Experimental analysis and modeling aspects of the removal of PAHs in soil slurry bioreactor

Douglas Oswaldo Pino Herrera

Thesis committee

Thesis Promotor
Prof. Mehmet A. Oturan
Université Paris-Est
Marne-la-Vallée, France

Thesis Co-Promotors
Dr. Hab. Eric D. van Hullebusch,
Université Paris-Est
Marne-la-Vallée, France

Dr. Giovanni Esposito,
University of Cassino and Southern Lazio
Cassino, Italy

Thesis Supervisor
Dr. Yoan Pechaud
Université Paris-Est
Marne-la-Vallée, France

Reviewers
Prof. Marie-Odile Simonnot
Université de Lorraine
Nancy, France

Prof. Francesca Beolchini
Università Politecnica delle Marche
Ancona, Italy

Examiners
Prof. Piet Lens
UNESCO-IHE Delft
Delft, The Netherlands

Dr. Yannick Fayolle
Irstea
Antony, France

Dr. Matthieu Peyre Lavigne
INSA Toulouse
Toulouse, France

This research was conducted under the auspices of the Erasmus Mundus Joint Doctorate in Environmental Technologies for Contaminated Solids, Soils, and Sediments (ETeCoS3). This joint PhD degree in Environmental Technology is funded by the Education, Audiovisual & Culture Executive Agency (EACEA) of the European Commission. The research training, academic courses undertaken and traveling expenses for presentation of the research outcome to conferences and seminars are funded by the programme.

Joint PhD degree in Environmental Technology

Docteur de l'Université Paris-Est
Spécialité : Science et Technique de l'Environnement

Dottore di Ricerca in Tecnologie Ambientali

Degree of Doctor in Environmental Technology

Tesi di Dottorato – Thèse – PhD thesis

Douglas Oswaldo Pino Herrera

Experimental analysis and modeling aspects of the removal of polycyclic aromatic hydrocarbons in soil slurry bioreactors

Defended on October 29th, 2018

In front of the PhD committee

Prof. Marie-Odile Simonnot	Reviewer
Prof. Francesca Beolchini	Reviewer
Prof. Piet Lens	Examiner, Jury President
Dr. Yannick Fayolle	Examiner
Dr. Matthieu Peyre Lavigne	Examiner
Prof. Mehmet A. Oturan	Promotor
Prof. Giovanni Esposito	Co-Promotor
Dr. Yoan Pechaud	Supervisor

Erasmus Joint doctorate programme in Environmental Technology for Contaminated Solids, Soils and Sediments (ETeCoS3)

Abstract

Polycyclic Aromatic Hydrocarbon (PAH)-contaminated soils are a great environmental and public health concern nowadays. Aerobic soil-slurry bioreactor technology has emerged as an effective and feasible technique with a high remediation potential, especially for the fine soil fractions, which often contain the highest pollution levels and are hard to treat with conventional approaches. However, the mechanisms involved in the PAH removal in the bioreactor are still not completely understood. In addition to the biological processes, important mass transfer mechanisms need to be considered (gas-liquid oxygen mass transfer, sorption-desorption, volatilization, etc.). For this study, a mechanistic approach was developed, in which the bioslurry process was deconstructed using a model system. Each part was isolated and analyzed individually. Then, the global process was studied and the results of the analysis of the individual parts were used to understand the global bioremediation treatment. Among the results obtained, it was demonstrated that clay presence in soils can strongly affect oxygen transfer in slurry systems, the pollutant bioavailability was limited by the desorption process, particularly when organic matter was present in the soil and volatilization can be the major removal process during the lag phase period in biodegradation. The results of this research work can be extrapolated to the study of real contaminated soil remediation. The mechanistic approach can be used as a generic method to investigate the slurry bioreactor treatment for any type of soil, different pollutants and microbial communities, and other operating conditions.

Keywords: Slurry bioreactor**,** PAHs, Soil remediation, Biological treatment, Mass transfer processes

Résumé

Les sols contaminés par des hydrocarbures aromatiques polycycliques (HAP) constituent un problème environnemental et de santé publique majeur. La technologie « bioslurry » aérobie s'est révélée être une méthode efficace avec un fort potentiel de remediation, en particulier pour les fractions de sol fines, qui contiennent souvent les niveaux de pollution les plus élevés et sont difficiles à traiter avec les approches conventionnelles. Cependant, les mécanismes impliqués dans l'élimination des HAP dans le bioréacteur ne sont toujours pas complètement compris. Outre les processus biologiques, d'importants mécanismes de transfert de masse doivent être pris en compte (transfert gaz-liquide d'oxygène, sorption-désorption, volatilisation, etc.). Pour cette étude, une approche mécanistique a été développée, dans laquelle les processus impliqués dans le « bioslurry » ont été isolée et analysée individuellement. Ensuite, le processus global a été étudié et les résultats de l'analyse des différents processus ont été utilisés pour comprendre le traitement de bioremédiation global. Parmi les résultats obtenus, il a été démontré que la présence d'argile dans les sols peut fortement affecter le transfert d'oxygène. Également, la biodisponibilité des polluants a été limitée par le processus de désorption, en particulier lorsque de la matière organique est présente dans le sol. En outre, la volatilisation peut être le principal processus d'élimination au cours de la phase de latence des microorganismes pendant le processus de biodégradation. Les résultats de ces travaux de recherche peuvent être extrapolés à l'étude de l'assainissement des sols contaminés réels. L'approche mécanistique peut être utilisée comme une méthode générique pour étudier le traitement par bioréacteur pour tout type de sol, différents polluants et communautés microbiennes, ainsi que d'autres conditions opératoires.

Mots-clés : Réacteur bioslurry, HAP, Dépollution des sols, Traitement biologique, Transfert de masse

Sintesi

Al giorno d'oggi i terreni inquinati da idrocarburi policiclici aromatici (IPA) rappresentano una grande preoccupazione per l'ambiente e la salute pubblica. La tecnologia “aerobic soil slurry bioreactor” è emersa come una tecnica efficace e attuabile con un alto potenziale per la bonifica, specialmente per le frazioni fini del terreno, che spesso contengono i livelli di inquinamento più elevati e sono difficili da trattare con approcci convenzionali. Tuttavia, i meccanismi coinvolti nella rimozione di IPA nel bioreattore non sono ancora completamente compresi. Oltre ai processi biologici, devono essere considerati importanti meccanismi di trasferimento di massa (trasferimento di massa di ossigeno gas-liquido, adsorbimento, volatilizzazione, ecc.). Per questo studio, è stato sviluppato un approccio meccanicistico, in cui il processo di bioslurry è stato decostruito utilizzando un sistema modello. Ogni parte è stata isolata e analizzata individualmente. Successivamente, è stato studiato il processo globale e sono stati utilizzati i risultati dell'analisi delle singole parti per comprendere il trattamento globale di biorimediazione. Tra i risultati ottenuti, è stato dimostrato che la presenza di argilla nei terreni può influenzare fortemente il trasferimento di ossigeno nei sistemi, la biodisponibilità degli inquinanti è limitata dal processo di desorbimento, in particolare quando la materia organica è presente nel suolo e la volatilizzazione può essere il principale processo di rimozione durante il periodo di fase di ritardo in biodegradazione. I risultati di questo lavoro di ricerca possono essere estrapolati allo studio di una bonifica del suolo inquinato reale. L'approccio meccanicistico può essere utilizzato come metodo generico per indagare il trattamento del bioslurry per qualsiasi tipo di terreno, per diversi inquinanti e comunità microbiche e altre condizioni operative.

Parole chiave: Bioslurry, IPA, bonifica del suolo, trattamento biologico, Trasferimento di massa

Samenvatting

Polycyclische aromatische koolwaterstof (PAK) -verontreinigde bodems zijn tegenwoordig een groot probleem voor de volksgezondheid en de volksgezondheid. Aërobe bodemsuspensie-bioreactor-technologie is naar voren gekomen als een effectieve en haalbare techniek met een hoog saneringspotentieel, vooral voor de fijne bodemfracties, die vaak de hoogste verontreinigingsniveaus bevatten en moeilijk te behandelen zijn met conventionele benaderingen. De mechanismen die betrokken zijn bij de PAK-verwijdering in de bioreactor zijn echter nog steeds niet volledig begrepen. Naast de biologische processen, moeten belangrijke mechanismen voor massaoverdracht worden overwogen (gas-vloeistof zuurstofmassaoverdracht, sorptie-desorptie, vervluchtiging, enz.). Voor deze studie werd een mechanistische benadering ontwikkeld, waarbij het bioslurryproces werd gedeconstrueerd met behulp van een modelsysteem. Elk onderdeel werd afzonderlijk geïsoleerd en geanalyseerd. Vervolgens werd het globale proces bestudeerd en werden de resultaten van de analyse van de afzonderlijke delen gebruikt om de globale bioremediatingsbehandeling te begrijpen. Onder de verkregen resultaten werd aangetoond dat de aanwezigheid van klei in de bodem de zuurstofoverdracht in slurrysystemen sterk kan beïnvloeden, de biologische beschikbaarheid van de verontreinigende stof werd beperkt door het desorptieproces, met name wanneer organisch materiaal in de grond aanwezig was en vervluchtiging het belangrijkste verwijderingsproces tijdens de de lag-faseperiode bij biologische afbraak. De resultaten van dit onderzoek kunnen worden geëxtrapoleerd naar de studie van echte verontreinigde bodemsanering. De mechanistische benadering kan worden gebruikt als een generieke methode om de behandeling met slurriebioreactor voor elk type bodem, verschillende verontreinigende stoffen en microbiële gemeenschappen en andere bedrijfsomstandigheden te onderzoeken.

Trefwoorden: Slurry-bioreactor, PAK's, Bodemsanering, Biologische behandeling, Massa-overdrachtsprocessen

Acknowledgements

Firstly, I would like to thank the coordinators of the program for having given me the opportunity to take part in the Erasmus Mundus Joint Doctorate programme ETeCoS^3: Dr. Giovanni Esposito (Università degli studi di Cassino e del Lazio Meridionale, Italy), Dr. Eric D. van Hullebusch (Université Paris-Est, France) and Prof. Piet Lens (Unesco-IHE, The Netherlands). I am proud of having been part of such a succesful and interesting programme.

I would like to expresse my sincere gratitude to Prof. Mehmet A. Oturan (promotor). It has been a privilege and an honor to have his guidance and his scientific expertise during the research and the writing of this thesis. I would also like to thank to Dr. Eric D. van Hullebusch and Dr. Giovanni Esposito (co-promotors) for all the administrative and scientific support during my PhD.

I am very grateful to my supervisor Dr. Yoan Pechaud to whom I own a big part of the accomplishment of this thesis. Not only for his great (dayly) contributions to my research activities and writing, but also for his patience, constant support and wise advices, which are proof of his professional and human qualities. I could have not asked for a better mentor.

I would like to express my gratitude to our partners at the Irstea, Dr. Yannick Fayolle and Sylvain Pageot, for their support during the tests we ran on their institute and for always making me feel welcome. I want to thank specially to Dr. Fayolle for the very interesting discussions and the invaluable advice on the papers on which we worked together.

I would also like to thank Prof. Marie-Odile Simonnot and Prof. Francesca Beolchini for reviewing my dissertation and for their insightful comments and challenging questions. They enriched the content of this thesis. Many thanks to Dr. Matthieu Peyre Lavigne and to Dr. Piet Lens, examiners of this work, for their helpful and constructive comments and questions during the defense.

I am very grateful for the opportunity of working in the Laboratoire Géomatérieux et Environnement (LGE) with such an excellent team. I would like to heartily thank Dr. David Huguenot for the advices and disposition to help at all times, Dr. Nihal Oturan for the technical and personal support and precious advice, Dr. Clément Trellu, Dr. Chloé Fourdrin and Dr. Anne Perez, for all their help in lab tasks and for reviewing specific chapters of the

thesis, Prof. Stéphanie Rossano for all the administrative and academic support, and to the technicians Christopher Prochasson and Théo Isigkeit for their assistance and quality of work. All the people at the LGE made me feel at home away from home.

I would like to extend my gratitude to Dr. Stefano Papirio for his help and guidance. He was a wonderful supervisor during my stay at the University of Cassino. I would also like to thank Gelsomino Monteverde for all his assistance and to Davide Risi, Master student whom I have the opportunitiy to supervise and who made all the long lab days much shorter and funnier.

This experience would not have been the same without all the labmates, colleagues and friends with whom I shared inspiring discussion, problems and happy moments during all these years: my dear ETeCoS^3 and ABWET colleagues: Viviana, Jairo, Gabriele, Kirki, Clément, Vicente, Nilesh, Anastasiia, Gilbert, Ludovico, Carolina, Ania, Suchanya, Andreina, Erika, Arda, Manivannan, Chiara and Paolo; my fellow PhD students at the LGE: Ilyes, Jules, Florian, Hélène and Valentina; and all the Master and Bachelor students who I had the opportunity to supervise or to work with: Carla Gentile, Stefano Pizzuto, Marie Sereng, Idriss Mariami, Marco Fantozzi and Ricardo Axel Cruz.

Last but not least, I would like to thank my family for the support and encouragement: my mom for all her prayers and encouraging words that kept me going on at difficult moments, my dad who I am sure would be very proud of this achievement, Daniela and Daniel for their unconditional care and support, my grandparents for following every step of my life and sending me their love, and especially to Albert who has been an unique moral and spiritual support and with whom I shared all the happy, sad and stressing moment of this great adventure. Thank you all for your love.

Table of Contents

List of Figures

GENERAL INTRODUCTION

CHAPTER 1 – Literature Review

CHAPTER 2 – Gas-liquid oxygen transfer in aerated and agitated slurry systems

CHAPTER 3 – Study of the volatilization of light aromatic compounds

CHAPTER 4 – PAH sorption and desorption in soil

CHAPTER 5 – Culture enrichment and biodegradation kinetics

CHAPTER 6 – Slurry bioreactor and general discussion

List of Tables

GENERAL INTRODUCTION

CHAPTER 1 – Literature Review

CHAPTER 2 – Gas-liquid oxygen transfer in aerated and agitated slurry systems

CHAPTER 3 – Study of the volatilization of light aromatic compounds

CHAPTER 4 – PAH sorption and desorption in soil

CHAPTER 5 – Culture enrichment and biodegradation kinetics

CHAPTER 6 – Slurry bioreactor and general discussion

GENERAL INTRODUCTION

GENERAL INTRODUCTION

1. Background

1.1. Soil pollution

Soil constitute an essential part of numerous ecosystems. For human beings, basic needs (such as feeding and clothing) depend on the quality and availability of this precious resource. Paradoxically, the number of polluted sites in the world has been increasing in the last decades due to human activities. In Europe, there might be as many as 2.5 million potentially contaminated sites [1] and, only in France, 6893 potentially contaminated sites were listed in September 2018 [2]. Polluted soils constitute a potential or real risk for the environment and human health and its remediation has become a common concern for governments and international organizations. According to the European Environmental Agency (EEA), remediation treatments are expected to be needed in approximately 342 000 European sites [1]. In terms of costs, expenses related to the contaminated soils management are estimated at €6.5 billion per year in Europe [3]. Only in France, public entities spent around €670 million in soil and groundwater protection and remediation in 2013 [4]. The remediation of contaminated sites represents a great challenge for the next years and decades due to the increasing number of polluted sites linked to human activities.

The most frequent contaminants are mineral hydrocarbons, polycyclic aromatic hydrocarbons (PAHs) and heavy metals. In France, almost 19% of the contaminated sites are impacted by petroleum hydrocarbons and PAHs [2]. Due to their common presence in contaminated sites and their characteristics as pollutants, PAHs were targeted as a study case in this thesis.

1.2. PAHs as pollutants

PAHs are a group of chemical compounds composed of two or more fused benzene rings. There are more than 100 different compounds within this group and, generally, they occur as complex mixtures. PAHs can be found in great diversity in the environment and are considered as ubiquitous pollutants. Incomplete combustion of organic matter is the typical source of PAHs, and emission sources can be mobile (e.g. automobile exhausts) or stationary (e.g. coal-fired electricity power plants). Also, domestic sources (e.g. tobacco smoke, residential wood or coal combustion), and area sources (e.g. forest fires and agricultural burnings) produce significant amounts of these compounds [5].

Based on their toxicity, frequency of occurrence at hazardous waste sites and human exposure potential, the United States Environmental Protection Agency (US EPA) has classified 16 of the PAHs as priority pollutants [6]. Seven of them are considered as probable human carcinogens. In general, PAHs considered to be carcinogenic have higher molecular weight, which means, higher number of aromatic rings included in their structure. The physicochemical characteristics of PAHs contribute directly to their recalcitrant nature in the environment [7].

1.2.1. Physicochemical properties

PAHs are lipophilic carbon-based compounds, containing fused aromatic rings. They may contain other non-six-sided carbon rings, as well as other atoms (such as nitrogen, oxygen or sulfur) attached to their structure (Figure 1). Some of them can readily volatilize into the air and most do not burn easily. Pure PAHs generally exist as colorless, white, or pale yellow-green solids and they can have a faint, pleasant odor [6]. Table 1 shows some physicochemical properties of the 16 PAHs listed by the USEPA. In general, most of the PAHs are very little soluble in water and little mobile in soils because of their tendency to be adsorbed, particularly on the fine particles of the soil. They are stable, but their biodegradability varies according to the environmental conditions (such as pH, temperature), external mass transport, number and type of soil microorganisms, among others [8].

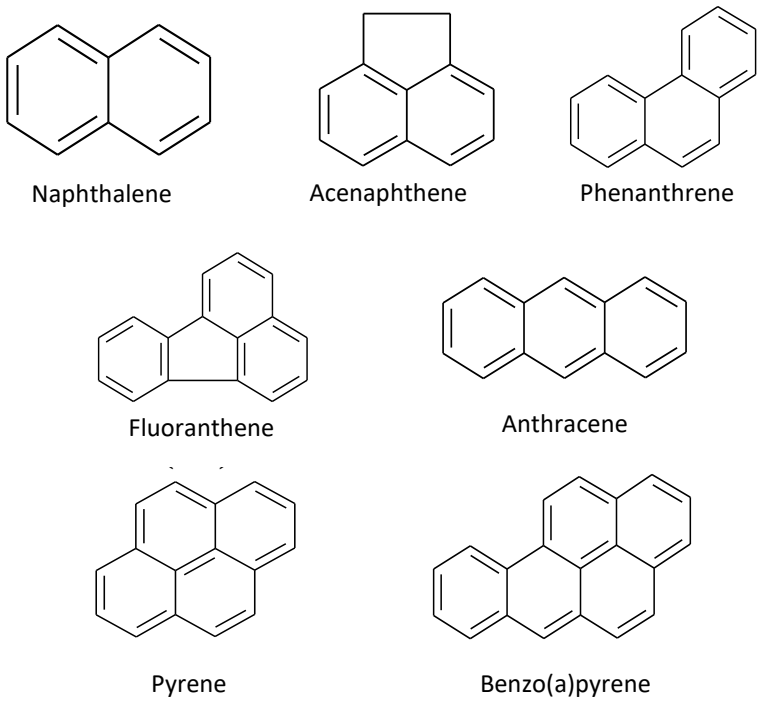

Figure 1 Structure of selected PAHs

PAHs' vapor saturate pressure decreases as long as the molecular molar mass increases, while water solubility varies in function of the molecular structure complexity. Generally, PAHs have a low solubility in water, between 32 mg/l for the lightest compound and values in the order of 10^{-4} mg/l for the heavier ones [9]. They are usually classified in two categories: low molecular weight (LMW) and high molecular weight (HMW) PAHs. LMW PAHs have only two or three fused rings and HMW PAHs have four or more. Therefore, the firsts are usually degraded and volatilized more rapidly than the latter [10].

Table 1. Physicochemical properties of the 16 PAHs listed by USEPA.

PAHs	Formula	MW (g/mol)	Density[(a)] (kg/l)	Water solubility[(b)] at 25°C (mg/l)	Log KOC[(a)]	Henry Constant[(a)] at 25°C (Pa m3/mol)
NAP	$C_{10}H_8$	128.2	1.162	3.2×101	3.15	4.9×101
ACY	$C_{12}H_8$	152.2	1.194	3.9×100	1.40	-
ACE	$C_{12}H_{10}$	154.2	1.024	3.4×100	3.66	1.5×101
FLE	$C_{13}H_{10}$	166.2	1.203	1.9×100	6.20	9.2×100
PHE	$C_{14}H_{10}$	178.2	1.172	1.3×100	4.15	4.0×100
ANT	$C_{14}H_{10}$	178.2	1.240	7.0×10-2	4.15	5.0×100
FLA	$C_{16}H_{10}$	202.3	1.236	2.6×10-1	4.58	1.5×100
PYR	$C_{16}H_{10}$	202.3	1.271	1.4×10-1	4.58	1.1×10-3
B(a)A	$C_{18}H_{12}$	228.3	1.174	1.0×10-2	5.30	2.0×10-2
CHRY	$C_{18}H_{12}$	228.3	1.274	2.0×10-3	5.30	1.0×10-2
B(b)F	$C_{20}H_{12}$	252.3	-	1.5×10-3	5.74	5.0×10-2
B(k)F	$C_{20}H_{12}$	252.3	-	8.0×10-3	5.74	6.9×10-2
B(a)P	$C_{20}H_{12}$	252.3	1.282	3.8×10-3	6.74	5.0×10-2
dB(a,h)A	$C_{22}H_{14}$	278.3	1.252	5.0×10-4	6.52	4.8×10-3
B(ghi)P	$C_{22}H_{12}$	276.3	1.329	3.0×10-4	6.20	1.4×10-2
I(1,2,3-c,d)P	$C_{22}H_{12}$	276.3	-	2.0×10-4	6.20	2.9×10-2

[(a)] INERIS [11]
[(b)] Manoli and Samara [12]

1.2.2. PAHs in soil

In soil, most PAHs are not available for degradation processes because they are usually strongly sorbed to organic matter. This is especially true for HMW PAHs [13]. LMW PAHs can be partially released from soils through volatilization, biodegradation and leaching. Higher concentrations can be found nearby emission sources, urban soils and roadside soils and may exceed 10,000 mg/kg soil for contaminated sites. In these sites usually industrial activities have been carried out and the production or the use of fossil fuels or derivative

products is involved [5]. Other industrial PAH sources may be waste of manufacturing and synthesis of organic compounds, such as pesticides, fungicides, detergents, dyes and mothballs [14].

Additionally, degradability and extractability of organic compounds in soil have proved to decrease according to the time they have been in contact with soil. This process is commonly known as “aging” or “weathering” [15]. Slow diffusion into the soil organic matter is the main responsible mechanism for aging. But also, formation of bound residues and physical entrapment within soil micro-pores can occur [5].

2. What treatment to use?

2.1. Remediation strategies for soils contaminated with organic pollutants

Traditional remediation involves the excavation and the disposition of the contaminated soil in another location [1]. However, other ways to remove organic pollutants from soil have been studied. According to Colombano et al. [16], they can be grouped into the four categories: physical processes, physicochemical process, thermal processes and biological process.

Physical processes consist mainly in containment and landfilling, whose goal is to avoid the extension of the pollution, but the contaminant is not removed. Physicochemical remediation techniques, such as chemical oxidation, soil flushing or soil washing, imply the use of substances (namely oxidizers or surfactants) to remove the contamination from the soil. These treatments are generally efficient, but substances used need to be environmentally friendly, which may limit its application. Thermal treatments are in general expensive and highly energy-consuming. Biological remediation constitute environmentally friendly, robust, low-maintenance treatments, but have the disadvantage of being slower than the other techniques. Therefore, the enhancement of their efficiency have been of interest during the last decades.

2.2. Bioremediation of PAH-contaminated soils

Bioremediation of PAHs has been well studied [17,18]. It represents an option to transform PAHs into less harmful compounds, with less addition of chemicals and energy to the process than other treatments. Different types of organisms (e.g. algae, bacteria and fungi) can be used for this purpose. The degradation rate of PAHs by biological treatments depends strongly on the environmental conditions, diversity and concentration of microorganisms, physicochemical properties and the chemical structure of the particular PAH to be degraded [19]. In general, LMW PAHs are biodegraded more easily than HMW PAHs. The reason for

this may be the physicochemical characteristics of the latter, which are highly lipophilic and water insoluble compounds. Only few microorganisms are able to degrade this kind of contaminants. Moreover, mineralization half-lives of LMW PAHs are in order of days compared to months or years for the HMW PAHs. Hence, bioremediation can be a time-consuming treatment when high concentrations of HMW PAHs are present [20].

2.2.1. Selection of the bioremediation technique

Bioremediation techniques for soil remediation can be classified in two types: *in situ* and *ex situ*. *In situ* remediation processes consist in the treatment of the soil in place. This type of remediation is applied mostly within the saturated zone of the soil and involves the addition of nutrients, an oxygen source, and sometimes specific adapted microorganisms in order to improve biodegradation. All these elements are added by drilling wells throughout the contaminated area and injecting the appropriate substances or solutions. In general, this type of treatments are slow and not efficient for recalcitrant, toxic compounds [21]. *Ex situ* remediation technologies include landfarming, prepare beds or composting. In landfarming, waste material is applied to the soil as slurry, in order to enhance microbial activity, and conditions are given for indigenous microorganisms to degrade the contaminants. However, contaminants can possibly move from the treatment area and this represents a major disadvantage. For prepared beds, contaminated soil is removed and put in a specific prepared area, which is managed with fertilization, irrigation, pH control and maybe microbial and/or surfactant addition. This allows an enhancement of the biodegradation process, but remediation time can still be low [16].

A more efficient technique consisting in removing the soil and placing it into a bioreactor can also be used. In the reactor, the soil is slurred with water and other substances to mobilize the contaminants and promote biodegradation**.** This process is called slurry bioreactor and have demonstrated to have a better performance at PAH degradation than other *in situ* and *ex situ* treatments of the same soil [22]. For this reason, this technique was selected as a subject of study. However, even if this technology has been investigated during the last decades, the process is not completely understood.

2.2.2. Slurry bioreactor for PAH removal from soil

Typically, three phases are present in soil slurry bioreactors, i.e. the aqueous medium, the solid phase (the soil to be remediated and the biomass), and an air flow providing oxygen to the system. To remove PAHs from soil, a series of processes have to occur. Pollutants must be

desorbed from soil, and microorganisms must have access to these pollutants and other nutrients, and, in the case of aerobic biodegradation, oxygen must be readily available [23]. Only when these conditions are fulfilled, biodegradation process can start. However, other processes, which are not necessarily related to the biotransformation of the pollutants, could happen simultaneously. For instance, LMW PAHs could volatilize [24]. To simplify and better understand these mechanisms, it easier to classify them into three groups: i) gas-liquid transfer processes; ii) solid-liquid transfer processes; and iii) biodegradation processes. These mechanisms take place simultaneously in the reactor and can influence one another.

3. Objectives of the study

3.1. Innovative approach

Most studies found in the literature regarding soil slurry bioreactors are focused on the optimization of the process efficiency for specific contaminated soils. This has allowed the identification of the advantages and the utility of the treatment. However, the mechanisms permitting the success of the treatment are not completely understood. Therefore, for this thesis project, a mechanistic approach was developed, in which the global process was deconstructed. Each part was isolated and analyzed individually. Then, the global process was studied and the results of the analysis of the individual parts were used to understand it. As a result, the global process was comprehended as an addition of the individual parts plus the interactions between them.

3.2. Structure of the thesis.

The structure of the thesis is depicted in Figure *2*. The thesis manuscript is divided in six chapters:

- **Chapter 1:** Literature review. The state-of-the-art studies on slurry bioreactors for remediation of soil and sediments contaminated with hydrophobic organic compounds is presented.

The following chapters study the individual mechanisms influencing the removal of PAHs in the soil slurry bioreactor.

- **Chapter 2:** Gas-liquid oxygen transfer in aerated and agitated slurry systems. The effect of selected operational parameters of the reactor on the gas-liquid oxygen transfer is studied.
- **Chapter 3:** Study of the volatilization of aromatic compounds. The study and modeling of the surface volatilization of PAHs in the reactor is done, using a model and two reference compounds.

- **Chapter 4:** PAH sorption-desorption in soil. The influence of soil concentration and composition on polycyclic aromatic hydrocarbon sorption and desorption is measured. Sorption-desorption equilibria and desorption kinetics of PAHs in soil slurry is investigated.
- **Chapter 5:** Culture enrichment. The influence of acclimation and co-substrate enrichment on the polycyclic aromatic hydrocarbon aqueous biodegradation by a mixed culture is investigated. The development of an acclimated, enriched mixed culture is done and the influence of co-substrate on the phenanthrene kinetic degradation is measured.

The last two chapters concern the study of the global process, discussions and conclusions of the project.

- **Chapter 6:** Soil slurry bioreactor and the removal mechanisms. Interactions between mass transfer and biodegradation mechanisms in a soil slurry bioreactor are experimentally analyzed and discussed. The study of the complete process in the reactor is performed.
- **Chapter 7:** Conclusions and perspectives.

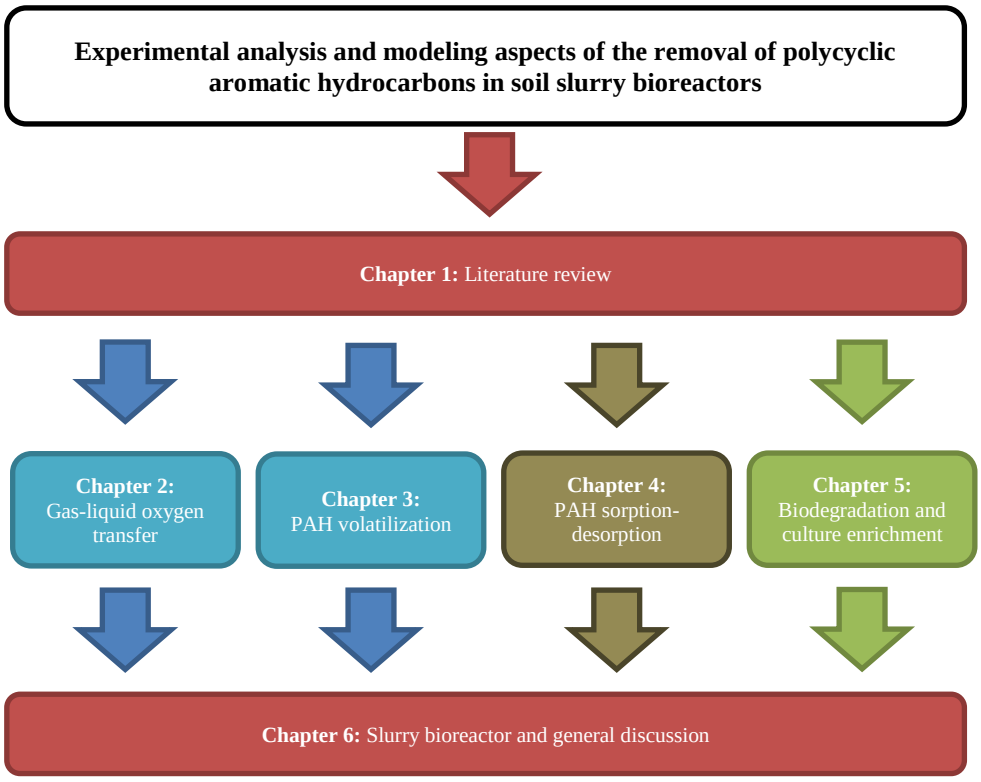

Figure 2 Structure of the thesis

References

[1] Soil contamination widespread in Europe, Eur. Environ. Agency. (n.d.). https://www.eea.europa.eu/highlights/soil-contamination-widespread-in-europe (accessed October 1, 2018).

[2] BASOL - Ministère de la Transition écologique et solidaire, (n.d.). https://basol.developpement-durable.gouv.fr/tableaux/home.htm (accessed October 1, 2018).

[3] Progress in management of contaminated sites, Eur. Environ. Agency. (n.d.). https://www.eea.europa.eu/data-and-maps/indicators/progress-in-management-of-contaminated-sites-3/assessment (accessed September 20, 2018).

[4] La dépense de protection et d'assainissement du sol, des eaux souterraines et des eaux de surface [L'essentiel sur…, Environnement, Dépenses de protection de l'environnement] : Observation et statistiques, Ministère Transit. Ecol. Solidaire. (n.d.). http://www.statistiques.developpement-durable.gouv.fr/lessentiel/ar/375/0/depense-protection-dassainissement-sol-eaux-souterraines.html (accessed September 20, 2018).

[5] S. Lundstedt, Analysis of PAHs and their transformation products in contaminated soil and remedial processes., Umeå Universitet, Umeå, 2003.

[6] ATSDR, Toxicological Profile for Polycyclic Aromatic Hydrocarbons, ATSDR, Atlanta, 1995.

[7] R.A. Kanaly, S. Harayama, Biodegradation of high-molecular-weight polycyclic aromatic hydrocarbons by bacteria, J. Bacteriol. 182 (2000) 2059–2067.

[8] A.R. Johnsen, L.Y. Wick, H. Harms, Principles of microbial PAH-degradation in soil, Environ. Pollut. 133 (2005) 71–84. doi:10.1016/j.envpol.2004.04.015.

[9] O. Bour, Hydrocarbures Aromatiques Polycyliques Guide méthodologique, INERIS, 2005.

[10] A.F. Wick, N.W. Haus, B.F. Sukkariyah, K.C. Haering, W.L. Daniels, Remediation of PAH-contaminated soils and sediments: A literature review, Va. Polytecnic Inst. Blacksbg. VA. (2011). http://www.landrehab.org/UserFiles/DataItems/66647A54537164594C6F513D/Virginia%20Tech%20PAH%20Remediation%20Lit%20Review%202011.pdf (accessed November 25, 2014).

[11] INERIS, Hydrocarbures Aromatiques Polycycliques. Guide méthodologique. Acquisition des données d'entrée des modèles analytiques ou numériques de transferts dans les sols et les eaux souterraines, INERIS, France, 2005.

[12] E. Manoli, C. Samara, The removal of Polycyclic Aromatic Hydrocarbons in the wastewater treatment process: Experimental calculations and model predictions, Environ. Pollut. 151 (2008) 477–485. doi:10.1016/j.envpol.2007.04.009.

[13] L.R. Brooks, T.J. Hughes, L.D. Claxton, B. Austern, R. Brenner, F. Kremer, Bioassay-directed fractionation and chemical identification of mutagens in bioremediated soils., Environ. Health Perspect. 106 (1998) 1435–1440.

[14] S.K. Samanta, O.V. Singh, R.K. Jain, Polycyclic aromatic hydrocarbons: environmental pollution and bioremediation, TRENDS Biotechnol. 20 (2002) 243–248.

[15] A.-S. Allard, M. Remberger, A.H. Neilson, The negative impact of aging on the loss of PAH components in a creosote-contaminated soil, Int. Biodeterior. Biodegrad. 46 (2000) 43–49. doi:10.1016/S0964-8305(00)00050-0.

[16] S. Colombano, A. Saada, V. Guerin, P. Bataillard, G. Bellenfant, S. Beranger, D. Hube, C. Blanc, C. Zornig, I. Girardeau, Quelles techniques pour quels traitements–Analyse coûts-bénéfices, Rapp. Final BRGM-RP-58609-FR. (2010).

[17] C.E. Cerniglia, Biodegradation of polycyclic aromatic hydrocarbons, Biodegradation. 3 (1992) 351–368.

[18] A.K. Haritash, C.P. Kaushik, Biodegradation aspects of Polycyclic Aromatic Hydrocarbons (PAHs): A review, J. Hazard. Mater. 169 (2009) 1–15. doi:10.1016/j.jhazmat.2009.03.137.

[19] A.K. Haritash, C.P. Kaushik, Biodegradation aspects of Polycyclic Aromatic Hydrocarbons (PAHs): A review, J. Hazard. Mater. 169 (2009) 1–15. doi:10.1016/j.jhazmat.2009.03.137.

[20] C.E. Cerniglia, Biodegradation of polycyclic aromatic hydrocarbons, Curr. Opin. Biotechnol. 4 (1993) 331–338.

[21] S.C. Wilson, K.C. Jones, Bioremediation of soil contaminated with polynuclear aromatic hydrocarbons (PAHs): a review, Environ. Pollut. 81 (1993) 229–249.

[22] B.E. Rittmann, N.M. Johnson, Rapid biological clean-up of soils contaminated with lubricationg oil, in: Water Pollut. Res. Control Brighton, Pergamon, 1988: pp. 209–219. doi:10.1016/B978-1-4832-8439-2.50024-9.

[23] S.H. Woo, J.M. Park, B.E. Rittmann, others, Evaluation of the interaction between biodegradation and sorption of phenanthrene in soil-slurry systems, Biotechnol. Bioeng. 73 (2001) 12–24.

[24] V. Jee, D.M. Beckles, C.H. Ward, J.B. Hughes, Aerobic slurry reactor treatment of phenanthrene contaminated sediment, Water Res. 32 (1998) 1231–1239.

CHAPTER 1

Literature Review

This chapter has been published as:

D.O. Pino-Herrera, Y. Pechaud, D. Huguenot, G. Esposito, E.D. van Hullebusch, M.A. Oturan, Removal mechanisms in aerobic slurry bioreactors for remediation of soils and sediments polluted with hydrophobic organic compounds: An overview, J. Hazard. Mater. 339 (2017) 427–449. doi:10.1016/j.jhazmat.2017.06.013.

CHAPTER 1 – Literature Review

First, it is necessary to know the state of the art of the technology to be studied. In this chapter the soil slurry bioreactor treatment for hydrophobic organic compound (HOC)-contaminated soil is reviewed. This review includes the current and the matured research on mass transfer and biodegradation processes, as well as bioslurry studies, going from theoretical aspects through experimental work and modeling of each mechanism.

Abstract

Hydrophobic organic compound (HOC)-contaminated soils are a great environmental and public health concern nowadays. Further research is necessary to develop environmentally friendly biotechnologies that allows public and private sectors to implement efficient and adaptable treatment approaches. Aerobic soil-slurry bioreactor technology has emerged as an effective and feasible technique with a high remediation potential, especially for silt and clay soil fractions, which often contain the highest pollutant concentration levels and are usually difficult to remove by implementing conventional methods. However, the mechanisms involved in the HOC removal in bioslurry reactor are still not completely understood. Gas-liquid and solid-liquid mass transfer, mass transport and biodegradation phenomena are the main known processes taking place in slurry bioreactors. This review compiles the most up-to-date information available about these phenomena and tries to link them, enlightening the possible interactions between parameters. It gathers the basic information needed to understand this complex bioremediation technology and raises awareness of some considerations that should be made.

Keywords: Slurry bioreactor, biological treatment, contaminated soil treatment, aerobic process, HOC removal

Graphical abstract

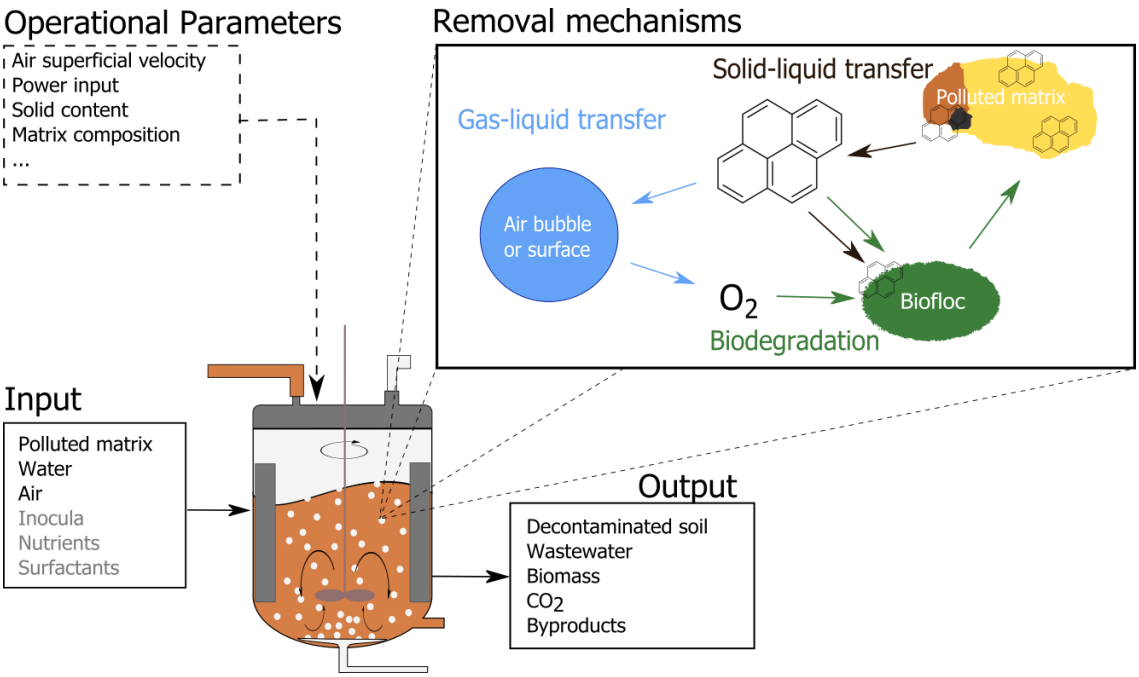

1. Introduction

Hydrophobic organic compounds (HOCs) are a wide group of chemical substances that includes aliphatic, aromatic and polyaromatic hydrocarbons, contained in petroleum residues, tars, creosotes, chlorinated solvents, herbicides, pesticides, explosives and other substances [1]. Due to their hydrophobic nature, HOCs can remain sorbed in soils or sediments for a long time and this fact places them among the recalcitrant materials. Additionally, many of them are known to have high impacts on ecosystems and human health. For all these reasons, remediation of HOC-contaminated soils and sediments has become an important field of research.

Several remediation techniques have been developed with the purpose of removing HOCs from soil and sediments [2]. They can be classified either by their nature (thermal, physicochemical, chemical or biological treatments) or by the type of application (*in situ* or *ex situ*, on-site or off-site). In general, thermal and chemical treatments are comparatively more expensive than biological treatments. The latter is also considered to be more environmentally friendly compared to the former ones [3,4]. Conversely, biological treatments are usually slow processes with long remediation time [5].

Regarding the type of application, *in situ* biological remediation consists in the treatment of the soil in place, remaining practically undisturbed. It is applied mostly within the saturated zone of the soil and involves the addition of nutrients, an oxygen source, and sometimes specific adapted microorganisms to improve contaminant degradation rate. On the other hand, *ex situ* remediation includes several technologies such as landfarming, prepared beds, biopiles or composting, which can be applied on-site [6,7]. It also includes off-site technologies which imply the excavation and treatment of the soil on a different place (that could be close or not to the contaminated site).

Slurry bioreactor technology is an off-site technology that consists in the biological treatment of contaminated soil or sediments in a large and possible mobile reactor, which is provided with the conditions to enhance natural attenuation of a great variety of contaminants in slurry phase [8]. This remediation process has also been called by other names; i.e., soil-slurry bioreactors, slurry-phase biological treatment, bio-slurry reactors, etc. In general, bioreactors are chosen as soil remediation treatment when fast and safe remediation is needed and when suitable conditions for more conventional biological treatments are not given (pollution in the unsaturated zone or dry conditions, recalcitrant pollutants, elevated toxicity levels, low

permeability, etc.). Several reasons for this choice can be enumerated: firstly, these systems allow the enhancement of surface phenomena, such as gas-liquid and solid-liquid mass transfer, which usually leads to an increment of the bioavailability of contaminants; secondly, if a toxic concentration of pollutants is present in the soil, the addition of water can reduce it, allowing a less hostile environment for biodegradation; thirdly, by using bioreactors, it is possible to control and optimize the bioremediation process accurately by adjusting the most critical parameters [6,9].

Therefore, it is not surprising that several studies have demonstrated that bioreactors have a better performance in HOCs degradation compared to other on-site treatments of the same soil, which has led to consider this treatment as one of the best options for subsurfaces polluted with recalcitrant compounds [10,11]. However, as a consequence of the excavation, the soil and slurry handling and the process control needed, the costs of the treatment are usually higher than other conventional bioremediation processes [3].

As a pretreatment, soil or sediments can be dried, crushed and separated into a coarse fraction (gravel and sand) and a fine fraction (fine sand, silt and clay). Often, only the fine fraction (< 2 mm) is considered in the bioremediation process for two reasons: (i) pollutants such as HOCs are mainly concentrated in the fine particles [12], where they are less mobile and hard to treat; and (ii) heavier particles might be difficult to maintain in suspension and the entire process might become more expensive. This means that silt and clay fractions of soils or sediments are, indeed, more interesting to treat from an environmental and an economical point of view.

After pretreatment, the selected fraction of the polluted soil is placed in a reactor and it is slurred with water to mobilize the contaminants and promote biodegradation. Figure 1.1A shows a typical configuration of a soil slurry bioreactor. To maintain homogeneous conditions, mechanical and/or pneumatic mixing is applied. Mechanical mixing is usually provided by a stirrer connected to a motor. However, mechanical rotational agitation (roller or drum bioreactors) have been also used [13–16]. Additionally, air spargers or diffusers are often installed in the reactor with the purpose of ensuring aerobic conditions. In fact, aerobic operation has demonstrated to be an effective and feasible technique with a higher remediation potential over other metabolic functions [17].

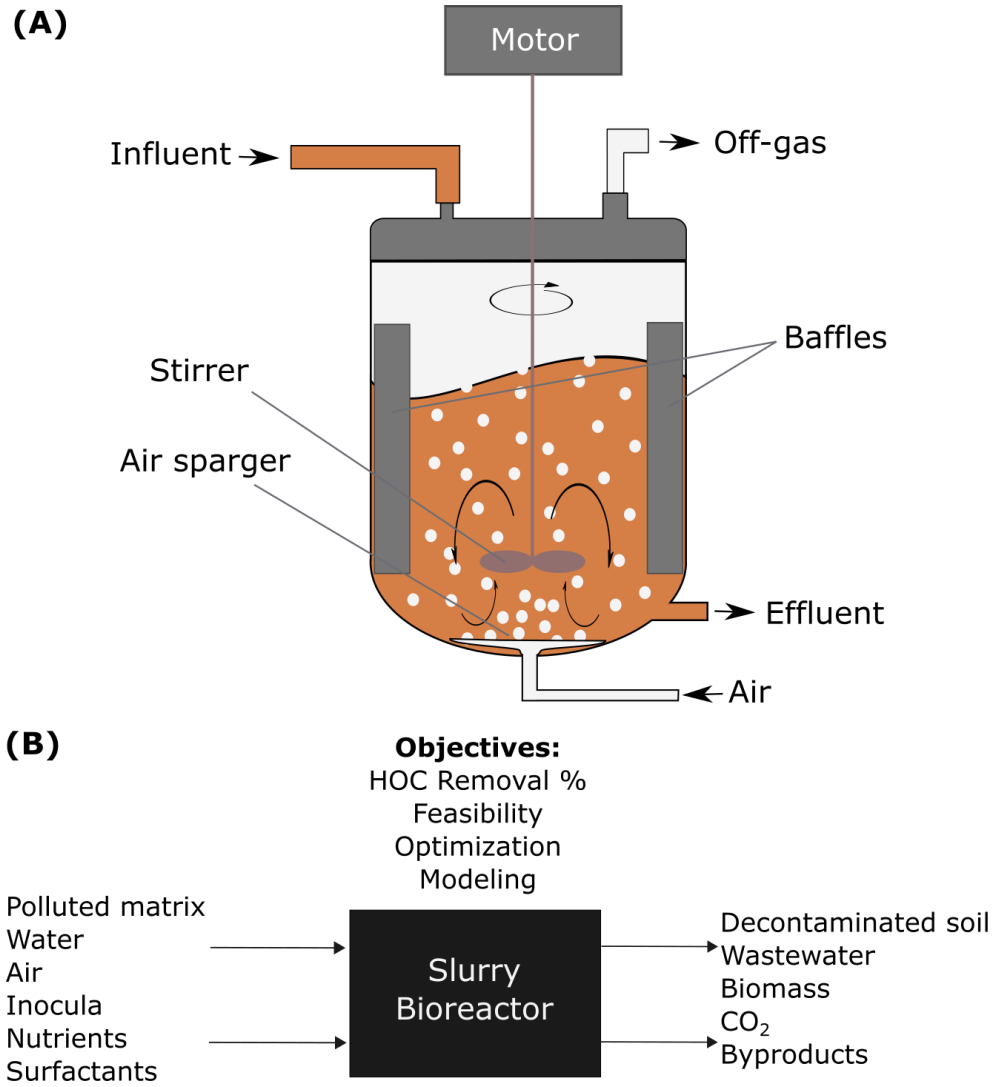

Figure 1.1 Slurry bioreactor technology: (a) Typical configuration (b) black box approach used in most studies

Soil-slurry bioreactors are usually operated in batch or semi-continuous (Sequencing Batch Reactor or SBR) mode because these operation modes facilitate the handling of soils and slurries [18–21]. The operation in continuous mode is also possible but remains uncommon [17]. This might be due to a demonstrated lower pollutant removal efficiency for some pollutants compared to batch operation [22].

Although slurry bioreactors for soil remediation have been studied for more than three decades, there is still a lack of knowledge about the mechanisms that control this treatment. In fact, many papers discussing this topic consider only biological processes and very few of them address and discuss important transfer phenomena. Therefore, the present article aims to review, identify and summarize the role and the importance of mass transfer, mass transport and biodegradation processes as well as the main operational parameters concerned in the

system, with the purpose of providing a practical understanding and a glimpse of the potential research work required on the subject. This review includes a summary of the most important results and conclusions drawn in publications addressing the subject during the last 20 years, as well as a description of the main mechanisms involved in the HOC removal in aerobic soil-slurry systems (with a focus on stirred and aerated bioreactors), the identification of some important operational parameters and perspectives on the future research about this topic.

2. State-of-the-art research on soil slurry bioreactor treatment

In this section, selected papers addressing the use of slurry bioreactors as treatment for contaminated soils and sediments and their results and conclusion are condensed. Table 1.1 shows a summary of the objectives of the papers included in this review, classifying them by the type of contaminant studied and the type of pollution (spiked or real).

The most typical applications reviewed involve hydrocarbons, both aliphatic and aromatic. Particularly, polycyclic aromatic hydrocarbons (PAHs) represent the clear majority of targeted contaminants. Their recalcitrance and toxicity make them hard to treat by other biological processes, hence this technology represents one of the best options for a quick and effective treatment [11]. However, the treatment has been studied mainly at the laboratory scale (meaning working volume less than 1 liter). Few works can also be found at bench or the pilot scale (considered in this paper as greater than or equal to 1 liter).

Concerning the objectives of the publications, the study of soil-slurry bioreactors has been carried out to identify and to quantify the main effects of several variables on the removal rate and the efficiency of the overall process. These variables include the soil constituents, the use of external microorganisms (bioaugmentation), the supplementation of nutrients or other carbon sources (biostimulation), and some operating conditions (for instance, mixing rate and regime, air flow, temperature and pH, among others).

Most studies reviewed in this article developed a “black-box” approach (Figure 1.1B), meaning that only the overall efficiency is concerned, and the local mechanisms involved in the removal of pollutants are hardly addressed. However, some biological studies have been made to identify biodegradation pathways of pollutants, microbial population dynamics and specific or mixed microbial strains performance on degradation in slurry conditions. Finally, only few research works have tried to understand the process using a mechanistic approach, in which both abiotic and biotic mechanisms have been studied and modeled.

Table 1.1 Objectives, contaminant targeted and pollution type in selected papers

Objectives of the study		PAHs		Aliphatic Hydrocarbons		Others*	
		Spiked matrix	Real pollution	Spiked matrix	Real pollution	Spiked matrix	Real pollution
Study of the treatment feasibility	Batch operation	[23][a] [24][a]	[25][b] [26][a] [27][a] [28][b]	[19][b]	[26][a] [28][b]	[29][a] [14][a]	[30][b] [31][b]
	SBR operation, effect of HRT and/or loading rate	[18][b] [20][a] [21][a]	[32][b]	[33][a, b]	[22][b] [34][b]		[31][b]
	Continuous operation				[22][b]		
Study of pollutant removal	Effect of soil constituents	[35][b]	[26][a]	[36][a]	[26][a]		
	Effect of Operational parameters (aeration, mixing, slurry concentration)	[37][a] [16][a] [38][a] [15][a]		[36][a]		[39][a] [40][a] [14][a]	[41][a] [42][b]
	Effect of (bio)surfactant addition	[35][b] [43][a] [44][a] [45][b]	[46][a]			[40][a] [14][a]	
	Effect of bioaugmentation	[20][a] [21][a] [47][a] [23][a] [38][a] [15][a]	[27][a] [13][a] [48][b]		[49][b] [13][a]	[40][a]	
	Effect of biostimulation	[50][a] [16][a]	[26][a] [46][a] [28][b]		[26][a] [28][b]	[51][a] [40][a]	[41][a]
	Effect of cell metabolism			[19][b]	[52][a]	[29][a]	
	Effect of co-contamination	[53][a]	[53][a]				
Study of dynamics of microbial population	Byproduct identification	[53][a]	[53][a]			[29][a]	[30][b]
	Study of microorganisms' capabilities and optimal biodegradation conditions	[48][b]					
Mechanisms modeling	Biodegradation	[48][b]				[54][a]	[31][b]
	Biodegradation and abiotic mechanisms	[38][a] [55][a] [53][a] [45][b]	[53][a]	[56][a]		[14][a]	

* Others: explosives, herbicides and pesticides.
[a] Laboratory scale
[b] Bench or pilot scale

Pollutant removal efficiencies are in general high for this treatment in batch operation mode (Table 1.2), achieving up to 100% in some cases. However, it is necessary to observe the individual conditions in which each experiment was performed to conclude about the removal efficiency of contaminants. For instance, the duration of the experiments should be considered to draw any firm conclusion about the efficiency of the treatment. Other important factors that play important roles on the soil slurry treatment are: (i) additions to the reactor, such as surfactants or external microorganisms [25,27,37,57]; (ii) characteristics of the soil; and (iii) origin and aging of the pollution and the environmental conditions of each polluted site.

The study of the SBR and continuous operation mode has also been investigated by some researchers to evaluate its feasibility for the remediation of specific soil or sediment matrices or pollutants. These research works are focused on the influence of specific operating conditions, such as hydraulic retention time (HRT), solid retention time (SRT) or substrate loading rate (SLR), on the overall efficiency of the process. Table 1.3 shows the main parameters used in some of these publications. It is possible to observe also in these cases that different operational parameters are adjusted and optimized for specific soil or sediments treatment evaluation and information of the general process is sometimes missing or incomplete. In these studies, HRT and SRT are often synonyms, meaning that the same quantities of water and solids are feed and withdrawn to avoid accumulation in the reactor.

Nevertheless, an interesting fact that can be deduced from the efficiency results (in Table 1.2) is that, in PAH-contaminated soils or sediments, natural microflora can remove Low Molecular Weight PAHs (LMW PAHs) without any addition of microorganisms, reaching in some cases full degradation. However, removal efficiencies for high molecular weight PAHs (HMW PAHs) are always less important than for their lighter counterparts [16,32,46]. Many authors explain this in terms of bioavailability: HMW PAHs are more hydrophobic and less soluble and, hence, less bioavailable for microorganisms [58]. But, in this type of systems, pollutant bioavailability results to be rather complicated to study when one considers interactions with soil components, pollution aging, pollutants and metabolites toxicity towards microbial population and operational parameters effects.

For instance, regarding the operational parameters, it is possible to consider soil or sediment slurry concentration (% w/v) and notice that it fluctuates from 4% to 50% among the papers summarized in Tables 1.2 and 1.3. What are the criteria for the selection of this specific parameter? What is its influence on the biodegradation process, the pollutants bioavailability

and the remediation time? What about the other operational parameters (air flow rate, stirring rate, temperature, etc.)? These are questions which researchers on this topic struggle with when deciding which parameters to fix and which to assess in order to understand and optimize the process.

Additionally, the arbitrary selection of these conditions makes impossible drawing any comparison between studies, limiting the comprehension of local transport phenomena and biodegradation dynamics. This means that further research on the mechanisms that rule and control the treatment are needed. A common knowledge about this proved efficient treatment can be useful for future process design and optimization of real scale applications. Therefore, next sections aim to compile information about the most important known mechanisms of HOCs removal in a soil slurry bioreactor.

Table 1.2 Removal of contaminants reported in selected papers using aerobic soil slurry reactors used in batch operation

Matrix	Soil % (w/v)	Contaminant [Concentration]	Removal efficiency	Remarks	Operational conditions	Reference
Real contamination						
Creosote contaminated soil	30%	Total 2-3 rings	96%	Bioaugmented with *Pseudomonas fluorescens*, *Pseudomonas stutzeri*, and an *Alcaligenes* specie	• 64-l reactor. • Complex system of aeration and homogenization. • 14-day operation.	[25]
		Total 4-6 rings	82%			
		Total	89%			
Sandy soil	N.R.	Pentachlorophenol (PCP)	98%	Bioaugmented with enriched indigenous microbial consortium immobilized in soil and as flocculent biomass (similar results).	• 4-l jar. • Mixed manually every three day for aeration. • 130-day operation.	[59]
Loam soil	20%	No-carcinogenic PAHs	93%	Bioaugmented with an inoculum developed in a 2-l reactor fed with PAHs contaminated soil for several months. Abiotic removal (volatilization) observed for light PAHs (around 20%)	• 750-ml flasks. • 0.02 l/min aeration. • 35-day operation. • Pre-treatment with solvents tested.	[57]
		Carcinogenic PAHs	42%			
Sandy loam soil	20%	No-carcinogenic PAHs	93%-99%			
		Carcinogenic PAHs	50%-52%			
Sandy clay loam	20%	No-carcinogenic PAHs	93%			
		Carcinogenic PAHs	59%			
Soil	10%	2,4,6-trinitrotoluene (TNT)	100%	Bioaugmented with *Pseudomonas putida* KP201 isolated from a TNT-contaminated site and biostimulated with 1% corn steep liquor. Amended with 0.1% tween 80	• 500-ml flasks. • Aerated (Not specified) • 30-day operation.	[42]
	20%		100%			
	30%		100%			
	40%		90%			
	50%		60%			
Contaminated soil from former coke plant	25%	Naphthalene	63%	Native microflora degradation. Abiotic removal was not tested and not considered. Effect of humic substances and soy lecithin as additive tested (results not shown here).	• 300-ml flasks. • No aeration (partially open reactors). • 150-day operation.	[46]
		2-Methylnaphthalene	56%			
		2-Ethenylnaphthalene	43%			
		Dimethylnaphthalene	73%			
		Dibenzofuran	49%			
		Fluorene	11%			
		Anthracene	49%			

Matrix	Soil % (w/v)	Contaminant [Concentration]	Removal efficiency	Remarks	Operational conditions	Reference
		Fluoranthene	36%			
		Pyrene	17%			
		11H-Benzo[B]fluorene	0%			
		Triphenylene	0%			
Aged oil-contaminated surface soil	50%	Anthracene	57%	Native soil microflora. Abiotic removal not considered	• 50-ml tubes. • Covered with sterilized tier gauze. • 30-day operation	[27]
		Fluoranthene	60%			
		Benzo(a)anthracene	59%			
		Anthracene	57%	Bacterial consortium isolated from contaminated soil. Abiotic removal not considered		
		Fluoranthene	62%			
		Benzo(a)anthracene	65%			
		Anthracene	66%	Fungal consortium isolated from contaminated soil. Abiotic removal not considered		
		Fluoranthene	77%			
		Benzo(a)anthracene	76%			
		Anthracene	55%	Mixed bacterial and fungal consortia isolated from contaminated soil. Abiotic removal not considered		
		Fluoranthene	71%			
		Benzo(a)anthracene	67%			
Marine sediment	20%	PAHs[1]	40%	Natural soil microflora. Abiotic removal not considered.	• 100-ml flask. • Open system (no aeration). • 35-d operation.	[26]
MGP contaminated sandy soil	50%	7 PAHs, 2-5 rings (Native microflora)	88%	Natural soil microflora.	• 2-l jar (1-l working volume). • Jars tilled twice per week for aeration. • 105-day operation.	[48]
		7 PAHs, 2-5 rings	93%	Inoculum A: Microbial consortium isolated from contaminated soil (identified)		
		7 PAHs, 2-5 rings	94%	Inoculum N: Enriched microbial consortium from contaminated soil (identified).		
Spiked contamination					•	
Sediment	5%	Phenanthrene	29%	Native microflora degradation. Volatilization was considered and quantified.	• 300-ml flasks. • Aeration 0.015 l/min. • 7-day operation.	[24]
	10%		41%			
	15%		31%			

Matrix	Soil % (w/v)	Contaminant [Concentration]	Removal efficiency	Remarks	Operational conditions	Reference
Loam sand (silt/clay fraction)	2%	Phenanthrene	100%	Bioaugmented with a mixed culture from a real PAH-contaminated soil. 10% of removal in abiotic control (considered not important)	• 250-ml flasks. • No aeration. • 100% removal was achieved in 2.92 d, 4.58 d and 5.83 d for 2%, 6% and 18% w/v slurry, respectively.	[16]
	6%		100%			
	18%		100%			
Loam sand (silt/clay fraction)	2%	Phenanthrene [25 mg/kg]	100%	Bioaugmented with a mixed culture from a real PAH-contaminated soil. 10% of removal in abiotic control (considered not important)	• 250-ml flasks. • No aeration. • 100% removal was achieved in 2.92 d, 2.92 d and 3.33 d for 25, 50 and 75 mg/kg of PHE initial concentration respectively.	[44]
	2%	Phenanthrene [50 mg/kg]	100%			
	2%	Phenanthrene [75 mg/kg]	100%			
Soil	33%	Naphthalene	100%	*Pseudomonas putida* used as pure culture. Modeling of volatilization and biodegradation contributions.	• 700-ml flask. • 0.1 l/min aeration. • 1-day operation.	[37]
Surface soil	33%	Phenanthrene (sterilized soil) [10 mg/kg]	69%	Immobilized *Zoogloea* sp.in slurry conditions tested as PAH degrader in combination (or not) with indigenous microflora from soil. Biocarrier pre-tested and selected.	• 150-ml flasks. • Aeration conditions not specified. • 5-day operation.	[23]
		Phenanthrene (sterilized soil) [50 mg/kg]	80%			
		Phenanthrene (sterilized soil) [100 mg/kg]	85%			
		Phenanthrene (sterilized soil) [200 mg/kg]	86%			
		Phenanthrene (unsterilized soil) [100 mg/kg]	85%			
		Pyrene (sterilized soil) [10 mg/kg]	56%			
		Pyrene (sterilized soil) [50 mg/kg]	61%			
		Pyrene (sterilized soil) [100 mg/kg]	74%			
		Pyrene (sterilized soil) [200 mg/kg]	47%			
		Pyrene (unsterilized soil) [100 mg/kg]	77%			
Agricultural mineral soil	25%	2,4-dichlorophenoxiacetic acid	92%	Acclimated mixed culture from seed reactor (20% v/v). Biostimulation with sucrose	• 100-ml flasks. • Open system (no aeration). • 14-day operation.	[51]
Marsh soil	10%	Dibenzotiophene	65-93 %	White-rot fungus *Bjerkandera*	• 5-l tank reactor, 4-l	[60]

Matrix	Soil % (w/v)	Contaminant [Concentration]	Removal efficiency	Remarks	Operational conditions	Reference
		Fluoranthene	41-81%	sp. BOS55 and biostimulated with glucose, peptone and BIII mineral medium. Gas outlet cooled down to minimize losses of volatile compounds	working volume. • Aeration 1 vvm*, stirring speed 250 rpm.	
		Pyrene	43-81%			
		Chrysene	21-31%			
Soil	50%	LMW PAHs[2] (2-3 rings)	>90%	Enriched heavy metal-tolerant consortium isolated from MGP contaminated site. Biostimulated with optimized mineral medium.	• 40-ml glass vials. • No aeration. Stirring rate: 175 rpm • 60-day operation	[53]
		Pyrene	77%			
		Benzo(a)Pyrene	48%			
Clay (Kaolin)	33%	n-Hexadecane (Air flow 0 vvm)	43%	Bioaugmented with *Pseudomonas* sp.	• 1-l glass reactor • Aeration varied (0, 2.5 and 5 vvm*). • 9-day operation. 5% abiotic removal.	[36]
		n-Hexadecane (Air flow 2.5 vvm)	54%			
		n-Hexadecane (Air flow 5 vvm)	20%			
Sandy loam soil	N.R.	2,4-dichlorophenoxyacetic acid [200 mg/kg]	100%	Sewage sludge as microorganisms' source	• 5-l glass bottle, working volume 1 l. Roller bioreactor (50 rpm). • Aeration 3.5 L/min. • 11-day operation.	[14]
		2,4-dichlorophenoxyacetic acid [300 mg/kg]	99%			
		2,4-dichlorophenoxyacetic acid [500 mg/kg]	97%			
Agricultural soil	N.R.	Diesel	>90%	Enriched microbial consortium isolated from a polluted site in an oil refinery		[56]

[1] PAHs: Polycyclic aromatic hydrocarbons: [2] LMW PAHs: Low molecular weight PAHs; *vvm: volume-volume-minute [$L^3.L^{-3}T^{-1}$]; N.R: not reported

Table 1.3 Removal efficiency, biodegradation rate and main operational conditions of bioreactors used in SBR operation

Matrix	Operation Phase	Soil % (w/v)	Pollutant	SRT(d)	Substrate Loading Rate ($mg.kg^{-1}.d^{-1}$)	Overall Biodegradation rate ($mg.l^{-1}.d^{-1}$)	Removal Efficiency	Remarks	Reference
Real Contamination									
Silt clay loam soil	-	40%	Diesel	10	2100	619.2	78.9%	• Biostimulated with Ammonia and phosphate to C:N:P 60:2:1. • 7% removal by volatilization.	[34]
				20	1050	350.4	79.7%		
				10	1921	696	83.4%		
				10	1255	693.6	81.8%		
				10	595	619.2	78.9%		
Soil	-	10.50%	Diesel	8	2650	250	96%	• Biostimulated with nutrient (C:N:P 60:2:1). • Biosurfactant production and foaming problems. • T: 23-25°C.	[22]
Soil	-	50% (w/w)	BEHP	3	2350	2310	70%	• Bioaugmented with enriched BEHP-utilizing microorganism. • Biostimulated with phosphate-ammonium medium. • Room temperature 20-22°C	[31]
				6	1067	1270	75%		
				10	665	780	78%		
				20	165	350	88%		
				25	96	280	86%		
				30	92	230	92%		
Sediment	2	10%	Total PAHs	70	0.30	1.66	55%	• Aeration (6.04e-4 m/s) (0.119 vvm). • No bioaugmentation in any phase • Phase 1: starting up • *Phase 4, biostimulated with lactose	[32]
			2-3 rings			0.37	70%		
			4 rings			0.66	64%		
			5-6 rings			0.63	43%		
	3	10%	Total PAHs	35	0.47	2.63	56%		
			2-3 rings			0.74	65%		
			4 rings			1.00	66%		
			5-6 rings			0.89	44%		
	4*	10%	Total PAHs	35	0.47	2.60	55%		
			2-3 rings			0.80	70%		
			4 rings			0.97	64%		
			5-6 rings			0.83	41%		
Spiked contamination									
Soil	-	4%	Pendimethalin	8.3	133200	N.R.	80%	• Bioaugmented with ETP-microflora	[39]
		5					95%		
		6.67%					91%		
		10%					89%		
		14.3%					82%		

Matrix	Operation Phase	Soil % (w/v)	Pollutant	SRT(d)	Substrate Loading Rate ($mg.kg^{-1}.d^{-1}$)	Overall Biodegradation rate ($mg.l^{-1}.d^{-1}$)	Removal Efficiency	Remarks	Reference
		20%					84%		
Soil	-	10%	Pyrene	5.60	120 (N.Ba.)	2000	33.3%	• Results are an average of 19th and 20th cycles.	[21]
					120	5400	90%	• Bioaugmentation with sewage,	
					240	8136	67.8%	• T: 30°C; pH 7.	
								• Decantation phase (anoxic)	
					360	9180	51%		
Soil	-	10%	Anthracene	6.7	100 (N.Ba.)	73	65.7%	• T: 30°C; pH 7.	[20]
					100	597	89.6%	• Decantation phase (anoxic)	
					200	1036	77.7%		
					300	994	49.7%		
Sediment	2	10%	Fluoranthene, Anthracene,	44	0.34-0.68	N.R.	90%	• No bioaugmentation.	[18]
	3		Pyrene and Chrysene	70	0.43-0.57	N.R.	> 90%	• Initial PAHs concentration was variated to avoid accumulation of chrysene (not completed biodegraded)	
	4			70	1-1.6	N.R.	>90%		
Soil	-	5%	Dodecane	1.8	5455	4739	47.4%	• Native microorganisms killed heating soil at 160 °C	[19]
					21818	15364	38.4%	• Bacterial consortium: Acinetobacter radioresistens, Bacillus subtilis, Pseudomonas aeriginosa. *Co-metabolism with glucose.	
					38182	19621	28%		
					54545	17460	17.5%		
					5455*	4595	46%		

N.R.: Not reported; N.Ba.: Not bioaugmented

3. Mechanisms involved in HOCs removal in slurry bioreactors

In this section, the key known mechanisms involved in the HOCs removal in slurry bioreactors are identified and explained. Figure 1.2 shows a simplified conceptual model of the main mechanisms taking place in a slurry phase bioreactor treating HOC contaminated soils or sediments reported in the literature. They can be separated in three type of processes, i.e., solid-liquid mass transfer, gas-liquid mass transfer and biodegradation processes. It is important to highlight that Non-Aqueous Phase Liquids (NAPLs) might be present in soil-slurry systems, meaning that liquid-liquid mass transfer should be considered. However, very few papers have addressed this issue and, therefore, this review does not include this process as a main mechanism. Alternatively, another solid or liquid phase can be added to the system (as it is done in two-phase partitioning bioreactors or TPPBs) [7]. In this case, new mechanisms including the new phase must be considered.

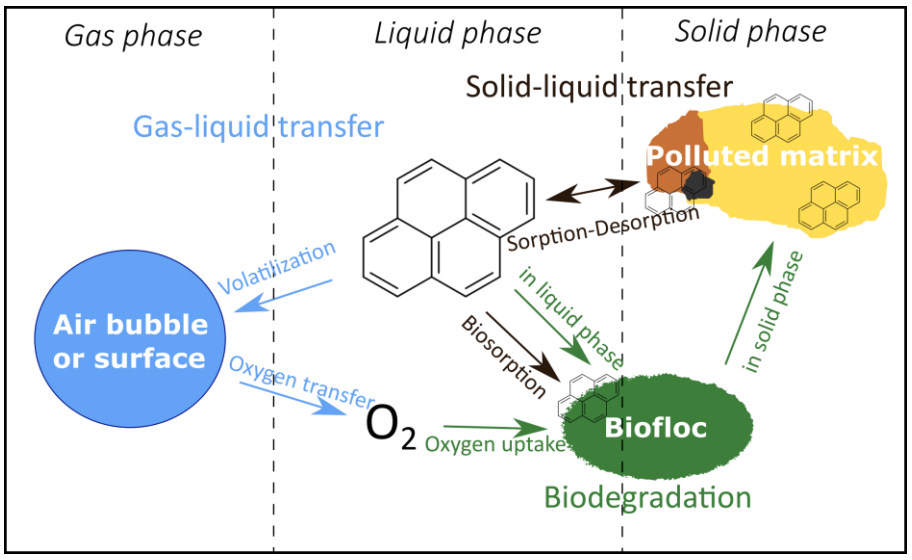

Figure 1.2 Simplified conceptual model of the main HOCs removal mechanisms in a slurry bioreactor treating contaminated soil or sediments

3.1. Mass transfer processes

In this section, the main studied mass transfer processes are explained and their importance in the soil-slurry bioreactor remediation process is described. The two key mechanisms identified are: solid-liquid mass transfer and gas-liquid mass transfer.

3.1.1. Solid-liquid mass transfer

Biodegradation of organic compounds in soil can only be achieved if the microorganisms have access to them (in other words, if pollutants are bioavailable) [61]. Considering that microorganisms are mostly able to consume pollutants in their soluble form, the release of HOCs from the solid matrix to the liquid phase play an important role in the contaminants removal [62]. Particularly, mass transfer related to sorption and desorption processes are important mechanisms to consider in the study of a soil-slurry bioreactor. This section explains the main solid-liquid mass transfer phenomena occurring in a slurry bioreactor.

3.1.1.1. Sorption and desorption

Adsorption is a surface phenomenon in which the molecules of a substance in gas, liquid or diluted phase (called adsorbate) adhere to an interface due to surface forces, increasing their concentration on it. Desorption is the opposite mechanism in which the adhered molecules are released from the interface [63]. In the case of slurry bioreactors, these processes occur at the solid/liquid interface between soil components and water, represented by the solid surface. In general terms, for soil-slurry systems, the term “sorption” is more used than the term “adsorption”, since the first includes not only the surface adhesion of pollutants, but also other types of “retention” processes, such as slow pollutant diffusion within nanopores in soil particles or even absorption in amorphous and condensed organic matter materials that might be present in natural and contaminated soils [1,64–67]. In this context, “desorption” is not only the opposite mechanisms to adsorption, but also any release of pollutants from the solid matrix to the liquid phase.

For HOCs, desorption rate from the soil to the aqueous phase may be low compared to other compounds, even at high sorbed phase concentration. The low HOC availability due to slow desorption, in turn, can determine the overall rate of bioremediation [61]. Therefore, sorption and desorption of HOCs sorbed on soils, sediments or some of their constituents have been widely investigated.

To study sorption-desorption phenomena, the main characteristics to consider are those related with the soil/water interface, such as the specific surface area (SSA), the nature of the active sites available for adsorption (associated to the type of adsorbent), the pollutant nature (ionic, polar, non-polar, amphiphilic), among others. Also, particle related characteristics such as intra- and interparticle porosity, particle size and tortuosity influence the overall phenomenon. Finally, temperature, pH, soil content and mixing conditions are important parameters that affect these processes [1,68].

Soils and sediments are heterogeneous materials typically separated by the particle size of their components in three fractions, i.e. sand (between 2000 µm and 63 µm), silt (between 63 µm and 2 µm) and clay (< 2 µm) [69]. In addition, all these fractions may contain organic matter in different forms. Therefore, it is interesting to observe HOCs' affinity with each fraction separately to understand their role in sorption and desorption mechanisms. Figure 1.3 shows a representation of the different places on which HOC molecules can be sorbed by the different soil components of the soil, as well as some possible interactions between the soil components.

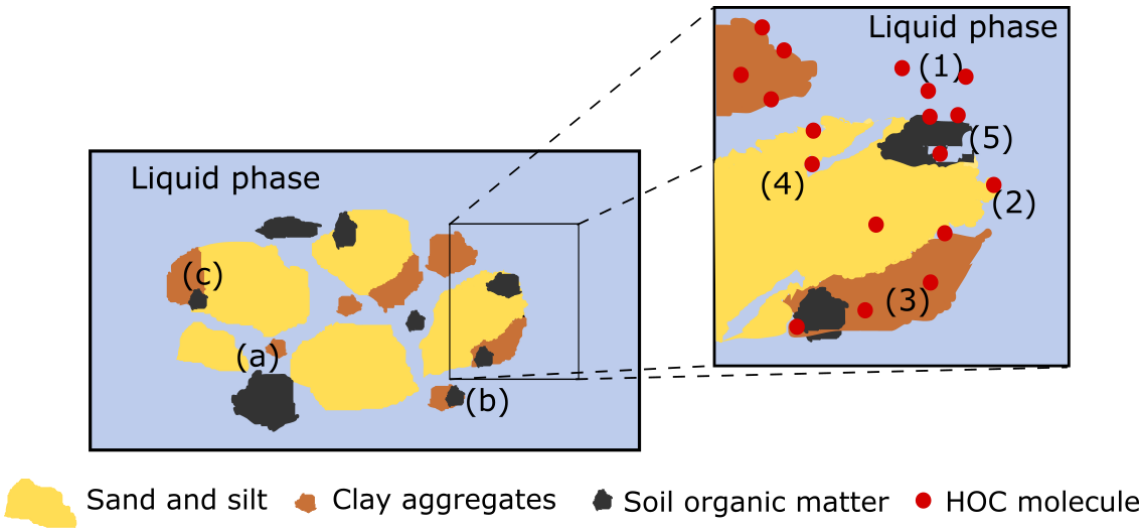

Figure 1.3 Interactions between soil components and HOC sorption mechanisms in soil: (a) individual particles, (b) clay-SOM aggregates, (c) sand-clay-SOM aggregates; (1) HOC in liquid phase, (2) external surface sorption, (3) clay micropores sorption, (4) mineral pores sorption, (5) SOM sorption

Regarding HOC-soil particle interactions, two distinctive types of sorption can be identified: HOC-mineral surface and HOC-soil organic matter. Organic compounds can be adsorbed onto mineral surfaces due to possible interactions with iron oxides and other mineral components, as showed in Figure 1.3 (mechanism 2 and 3). According to Lützow et al. [70], these interactions include ligand exchange, polyvalent cation bridges, weak interactions (such

as van der Waals forces and hydrogen bonds) and complexation. However, soil fractions may interact differently with HOCs depending on their particle characteristics. For instance, clays are a group of minerals with a wide range of SSA (~10^6 cm^2/g for kaolinites, ~10^8 cm^2/g for smectites) [71]. On the other hand, sandy materials usually have SSA values much lower than clays (~10^3 cm^2/g). This difference is attributable to both the particle size and the spaces between clay sheets, which constitute micropores wherein adsorbents can diffuse and be fixed by capillary condensation [72]. Müller et al. [73] highlighted the impact of this difference by comparing the adsorptive capacity of different mixtures of soil constituents for selected PAHs and found that the presence of clay increased about ten times the PAH solid concentration at equilibrium compared to sandy materials alone. Additionally, silt and clay (also called soil fine fraction) usually concentrate the largest part of sorbed and bioavailable contaminants in HOC polluted sediments and soils [64,68]. Therefore, as explained above, slurry bioreactors are used to treat mainly this fraction of soils or sediments.

Soil or sediment organic matter (SOM) have a big influence on sorption and desorption mechanisms. Cui et al. [74] and Oen et al. [75] demonstrated that there is a correlation between the PAHs mass content and the total organic carbon (TOC) in each fraction for different types of sediments and concluded that organic carbon controls the distribution of PAHs among them. Indeed, SOM particles are present in soils and sediments in all sizes, from plant or animal debris to single macromolecules, such as proteins and lipids [76]. This gives a wide range of characteristic of SOM as adsorbent that should be considered for each type of soil. For example, in the liquid phase, humic-like substances are able to form structures similar to membranes or micelles with an hydrophobic inner side, in which HOCs can be retained [76,77]. The presence of anthropogenic altered organic matter, such as kerogen, coal or black carbon, in contaminated soil may lead to the accumulation of high concentrations of organic pollutants due to hydrophobic interactions [64]. Thus, apparent diffusion in micro- and mesoporous soil organic matter is an important aspect to consider in sorption and desorption studies. Additionally, mineral-SOM aggregates can be formed (interactions b and c in Figure 1.3), in which HOC can diffuse and sorbed, reducing their bioavailability. Also, these interactions can reduce the number of available active sites for HOC adsorption compared to soil components alone.

To study the sorption and desorption mechanisms of HOCs on soil, several models have been developed. Both equilibrium and kinetic models are necessary to understand the global mass transfer process of sorption-desorption. The most used equilibrium models are called sorption

or desorption isotherms and relate HOCs concentrations in liquid phase and solid phase at constant temperature and pH. The most used sorption isotherms are summarized in Table 1.4.

Table 1 4 Most used isotherm models for HOCs sorption on soil

Model	Equation	
Linear partition	$q_e = k_D C_e$	(1)
Langmuir	$q_e = \frac{q_{max} k_L C_e}{1 + k_L C_e}$	(2)
Freundlich	$q_e = k_F {C_e}^{1/n}$	(3)
Dual-mode site limited	$q_e = k_D C_e + \frac{q_{max} k_L C_e}{1 + k_L C_e}$	(4)
Dual-mode multi-site	$q_e = k_D C_e + k_F {C_e}^{1/n}$	(5)

where q_e is the pollutant sorbed concentration [$M.M^{-1}$] and, C_e, is the pollutant liquid concentration at equilibrium [$M.L^{-3}$]

k_D, is the linear partition coefficient [$L^3.M^{-1}$].

q_{max}, is the maximum adsorption capacity in a monolayer [$M.M^{-1}$] and, k_L, is the Langmuir sorption constant [$L^3.M^{-1}$].

k_F, is the Freundlich sorption constant [$M.L^{-3}M\ {}^{n}L^{3n}$] and, n, is the exponent constant in Freundlich equation.

At low concentration, the linear partition model (Eq. 1) usually fit well to isotherms in systems with presence of amorphous organic matter and mineral surfaces exposed to water [1]. Isotherms fitted by Langmuir model (Eq. 2) correspond to sorption in a monolayer (surface adsorption) with q_{max} as maximum adsorption capacity (when all active sites of the monolayer are filled). Freundlich isotherm (Eq. 3) is the most widely model used because it accounts for the deviations of linear isotherms introduced by sorption in micropores in clay or SOM and by multilayer adsorption [1,78]. Dual-mode isotherms (Eq. 4 and 5) are developed for systems where external surface sorption is differentiated from sorption in meso- or micropores. In this case, the first is usually modeled as a linear isotherm and the latter as Langmuir or Freundlich isotherm [79]. However, for HOC-soil system, they are currently not often used.

Table 1.5 shows the parameter values of linear partition isotherm and Freundlich isotherms in selected papers. As expected, at equilibrium, linear partition coefficient in systems using SOM as adsorbent is higher than in those using mineral surfaces. This can be explained by the higher affinity of HOCs to SOM compared to the affinity to minerals, due to hydrophobic interactions and higher availability of active sites. This is also true for the Freundlich sorption constant (k_F), for which distinctions between clayey and sandy soils can also be established (SOM > clay > sand). Moreover, even if only one compound is considered (e.g.

Phenanthrene) both coefficients in Freundlich isotherm are within a wide range of values (k_F: [0.21; 31.2] (mg.kg^{-1})/(mg.L^{-1})^n; n: [0.45, 1.56]). This is due to the different characteristics of soils or sediments, their composition, type and size of organic matter present in the soil and the operational conditions (particularly temperature).

Additionally, mineral affinities and hydrophobic interactions may cause some irreversible effects on the sorption-desorption process. Several works have demonstrated the hysteresis of the isotherms of HOCs sorbed on soil constituents and they attribute it to several factors: (i) sorption on dissolved organic carbon or clay-SOM colloids; (ii) diffusion and irreversibility in sorption on SOM [66]; and (iii) non-equilibrium conditions at the end of isotherm experiments due to slow diffusion in micropores [80]. The hysteresis index (HI) represents the measurement of the difference between equilibrium sorption and desorption solid concentration of pollutant evaluated at the same equilibrium liquid concentration and conditions and it is calculated as follows:

$$HI = \left. \frac{{q_e}^d - {q_e}^s}{{q_e}^s} \right|_{T,C_e} \quad (6)$$

Huang and Weber [81] investigated the HI for a variety of SOM and they found that SOM can contribute significantly to sorption-desorption hysteresis for phenanthrene. However, it highly varies depending on the type of SOM studied (HI ranging from 0.02 to 1.48 at different equilibrium concentration levels). The explanation of such variation comes from the heterogeneity of the SOM. HOCs can adsorb and diffuse freely on SOM macromolecules, and, in turn, these macromolecules can accommodate HOC molecules in flexible, amorphous matrices characterized by highly oxidized regions. In fact, they also found positive linear correlations between the "oxygen to carbon ratio" of the SOM in relation with the Freundlich n parameter and the hysteresis index (HI) using phenanthrene as adsorbate.

For the kinetic study, Geerdink et al. [82] explain that desorption rate from the soil phase in a slurry bioreactor can be expressed by characterizing the contribution of each soil component in batch reactor as follows:

$$r_{des} = f_{SOM}\frac{dC_S}{dt} + f_{Clay}\frac{dC_S}{dt} + f_{Sand}\frac{dC_S}{dt} \quad (7)$$

where r_{des} is the desorption rate [M.M^{-3}.T^{-1}], m is the soil or sediment mass [M], C_S is the concentration of the sorbed pollutant [M.M^{-1}], t is the time [T], f_{SOM}, f_{Clay} and f_{Sand} are the

fractions of soil organic matter, clay and sand, respectively. In this case, silt is considered in the clay fraction due to the similar behavior of these two soil constituents regarding desorption mass transfer. Interactions among the individual contributions are neglected.

In general, desorption kinetics of HOCs from soil matrix to aqueous phase is modelled by a first-order model, as follows:

$$r_{des} = -k_{des} C_S \quad (8)$$

where k_{des} is the kinetic constant of desorption [T^{-1}].

However, other theoretical models have been developed. One of them is the diffusion model, which is based on Fick's second law. This model, expressed in radial coordinates and assuming that soil is represented by spherical particles, can be written as:

$$\frac{\partial C_S}{\partial t} = D_e \left[\frac{\partial^2 C_S}{\partial r^2} + \frac{2 \partial C_S}{r \partial r} \right] \quad (9)$$

where r is the soil particle radius [L] and, D_e, is the effective diffusion coefficient [$L^2\ T^{-1}$]. D_e can be defined in several ways, according to the considerations and simplifications made on the model development. The most common assumption is that sorption and desorption equilibrium is given by a linear model. In that case, effective diffusion coefficient is constant and can be defined as follows:

$$D_e = \frac{D \epsilon}{k_D (1 - \epsilon) \rho_s} \quad (10)$$

where ϵ is the particle porosity [$L^3.L^{-3}$] and ρ_s is the particle density [$M.L^{-3}$].

However, this simplification is not always valid, since diffusion can depend also on the soil sorbed concentration [79]. Moreover, as explained, soil composition considerations should be made. For instance, Chen et al. [86] found that, for phenanthrene desorption in sediments, the higher the content of both, clay and organic matter is, the lower the effective diffusion coefficient is. Therefore, soil content and soil composition are key parameters to consider in this kind of systems.

Table 1.5 Parameters for linear and Freundlich isotherms in selected papers

Isotherm model	Adsorbent	Pollutant	Parameters		Reference
Linear partition			k_D (l.kg^{-1})		
	Clay	Hexachlorohexane	2400		[82]
	SOM		9900		
	Sediment	1,2,4-trichlorobenzene	265		[65]
	Sediment	1,4-dichorobenzene	87		
	Soil	1,2,3,4-tetrachlorobenzene	58		
	Soil	Pentachlorobenzene	239		
	Sediment	1,2,3,4-tetrachlorobenzene	418		
	Sediment	Pentachlorobenzene	1560		
	Sediment	1,2,3,4-tetrachlorobenzene	1220*		
	Sediment	1,2,3,4-tetrachlorobenzene	418 *		
	Sediment	Phenanthrene	240 *		[24]
	Loan sand (silt/clay fraction)	Phenanthrene	57.1 *		[16,38]
Freundlich			k_F (mg kg^{-1}).(mg L)$^{-n}$	n^{-1}	
	Different types of SOM	Phenanthrene	[2.26; 33.97]	[0.45; 0.92]	[81]
			[2.03; 37.96] *	[0.51; 1.02] *	
	Four different soil and sediments	Phenanthrene	1.26	0.727	[83]
			0.87	0.89	
			0.83	0.76	
			0.94	0.73	
	Dark limestone	Phenanthrene	At 20 °C		[80]
			25.03	0.48	
			At 40°C		
			19.49	0.53	
	Triassic limestone	Phenanthrene	At 20 °C		
			13.07	0.75	
			At 40 °C		
			8.25	0.83	
	Sediment in fresh water	Phenanthrene	17.12	0.81	[66]
			18.73*	0.78*	

Isotherm model	Adsorbent	Pollutant	Parameters		Reference
	Soil in fresh water	Phenanthrene	21.76	0.66	
			29.96*	0.57*	
	Sediment in saline water	Phenanthrene	19.30	0.79	
			19.69*	0.78*	
	Soil in saline water	Phenanthrene	27.94	0.61	
			31.19*	0.58*	
	Pahokee peat	Phenanthrene	6310†	0.66	[84]
			6457*,†	0.66*	
	Lignite	Phenanthrene	19055†	0.83	
			18197*,†	0.82*	
	Anthropogenic soil	Phenanthrene	1995†	0.95	
			1995*,†	0.94*	
	Mineral soil	Phenanthrene	166†	0.77	
			166*,†	0.76*	
	K-hectorite	Phenanthrene	140.5†	1.56	[85]
	Na-hectorite	Phenanthrene	116.6†	1.31	
	Different types of Ca-Montmorillonite	Phenanthrene	[22.18; 50.36] †	[1.01; 1.18]	
	Different types of K-montmorillonite	Phenanthrene	[17.46; 62.16] †	[0.96; 1.05]	
	Different types of Na-montmorillonite	Phenanthrene	[14.93; 49.68] †	[0.82; 0.96]	
	Quartz	Phenanthrene	0.21	1.04	[73]
		Pyrene	0.36	0.85	
	Goethite-coated quartz	Phenanthrene	0.31	1	
		Pyrene	1.35	0.93	
	Quartz-montmorillonite	Phenanthrene	2.46	1.13	
		Pyrene	3.43	0.81	
	Sand	Naphthalene	0.001	0.85	[55]
	Clay		0.003	0.75	
	SOM		0.06	1.64	
	Artificial soil		0.004	0.69	

* Parameters for desorption isotherms; † Values correspond to the modified Freundlich constant ($K'_F = K_F S_{scl}^{1/n}$; where S_{scl} is the subcooled liquid solubility [85])

It is also possible to consider two types of desorption for the same compound in the same matrix for modeling. First, a rapid desorption from the external mineral and organic surfaces. Then, a slower desorption in which pore size, intraparticle porosity and tortuosity are considered in the apparent diffusion of the molecule leaving the soil particles [74,87]. Both steps can be modelled using first-order equations in a "two-box model", as follows:

$$r_{des} = -k_{Rapid} C_S - k_{Slow} C_S \quad (11)$$

where k_{Rapid} is the kinetic constant for rapid desorption [T^{-1}] and k_{Slow} is the kinetic constant for slow desorption [T^{-1}].

Additionally, a third parameter can be added to Eq. (11) to normalize the two fractions and to stablish the contribution of each one of them to the total desorption rate.

$$r_{des} = -\phi_R k_{Rapid} C_S - (1 - \phi_R) k_{Slow} C_S \quad (12)$$

where ϕ_R is the fraction of soil with a rapid desorption kinetics.

Table 1.6 shows applied examples of these models in selected publications retrieved from the literature. The kinetic parameters depend on both the pollutant and the solid matrix physicochemical characteristics. Therefore, even for the same contaminant, the range of values can be wide, considering organic matter content, clay content and mixing conditions. Moreover, some studies show the difference of kinetic behaviors on sorption and desorption, which is generally explained by the same mechanisms producing isotherm hysteresis, but not only.

Likewise, desorption kinetics is strongly influenced by the aging of the contamination. Usually, aged contamination has lower kinetics parameters due to: i) a more pronounced diffusion of pollutants in the interior of soil particles, which causes a retention of pollutants within the solid matrix longer time [88]; and ii) a condensation of non-aqueous phase liquids possibly present in the contaminated soil into a "hard" glassy carbonaceous material which traps the pollutants avoiding their release to the aqueous phase [1,64,68]. Reid et al. [89] detail this issue from the point of view of the pollutant bioavailability.

Table 1.6 Parameters for desorption kinetic models in selected papers

Model	Adsorbent	Pollutant	Parameters			Reference
First order			k_{des} (d^{-1})			
					Biosurfactant concentration	
	Soil	Phenanthrene	0.06		0 mg/L	[45]
			0.15		400 mg/L	
			0.18		700 mg/L	
					Initial concentration	
	Sandy loam soil	2,4-dichlorophenoxyacetic acid	0.47		200 mg/kg	[14]
			0.42		300 mg/kg	
			0.2		500 mg/kg	
	Artificial spiked soil	Naphthalene	0.12			[55]
First order two phases, two parameters			k_{Rapid} (d^{-1})		k_{Slow} (d^{-1})	
	Loam sand (silt/clay fraction)	Phenanthrene	215.04		20.4	[16,38]
First order Two phases, three parameters			ϕ_R	k_{Rapid} (d^{-1})	k_{Slow} (d^{-1})	
	Young topsoil	Phenanthrene	[0.299;0.59]	[0.32;7.3]	[4.2×10^{-3}; 1.48×10^{-1}]	[90]
	Geological old sediment		[0.144;0.367]	[0.0289;0.18]	[8.59×10^{-4}; 2.92×10^{-3}]	
	Sandy soil		[0.26;0.343]	[0.134;0.332]	[1.38×10^{-3}; 2.63×10^{-3}]	
	Real contaminated Sediment	Pyrene	0.29	1.24	0.021	[74]
	Real contaminated Sediment		0.31	4.30	0.019	
Diffusion model			D_{eff} (cm^2/s)			
			Sorption			[65]
	Sediment	1,2,4-trichlorobenzene	3.3×10^{-10}			
	Sediment	1,4-dichorobenzene	1.0×10^{-9}			
	Soil	1,2,3,4-tetrachlorobenzene	1.0×10^{-9}			
	Soil	Pentachlorobenzene	2.5×10^{-10}			
	Sediment	1,2,3,4-tetrachlorobenzene	5.0×10^{-11}			
	Sediment	Pentachlorobenzene	8.3×10^{-11}			
			Desorption			
	Sediment	1,2,3,4-tetrachlorobenzene	8.3×10^{-11}			
	Sediment	1,2,3,4-tetrachlorobenzene	1.3×10^{-10}			

3.1.1.2. Biosorption

Another mass transfer phenomenon that may be considered is the adsorption of HOCs onto biomass (or biosorption). Since mixed cultures are usually responsible for the biodegradation in soil slurry systems, HOCs can be sequestrated by non-degraders and decrease the efficiency of pollutants removal. Other substances present in the bioflocs or biofilms structures (such as extracellular polymeric substances or EPS) can also act as sorbents for HOCs due to the presence of an hydrophobic surface [91,92]. Whereas this mechanism has not been properly addressed in soil-slurry systems, in water and wastewater treatment it has been extensively studied for both heavy metals and organic pollutants and even considered as a separated treatment for their removal [93].

In general, biosorption is believed to be a rapid process due to the HOC affinity to the cell walls, and compared to the other mechanisms studied in the present work, equilibrium is reached almost instantaneously (2-3 h) [94]. Besides, it is important to notice that the biosorption capacity of a specific bacterial species or strain cannot be correlated with its degradation capacity for a given contaminant [95]. Biosorbed HOCs and HOC by-products can constitute a source of error in the bioreactor mass balance and the total removal calculations when not considered properly.

3.1.1.3. Solubilization and surfactant use

Depending on the origin, level and aging of the soil or sediment contamination, some HOCs may exist in solid or semisolid phases. Hence, solubilization may exist as a mass transfer process in soil-slurry systems [55]. However, due to the difficulty of differentiating this phenomenon from sorption-desorption, it is often included in an overall solid-liquid transfer mechanism also called “desorption”. Moreover, the separation of these solid organic phases can be intricate or, in some cases, even impossible, which complicates their characterization and the study of their individual impact on the process. Despite the development of some physical techniques to achieve separation [68], overall solid-liquid mass transfer is still the most used approach.

In addition, to improve the overall transfer rate, many researchers have considered the supplement of surfactants. These substances have the ability of creating micelles. Micelles are aggregates of colloidal dimensions [63] which, in aqueous phase, typically have a hydrophilic outside and a hydrophobic inside. HOCs can be mobilized to the interior part of these structures, accelerating both desorption and solubilization mechanisms, and therefore, HOCs’

bioavailability. Despite this fact, the use of surfactants has produced contradictory results regarding the improvement of the bioremediation process [96–98].

Some surfactants, particularly those with cationic functional groups, have been found to be toxic for microorganisms and, hence, inhibitory of pollutant biodegradation, even at low concentrations [99]. This problem has led to privilege the use of anionic or nonionic surfactants. Table 1.8 shows the enhanced biodegradation due to the use of specific surfactants in soil or sediment slurry systems. Paradoxically, whereas some researchers have found a higher biodegradation rate using nonionic surfactants [35,40,43], some others have noticed no significant enhancement by adding them [14,25], from which it is possible to infer that increasing apparent solubility does not necessarily mean an enhancement of the pollutant bioavailability.

Furthermore, studies have found some undesired effects of the surfactant addition. The explanation seems to lie in two different mechanisms: on one hand, micelles formed by surfactants can trap and isolate pollutants from microorganisms by forming a barrier and decreasing their bioavailability [44]; on the other hand, association between surfactants and mineral or organic phases of the soil can cause pollutants retention on the sorbed phase [97]. Moreover, surfactant sorption on soil components decrease their availability to form micelles, which means that the presence of soil limits their HOC solubilization efficiency. For instance, Ahn et al. [100] studied the effect of SOM content on the solubilization of phenanthrene by Triton X-100 and found that using a soil with 10 times higher SOM content, apparent pollutant concentration was reduced by half.

Additionally, Lippold et al. [101] studied the combined effect of five surfactants (the cationic dodecyltrimethylammonium bromide and hexadecyltrimethylammonium bromide; the anionic sodium dodecylsulfate and sodium dodecylbenzenesulfonate; and the non-ionic dodecyl-b-D-glucopyranoside) and dissolved organic matter on PAH solubility. They found that these compounds have a very limited influence on it. Moreover, ionic surfactants have a negative effect neutralizing the dissolved organic matter electric charges and decreasing PAH solubility. In any case, the final concentration of the surfactant in the reactor will define the positive or negative effect of its addition on the slurry system [99].

Also, some microorganisms have developed strategies to make HOCs bioavailable either by producing emulsifiers or biosurfactants [102] or by having a hydrophobic cell surface themselves, which attracts the HOCs to be consumed [103]. Some researchers have developed

methods to produce and isolate biosurfactants in order to use them as amendments for slurry bioreactors [45,49]. Although some interesting results have been obtained from their use in soil-slurry systems (Table 1.7), very few works have addressed this topic, mainly at laboratory scale. Further research is needed on this subject.

Table 1.7 Enhancement of biodegradation by nonionic surfactants in soil slurry bioreactors

Matrix	Pollutant [Concentration]	Surfactant [Concentration]	Removal Unamended	Removal Amended	Enhanced Removal	Remarks	Ref.
Real Contamination							
Soil	PAHs and VOCs [10972.9 mg/k]	Tween 80 [5.93 ml/64L]	Addition of Tween 80 did not show any significant improvement in degradation			Bioaugmented with *Pseudomonas fluorescens*, *Pseudomonas stuzeri* and an *Alcaligenes* specie.	[25]
Former MGP* soil	PAHs	Brij 30 [5 mg/kg]	Enhanced desorption kinetics, but not enhanced PAHs biodegradation			Native soil microflora	[43]
WIP** soil	PAHs	Biosurfactant produced by *P. aeruginosa* [3 g/kg]	57%	86.50%	29.50%	Enriched culture from soil	[45]
Spiked contamination							
Sand	Naphthalene	Brij 30	Not tested	>95%	-	Mixed cultured acclimatized to PHE from municipal wastewater facility	[35]
Clay	Phenanthrene		Not tested	>90%	-	Other nonionic surfactants tested, but only in aqueous phase	
Surface playground soil	Phenanthrene [13 mg/kg]	Triton X-100 [3g/L]	100%	73%	-27%	Mixed culture isolated from PAH-contaminated soil	[44]
		[10 g/L]	100%	31%	-69%		
Clay (Kaolin)	TNT [1000 mg/kg]	Tween 80 [4.92 g/L]	5%	85%	80%	Bioaugmented with *P. putida*. Biostimulated with glucose. Several conditions tested.	[40]

*MGP: Manufactured gas plant; **WIP: Wood impregnation plant

3.1.2. Gas-liquid mass transfer

The gas phase plays an important role in the aerobic biodegradation process. Aerobic slurry bioreactors usually are provided with enough air flow to maintain aerobic conditions and avoid oxygen to be a limiting factor. However, many studies assume aeration to be enough in their systems and do not measure its real impact on their processes. Furthermore, when volatile or semi-volatile HOCs are present in the system, volatilization becomes an important

removal mechanism, which is neglected in most cases. Figure 1.4 shows the processes of oxygen transfer and volatilization explained by the two-film theory, which is the most commonly used model due to its simplicity and to its good fitting for this transfer phenomena in reactors [104]. This theory proposes that near the interface between the gas-liquid interphase thin films are formed, with length δ_L and δ_G for the liquid film and the gas film respectively, in which there is a concentration gradient of the transferred compounds.

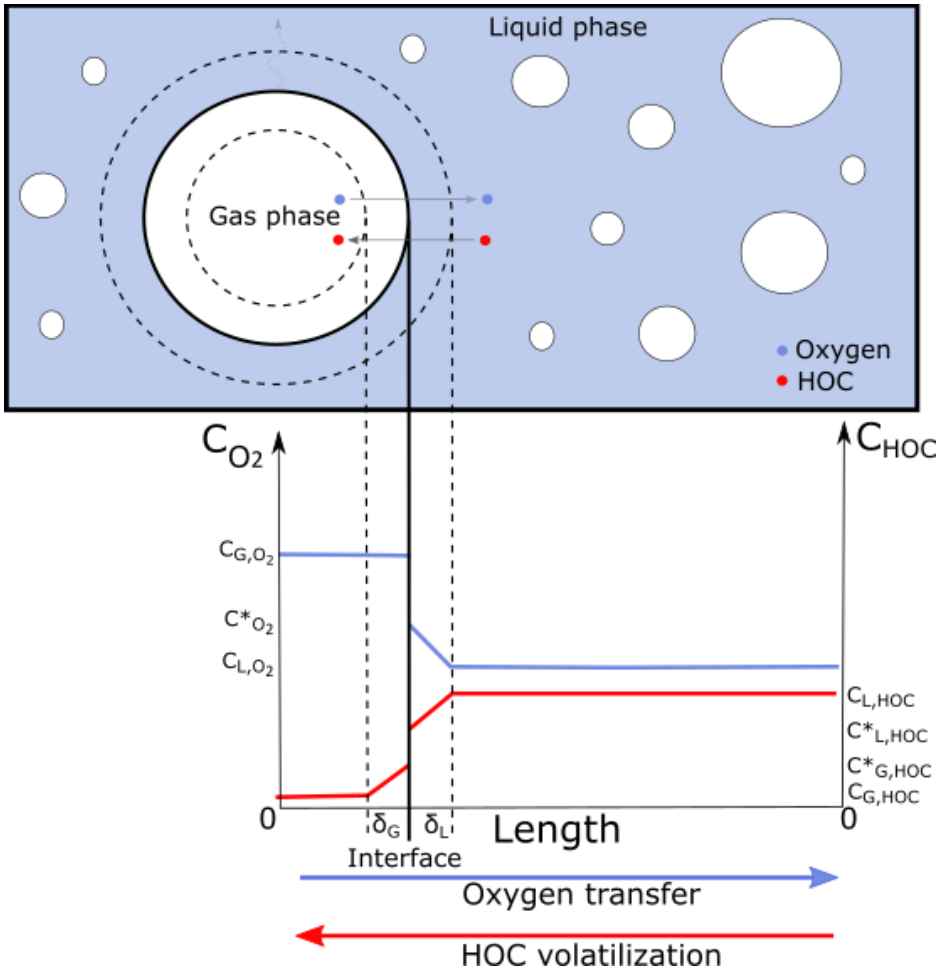

Figure 1.4 Two film model for gas-liquid mass transfer in a soil slurry bioreactor

In each film, the compound flow, by Fick's first law, is assumed to be linear and is given by the next equations:

$$\dot{N}_L = k_L a(C_L - C_L{}^*) \quad (13)$$

$$\dot{N}_G = k_G a(C_G - C_G{}^*) \quad (14)$$

where the subscripts L and G stand for liquid phase and gas phase, respectively, $\dot{N}$ is the compound's volumetric transfer rate [$M.L^{-3}.T^{-1}$], k is the compound transfer constant [$L.T^{-1}$],

a is the specific interfacial area [$L^2.L^{-3}$], C the bulk concentration, C^* the equilibrium concentration at the interface [$M.L^{-3}$] and V is the total volume of the system [L^3]. If there is no accumulation of compounds in the layers, the next assumption can be made:

$$\dot{N}_L = \dot{N}_G = \dot{N} \quad (15)$$

Moreover, k_L and k_G are defined as follows:

$$k_L = D_L/\delta_L \quad (16)$$

$$k_G = D_G/\delta_G \quad (17)$$

where D_L and D_G are the diffusivities of the compound in the liquid phase and the gas phase respectively [L^2T^{-1}].

For diluted solutions, when the compound reaches the interface, the change of concentration from one phase to the next is given by an equilibrium process explained by Henry's law and it can be represented by the next equation:

$$C_L{}^* = H_C C_G{}^* \quad (18)$$

where H_C is the dimensionless Henry's law constant.

3.1.2.1. Oxygen transfer

The required dissolved oxygen concentration (DO) for achieving pollutant biodegradation in soil slurry systems is reached, usually, by aeration. Depending on the type of reactor, air can be introduced superficially by simple mechanical mixing or by spargers or diffusers located on the bottom of the reactor. If oxygen is not provided at an adequate rate, it becomes a limiting factor, affecting and controlling the biodegradation process. Garcia-Ochoa and Gomez [104] explained that the oxygen transfer rate (OTR) depends on the physical properties of the medium (viscosity, density, and superficial tension), geometric parameters, operational conditions (air superficial velocity, stirring rate), physicochemical properties (pH, conductivity, etc.) and the presence of solids and colloidal compounds.

For oxygen transfer, the diffusion of oxygen in the (air) gas phase is considered much faster than the diffusion in the liquid phase, meaning that the gas phase offers no resistance to the transfer, the gradient in the gas layer is almost inexistent and the overall oxygen transfer rate

is controlled by the liquid film. Then, the oxygen mass transfer rate from gas phase to liquid phase in a slurry bioreactor can be expressed as follows:

$$OTR = k_L a\left(C_{L,O_2}{}^{*} - C_{L,O_2}\right) \quad (19)$$

where OTR is the oxygen transfer rate [$M.L^{-3}.T^{-1}$], $k_L a$ is defined as the volumetric oxygen mass transfer coefficient [T^{-1}], due to the difficulty of measuring or estimating the volumetric area, a. The oxygen mass transfer has been well studied for water and wastewater treatment systems, where the mass transfer coefficients have been investigated as function of different operational conditions to optimize the process. They depend on several parameters such as bubble diameter, gas hold up and exposure time [104–106].

The effect of solids addition on the oxygen transfer has been addressed in the literature, but very poorly in the context of soil-slurry reactors. It seems to depend on the solid characteristics such as particle size, density, hydrophobicity and concentration [107,104]. The presence of solids can lead to: (i) a steric effect that reduces the transfer area available, due the tendency of hydrophobic surfaces to adsorb at the G-L interface; (ii) a buoyancy effect, modifying the bubble rising velocity and the gas hold-up by changing the density of the suspension; (iii) an alteration of the apparent viscosity of the suspension, which can cause a possible bubble size growth (by bubble coalescence and bubble growth time increase) and a rising velocity decrease [105]. Furthermore, Mena et al. [108] explain that particle size plays an important role on the determination of positive or negative effects of solids presence on oxygen transfer. Decreasing expanded polystyrene PS particles diameter from 1100 µm to 590 µm caused, in general, a reduction of the oxygen transfer coefficient. Very fine expanded PS particles (0.1 µm) act as contamination on the bubble surface, decreasing the transfer area. However, up to a certain solid loading (3% vol.), 9.6-µm hollow glass spheres increased the transfer coefficient by increasing the surface renewal and turbulence of the system and by avoiding bubble coalescence.

Therefore, it is important to consider all these effects in the study of oxygen transfer in soil-slurry systems. The only investigation regarding this topic found in the literature was made by Woo and Park [109]. According to them, different sandy and silty soils caused a similar $k_L a$ coefficient reduction compared to clean water at different solid concentrations, mainly due to bubble coalescence. Besides, SOM content had a very limited effect, regardless its proportion in soil (1.1 - 14.5%). On the other hand, clayey soil (55% of clay content) decreased dramatically the global transfer coefficient because of an apparent viscosity increase. This

change was noticed even at solid concentrations in slurry as low as 2% w/v and the decrease was as large as 40% at 5% w/v of soil content. Due to the importance of this mechanism for pollutant biodegradation, further investigation is needed.

3.1.2.2. Pollutant volatilization

HOC mass losses due to volatilization may be important in slurry bioreactors and this transfer process can even be considered as the main abiotic removal mechanism for some light compounds [110]. Moreover, competition between volatilization and biodegradation is significant for volatile and semi-volatile substances in aqueous systems. Nevertheless, many of the research articles included in this review do not consider at all volatilization as a possible removal mechanism of HOCs for a slurry bioreactor. Neglecting this mechanism will most likely lead to miscalculations in the general mass balance of the system and overestimations of the pollutant removal by biodegradation. HOCs can be transferred to the gas phase by both surface and air bubbles from the spargers [111]. This means that aeration and agitation parameters should be adjusted in order to regulate the competition in soil slurry bioreactors [37].

For volatilization modeling using the two-film theory, the pollutant concentration in the gas phase is typically assumed as zero, meaning that the kinetic model can be written as a first order equation, as follows:

$$r_{vol} = -k_{vol} C_L \quad (20)$$

where r_{vol} is the volatilization rate [$M.L^{-3}.T^{-1}$], k_{vol} is the gas/liquid transfer constant or volatilization constant [T^{-1}]. Gas resistance phase is usually not considered for volatile compounds, due to the high mass transfer coefficient in the gas phase. However, some HOCs are considered to have low volatility or to be “semi-volatile” compounds, which means that the gas resistance can be equally important as the liquid resistance or can even control the entire volatilization process.

Lewis [25] explained that, during their bioslurry treatment experiments, volatilization of some volatile and semi-volatile PAHs occurred mainly at the beginning of the treatment due to their higher concentration at this stage. Also, these (generally light) compounds are biologically removed relatively faster from the slurry bioreactor, and after some time no significant volatilization rates are evidenced. However, biodegradation process might have a lag period in which volatilization becomes the main removal process in the reactor [24]. For this reason,

it is recommended to check losses by volatilization. In case this process proves to be significant, control mechanisms must be implemented, which may imply off-gas treatment and cost increments for the overall treatment.

3.2. Biodegradation

3.2.1. HOCs biodegradation

Once soil is removed and placed in the reactor, suitable conditions are set for indigenous microorganisms to perform the HOCs removal. But not all of them respond to the same stimulus in the same way. For this reason, it is necessary to study the microorganisms responsible for the biodegradation processes and understand the conditions in which they are able to perform the expected work at a convenient rate.

Several types of microorganisms, namely bacteria, fungi and algae, have been extensively studied for their capacity to degrade and mineralize different types of organic compounds, among which HOCs can be found. Interesting reviews on biodegradation aspects have been done, targeting specific groups of HOCs present in diverse matrices (soil, sediments, water, groundwater, etc.). Within the aimed contaminants it is possible to find PAHs [112–114], petroleum hydrocarbons [115–117], nitroaromatic compounds [118,119], pesticides and herbicides [120–123], among others.

Since HOC solubility and concentration in aqueous phase are very low, HOC consumption in aqueous phase by microorganisms or the substrate utilization rate (r_S) [$M.L^{-3}.T^{-1}$] is often modeled by a first order kinetic equation, assuming that biomass is constant, and is written as:

$$r_S = -k_{bio} S \quad (21)$$

where S is the specific limiting substrate concentration and k_{bio} is the first order constant for biodegradation [T^{-1}]. Table 1.8 shows the models used when biomass is not considered constant. These models are based on the biomass growth.

Usually, for the models shown in Table 1.8, the substrate consumption rate (r_S) is related to the growth rate and expressed as:

$$r_S = \mu \frac{X}{Y} \quad (22)$$

where Y is the yield coefficient [$M.M^{-1}$].

Table 1.8 Models for biomass specific growth used in slurry bioreactors modeling

Model	Equation	
Logistic equation	$r_X = k_{log} X(1 - \beta X)$	(23)
Monod growth	$\mu = \mu_{max} \frac{S}{K + S}$	(24)
Andrews inhibitory growth	$\mu = \mu_{max} \frac{S}{K + S + \frac{S^2}{K_i}}$	(25)

where r_X is the biomass growth rate [M.L^{-1}.T^{-1}], X is the total biomass concentration in the reactor [M.L^{-3}], k_{log} is the proportionality constant [T^{-1}] and β is the inverse of the carrying capacity [L^3.M^{-1}].

where μ is the specific growth rate [M.M^{-1}.T^{-1}], μ_{max} is the maximum substrate utilization rate [M.M^{-1}.T^{-1}], S is the substrate concentration [M.L^{-3}], K is the half-velocity constant [M.L^{-3}] and K_i is the inhibition constant [M^{3}L^{-6}].

The logistic equation (Eq. 23) was derived for self-limiting growth of a biological population, but it has not been often used for soil slurry systems. Indeed, the most commonly used model for organic compounds biodegradation is Monod equation (Eq. 24), which relates microbial growth (in general, in aqueous systems) to the concentration of a limiting nutrient. However, if there is more than one limiting nutrient, similar terms can be added to consider them as well. Finally, Andrews model (Eq. 25) is used when the substrate has an inhibitory effect on the microbial growth. It is important to consider that, during the aerobic biodegradation of HOCs, derivatives or metabolites are likely to be produced. Polar metabolites, more soluble in water, are potentially more toxic than their precursors [124] and can be accumulated either on the solid phase (by sorption) or in the liquid phase, causing inhibition in some cases [29].

Additionally, cell death rate (r_d) should be considered to obtain an accurate representation of the system. In most models, this is represented as a simple first order equation, as follows:

$$r_d = -bX \qquad (26)$$

where b is the cell death constant [T^{-1}].

Table 1.9 summarizes some kinetic constants for biomass growth and substrate consumption according to the model in selected papers found in the literature. In general, authors consider the slurry as a homogeneous phase, and models are fitted without consideration of other mechanisms such as desorption or volatilization. This means that most kinetic constants found in the literature (especially those using first-order model and logistic model) are, in fact, apparent kinetic constants, which also include the solid-liquid mass transfer step. Hence,

values seem to be very low in comparison with aqueous phase kinetic constants. Similarly, many papers do not consider gas-liquid mass transfer, causing in some cases an overestimation of biodegradation rates.

Although many authors have demonstrated the importance of the desorption process for the bioavailability of HOCs in slurry conditions, biodegradation occurring directly on the sorbed phase has been suggested as another mechanism to consider. For instance, Woo et al. [38] developed a model in which phenanthrene is also taken up directly from soil, without the desorption step. The kinetic parameters of these processes have been calibrated to fit the experimental points (see Table 1.9), and the maximum utilization rate (μ_{max}) is between 25 and 100 times lower than the one of the dissolved contaminants. This mechanism has been poorly addressed and generally not considered in models reported in the literature.

Table 1.9 Modeling parameters for biodegradation in soil slurry bioreactors from selected papers

Model	Matrix	Pollutant (concentration)	Parameters	Remarks	Reference
First order			k_{bio} (d^{-1})		
	Top horizon soil	Acenaphthene	0.079	Natural attenuation	[48]
	real aged	Phenanthrene	0.059	T: 25°C	
		Anthracene	0.052		
		Fluoranthene	0.044		
		Pyrene	0.061		
		Benzo(a)anthracene	0.036		
		Benzo(a)fluoranthene	0.037		
		Acenaphthene	0.091	Bioaugmentation	
		Phenanthrene	0.093	Consortium A	
		Anthracene	0.154	T: 25°C	
		Fluoranthene	0.051		
		Pyrene	0.075		
		Benzo(a)anthracene	0.053		
		Benzo(a)fluoranthene	0.052		
		Acenaphthene	0.09	Bioaugmentation	
		Phenanthrene	0.104	Consortium N	
		Anthracene	0.186	T: 25°C	
		Fluoranthene	0.057		
		Pyrene	0.079		
		Benzo(a)anthracene	0.058		
		Benzo(a)fluoranthene	0.06		
	Real	BEHP* (Co = 7050 mg/kg)	0.28	Enriched culture from	[31]
	contaminated soil	BEHP (Co = 6650 mg/kg)	0.398	contaminated soil	
		BEHP (Co = 6400 mg/kg)	0.315	Room Temperature	
		BEHP (Co = 3300 mg/kg)	0.146	(20-22°C)	
		BEHP (Co = 2760 mg/kg)	0.263		
		BEHP (Co = 2400 mg/kg)	0.137		
	Sandy loam soil	2,4-dichlorophenoxyacetic acid	0.49	Sewage sludge	[14]
		(Co 200 mg/kg)		bioaugmentation	

Model	Matrix	Pollutant (concentration)	Parameters				Remarks	Reference
		2,4-dichlorophenoxyacetic acid (Co 300 mg/kg)	0.43				T: N.R.	
		2,4-dichlorophenoxyacetic acid (Co 500 mg/kg)	0.23					
	Artificial spiked soil	Naphthalene	0.48				*Flavobacterium sp.* Isolated from crude oil contaminated water T: N.R.	[55]
Logistic equation			k_{log} (d^{-1})	β ($L.mg^{-1}$)	Y ($mg.mg^{-1}$)			
	Spiked marine sediments	Aliphatic hydrocarbons (500 mg/kg) and 13 PAHs (6.1 mg/kg)	0.24	0.1	0.16		No bioaugmentation T: 30°C	[26]
			0.39	0.04	0.73		Amended (nutrients) T: 30°C	
			0.18	0.08	0.09		Amended (sand) T: 30°C	
			0.35	0.04	0.32		Amended (nutrients and sand) T: 30°C	
Monod			μ_{max} (d^{-1})	K (mg/L)	b (d^{-1})	Y ($mg.mg^{-1}$)		
	Loam sand (silt/clay fraction)	Phenanthrene	0.96 (Dissolved)	0.1	0.12	1.696 (Oxygen to Substrate)	Enriched culture from contaminated soil T: 25°C	[16,38]
			0.04 (Sorbed on biomass)			1.416 (Oxygen to Biomass)		
			0.052 (Sorbed on soil 2% slurry)			0.897 (Biomass to substrate)		
			0.02 (Sorbed on soil 6% slurry)					
			0.01 (Sorbed on soil 18% slurry)					
	Aqueous phase	Pyrene	4.2 (Unamended)	NR	NR		Enriched culture from	[45]

Model	Matrix	Pollutant (concentration)	Parameters			Remarks	Reference
			16.1 (400 mg/L biosurfactant)	NR	NR	Creosote contaminated soil	
			19.4 (700 mg/L biosurfactant)	NR	NR	T: 37°C	

NR = Not reported

*BEHP: Bis(2-ethylhexyl)phthalate

3.2.2. Biostimulation and bioaugmentation

The addition of nutrients or alternative carbon sources to improve the biodegradation rates is called biostimulation. Although the implementation of slurry conditions can be enough to mobilize nutrients in the soil and improve the soil bioremediation, in some cases biostimulation may be used to enhance the process. Some research works in soil-slurry conditions have performed experiments using external carbon sources [19,32,40,51] or nutrients supplementation (mainly nitrogen and phosphorous) [26,36,53].

Even if native microorganisms of polluted soils can degrade the pollutants successfully given the optimal conditions of temperature, pH and agitation, in some cases, it is possible to enhance the biodegradation rate by adding pure or mixed cultures. This is called bioaugmentation. The sources may include activated sludge from domestic or industrial wastewater treatment plants [14,20,30,35,52], pure microbial cultures [25,37,47], mixed microbial cultures isolated from contaminated sites [15,19,27,29,36,125,126] or acclimatized mixed cultures [51]. It is important that the added inoculum be compatible with the native microbial communities of the soil. Otherwise, negative effects might be produced, reducing the treatment efficiency.

Table 1.10 shows some applications of bioaugmentation and biostimulation found in the literature. It is noticeable that, when spiked soils are studied, bioaugmentation is generally useful and sometimes necessary. This is because the soil spiking is usually performed by impregnating the soil with a solution of the target pollutant in an organic solvent (such as acetone or dichloromethane). This process certainly affects soil native microorganisms, making the indigenous microflora of the soil inviable [127]. Therefore, a comparison of bioaugmented reactors with not bioaugmented reactors is often not possible using spiked soils.

Moreover, in real soils, the native microbiota may be adapted to the presence and the consumption of the often toxic HOCs present in the matrix. Consequently, these indigenous microorganisms are considered as a powerful starting point for the development of inocula of pure or mixed microbial strains that are later tested at different operational conditions in the slurry bioreactor. In fact, some studies have reached up to 25% of pollutants biodegradation increments, compared to non-bioaugmented reactors [27,52]. Yet, in some cases, the bioaugmentation techniques have not shown a significant enhancement of the biodegradation process at the same conditions [25]. In any case, thoughtful investigation of contaminated

sites and the final fate of the polluted soil should be carried out before deciding the application of bioaugmentation and or biostimulation [48].

Table 1.10 Bioaugmentation and biostimulation used in aerobic slurry bioreactors

Pollutant	Bioaugmentation	Biostimulation	Enhanced removal	Remarks	Reference
Spiked soil					
Naphthalene and Phenanthrene	+	-	N.T.	Acclimatized sludge from municipal wastewater treatment	[35]
Naphthalene	+	-	N.T.	Pure culture: Pseudomonas putida	[37]
2,4-dichlorophenoxyacetic acid	+	+	N.T.	Acclimatized aerobic and sulfate reducing microorganisms and sucrose	[51]
Dibenzothiophene, Fluoranthene, Pyrene and Chrysene	+	+	30-75%	White-rot fungus *Bjerkandera sp.* BOS55, glucose, peptone and mineral medium	[60]
Pyrene	+	-	57%	Aerobic domestic sewage	[21]
TNT	+	+	N.T.	Pure culture: *Pseudomonas putida* and sucrose	[40]
Phenanthrene	+	-	N.T.	Consortium of adapted microorganisms	[50]
Real Contaminated soil					
14 PAHs	+	+	3%	PAH degraders and inorganic nutrients	[25]
16 PAHs	+	-	25%	Bacterial consortium, Fungal consortium and both	[27]
Hydrocarbons	+	+	14%	7 bacterial strains and biosurfactants addition	[49]
Phthalates, adipate and alcohols	+	-	N.T.	Activated sludge acclimatized from wastewater treatment plant	[30]
7 PAHs	+	-	5%	Inoculum A (see Table 1.2)	[48]
			6%	Inoculum N (see Table 1.2)	

3.2.3. Microorganisms' oxygen uptake

As discussed in section 3.1.2, oxygen is an important nutrient involved in aerobic biodegradation and it can be a limiting factor in aerobic systems. The presence of biomass affects the hydrodynamic conditions of the systems that, at the same time, affect the oxygen transfer rate. Thus, the microorganisms' oxygen uptake can be directly affected by the OTR.

Moreover, depending on the type of microorganisms, the importance of the dissolved oxygen concentration can vary [128]. Only few studies in the literature consider the oxygen uptake as an important parameter to measure or follow in soil slurry systems, although it can provide useful information of the HOC biodegradation process.

The oxygen mass balance in the aqueous phase of the bioreactor is given by the next equation.

$$r_{O_2} = OTR - OUR \quad (27)$$

where r_{O_2} is the accumulation rate of oxygen in the liquid phase [$M.L^{-3}.T^{-1}$], OTR is the oxygen transfer rate (explained in the gas-liquid transfer section) [$M.L^{-3}.T^{-1}$] and OUR is the oxygen uptake rate [$M.L^{-3}.T^{-1}$]. The OUR is usually defined as:

$$OUR = q_{O_2} X \quad (28)$$

where q_{O_2} is the specific oxygen uptake rate ($M_{O2}.M_X^{-1}.T^{-1}$) and it is characteristic for each microorganism. This parameter is usually considered constant, but there is evidence that it may depend on physicochemical and operational parameters. Moreover, OUR can be in some cases an indicator of hydrodynamic stress, cell damage and cell death [128].

The OUR has been used by some authors as an indirect parameter to follow HOC biodegradation in soil-slurry bioreactors [18,32]. It can also be related with the consumption of SOM and other substances added to the reactor (such as surfactants or other amendments) depending of their bioavailability. Endogenous respiration, concerning consumption of dead cells and other microbial products, can be calculated and used in the microbial growth modeling by measuring the OUR when substrate has been totally consumed [32]. In the presence of soil and SOM, other chemical oxidation processes can occur, increasing the oxygen needs of the system. However, OUR measurements in soil slurry bioreactors are rarely carried out and, hence, no information about the possible effects of soil presence have been found.

4. Influence of Operational Parameters on the HOC Removal Mechanisms in a Soil Slurry Bioreactor

In this section, some of the most important operational parameters of slurry bioreactors are identified and their influence on the mechanisms mentioned above are explained. Table 1.11 shows the main parameters monitored and controlled in soil slurry system for some cases found in the literature.

Some physical parameters such as temperature and pH are known to have an important impact on bioprocesses. However, it is also known that optimal temperatures varies between 20°C and 30°C and adequate pH values between 6.75 and 7.25 for most microorganisms used in a slurry bioreactor [51]. Therefore, these parameters are not commonly studied. They are instead chosen by standard weather conditions and natural soil pH or they are just followed as indicators of the bioprocess state. Nevertheless, these parameters may have a strong influence in all other mechanisms (desorption, diffusion, microbial kinetics, volatilization etc.), and, moreover, an impact on the costs of the treatment at real scale (i.e., need of pH adjustments or temperature control).

4.1. Air superficial velocity and stirring speed

In slurry phase bioreactors, solids need to be maintained in suspension and well mixed and oxygen need to be provided in proper amounts. Therefore, as explained in section 1, reactors are usually mechanically agitated by stirrers whereas air bubbles are generated by the air flow input passing through spargers located on the bottom. The introduction of this current of air has an impact on the agitation of the system by modifying the input power [129]. Both air superficial velocity (U_G) and stirring speed (N) influence directly the mixing and the hydrodynamic conditions in the reactor. These parameters have a great influence on the oxygen transfer, which, at the same time, has a significant impact on the biodegradation rate and other chemical oxidation processes in the reactor. Empirical models have been developed to understand this influence on water and wastewater treatments, particularly in terms of the variation of the volumetric oxygen transfer coefficient ($k_L a$) [104]. In general, they are expressed as follows:

$$k_L a = A\, {U_G}^B \left(\frac{P_G}{V}\right)^C {\mu_a}^D \qquad (29)$$

where A, B, C and D are empirical constants, depending mainly on the geometric characteristics of the system, V is the reactor volume, P_G is the power applied to the system (depending mostly on N, but not only) and μ_a is the slurry apparent viscosity (which can vary in the presence of solids, as explained before). However, no comprehensive studies or models regarding this subject have been found in the literature for soil-slurry bioreactors. In fact, most research works set these parameters to assure aerobic conditions, without investigating the real influence on oxygen transfer and biodegradation.

Table 1.11 Parameters commonly measured or followed in the study of slurry bioreactors, their main influence on the removal mechanisms in soil-slurry systems and ranges observed in reviewed articles.

Parameters	Influence on removal mechanisms	Range
Physical and biological parameters		
Temperature	Direct effect on volatilization and desorption rates of pollutants and on biodegradation and bacterial growth.	20 – 30 °C
pH	Effect on hydrodynamic conditions in the presence of soil and on the biodegradation rate according to the microorganism type and affinity.	5.7 – 8.4
Pollutant concentration in soil	High level of pollutants can be toxic for certain types of microorganism. Low concentrations can cause low bacterial growing rates. Possible effect on desorption kinetics (if initial-concentration dependent desorption).	Depending on contaminant
Dissolved oxygen (DO)	Low DO concentrations can lead to low biodegradation rates and low removal efficiencies.	2 mg/L - Saturation
Biomass concentration	Control of biodegradation rate and removal efficiency. Control of bioprocess. Effect on rheology and reactor hydrodynamics.	Used as indicator. 10^4 – 10^9 CFU/ml
Soil composition	High clay content can decrease oxygen transfer and change rheological properties. High organic matter contents are related to slower desorption rate of pollutants.	Natural conditions
Operational parameters		
Mixing (stirring speed)	Enhancement of the homogeneity of the system and oxygenation of non-aerated systems. High mixing speeds lead to higher desorption rates, but also to bubble coalescence (and decreased oxygen transfer rate). Low stirring speed may cause poor homogenization.	20 – 500 rpm (depending on reactor volume)
Aeration (air superficial velocity)	Control of DO and enhancement of oxygen uptake rate. Too high aeration rates can lead to bubble coalescence, higher volatilization of pollutants and lesser biodegradation efficiencies.	10^{-4} – 10^{-1} m/s
Soil content	Control of pollutant concentration in reactor (substrate loading). High soil content can modify the rheological properties and affect oxygen transfer.	4% – 50% (w/v)
Substrate loading rate (SLR), HRT and SRT	These parameters are to be regulated for optimization of SBR and continuous operation mode.	SLR: 10^{-1} – 10^4 mg/kg/d HRT = SRT: 1 – 70 d
Surfactant concentration	Effect on pollutants solubility and bioavailability. Possible toxic effect for microorganisms. Negative impact on oxygen transfer.	Depending on CMC* of surfactant used
Nutrients concentration	Effect on bacterial growth and possible enhancement biodegradation rate.	Depending on microorganism needs and system lacks
Bioaugmentation dose	Enhancement of biodegradation rates and removal efficiency of pollutants	Depending on types of microorganisms and their biodegradation capacity

*Critical micelle concentration

Besides, volatilization is an important mechanism to consider when these operational parameters are fixed in soil-slurry systems working with volatile and semi-volatile substances. For instance, Collina et al. [37] tested their influence on the apparent biodegradation and volatilization rates in a bioreactor treating naphthalene spiked soil. Their results are depicted in Table 1.12. It is interesting to observe that, for an aeration rate of 0.05 l.min^{-1} and a stirring rate of 350 min^{-1}, the volatilization kinetic coefficient (k_{vol}) is higher than the apparent biodegradation kinetic coefficient (k_{bio}). They concluded that, for a fixed air flow rate, an optimum agitation rate that maximizes biodegradation and minimizes volatilization can be found. However, they did not consider the desorption mechanism in their model, meaning that this process is implicitly expressed in the apparent k_{bio}. Therefore, the variations in biodegradation and volatilization rate may also be due to the variation of the desorption rate. Their conclusions demonstrate, nonetheless, the importance of considering volatilization in soil-slurry systems. Few empirical correlations have been proposed in the literature relating k_{vol} for volatile compounds to U_G and $\frac{P_G}{V}$ (similar to Eq. 29) in aqueous systems [130,131], however, no information has been found in the context of soil-slurry systems.

Table 1.12 Influence of air flow rate and stirring rate on the apparent biodegradation and volatilization kinetic coefficients in a slurry bioreactor treating naphthalene contaminated soil [37]

Air flow rate (l.min^{-1})	Stirring rate (min^{-1})	k_{vol} (d^{-1})	k_{bio} (d^{-1})
0.05	130	0.43	3.53
	200	1.22	5.74
	350	1.51	1.20
1	200	0.58	2.88
	350	1.44	7.20
	500	1.68	4.56

If agitation is not enough, homogenization problems may occur. This creates limitations in pollutants and oxygen transfer through the different phases. But, if the agitation rate is too high, other problems may be generated, such as bubble coalescence and soil particle size decrease. For instance, Park et al. [42] found an optimum agitation range in which TNT removal was maximal by testing the influence of the stirring speed (20 to 80 rpm) on the bioremediation of real TNT-contaminated soil, at fixed aeration conditions (U_G) using Tween 80. In their case, high stirring speeds produced other adverse effects, such as foaming. However, a contradictory result was found by Woo et al. [16], who observed that, at low mass transfer regime (roller-bottle reactor at 2 min^{-1}), the biodegradation rate of phenanthrene in a

spiked soil was higher than at high mass transfer regime (agitated flask reactor at 150 min^{-1}) at slurry concentrations of 6% and 18% w/v. They attributed their results to a higher attachment of microorganisms to soil particles in mild conditions, which would lead to a direct (and faster) sorbed-phase pollutants biodegradation. Nevertheless, air was not supplied, and oxygen needs where not measured in their systems, which makes difficult to draw conclusions on the biodegradation process.

4.2. Soil content and soil composition

Soil content (typically ranging between 5% and 50% w/v) can be changed to adjust the optimal conditions for biodegradation. As discussed in section 3.1, HOCs removal efficiency in slurry phase bioreactors depends on the pollutant mass transfer rate (from soil to aqueous phase), which is directly influenced by the soil/water ratio [39]. This parameter can also highly affect other mechanisms within the system. For instance, rheological properties can be affected, distancing the fluid properties from Newtonian conditions, particularly at high clay content [132]. Other factors affecting rheological properties are the power input, pH variations and electrolytes presence [133]. Thus, the power input needed to maintain solids in suspension and complete mixed conditions might be significant for high soil concentration, increasing operational costs. Moreover, rheological changes due to soil presence can affect gas-liquid oxygen transfer (as shown in Eq. 29), by changing gas hold-up, increasing or decreasing bubble coalescence and varying bubble size [134].

Likewise, as discussed in section 3.1, soil composition (and particle characteristics) determines the effect of soil presence on the biodegradation process. Some practical examples can be found in the literature. For instance, Beolchini et al. [26] investigated the effect of adding sand amendments in a slurry bioreactor treating aliphatic and polyaromatic hydrocarbons. They found that the sand amendments enhanced the biodegradation of pollutants by increasing the gas-liquid interface (smaller and more stable bubbles), oxygen diffusion and mass transfer rate. However, in the presence clayey soils, increasing air flow rate with the purpose of enhancing the biodegradation rate may be counterproductive. Two other examples are those provided by Woo et al. [36] (using clayey soil spiked with n-hexadecane) and Sheibani et al. [40] (using spiked TNT-contaminated clay). They explained that clay presence at high aeration rates can lead to bubble coalescence, which, in turn, decreases oxygen transfer rate and impacts negatively the biodegradation process. In all cases, soil content and composition must be studied carefully to avoid negative effects disturbing the overall pollutant removal.

4.3. Nutrient concentration

As discussed in section 3.2.1, nutrient addition (or biostimulation) can be used to enhance microbial growing. Moreover, the nutrient concentration might be used as a tool to steer the microbial community and its dynamics. It can even be critical for certain growing phases or specific biological compound productions (such as EPS and biosurfactants) [135,136]. For instance, Irvine et al. [137] explained that adequate levels of N and P can avoid a prolonged lag phase at the starting of the slurry reactor and can enhance biodegradation of Bis(2-ethylhexyl)phthalate (BEHP)-contaminated soil. Kalantary et al. [50] carried out experiments to determine the effect of three macronutrients (N, P and K), eight micronutrients (Mg, S, Fe, Cl, Zn, Mn, Cu and Na) and four trace elements (B, Mo, Co and Ni) in the biodegradation of spiked phenanthrene contaminated soil in slurry conditions. Placket-Burman statistical design was used to evaluate significance of the variables. They found that N, K, P, Cl, Na and Mg were the main elements affecting phenanthrene degradation under the experiment conditions. The effect of the other elements was less than 1% in the range of concentrations tested. This means that it is important to verify the nutrient needs and balance of the system, which depends not only on the soil characteristics, but also on the microorganisms and on the specific pollutants to be biodegraded.

On the other hand, the addition of external carbon sources can increase biological activity and the biomass concentration, but this is not necessarily linked to an enhancement of the biodegradation rate of targeted compounds. For example, Giordano et al. [32] added lactose as external carbon source to a slurry bioreactor treating PAH-contaminated sediments in SBR mode and no improvement of the PAHs removal was achieved. Similarly, Robles-González et al. [51] added sucrose for biostimulation purposes in the bioremediation of spiked soil contaminated with 2,4-dichlorophenoxyacetic acid and they found no effect compared to non-amended conditions.

4.4. Biomass concentration

Mozo et al. [111] showed that biomass concentration can affect the volatilization and biodegradation competition in aqueous phase. The fraction of biodegraded substrate is related to the amount of biomass capable of utilizing it as a carbon source. This means that increasing biomass amount, biodegradation is favored to volatilization as removal mechanism of volatile and semi-volatile compounds. To enhance the biomass concentration, the optimization of parameters like pH or temperature is critical [115]. Moreover, if a strategy of bioaugmentation

is being used, specialized microorganisms, the inocula volume and its concentration can play important roles in the microbial growth rate [48].

Biomass concentration also affects the slurry rheological properties [138]. Microorganisms might be able to form structures with the soil, which may change the rheological behavior of the system in the reactor, but biofilms around soil particles or bioflocs with both mineral and biological parts have not been studied to our knowledge. However, it is possible to find interesting results of the rheological properties of suspended biomass on wastewater treatment [105].

4.5. Surfactants concentration

Many studies have used surfactants to enhance HOC solubility and HOC desorption from soil, as mentioned in section 3.1.1.3. However, the properties of the surfactant used and its dose (relative to their critical micelle concentration in aqueous phase) are important factors to consider when designing surfactant-enhanced bioremediation of HOC-contaminated soils [43]. An interesting application was made by Mozo et al. [35], who investigated the effect of nonionic surfactants on the solubility and biodegradation of PAHs in both aqueous and slurry phases using spiked sand and spiked clay as model soils. Phenanthrene desorption was successfully enhanced and the surfactant did not cause substrate consumption inhibition and, moreover, it was used as carbon source by microorganisms. Spiked soil was completely remediated (>99%) in less than 120 h. However, no comparison with unamended systems was made, which does not allow of measuring the real impact of the surfactant addition on the soil-slurry system.

On the hydrodynamics point of view, surfactants affect also surface tension, apparent viscosity increasing bubble coalescence, particle aggregation and gas hold up, decreasing the oxygen transfer rate [106]. However, all these combined effects have been poorly addressed for soil slurry bioreactors.

Alternatively, biosurfactants have become an interesting option. Trejo-Castillo et al. [49] tested the addition of biosurfactants produced by a mixed culture on the treatment of hydrocarbon contaminated soil in a slurry bioreactor. When biosurfactants were added as a pretreatment before the inoculum, the hydrocarbons removal was more efficient than when they were added at the same time. This means that biosurfactants may have been used as a carbon source to the detriment of hydrocarbons biodegradation. Other substances can also act as surface active compounds. For example, Fava et al. [46] used soy lecithin and humic

substances as surface active substances to enhance PAHs mobility from a real aged soil. These substances increased the PAHs removal and were also metabolized by the microorganisms in the system.

5. Final considerations and perspectives

Slurry bioreactors are very complex systems, combining several interacting phases. Most mechanisms described in this review have been studied independently and isolated from other interactions. Moreover, most studies in this field are performed focusing on the biodegradation process and using a "black box" approach, in which pollutants removal efficiency is related to specific parameters, without observing possible side or chain effects in the system. Modeling of the mechanisms have been rarely developed, particularly for combined phenomena. However, from the available information it was possible to identify the main physical, chemical, physicochemical and biological interactions, as well as the influence of the operational conditions and the soil and pollutants characteristics. They set the rules for the competition of removal mechanisms and will determine the limiting step in the system.

Figure 1.5 shows the characteristic time for the mechanisms exposed in this review, calculated from the kinetic data available in the literature for soil slurry bioreactors. It is interesting to observe that, despite common beliefs stressing that biodegradation of HOCs is a slow process, it might not be the limiting step for bioremediation of HOC-contaminated soils. In fact, depending on the matrix, pollutant and operational conditions, solid-liquid mass transfer and oxygen availability may become the processes to optimize, particularly when enriched inoculum is used as bioaugmentation technique. Also, as discussed in section 4.1, Figure 1.5 shows that for HOC volatilization may be always in competition with biodegradation as a removal mechanism in the reactor for volatile and semi-volatile compounds. This means that operational conditions must be studied to minimize losses by volatilization and maximize biodegradation rate.

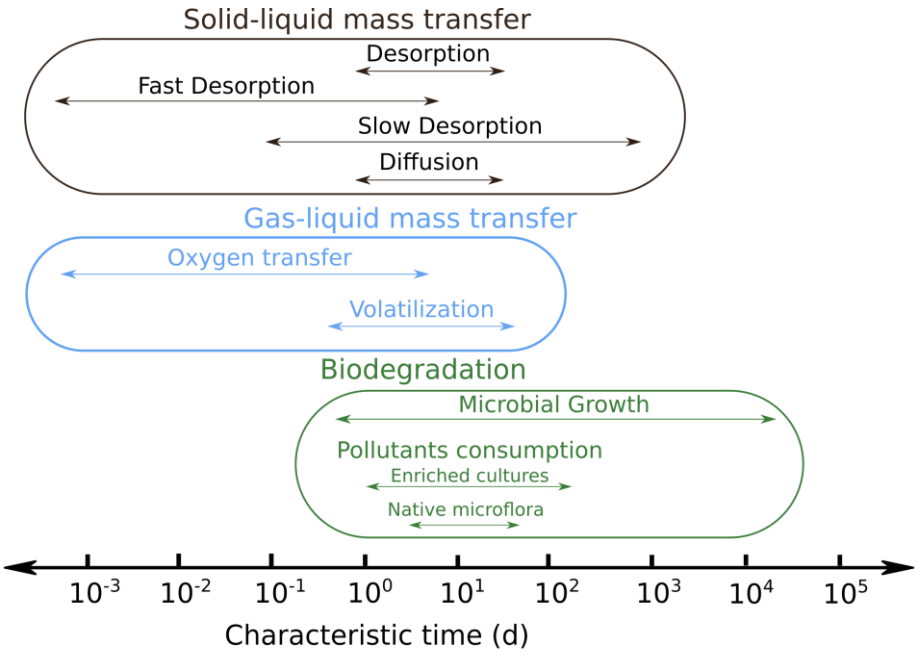

Figure 1.5 Characteristic time for the mechanisms present in the slurry bioreactor treating HOC-contaminated soil

This review is the first that, to the best of our knowledge, compiles available information from the main known mechanisms involved in the HOCs removal in soil or sediment slurry conditions and try to connect them, explaining the possible interactions between parameters. It gathers the basic information needed to understand the complex process of bioremediation occurring in slurry bioreactors and raises awareness on the considerations that should be made in the research of this technology. Several niches are to be explored regarding the effect of different parameters on the mechanisms involved in the removal of HOCs from contaminated soils or sediments in bioreactors. Among them, the next can be highlighted:

- Both aeration and mechanical agitation should be studied from the hydrodynamic point of view. Some studies have addressed this subject for three phase systems (gas-liquid-solid) but research on soil-slurry biological systems in which biomass and soil content affect the entire process are practically inexistent.

- The role of soil organic matter in different mechanisms should be further investigated. Dissolved organic matter can act as a surface-active compound and enhance the HOC solubilization or can adsorb on the mineral particle surface and retain HOCs. Also, non-soluble organic matter interacts with different mineral particles forming aggregates, which trap HOC molecules, but also reduce active sites for further HOC sorption.

- Deeper knowledge regarding the microbial diversity is needed to understand the efficiency of the bioaugmentation approach. Indeed, controversial results have been found in the application of this technique and, thus, several aspects are to be thoroughly investigated, such as origin, population dynamics and interactions, nutrient needs, enrichment approach, among others.

- The properties of mixed mineral-microbial bioflocs and their effect on the different mechanisms present in a soil slurry bioreactor have not been studied. Direct microorganism attachment or biofilm formation on the mineral or organic matter particle surfaces can lead to a direct consumption of HOCs, avoiding the desorption step. This is only true for sorbed HOCs on surfaces accessible to the microorganisms. Nevertheless, this subject needs to be better understood.

- No information about the final disposal of the soil or sediment was found in the literature. This is an issue that could depend on national or international regulations. Nonetheless, practical research about the separation and possible reutilization of soils or sediments after the slurry bioreactor treatment has not been taken into consideration. Similarly, wastewater produced in the slurry separation needs to be characterized and possible treatments or disposals proposed.

References

[1] R.G. Luthy, G.R. Aiken, M.L. Brusseau, S.D. Cunningham, P.M. Gschwend, J.J. Pignatello, M. Reinhard, S.J. Traina, W.J. Weber, J.C. Westall, Sequestration of hydrophobic organic contaminants by geosorbents, Environ. Sci. Technol. 31 (1997) 3341–3347.

[2] R.L. Crawford, Bioremediation, in: Encycl. Bioprocess Technol., John Wiley & Sons, Inc., 2002. http://dx.doi.org/10.1002/0471250589.ebt035.

[3] S. Colombano, A. Saada, V. Guerin, P. Bataillard, G. Bellenfant, S. Beranger, D. Hube, C. Blanc, C. Zornig, I. Girardeau, Quelles techniques pour quels traitements–Analyse coûts-bénéfices, Rapp. Final BRGM-RP-58609-FR. (2010).

[4] A.M. Thayer, Bioremediation: Innovative Technology for Cleaning Up Hazardous Waste, Chem. Eng. News. 69 (1991) 23–44. doi:10.1021/cen-v069n034.p023.

[5] R. Boopathy, Factors limiting bioremediation technologies, Bioresour. Technol. 74 (2000) 63–67.

[6] M. Vidali, Bioremediation. an overview, Pure Appl. Chem. 73 (2001) 1163–1172.

[7] M.C. Tomei, A.J. Daugulis, Ex Situ Bioremediation of Contaminated Soils: An Overview of Conventional and Innovative Technologies, Crit. Rev. Environ. Sci. Technol. 43 (2013) 2107–2139. doi:10.1080/10643389.2012.672056.

[8] U.S. Environmental Protection Agency (USEPA), Selecting Remediation Technique for Contaminated Sediment, Environmental Protection Agency. Office of Water, Washington DC, 1993. https://nepis.epa.gov/Exe/ZyPURL.cgi?Dockey=20003Q0N.txt.

[9] S. Gan, E.V. Lau, H.K. Ng, Remediation of soils contaminated with polycyclic aromatic hydrocarbons (PAHs), J. Hazard. Mater. 172 (2009) 532–549. doi:10.1016/j.jhazmat.2009.07.118.

[10] S. Kuppusamy, T. Palanisami, M. Megharaj, K. Venkateswarlu, R. Naidu, Ex-Situ Remediation Technologies for Environmental Pollutants: A Critical Perspective, in: P. de Voogt (Ed.), Rev. Environ. Contam. Toxicol. Vol. 236, Springer International Publishing, Cham, 2016: pp. 117–192. http://link.springer.com/10.1007/978-3-319-20013-2_2 (accessed October 4, 2016).

[11] S.C. Wilson, K.C. Jones, Bioremediation of soil contaminated with polynuclear aromatic hydrocarbons (PAHs): a review, Environ. Pollut. 81 (1993) 229–249.

[12] R.L. Crawford, D.L. Crawford, Bioremediation: Principles and Applications, Cambridge University Press, 2005.

[13] C. Machín-Ramírez, A.I. Okoh, D. Morales, K. Mayolo-Deloisa, R. Quintero, M.R. Trejo-Hernández, Slurry-phase biodegradation of weathered oily sludge waste, Chemosphere. 70 (2008) 737–744. doi:10.1016/j.chemosphere.2007.06.017.

[14] Y.A. Mustafa, H.M. Abdul-Hameed, Z.A. Razak, Biodegradation of 2,4-Dichlorophenoxyacetic Acid Contaminated Soil in a Roller Slurry Bioreactor: Soil, CLEAN - Soil Air Water. 43 (2015) 1241–1247. doi:10.1002/clen.201400623.

[15] S.H. Woo, J.M. Park, Evaluation of drum bioreactor performance used for decontamination of soil polluted with polycyclic aromatic hydrocarbons, J. Chem. Technol. Biotechnol. 74 (1999) 937–944. doi:10.1002/(SICI)1097-4660(199910)74:10<937::AID-JCTB128>3.0.CO;2-Q.

[16] S.H. Woo, M.W. Lee, J.M. Park, Biodegradation of phenanthrene in soil-slurry systems with different mass transfer regimes and soil contents, J. Biotechnol. 110 (2004) 235–250. doi:10.1016/j.jbiotec.2004.02.007.

[17] I.V. Robles-González, F. Fava, H.M. Poggi-Varaldo, A review on slurry bioreactors for bioremediation of soils and sediments, Microb. Cell Factories. 7 (2008) 5. doi:10.1186/1475-2859-7-5.

[18] A. Chiavola, R. Baciocchi, R. Gavasci, Biological treatment of PAH-contaminated sediments in a Sequencing Batch Reactor, J. Hazard. Mater. 184 (2010) 97–104. doi:10.1016/j.jhazmat.2010.08.010.

[19] M. Nozari, M. Reza, M. Dehgani, Investigation of the Effect of Co-Metabolism on Removal of Dodecane by Microbial Consortium from Soil in a Slurry Sequencing Bioreactor, J. Bioremediation Biodegrad. 05 (2014). doi:10.4172/2155-6199.1000253.

[20] D. Prasanna, S. Venkata Mohan, B. Purushotham Reddy, P.N. Sarma, Bioremediation of anthracene contaminated soil in bio-slurry phase reactor operated in periodic discontinuous batch mode, J. Hazard. Mater. 153 (2008) 244–251. doi:10.1016/j.jhazmat.2007.08.063.

[21] S. Venkata Mohan, D. Prasanna, B. Purushotham Reddy, P.N. Sarma, Ex situ bioremediation of pyrene contaminated soil in bio-slurry phase reactor operated in periodic discontinuous batch mode: Influence of bioaugmentation, Int. Biodeterior. Biodegrad. 62 (2008) 162–169. doi:10.1016/j.ibiod.2008.01.006.

[22] D.P. Cassidy, S. Efendiev, D.M. White, A comparison of CSTR and SBR bioslurry reactor performance, Water Res. 34 (2000) 4333–4342.

[23] P. Li, X. Wang, F. Stagnitti, L. Li, Z. Gong, H. Zhang, X. Xiong, C. Austin, Degradation of phenanthrene and pyrene in soil slurry reactors with immobilized bacteria Zoogloea sp., Environ. Eng. Sci. 22 (2005) 390–399.

[24] V. Jee, D.M. Beckles, C.H. Ward, J.B. Hughes, Aerobic slurry reactor treatment of phenanthrene contaminated sediment, Water Res. 32 (1998) 1231–1239.

[25] R.F. Lewis, SITE Demonstration of Slurry-Phase Biodegradation of PAH Contaminated Soil, Air Waste. 43 (1993) 503–508. doi:10.1080/1073161X.1993.10467149.

[26] F. Beolchini, L. Rocchetti, F. Regoli, A. Dell'Anno, Bioremediation of marine sediments contaminated by hydrocarbons: Experimental analysis and kinetic modeling, J. Hazard. Mater. 182 (2010) 403–407. doi:10.1016/j.jhazmat.2010.06.047.

[27] X. Li, P. Li, X. Lin, C. Zhang, Q. Li, Z. Gong, Biodegradation of aged polycyclic aromatic hydrocarbons (PAHs) by microbial consortia in soil and slurry phases, J. Hazard. Mater. 150 (2008) 21–26. doi:10.1016/j.jhazmat.2007.04.040.

[28] C.B. Chikere, B.O. Chikere, G.C. Okpokwasili, Bioreactor-based bioremediation of hydrocarbon-polluted Niger Delta marine sediment, Nigeria, 3 Biotech. 2 (2012) 53–66. doi:10.1007/s13205-011-0030-8.

[29] M.K. Tiwari, S. Guha, Kinetics of biotransformation of chlorpyrifos in aqueous and soil slurry environments, Water Res. 51 (2014) 73–85. doi:10.1016/j.watres.2013.12.014.

[30] I.D. Ferreira, C.B.A. de Menezes, V.M. de Oliveira, D.M. Morita, Slurry Phase Biological Treatment of Latosol Contaminated with Phthalates, Adipate, and Alcohols, J. Environ. Eng. 141 (2014) 04014046.

[31] C. Juneson, O.P. Ward, A. Singh, Biodegradation of bis (2-ethylhexyl) phthalate in a soil slurry-sequencing batch reactor, Process Biochem. 37 (2001) 305–313.

[32] A. Giordano, L. Stante, F. Pirozzi, R. Cesaro, G. Bortone, Sequencing batch reactor performance treating PAH contaminated lagoon sediments, J. Hazard. Mater. 119 (2005) 159–166. doi:10.1016/j.jhazmat.2004.12.002.

[33] G. Nano, A. Borroni, R. Rota, Combined slurry and solid-phase bioremediation of diesel contaminated soils, J. Hazard. Mater. 100 (2003) 79–94. doi:10.1016/S0304-3894(03)00065-7.

[34] D.P. Cassidy, R.L. Irvine, Biological treatment of a soil contaminated with diesel fuel using periodically operated slurry and solid phase reactors, Water Sci. Technol. 35 (1997) 185–192.

[35] I.S. Kim, J.-S. Park, K.-W. Kim, Enhanced biodegradation of polycyclic aromatic hydrocarbons using nonionic surfactants in soil slurry, Appl. Geochem. 16 (2001) 1419–1428.

[36] A. Partovinia, F. Naeimpoor, P. Hejazi, Carbon content reduction in a model reluctant clayey soil: Slurry phase n-hexadecane bioremediation, J. Hazard. Mater. 181 (2010) 133–139. doi:10.1016/j.jhazmat.2010.04.106.

[37] E. Collina, G. Bestetti, P. Di Gennaro, A. Franzetti, F. Gugliersi, M. Lasagni, D. Pitea, Naphthalene biodegradation kinetics in an aerobic slurry-phase bioreactor, Environ. Int. 31 (2005) 167–171. doi:10.1016/j.envint.2004.09.011.

[38] S.H. Woo, J.M. Park, B.E. Rittmann, others, Evaluation of the interaction between biodegradation and sorption of phenanthrene in soil-slurry systems, Biotechnol. Bioeng. 73 (2001) 12–24.

[39] S. Venkata Mohan, M. Ramakrishna, S. Shailaja, P. Sarma, Influence of soil–water ratio on the performance of slurry phase bioreactor treating herbicide contaminated soil, Bioresour. Technol. 98 (2007) 2584–2589. doi:10.1016/j.biortech.2006.09.018.

[40] G. Sheibani, F. Naeimpoor, P. Hejazi, Statistical factor-screening and optimization in slurry phase bioremediation of 2,4,6-trinitrotoluene contaminated soil, J. Hazard. Mater. 188 (2011) 1–9. doi:10.1016/j.jhazmat.2011.01.112.

[41] B. Xin, M. Shen, H. Aslam, F. Wu, Remediation of explosive-polluted soil in slurry phase by aerobic biostimulation, J. Phys. Conf. Ser. 439 (2013) 012047. doi:10.1088/1742-6596/439/1/012047.

[42] C. Park, T.-H. Kim, S. Kim, J. Lee, S.-W. Kim, Bioremediation of 2, 4, 6-trinitrotoluene contaminated soil in slurry and column reactors, J. Biosci. Bioeng. 96 (2003) 429–433.

[43] H. Zhu, M.D. Aitken, Surfactant-Enhanced Desorption and Biodegradation of Polycyclic Aromatic Hydrocarbons in Contaminated Soil, Environ. Sci. Technol. 44 (2010) 7260–7265. doi:10.1021/es100112a.

[44] S.H. Woo, C.O. Jeon, J.M. Park, Phenanthrene biodegradation in soil slurry systems: Influence of salicylate and Triton X-100, Korean J. Chem. Eng. 21 (2004) 412–418.

[45] F.A. Bezza, E.M. Nkhalambayausi Chirwa, Biosurfactant-enhanced bioremediation of aged polycyclic aromatic hydrocarbons (PAHs) in creosote contaminated soil, Chemosphere. 144 (2016) 635–644. doi:10.1016/j.chemosphere.2015.08.027.

[46] F. Fava, S. Berselli, P. Conte, A. Piccolo, L. Marchetti, Effects of humic substances and soya lecithin on the aerobic bioremediation of a soil historically contaminated by polycyclic aromatic hydrocarbons (PAHs), Biotechnol. Bioeng. 88 (2004) 214–223. doi:10.1002/bit.20225.

[47] S. Nasseri, R.R. Kalantary, N. Nourieh, K. Naddafi, A.H. Mahvi, N. Baradaran, Influence of bioaugmentation in biodegradation of PAHs-contaminated soil in bio-slurry phase reactor, Iran. J. Environ. Health Sci. Eng. 7 (2010) 199.

[48] S. Kuppusamy, P. Thavamani, M. Megharaj, R. Naidu, Bioaugmentation with Novel Microbial Formula vs. Natural Attenuation of a Long-Term Mixed Contaminated Soil—Treatability Studies in Solid- and Slurry-Phase Microcosms, Water. Air. Soil Pollut. 227 (2016). doi:10.1007/s11270-015-2709-7.

[49] R. Trejo-Castillo, M.A. Martínez-Trujillo, M. García-Rivero, Effectiveness of crude biosurfactant mixture for enhanced biodegradation of hydrocarbon contaminated soil in slurry reactor, Int. J. Environ. Res. 8 (2014) 727–732.

[50] R.R. Kalantary, A. Mohseni-Bandpi, A. Esrafili, S. Nasseri, F.R. Ashmagh, S. Jorfi, M. Ja'fari, Effectiveness of biostimulation through nutrient content on the bioremediation of phenanthrene contaminated soil, J. Environ. Health Sci. Eng. 12 (2014). doi:10.1186/s40201-014-0143-1.

[51] I. Robles-González, E. Ríos-Leal, R. Ferrera-Cerrato, F. Esparza-García, N. Rinderkenecht-Seijas, H.M. Poggi-Varaldo, Bioremediation of a mineral soil with high contents of clay and organic matter contaminated with herbicide 2,4-dichlorophenoxyacetic acid using slurry bioreactors: Effect of electron acceptor and supplementation with an organic carbon source, Process Biochem. 41 (2006) 1951–1960. doi:10.1016/j.procbio.2006.04.004.

[52] S. Venkata Mohan, B. Purushotham Reddy, P.N. Sarma, Ex situ slurry phase bioremediation of chrysene contaminated soil with the function of metabolic function: Process evaluation by data enveloping analysis (DEA) and Taguchi design of experimental methodology (DOE), Bioresour. Technol. 100 (2009) 164–172. doi:10.1016/j.biortech.2008.06.020.

[53] P. Thavamani, M. Megharaj, R. Naidu, Bioremediation of high molecular weight polyaromatic hydrocarbons co-contaminated with metals in liquid and soil slurries by metal tolerant PAHs degrading bacterial consortium, Biodegradation. 23 (2012) 823–835. doi:10.1007/s10532-012-9572-7.

[54] G. Misra, S.G. Pavlostathis, Biodegradation kinetics of monoterpenes in liquid and soil-slurry systems, Appl. Microbiol. Biotechnol. 47 (1997) 572–577.

[55] S.-Y. Wang, C. Vipulanandan, Biodegradation of naphthalene-contaminated soils in slurry bioreactors, J. Environ. Eng. 127 (2001) 748–754.

[56] E.L. Fernández, E.M. Merlo, L.R. Mayor, J.V. Camacho, Kinetic modelling of a diesel-polluted clayey soil bioremediation process, Sci. Total Environ. 557–558 (2016) 276–284. doi:10.1016/j.scitotenv.2016.03.074.

[57] P.-H. Lee, S.K. Ong, J. Golchin, G.S. Nelson, Use of solvents to enhance PAH biodegradation of coal tar, Water Res. 35 (2001) 3941–3949.

[58] K.T. Semple, A.W.J. Morriss, G.I. Paton, Bioavailability of hydrophobic organic contaminants in soils: fundamental concepts and techniques for analysis, Eur. J. Soil Sci. 54 (2003) 809–818.

[59] C. Barbeau, L. Deschenes, D. Karamanev, Y. Comeau, R. Samson, Bioremediation of pentachlorophenol-contaminated soil by bioaugmentation using activated soil, Appl. Microbiol. Biotechnol. 48 (1997) 745–752.

[60] L. Valentín, T.A. Lu-Chau, C. López, G. Feijoo, M.T. Moreira, J.M. Lema, Biodegradation of dibenzothiophene, fluoranthene, pyrene and chrysene in a soil slurry reactor by the white-rot fungus Bjerkandera sp. BOS55, Process Biochem. 42 (2007) 641–648. doi:10.1016/j.procbio.2006.11.011.

[61] W. Zhang, E.J. Bouwer, W.P. Ball, Bioavailability of Hydrophobic Organic Contaminants: Effects and Implications of Sorption-Related Mass Transfer on Bioremediation, Groundw. Monit. Remediat. 18 (1998) 126–138.

[62] M.C. van Loosdrecht, J. Lyklema, W. Norde, A.J. Zehnder, Influence of interfaces on microbial activity., Microbiol. Rev. 54 (1990) 75–87.

[63] IUPAC, Compendium of Chemical Terminology, 2nd Edition (the "Gold book"), Blackwell Scientific Publications, Oxford, 2014. http://citeseerx.ist.psu.edu/viewdoc/download?doi=10.1.1.681.2291&rep=rep1&type=pdf (accessed October 4, 2016).

[64] C. Trellu, A. Miltner, R. Gallo, D. Huguenot, E.D. van Hullebusch, G. Esposito, M.A. Oturan, M. Kästner, Characteristics of PAH tar oil contaminated soils—Black particles, resins and implications for treatment strategies, J. Hazard. Mater. 327 (2017) 206–215. doi:10.1016/j.jhazmat.2016.12.062.

[65] S.C. Wu, P.M. Gschwend, Sorption kinetics of hydrophobic organic compounds to natural sediments and soils, Environ. Sci. Technol. 20 (1986) 717–725.

[66] W. Wu, H. Sun, Sorption–desorption hysteresis of phenanthrene – Effect of nanopores, solute concentration, and salinity, Chemosphere. 81 (2010) 961–967. doi:10.1016/j.chemosphere.2010.07.051.

[67] S. Kleineidam, C. Schüth, P. Grathwohl, Solubility-normalized combined adsorption-partitioning sorption isotherms for organic pollutants, Environ. Sci. Technol. 36 (2002) 4689–4697.

[68] J.W. Talley, U. Ghosh, S.G. Tucker, J.S. Furey, R.G. Luthy, Particle-scale understanding of the bioavailability of PAHs in sediment, Environ. Sci. Technol. 36 (2002) 477–483.

[69] FAO, Guidelines for soil description, 4th ed, Food and Agriculture Organization of the United Nations, Rome, 2006.

[70] M. v. Lützow, I. Kögel-Knabner, K. Ekschmitt, E. Matzner, G. Guggenberger, B. Marschner, H. Flessa, Stabilization of organic matter in temperate soils: mechanisms and their relevance under different soil conditions - a review, Eur. J. Soil Sci. 57 (2006) 426–445. doi:10.1111/j.1365-2389.2006.00809.x.

[71] A. Parker, J.E. Rae, Environmental Interactions of Clays: Clays and the Environment, Springer Science & Business Media, 1998.

[72] L.A.G. Aylmore, J.P. Quirk, The micropore size distributions of clay mineral systems, J. Soil Sci. 18 (1967) 1–17.

[73] S. Müller, K.U. Totsche, I. Kögel-Knabner, Sorption of polycyclic aromatic hydrocarbons to mineral surfaces, Eur. J. Soil Sci. 58 (2007) 918–931. doi:10.1111/j.1365-2389.2007.00930.x.

[74] X. Cui, W. Hunter, Y. Yang, Y. Chen, J. Gan, Biodegradation of pyrene in sand, silt and clay fractions of sediment, Biodegradation. 22 (2011) 297–307. doi:10.1007/s10532-010-9399-z.

[75] A.M. Oen, G. Cornelissen, G.D. Breedveld, Relation between PAH and black carbon contents in size fractions of Norwegian harbor sediments, Environ. Pollut. 141 (2006) 370–380.

[76] R.L. Wershaw, A new model for humic materials and their interactions with hydrophobic organic chemicals in soil-water or sediment-water systems, J. Contam. Hydrol. 1 (1986) 29–45.

[77] E.M. Murphy, J.M. Zachara, S.C. Smith, J.L. Phillips, T.W. Wietsma, Interaction of Hydrophobic Organic Compounds with Mineral-Bound Humic Substances, Environ. Sci. Technol. 28 (1994) 1291–1299. doi:10.1021/es00056a017.

[78] G. Limousin, J.-P. Gaudet, L. Charlet, S. Szenknect, V. Barthès, M. Krimissa, Sorption isotherms: A review on physical bases, modeling and measurement, Appl. Geochem. 22 (2007) 249–275. doi:10.1016/j.apgeochem.2006.09.010.

[79] D. Zhao, J.J. Pignatello, J.C. White, W. Braida, F. Ferrandino, Dual-mode modeling of competitive and concentration-dependent sorption and desorption kinetics of polycyclic aromatic hydrocarbons in soils, Water Resour. Res. 37 (2001) 2205–2212.

[80] S. Kleineidam, H. Rügner, P. Grathwohl, Desorption Kinetics of Phenanthrene in Aquifer Material Lacks Hysteresis, Environ. Sci. Technol. 38 (2004) 4169–4175. doi:10.1021/es034846p.

[81] W. Huang, W.J. Weber, A distributed reactivity model for sorption by soils and sediments. 10. Relationships between desorption, hysteresis, and the chemical characteristics of organic domains, Environ. Sci. Technol. 31 (1997) 2562–2569.

[82] M.J. Geerdink, M.C. van Loosdrecht, K.C.A. Luyben, Model for microbial degradation of nonpolar organic contaminants in a soil slurry reactor, Environ. Sci. Technol. 30 (1996) 779–786.

[83] W.J. Weber, W. Huang, A distributed reactivity model for sorption by soils and sediments. 4. Intraparticle heterogeneity and phase-distribution relationships under nonequilibrium conditions, Environ. Sci. Technol. 30 (1996) 881–888.

[84] G. Wang, S. Kleineidam, P. Grathwohl, Sorption/desorption reversibility of phenanthrene in soils and carbonaceous materials, Environ. Sci. Technol. 41 (2007) 1186–1193.

[85] L.S. Hundal, M.L. Thompson, D.A. Laird, A.M. Carmo, Sorption of Phenanthrene by Reference Smectites, Environ. Sci. Technol. 35 (2001) 3456–3461. doi:10.1021/es001982a.

[86] J.L. Chen, M.H. Wong, Y.S. Wong, N.F.Y. Tam, Modeling sorption and biodegradation of phenanthrene in mangrove sediment slurry, J. Hazard. Mater. 190 (2011) 409–415. doi:10.1016/j.jhazmat.2011.03.060.

[87] L.M. Carmichael, R.F. Christman, F.K. Pfaender, Desorption and mineralization kinetics of phenanthrene and chrysene in contaminated soils, Environ. Sci. Technol. 31 (1996) 126–132.

[88] A.-S. Allard, M. Remberger, A.H. Neilson, The negative impact of aging on the loss of PAH components in a creosote-contaminated soil, Int. Biodeterior. Biodegrad. 46 (2000) 43–49. doi:10.1016/S0964-8305(00)00050-0.

[89] B.J. Reid, K.C. Jones, K.T. Semple, Bioavailability of persistent organic pollutants in soils and sediments—a perspective on mechanisms, consequences and assessment, Environ. Pollut. 108 (2000) 103–112.

[90] M.D. Johnson, T.M. Keinath, W.J. Weber, A Distributed Reactivity Model for Sorption by Soils and Sediments. 14. Characterization and Modeling of Phenanthrene Desorption Rates, Environ. Sci. Technol. 35 (2001) 1688–1695. doi:10.1021/es001391k.

[91] F. Cao, I. Bourven, P.N.L. Lens, E.D. van Hullebusch, Y. Pechaud, G. Guibaud, Hydrophobic features of EPS extracted from anaerobic granular sludge: an investigation based on DAX-8 resin fractionation and size exclusion chromatography, Appl. Microbiol. Biotechnol. (2016). doi:10.1007/s00253-016-8053-z.

[92] S.S. Adav, D.-J. Lee, Extraction of extracellular polymeric substances from aerobic granule with compact interior structure, J. Hazard. Mater. 154 (2008) 1120–1126. doi:10.1016/j.jhazmat.2007.11.058.

[93] Z. Aksu, Application of biosorption for the removal of organic pollutants: a review, Process Biochem. 40 (2005) 997–1026. doi:10.1016/j.procbio.2004.04.008.

[94] K. Vijayaraghavan, Y.-S. Yun, Bacterial biosorbents and biosorption, Biotechnol. Adv. 26 (2008) 266–291. doi:10.1016/j.biotechadv.2008.02.002.

[95] W.T. Stringfellow, L. Alvarez-Cohen, Evaluating the relationship between the sorption of PAHs to bacterial biomass and biodegradation, Water Res. 33 (1999) 2535–2544.

[96] S.D. Haigh, A review of the interaction of surfactants with organic contaminants in soil, Sci. Total Environ. 185 (1996) 161–170.

[97] S. Laha, B. Tansel, A. Ussawarujikulchai, Surfactant–soil interactions during surfactant-amended remediation of contaminated soils by hydrophobic organic compounds: A review, J. Environ. Manage. 90 (2009) 95–100. doi:10.1016/j.jenvman.2008.08.006.

[98] C. Mulligan, R. Yong, B. Gibbs, Surfactant-enhanced remediation of contaminated soil: a review, Eng. Geol. 60 (2001) 371–380.

[99] D. Jin, X. Jiang, X. Jing, Z. Ou, Effects of concentration, head group, and structure of surfactants on the degradation of phenanthrene, J. Hazard. Mater. 144 (2007) 215–221. doi:10.1016/j.jhazmat.2006.10.012.

[100] C.K. Ahn, S.H. Woo, J.M. Park, Surface solubilization of phenanthrene by surfactant sorbed on soils with different organic matter contents, J. Hazard. Mater. 177 (2010) 799–806. doi:10.1016/j.jhazmat.2009.12.104.

[101] H. Lippold, U. Gottschalch, H. Kupsch, Joint influence of surfactants and humic matter on PAH solubility. Are mixed micelles formed?, Chemosphere. 70 (2008) 1979–1986. doi:10.1016/j.chemosphere.2007.09.040.

[102] S. Shekhar, A. Sundaramanickam, T. Balasubramanian, Biosurfactant Producing Microbes and their Potential Applications: A Review, Crit. Rev. Environ. Sci. Technol. 45 (2015) 1522–1554. doi:10.1080/10643389.2014.955631.

[103] G. Stucki, M. Alexander, Role of dissolution rate and solubility in biodegradation of aromatic compounds., Appl. Environ. Microbiol. 53 (1987) 292–297.

[104] F. Garcia-Ochoa, E. Gomez, Bioreactor scale-up and oxygen transfer rate in microbial processes: An overview, Biotechnol. Adv. 27 (2009) 153–176. doi:10.1016/j.biotechadv.2008.10.006.

[105] C. Durán, Y. Fayolle, Y. Pechaud, A. Cockx, S. Gillot, Impact of suspended solids on the activated sludge non-newtonian behaviour and on oxygen transfer in a bubble column, Chem. Eng. Sci. 141 (2016) 154–165. doi:10.1016/j.ces.2015.10.016.

[106] J. Henkel, Oxygen Transfer Phenomena in Activated Sludge, TU Darmstadt, Darmstadt, 2010. http://tuprints.ulb.tu-darmstadt.de/3008/.

[107] P.C. Mena, M.C. Ruzicka, F.A. Rocha, J.A. Teixeira, J. Drahoš, Effect of solids on homogeneous–heterogeneous flow regime transition in bubble columns, Chem. Eng. Sci. 60 (2005) 6013–6026. doi:10.1016/j.ces.2005.04.020.

[108] P. Mena, A. Ferreira, J.A. Teixeira, F. Rocha, Effect of some solid properties on gas–liquid mass transfer in a bubble column, Chem. Eng. Process. Process Intensif. 50 (2011) 181–188. doi:10.1016/j.cep.2010.12.013.

[109] S. Woo, J. Park, Estimation of oxygen transfer in soil slurry bioreactor, Biotechnol. Tech. 11 (1997) 713–716.

[110] S. Saponaro, L. Bonomo, G. Petruzzelli, L. Romele, M. Barbafieri, Polycyclic aromatic hydrocarbons (PAHs) slurry phase bioremediation of a manufacturing gas plant (MGP) site aged soil, Water. Air. Soil Pollut. 135 (2002) 219–236.

[111] I. Mozo, G. Lesage, J. Yin, Y. Bessiere, L. Barna, M. Sperandio, Dynamic modeling of biodegradation and volatilization of hazardous aromatic substances in aerobic bioreactor, Water Res. 46 (2012) 5327–5342. doi:10.1016/j.watres.2012.07.014.

[112] A.L. Juhasz, R. Naidu, Bioremediation of high molecular weight polycyclic aromatic hydrocarbons: a review of the microbial degradation of benzo[a]pyrene, Int. Biodeterior. Biodegrad. 45 (2000) 57–88. doi:10.1016/S0964-8305(00)00052-4.

[113] R.A. Kanaly, S. Harayama, Biodegradation of high-molecular-weight polycyclic aromatic hydrocarbons by bacteria, J. Bacteriol. 182 (2000) 2059–2067.

[114] A.K. Haritash, C.P. Kaushik, Biodegradation aspects of Polycyclic Aromatic Hydrocarbons (PAHs): A review, J. Hazard. Mater. 169 (2009) 1–15. doi:10.1016/j.jhazmat.2009.03.137.

[115] J.G. Leahy, R.R. Colwell, Microbial degradation of hydrocarbons in the environment., Microbiol. Rev. 54 (1990) 305–315.

[116] N. Das, P. Chandran, Microbial Degradation of Petroleum Hydrocarbon Contaminants: An Overview, Biotechnol. Res. Int. 2011 (2011) 1–13. doi:10.4061/2011/941810.

[117] T.J. McGenity, Hydrocarbon biodegradation in intertidal wetland sediments, Energy Biotechnol. • Environ. Biotechnol. 27 (2014) 46–54. doi:10.1016/j.copbio.2013.10.010.

[118] A. Esteve-Nunez, A. Caballero, J.L. Ramos, Biological Degradation of 2,4,6-Trinitrotoluene, Microbiol. Mol. Biol. Rev. 65 (2001) 335–352. doi:10.1128/MMBR.65.3.335-352.2001.

[119] J.C. Spain, Biodegradation of nitroaromatic compounds, Springer Science & Business Media, 2013.

[120] J. Aislabie, G. Lloyd-Jones, A review of bacterial-degradation of pesticides, Soil Res. 33 (1995) 925–942.

[121] S. Giacomazzi, N. Cochet, Environmental impact of diuron transformation: a review, Chemosphere. 56 (2004) 1021–1032. doi:10.1016/j.chemosphere.2004.04.061.

[122] S. Hussain, M. Arshad, D. Springael, S.R. SøRensen, G.D. Bending, M. Devers-Lamrani, Z. Maqbool, F. Martin-Laurent, Abiotic and Biotic Processes Governing the Fate of Phenylurea Herbicides in Soils: A Review, Crit. Rev. Environ. Sci. Technol. 45 (2015) 1947–1998. doi:10.1080/10643389.2014.1001141.

[123] B. Singh, K. Singh, Microbial degradation of herbicides, Crit. Rev. Microbiol. 42 (2016) 245–261. doi:10.3109/1040841X.2014.929564.

[124] L. Arias, J. Bauzá, J. Tobella, J. Vila, M. Grifoll, A microcosm system and an analytical protocol to assess PAH degradation and metabolite formation in soils, Biodegradation. 19 (2008) 425–434. doi:10.1007/s10532-007-9148-0.

[125] P.H. Lee, K.P. Chao, S.K. Ong, Solvent–water extraction method for the evaluation of polycyclic aromatic hydrocarbons bioavailability in coal–tar-contaminated soils, Int. J. Environ. Sci. Technol. 11 (2014) 1999–2008. doi:10.1007/s13762-013-0405-y.

[126] W. Xu, S. Guo, G. Li, F. Li, B. Wu, X. Gan, Combination of the direct electro-Fenton process and bioremediation for the treatment of pyrene-contaminated soil in a slurry reactor, Front. Environ. Sci. Eng. 9 (2015) 1096–1107. doi:10.1007/s11783-015-0804-z.

[127] B.J. Reid, G.L. Northcott, K.C. Jones, K.T. Semple, Evaluation of spiking procedures for the introduction of poorly water soluble contaminants into soil, Environ. Sci. Technol. 32 (1998) 3224–3227.

[128] F. Garcia-Ochoa, E. Gomez, V.E. Santos, J.C. Merchuk, Oxygen uptake rate in microbial processes: An overview, Biochem. Eng. J. 49 (2010) 289–307. doi:10.1016/j.bej.2010.01.011.

[129] M. Martín, F.J. Montes, M.A. Galán, Mass transfer rates from bubbles in stirred tanks operating with viscous fluids, Chem. Eng. Sci. 65 (2010) 3814–3824.

[130] J.A. Libra, Volatilization of organic compounds in an aerated stirred tank reactor, UNIVERSITY OF CALIFORNIA Los Angeles, 1991. http://www.seas.ucla.edu/stenstro/d/d11.pdf (accessed December 11, 2016).

[131] C. Munz, P.V. Roberts, Gas- and liquid-phase mass transfer resistances of organic compounds during mechanical surface aeration, Water Res. 23 (1989) 589–601. doi:10.1016/0043-1354(89)90026-2.

[132] P.F. Luckham, S. Rossi, The colloidal and rheological properties of bentonite suspensions, Adv. Colloid Interface Sci. 82 (1999) 43–92. doi:10.1016/S0001-8686(99)00005-6.

[133] E. Tombácz, M. Szekeres, Colloidal behavior of aqueous montmorillonite suspensions: the specific role of pH in the presence of indifferent electrolytes, Appl. Clay Sci. 27 (2004) 75–94. doi:10.1016/j.clay.2004.01.001.

[134] D.B. Mills, R. Bar, D.J. Kirwan, Effect of solids on oxygen transfer in agitated three-phase systems, AIChe J. 33 (1987) 1542–1549.

[135] F. Md, Biosurfactant: Production and Application, J. Pet. Environ. Biotechnol. 03 (2012). doi:10.4172/2157-7463.1000124.

[136] V. Musale, S.B. Thakar, Review: Biosurfactant and Hydrocarbon degradation, (2015). http://rjlbpcs.com/wp-content/uploads/2015/May-June/1.-Biosurfactant-and-Hydrocarbon-degradation.pdf (accessed February 5, 2017).

[137] R.L. Irvine, J.P. Earley, G.J. Kehrberger, B. Tod Delaney, Bioremediation of soils contaminated with bis-(2-ethylhexyl) phthalate (BEHP) in a soil slurry-sequencing batch reactor, Environ. Prog. 12 (1993) 39–44.

[138] B. Özbek, S. Gayik, The studies on the oxygen mass transfer coefficient in a bioreactor, Process Biochem. 36 (2001) 729–741. doi:https://dx-doi-org.fennec.u-pem.fr/10.1016/S0032-9592(00)00272-7.

CHAPTER 2

Gas-liquid oxygen transfer in aerated and agitated slurry systems

This chapter has been published as:

D.O. Pino-Herrera, Y. Fayolle, S. Pageot, D. Huguenot, G. Esposito, E.D. van Hullebusch, Y. Pechaud, Gas-liquid oxygen transfer in aerated and agitated slurry systems with high solid volume fractions, Chem. Eng. J. 350 (2018) 1073–1083. doi:10.1016/j.cej.2018.05.193.

CHAPTER 2 – Gas-liquid oxygen transfer in aerated and agitated slurry systems

Gas-liquid mass transfer, part I: In this chapter, the influence of three operational parameters (stirring speed, air superficial velocity and clay concentration) on the gas-liquid oxygen transfer is measured. Correlations between these parameters and the volumetric oxygen transfer coefficient are developped and a model to estimate this value from the total power input and clay content in the reactor is proposed.

Abstract

Oxygen transfer can be a limiting step in biodegradation processes. Therefore, this process has been widely investigated for wastewater treatment, but only few research works have been done on soil slurry systems. This study focuses on the gas-liquid oxygen mass transfer in clay slurry conditions in an aerated and agitated reactor using a marine propeller. Conversely to most studies on oxygen transfer, pneumatic power input was not negligible compared to mechanical power input. Clay presence has a negative impact on the oxygen transfer. However, the effect of agitation and aeration on this process remains unaffected at the clay concentrations tested. Three different phases explaining the depletion in the oxygen transfer rate were hypothesized. A model to predict the oxygen transfer coefficient in slurry reactors, including the three operational parameters tested within their respective ranges, was proposed.

Keywords: Slurry bioreactor, oxygen mass transfer, soil slurry, oxygen transfer coefficient model

Nomenclature

$A_{i=1...5}$	Constant of empirical Eqs. (10) to (14)
Ar	Dimensionless Archimedes number (-)
$B_{i=1...5}$	Exponents of empirical Eqs. (10) to (14)
b	Baffle width (m)
$C_{i=1...5}$	Exponents of empirical Eqs. (10) to (14)
D	Reactor diameter (m)
D_3	Exponent of empirical Eq. (12)
D_5	Exponent of empirical Eq. (14)
d_{50}	Particle median diameter (µm)
d_b	Bubble diameter (m)
d	Impeller diameter (m)
DO	Dissolved oxygen ($mg.L^{-1}$)
F	Y-intercept in Eq. 15 (s^{-1})
g	Gravitational constant ($m.s^{-2}$)
H	Reactor height (m)
K	Parameter in Eq. 15 ($W^{-1}.m^3.s^{-1}$)
k_La	Volumetric oxygen mass transfer coefficient (s^{-1})
L	Liquid height (m)
m	Slope of correlation in Eq. 20 (-)
N	Stirring speed (rpm)
N_P	Dimensionless power number (-)
Re	Dimensionless Reynolds number (-)
$\frac{P}{V}$	Specific power input ($W.m^3$)
$\frac{P_g}{V}$	Specific mechanical power input modified by the gas phase ($W.m^3$)
$\frac{P_N}{V}$	Specific mechanical power input ($W.m^3$)
$\frac{P_T}{V}$	Specific total power input ($W.m^3$)
$\frac{P_{U_G}}{V}$	Specific pneumatic power input ($W.m^{-3}$)
U_G	Air superficial velocity ($m.s^{-1}$)
V	Reactor volume (m^3)
V_S	Solid volume in the slurry (m^3)
V_T	Total slurry volume (m^3)
w	Impeller width (m)
X_S	Clay concentration ($kg.m^3$)

Greek letters

α	Ratio of mass transfer coefficient in slurry to that in tap water (-)
γ	Shear rate (s^{-1})
ε_G	Gas holdup (-)
$\varepsilon_{G,w}$	Gas holdup in clean water (-)
ε_r	Relative gas holdup (-)
ε_S	Solid volume fraction (-)
μ	Apparent viscosity (mPa.s)
μ_B	Bingham plastic viscosity (mPa.s)
ρ	Density ($kg.m^3$)
σ	Surface tension ($N.m^{-1}$)

τ	Shear stress (Pa)
τ_0	Yield stress (Pa)
φ_S	Solid mass fraction (-)

Sub-indexes

S	Relative to solid phase
Sl	Relative to slurry
W	Relative to water

1. Introduction

Biological treatments are advantageous technologies for contaminated soil remediation from economic and environmental points of view [1,2]. However, remediation time is a major disadvantage for these processes [3]. Slurry bioreactor technology is a promising remediation technique that can overcome some of the drawbacks of other biological treatments, by enhancing mass transfer processes and allowing to set up optimized conditions for biodegradation, particularly when pollution is constituted of hydrophobic organic compounds [4]. Moreover, aerobic slurry bioreactor technology has emerged as an effective and feasible technique with a high remediation potential, especially for silt and clay soil fractions, which often contain the highest pollution levels and are difficult to treat with more conventional approaches [5,6]. However, the mechanisms involved in the soil pollutants degradation within bioreactors are still not completely understood.

The main mechanisms occurring in a slurry bioreactor that are reported in the literature can be classified in three main groups, i.e. gas-liquid transfer processes, solid-liquid transfer processes and biodegradation processes. Within the gas-liquid transfer processes, it is possible to find the pollutant and by-product volatilization and the oxygen transfer from gas to liquid phase [7]. Oxygen consumption in aerobic reactors can be a limiting step if air supply is not sufficient during the process operation [8]. Therefore, oxygen transfer has been extensively studied in aerobic wastewater treatment systems. Several empiric correlations regarding the influence of diverse parameters on the volumetric oxygen mass transfer coefficient ($k_L a$) have been established and proved in stirred and aerated reactors [9].

One of the operational parameters studied for this kind of systems is the presence and concentration of different types of solids. In general, four different mechanisms explaining the effects of solids on mass transfer can be identified: i) solid particles can modify some physicochemical properties of the fluid, such as apparent density and viscosity, affecting bubble size, gas holdup and the mass transfer coefficient [10]; ii) the sole presence of solids can cause some steric effects affecting the trajectory of the bubbles, changing the bubble residence time in the reactor and causing coalescence in the system [11]; iii) solids can also attach or adsorb onto the gas-liquid interface, reducing the transfer area (surface and bubble contamination) [12,13] and; iv) if the affinity between oxygen and the solids is significant, oxygen molecules can be adsorbed on the solid surface enhancing the transfer rate [14].

Regarding soil particles, very few studies can be found in the literature. For instance, the study of Woo and Park [15] observed that $k_L a$ values in slurries at 40% w/v soil content were reduced from 80% to 60% compared to $k_L a$ values in water and that clay presence decreased drastically this parameter. However, there is still a lack of understanding regarding the reasons behind this phenomenon in soil slurries.

Besides, solid particles in soil are denser than most solids studied in the literature. Axial impellers, such as marine propellers, are hence used to improve homogenization of solids in the reactor and minimize the energy consumption [16]. But then gas dispersion can become inefficient. Moreover, clay particles can swell incrementing several times their size, which usually produces slurry with high solid volume fraction. The atypical conditions in which this kind of reactors are operated may hinder the use of classical correlation for oxygen transfer in wastewater treatment.

The main objective of this work is to study the oxygen gas-liquid mass transfer process in the presence of clay (in a large range of solid fraction volumes) in agitated and aerated conditions by using a mechanistic approach. To assess the influence of operational parameters on the gas-liquid mass transfer in a soil slurry bioreactor, three parameters were tested, i.e. specific power input, air superficial velocity and solid concentration.

2. Materials and methods

2.1. Reactor and operational parameters

The experiments were carried out in a standard glass reactor of diameter D = 17.5 cm. (Figure 2.1). The working volume was 4.2 L (with the height of liquid $L = D$). The reactor had a thermal jacket controlled at 20 °C and four baffles of width $b = D/10$. The total height was H = 30 cm. The gas phase was injected from the bottom of the reactor through a porous glass sparger of 5 cm of diameter connected to a three-port L-shaped valve, providing the choice between air and nitrogen, as needed. Mechanical agitation was supplied by a motor with digital controlled stirring speed coupled to a single marine propeller ($d = D/3$ and $w = d/3$) at a distance of a third of the liquid height from the bottom.

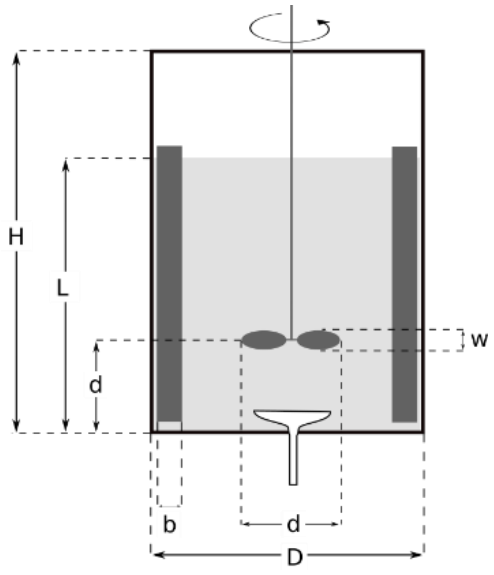

Figure 2.1 Schematic representation of the reactor

In aerated reactors, the definition of the power input is not always homogeneous throughout the literature. It is possible to find a purely specific mechanical power input due only to the agitation ($\frac{P_N}{V}$), a specific mechanical power input modified by the presence of gas ($\frac{P_g}{V}$) or even a specific total power input ($\frac{P_T}{V}$, in Eq. 1) which includes the pneumatic power input ($\frac{P_{U_G}}{V}$) given by the gas pressure drop in the reactor (due to the aeration). Mechanical specific power input can be estimated using the power number (N_P) and the stirring speed (N) (Eq.2), and the pneumatic specific power input from aeration can be calculated using the air superficial velocity U_G (Eq. 3) [17].

$$\frac{P_T}{V} = \frac{P_N}{V} + \frac{P_{U_G}}{V} \quad (1)$$

$$\frac{P_N}{V} = \frac{N_P \rho N^3 {d_i}^5}{V} \quad (2)$$

$$\frac{P_{U_G}}{V} = \rho g U_G \quad (3)$$

The power number N_P is constant and equal to 0.35 for a marine propeller at turbulent conditions ($Re > 10^4$), which is the case for all conditions tested in this study [18].

The soil used for this study was clay, provided by Argiles du Bassin Méditerranéen (France). It was composed of at least 65% of Sardinian montmorillonite (from Italy), with a particle size lower than 40 µm in ambient conditions. The chemical analysis of the clay was provided

by the supplier. The relative moisture of the clay was fairly constant at 10% when used in controlled laboratory conditions. Tap water was used for all experiments. Water conductivity was measured for each experiment to assure equal conditions. The reactor was operated varying the operational parameters in the ranges given in Table 2.1

Table 2.1 Operational parameter ranges used in this study

Operational parameter	Units	Range
Air superficial velocity, $\boldsymbol{U_G}$ ($\times 10^3$)	$m.s^{-1}$	1.53 – 8.87
Stirring speed, $\boldsymbol{N}$	s^{-1}	6.67 – 11.67
Clay concentration	% w/v, (wet basis)	0.1 – 20
	$kg.m^{-3}$, (dry basis)	0.9 – 180

2.2. Solid volume fraction and solid particle size

Some solids can increase their volume in slurry conditions (swelling). This is the case for some clay materials, which can make their volume rise up to 100 times, depending on the crystallographic structure [19]. Therefore, it is important to consider the solid volume fraction in the reactor, which is defined as the ratio of the volume occupied by the solids in the slurry to the total volume of the reactor (Eq. 4).

$$\varepsilon_S = \frac{V_S}{V} \tag{4}$$

Solid volume fraction was measured by the decantation method from 0.1% to 20% w/v (wet basis) of clay concentration. Tap water and clay were mixed at the desired concentration in the reactor and agitated for at least 30 minutes at 20°C. Then, 1 L of suspension was transferred to a graduated cylinder, covered and left to decant for 48h. The volume occupied by the solids was followed until no change was observed and the final value was reported as the solid volume fraction.

The solid particle size distribution in the slurry was measured using a particle size analyzer Malvern Mastersizer 3000. This technique provides particle size distributions in terms of a volume fraction in a size interval with respect to the volume equivalent size.

2.3. Rheology

Rheological parameters of clay-water mixture were measured using a capillary rheometer, for clay concentrations in soil slurry ranging from 0 to 30% w/v (wet basis). A rheological measure consists in determining the longitudinal pressure loss associated to the liquid flow rate through a capillary tube of known geometry. More details on the rheological device used

and on the calculations method are provided by Duran et al. [10]. The rheological measurements were performed for shear rates ranging between 150 and 1500 s^{-1} corresponding to shear rates that can be encountered in the reactor. To perform the rheological experiments, the slurry was pumped directly from the reactor (4.2-L working volume, 4 baffles, mechanical agitation, no aeration) using a helical rotor pump characterized by a pulseless and low shear flow.

2.4. Gas holdup

The gas holdup (ε_G) is the ratio of the gas phase volume to the total volume (Eq. 5).

$$\varepsilon_G = \frac{V_G}{V_T} \tag{5}$$

It was measured using two pressure sensors at different heights in the reactor. Difference on dynamic pressure due to agitation (without presence of air) was measured and subtracted from the total difference of pressure between the sensors. Differential pressure values were recorded, using a micro-manometer with a piezoresistive sensor, for at least 60 s and the average was used for the gas holdup calculation. This parameter was measured for each operating condition.

To compare changes on gas holdup in the presence of clay, a relative gas holdup, ε_r, was defined (Eq. 6). This is the ratio of gas holdup for the slurry at a specific solid concentration, ε_{Sl}, to the ratio of gas holdup using tap water, ε_w, for the same conditions of agitation and aeration.

$$\varepsilon_r = \frac{\varepsilon_{G,Sl}}{\varepsilon_{G,W}} \tag{6}$$

2.5. Oxygen mass transfer

Volumetric oxygen mass transfer coefficients were measured by the dynamic method (gassing out), described by García-Ochoa and Gomez [9]. Shortly, a nitrogen stream was injected to the system to remove the dissolved oxygen (DO). When the DO was less than 1 $mg.L^{-1}$, the nitrogen flow was interrupted, and air was introduced to the system. The curve of oxygen absorption was recorded using an inoLab® Oxi 7310 DO sensor connected to a Cellox 325 probe (WTW). From the oxygen absorption curves, volumetric mass transfer coefficients ($k_L a$) were obtained, taking into account the response time of the electrode. This parameter was determined for the operational condition ranges detailed in Table 2.1.

For studying the influence of operational parameters on the oxygen transfer, it is common to use a ratio between the transfer parameter at specific conditions to that in water [20–22]. Therefore, to compare the oxygen transfer process with and without soil, the alpha factor (α) has been defined (Eq.7) analogously to wastewater treatment. It stands for the ratio of the volumetric mass transfer coefficient in the slurry at a particular clay concentration to that in tap water, at the same aeration and agitation conditions. The study of this factor allows of spotting easily enhancements or reductions on the volumetric oxygen mass transfer coefficient due to clay addition.

$$\alpha = \frac{k_L a_{Sl}}{k_L a_W} \tag{7}$$

3. Results and discussion

3.1. Density, solid volume fraction and particle size

As in any solid-water system, the relation between the slurry density and clay concentration is linear and can be calculated from the weighted sum of the densities of the constituents (Eq. 8).

$$\rho_{Sl} = (\rho_S - \rho_W)\varphi_s + \rho_W \tag{8}$$

Moreover, the relation between the solid volume fraction (ε_S) and the clay concentration (X_S) is also linear in the range tested in this study (i.e. 0.9 kg.m^{-3} – 180 kg.m^{-3} on a dry basis), as it can be observed in Figure 2.2. However, it is interesting to notice that at the highest concentration (close to 20% w/v), the solid volume fraction represents already half of the total slurry volume.

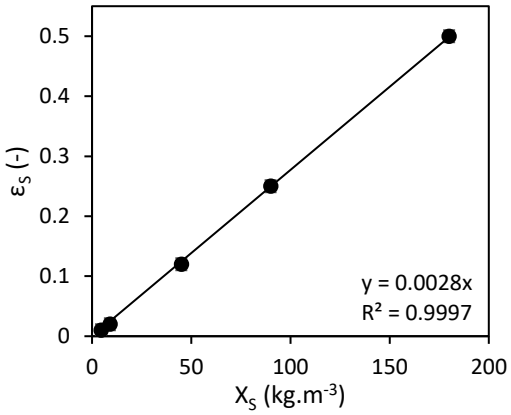

Figure 2.2 Total solid volume in slurry suspensions

Besides, clay minerals have the capacity of increasing several times its own size in the presence of water. Two mechanisms are involved in this phenomenon, namely, water absorption (called crystalline swelling) and surface ionization (called osmotic swelling) [23,24]. The latter represents a repulsion between the negative charged structural sheets and it is reserved for clay compositions containing monovalent cations (such as Na^+ or Li^+) [25]. To measure this property, the swelling factor has been defined as the ratio of the volume occupied by a determined amount of hydrated clay to its dry volume. The swelling factor depends on the crystallographic structure of the clay, the electrolytic composition of the bulk water as well as pH, among other factors. For instance, the swelling factor of montmorillonite in distilled water can vary from 10 to 100, while the one of illite can range from 9 to 19 [19]. On the other hand, kaolinite has almost no swelling capacity. Since the clay used in this study is a mixture containing at least 65% of montmorillonite, it was not pretreated before performing the experiments (meaning that it can contain a mixture of monovalent and divalent cations in its structure) and the water used for all experiments was tap water, the swelling factor was found to be 5. Additionally, the volume median diameter of clay particles in suspension is constant (i.e. about 7.5 µm) and independent of the shear rate (results not shown). One can therefore assume that the changes in the solid volume fraction due to agitation and/or aeration in the reactor are negligible.

3.2. Rheology

The rheological behavior of the clay-water system for shear rates in the range encountered in soil-slurry reactors was studied. Figure 2.3 shows that for the range of clay concentrations (45 $kg.m^{-3}$ – 270 $kg.m^{-3}$, corresponding to 5 to 20% w/v on wet bases) and shear rate (150 s^{-1} – 1500 s^{-1}) tested in this study, clay suspensions can be modelled as Bingham plastics, which agrees with the rheological behavior of clay suspensions containing montmorillonite [26,27]. The Bingham model is expressed by the Eq. 9. More complex models, such as Casson model or Herschel-Bulkley model, are usually utilized at lower shear rates [24,28].

$$\tau = \mu_B \gamma + \tau_0 \quad (9)$$

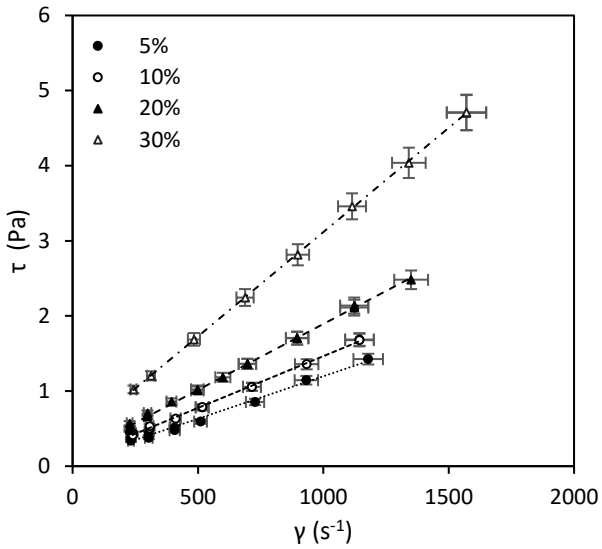

Figure 2.3 Rheogram of montmorillonite suspensions at different clay concentrations

An exponential correlation between both the plastic viscosity (μ_B) and the yield stress (τ_0) and the clay concentration in the slurry can be assimilated (Figure 2.4). This is in accordance with the studies of Ramos-Tejada et al. [29] and Robertson et al. [19], where both plastic viscosity and yield stress increased with the clay concentration. Similarly to the swelling factor mentioned in section 3.1, the increments in the rheological parameters depend on the mineralogical composition of the clay used, the electrolytes present in the bulk water as well as the bulk water pH, among other factors [30,31].

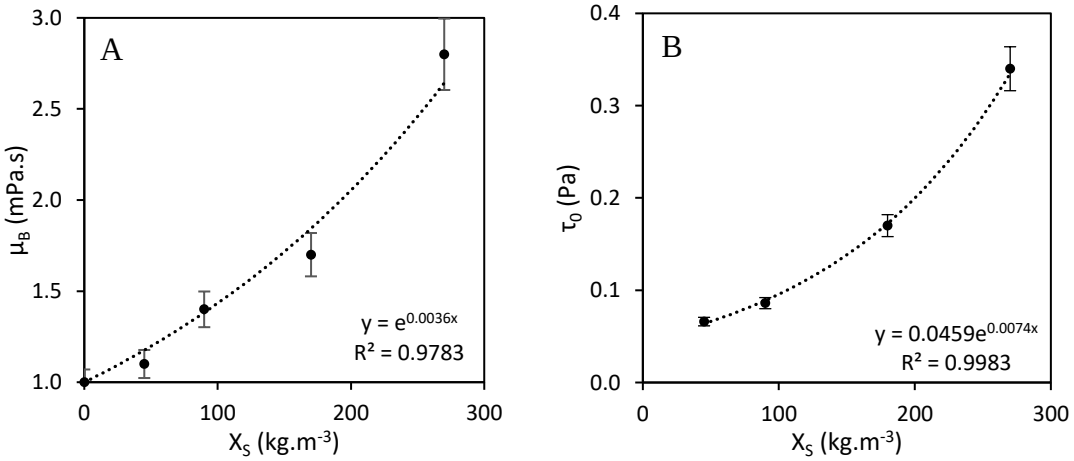

Figure 2.4 Rheological behavior of clay suspensions at different clay concentrations; (A) Plastic viscosity; (B) Yield stress

3.3. Gas holdup

Usually, for agitated stirred tanks with variable agitation speed, the dispersion of gas in the liquid phase at a constant gas flow comprises three cases [32]. In the first one (C1), the total power input is not sufficient to disperse uniformly the gas through the liquid and the impeller

is flooded. This means that, during this phase, the impeller is surrounded by the gas phase and the bubble rising is slightly impacted by mechanical mixing and mainly vertical (approaching the system to a bubble column). For higher power input, the dispersion of the gas becomes more efficient and the second case is observed. In this case (C2), both aeration and agitation structure the flow. However, in this phase the complete homogeneous dispersion of the gas in the overall reactor is not yet achieved. Finally, the third case (C3) is characterized by a complete and homogeneous dispersion, where large amounts of bubbles recirculate in the system. In general, for the three cases, increases in air superficial velocity and mechanical agitation have a positive impact on the gas holdup and correlations between these parameters (similar to those for the $k_L a$) have been proposed in literature according to each case [33].

For the air-water system (without soil addition) studied in this work (results provided as supplementary data), the gas holdup was almost not affected by the increments in the mechanical power input at the low range and at a fixed air flow (Figure S1A). However, when the mechanical power input is higher than 50 $W.m^{-3}$, the gas holdup increased considerably (even doubling the initial values). In contrast, when fixing the stirring speed, the gas holdup increases at the lower range of air superficial velocity (from 1.53×10^{-3} to 3.53×10^{-3} $m.s^{-1}$) and for higher values, it remains constant (Figure S1B). The same gas holdup behavior was observed at all clay concentrations (from 0.9 to 180 $kg.m^{-3}$) tested in this study (Figure S2-Figure S8).

From these results, it is possible to infer that at the lower range of power input and the higher range of air superficial velocity, the gas-liquid flow in the reactor could be assimilated to the previously described case C1. As the stirring speed increases or the air flow decreases, the system moves on to the second case (higher gas dispersion within the reactor). This conclusion is confirmed by direct observations of the bubble behavior in the reactor. This specific gas holdup behavior can be explained by the choice of the impeller. Indeed, the marine propeller provides an axial flow to the liquid in the system, which may reduce the gas dispersion efficiency for low power inputs, in comparison with other types of impeller, such as Rushton turbines. Nevertheless, it also facilitates the suspension of heavy solid particles at comparative low power inputs [16,34].

To assess the effect of solid particle presence on the gas holdup, the relative gas holdup (ε_r) was evaluated as a function of the mechanical power input, the air superficial velocity and the solid volume fraction (Figure 2.5). It can be observed that the power input due to mechanical

agitation has practically no influence on the relative gas holdup at 8.83×10^{-3} m.s^{-1} (Figure 2.5A). This is true for the whole range of clay concentrations investigated in this study. Figure 2.5B shows a similar behavior regarding the influence of the air superficial velocity (U_G). Moreover, most ε_r values are statistically similar to 1, meaning that the presence of solids has a very little effect on the gas holdup. Only at the lowest air superficial velocity tested (1.53×10^{-3} m.s^{-1}), a distinctive evolution on the relative gas holdup can be observed which can be translated as a net augmentation of ε_G in presence of solids at this air flow.

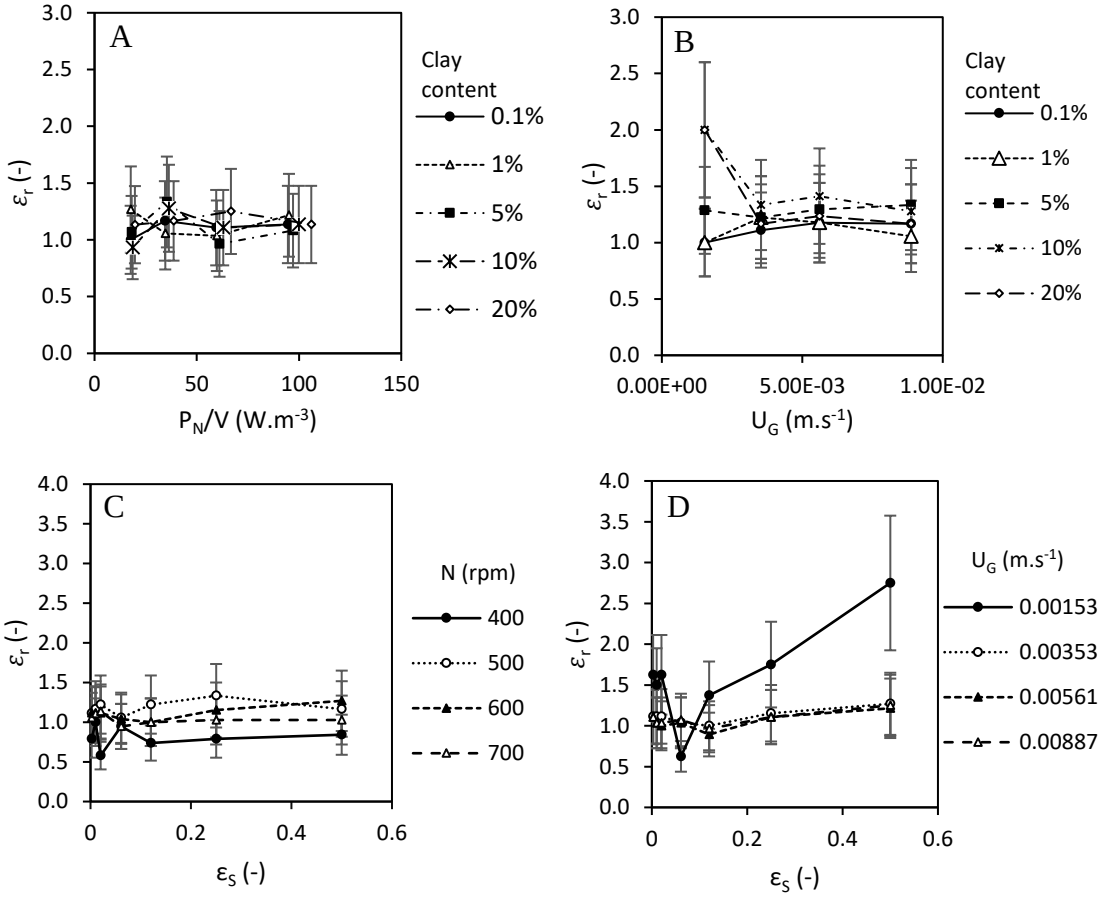

Figure 2.5 Effect of operational parameters on the relative gas holdup; (A) Effect of power input for different clay contents (% w/v) at UG=8.83×10-3 m.s-1; (B) Effect of air superficial velocity for different clay contents (% w/v) at N=500 rpm; Effect of the solid volume fraction on the relative gas holdup (C) at different stirring speed (rpm) at U_G= 3.53×10^{-3} m.s^{-1}; (D) at different air superficial velocities (m.s^{-1}) at N=600 rpm.

These conclusions are confirmed by Figures 2.5C and 2.5D. In fact, the variations of ε_r for different stirring speeds and air superficial velocities are, in general, around 30% from $\varepsilon_{G,W}$ (excluding the weakest air flow). The difference between the relative gas holdup values are statistically insignificant due to the measurement errors associated to the poor gas homogenization of the system (error bars represent an estimated error of 30% of the value).

This means that the impact of the presence of solids on the gas holdup cannot be established for the operational conditions tested in this study.

By comparing the results of this study with others reported in the literature [33,35,36], it is noticeable that most research works focusing on the gas holdup are in an agitation/aeration regime corresponding to the third case of the bubble dispersion zone (completely homogenized dispersion). Moreover, impellers and spargers used in these studies are different to those used in the present work. Therefore, none of the correlations proposed can be applied to the results of the experiments performed.

3.4. Operational parameters influence on the oxygen transfer in slurry phase

3.4.1. Power input considerations

Most research works performed on oxygen transfer in aerated and agitated reactors consider the pneumatic power input to be negligible in relation with the mechanical power input generated by the impeller. Indeed, Table 2.2 shows that for several impellers, range of agitation speeds and range of air superficial velocity, the ratio of power input due to aeration to the power input due to agitation is always less than 15%. This is because most gas-liquid transfer studies use radial impellers, which permit a better gas homogenization in the reactor. However, as discussed in section 3.3, they are less efficient in maintaining dense solids suspensions, such as soil slurries, than axial impellers.

Table 2.2 Ratio of power input due to aeration to power input due to agitation in selected articles

Type of impeller	Range of agitation speed (s^{-1})	Range of air superficial velocity ($m.s^{-1}$)	$\frac{P_{U_G}}{P_N}$	Reference
Rushton Turbine	4 – 15	1.0×10^{-2} – 7.5×10^{-2}	4.4×10^{-4} – 1.5×10^{-1}	[37]
	2.5 – 10	2.1×10^{-2} – 8.5×10^{-2}	1.0×10^{-4} – 2.5×10^{-2}	[38]
	1.7 – 8.3	5.2×10^{-4}	7.0×10^{-4} – 8.8×10^{-2}	[39]
	1.5 – 4.5	1.0×10^{-3} – 4×10^{-3}	5.4×10^{-4} – 5.9×10^{-2}	[35]
	10 – 13.3	3.6×10^{-3} – 1.1×10^{-2}	2.8×10^{-4} – 2.1×10^{-3}	[40]
Paddle four flat blades	8.3 – 11.7	1.0×10^{-4} – 5×10^{-4}	5.9×10^{-5} – 8.1×10^{-4}	[41]
Six blade pitch downflow turbine	2.5 - 7	1.0×10^{-3} – 4×10^{-3}	6.2×10^{-4} – 5.5×10^{-2}	[35]
Several combinations of impellers	2.5 – 10	2.1×10^{-2} – 8.5×10^{-2}	6.0×10^{-4} – 1.5×10^{-1}	[38]
Marine propeller	6.7 – 11.7	1.5×10^{-3} – 8.9×10^{-3}	1.6×10^{-1} – 4.9×10^{0}	This study

In the present study, $\frac{P_{U_G}}{V}$ can represent up to 83% of the total power input (Table 2.2), which means that it cannot be neglected. Therefore, the influence of both the purely mechanical

specific power input and the total specific power input on the gas-liquid transfer behavior were evaluated.

3.4.2. Correlations for k_La

A selection of the most typical correlations between the volumetric oxygen mass transfer coefficient and the operational parameters reported in the literature is shown in Table 2.3. Most of them relate k_La to the mechanical power input (Eq. 10) or the stirring rate (Eq. 11), as well as to the air superficial velocity. In general, by increasing agitation and/or aeration, most systems experience an increment in the volumetric oxygen mass transfer coefficient leading to an increased oxygen mass transfer rate. This enhancement is reflected in the exponents for these experimental parameters. It is possible to observe that the exponents obtained for this study are in the low range of typical values reported in the literature and the coefficients of determination show a good fit for these values. By analyzing these parameters, one can observe that the power input due to agitation has a greater influence on the oxygen transfer than air superficial velocity. This corresponds to the findings of most studies performed in clear water, as shown in the review of Garcia-Ochoa and Gomez [9]. However, the adjusted values of the correlations are slightly lower than those recollected by them and those found in the articles cited in Table 2.3, which can be explained by the type of agitator used and its comparative lower efficiency on gas dispersion. However, these correlations do not reflect the effect of the presence of solids.

Thus, some studies reported the effect of the viscosity on the oxygen gas-liquid transfer. Correlations including the liquid apparent viscosity have been proposed (Eq. 12). Application of Eq. 12 can be extended even for non-Newtonian fluids at homogeneous or heterogenous conditions [10,45]. For this study, the exponent of the apparent viscosity is out of the typical range and it shows an inflated negative effect of the viscosity on the oxygen transfer rate. Even if the coefficient of determination still shows a good correlation, changes in the apparent viscosity are not the only effect of the presence of solid particles in slurry systems [10,40,47,48].

Depending on the size of the particles and their interaction with the liquid phase, other effects on the slurry properties, and hence on the gas-liquid transfer process, can appear. Therefore, another way to represent the influence of solids on the k_La correlation is using the solid volume fraction (Eq. 13), which considers the steric effects linked to changes in bubble trajectory, bubble residence time and bubble coalescence. For the data in this study, the latter

correlation has a mediocre fitting ($R^2 = 0.88$), meaning that effects of other parameters related to solid presence are probably not being considered. A fifth correlation is then proposed (Eq. 14), in which these effects can be included adding a third parameter (exponent of solid volume fraction term, $D_5 > 1$) and, in this case, a good fitting can again be found ($R^2 = 0.96$). However, a correlation with this form has not been found in the literature and comparisons are not possible.

Table 2.3 Correlations for the volumetric oxygen mass transfer coefficient in selected literature

Correlation	Eq.	Parameter exponent value				References
			Typical Ranges	Present study		
Clear water						
$k_La = A_1\left(\frac{P}{V}\right)^{B_1} {U_G}^{C_1}$	(10)	Power input (B_1)	0.4 – 1.1	0.4	$R^2 = 0.98$	[32,36,42–44]
		Gas superficial velocity (C_1)	0.3 – 0.9	0.3		
$k_La = A_2\, N^{B_2} {U_G}^{C_2}$	(11)	Stirring speed (B_2)	0.9 – 2.7	1.2	$R^2 = 0.98$	[37,39]
		Gas superficial velocity (C_2)	0.5 – 0.7	0.3		
Slurry						
$k_La = A_3\left(\frac{P}{V}\right)^{B_3} {U_G}^{C_3}\mu^{-D_3}$	(12)	Power input (B_3)	0.6 – 1.0	0.4	$R^2 = 0.96$	[10,45]
		Gas superficial velocity (C_3)	0.3 – 0.7	0.4		
		Viscosity (D_3)	-0.4 – -1	-1.6		
$k_La = A_4\left(\frac{P}{V}\right)^{B_4} {U_G}^{C_4}(1-\varepsilon_S)$	(13)	Power input (B_4)	0.4 – 0.7	0.4	$R^2 = 0.88$	[40,46]
		Gas superficial velocity (C_4)	0.2 – 0.4	0.3		
$k_La = A_5\left(\frac{P}{V}\right)^{B_5} {U_G}^{C_5}(1-\varepsilon_S)^{D_5}$	(14)	Power input (B_5)	-	0.4	$R^2 = 0.96$	-
		Gas superficial velocity (C_5)	-	0.3		
		Solid volume fraction (D_5)	-	1.4		

*for the operational parameters range given in Table 2.1

Alternatively, a linear correlation between the volumetric mass transfer coefficient and the total power input is proposed (Eq. 15).

$$k_La\,[s^{-1}] = F\left(\frac{P_T}{V}[W.m^{-3}]\right) + K \qquad (15)$$

It was possible to apply the linear correlation given by Eq. 15 for the oxygen transfer in clear water, as well as in the slurry at 5%, 10% and 20% w/v (wet basis) of clay (Figure 2.6). Table 2.4 shows the adjusted parameters for the curves in Figure 2.6 using the correlation proposed in Eq. 15. Using this correlation and only knowing the total power input in the system,

the $k_L a$ can be estimated for the total power input range studied at a constant clay concentration. It is possible to notice that both the slope F and the y-intercept K decrease with the solid fraction volume, which means increasing the clay concentration, $k_L a$ values decrease and that the effect of the total power input on the oxygen transfer is less important. The linearity observed might be due to the impeller used and the consequences of its use on the system (pneumatic power input comparable to mechanical power input). It is highly possible that this behavior changes at very low P_{U_G} or P_N, where only one of these two parameters governs the oxygen transfer. This can also explain the fact that the y-intercept does not pass through the origin ($K \neq 0$).

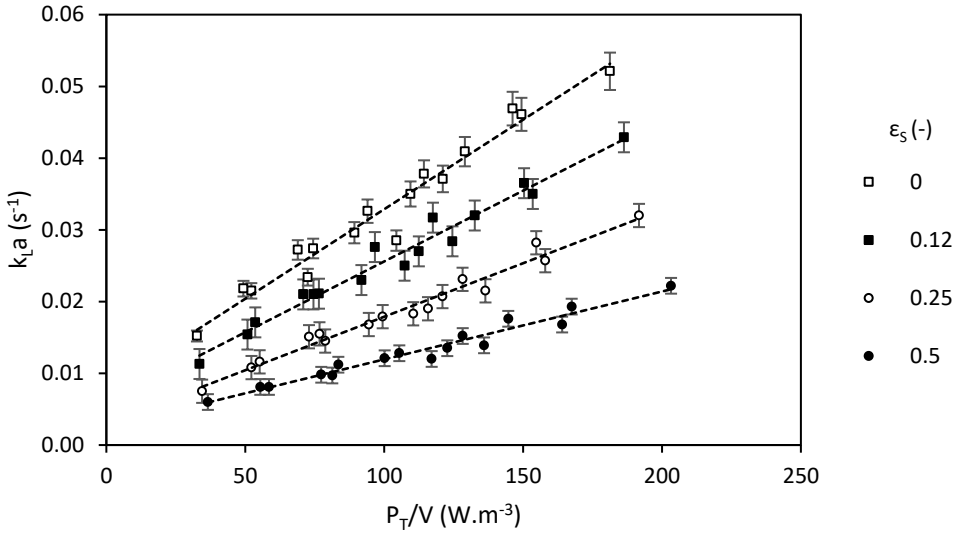

Figure 2.6 Effect of total power input on the oxygen transfer coefficient at different solid volume fractions

Table 2.4 Adjusted parameters for correlation in Eq. 15 at different solid contents (for the ranges of experimental parameters shown in Table 2.1)

Soil content (w/v%)	ε_S (-)	F ($m^3.W^{-1}.s^{-1}$)	K (s^{-1})	R^2
0%	0	2.5×10^{-4}	7.9×10^{-3}	0.96
5%	0.12	2.0×10^{-4}	5.9×10^{-3}	0.97
10%	0.25	1.5×10^{-4}	3.0×10^{-3}	0.97
20%	0.5	9.5×10^{-5}	2.5×10^{-3}	0.96

3.5. Alpha factor

3.5.1. Total power input and gas holdup effect

The effect of total power input and the gas holdup on the alpha factor for different solid volume fractions is shown in Figure 2.7. For all applied operating conditions, the alpha factor

is mainly controlled by the clay concentration. Furthermore, the alpha factor does not vary greatly with $\frac{P_T}{V}$ (Figure 2.7A) or ε_G (Figure 2.7B) for a fixed solid volume fraction (less than 15% from the average). This means that, for a fixed clay concentration in the slurry, the decrease on $k_L a$ values by the presence of solids is not significantly affected by power input or air superficial velocity at the clay concentrations tested. Hence, the reduction on the volumetric oxygen transfer coefficient in the slurry systems studied is mainly due to the presence of solid particles and the influences of $\frac{P_N}{V}$ and U_G are reduced proportionally for all conditions tested.

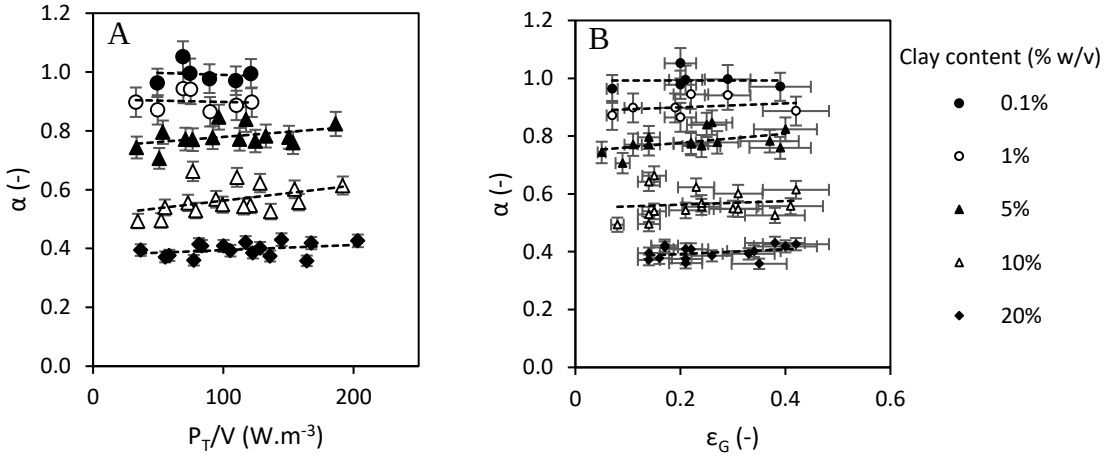

Figure 2.7 Effect of (A) total power input and (B) gas holdup on the alpha factor at different clay concentration (%w/v wet basis).

Since the total power input does not affect alpha values for a fixed clay concentration, an average alpha value for each clay concentration condition can be used. Table 2.5 shows the average α factor corresponding to each clay content. It can be noticed that the gas liquid transfer coefficient decreases while the clay content increases, even for low solid content (from 0.5%). This result agree with the results of Woo and Park [15] for soils with high clay content.

Table 2.5 Average alpha factor for each clay content (for the operational parameters range given in Table 2.1).

Clay content (%w/v wet basis)	ε_S (-)	Average α factor (-)
0.1%	0.002	0.99 ± 0.03
0.5%	0.01	0.93 ± 0.04
1%	0.02	0.90 ± 0.03
2.5%	0.06	0.82 ± 0.03
5%	0.12	0.79 ± 0.03
10%	0.25	0.57 ± 0.03
20%	0.5	0.40 ± 0.01

3.5.2. Slurry physicochemical properties effect

Furthermore, the behavior of the average alpha factor in relation with the solid volume fraction can be contrasted with the property changes of the slurry due to the clay concentration, namely viscosity and density. With this aim, the Archimedes number was used (Eq. 16).

$$Ar = \frac{\rho_L(\rho_L - \rho_G) g {d_b}^3}{\mu^2} \tag{16}$$

This dimensionless number represents the ratio of the buoyancy force to viscous forces, and in its definition the bubble size is needed. However, for this study, it was not possible to measure this parameter. Therefore, an estimation using the theoretical relation proposed by García-Ochoa and Gomez [49] (Eq. 17) was given.

$$d_b = \frac{0.7\sigma^{0.6}}{(P_T/V)^{0.4}{\rho_L}^{0.2}} \left(\frac{\mu_L}{\mu_G}\right)^{0.1} \tag{17}$$

Combining Eq. 17 with the definition of the total power input (Eq. 1, Eq. 2 and Eq. 3), it is possible to define a ratio of the bubble size in slurry to that in tap water, at the same stirring speed and air superficial velocity, as a function of the apparent density and apparent viscosity of the respective phases (Eq. 18).

$$\frac{d_{b,Sl}}{d_{b,W}} = \left(\frac{\rho_{Sl}}{\rho_W}\right)^{-0.6} \left(\frac{\mu_L}{\mu_G}\right)^{0.1} \tag{18}$$

Within the range of clay content investigated and by using Eq. 18, a slight decrease of the bubble average size due to presence of solids can be observed. However, this variation is lower than 2% for all clay concentrations (Figure 2.8). This means that changes in both apparent density and apparent viscosity does not seem to significantly affect the bubble size. Consequently, it can be concluded that the effect of clay concentration on the bubble size can be neglected and this parameter is considered to be constant at fixed N and U_G.

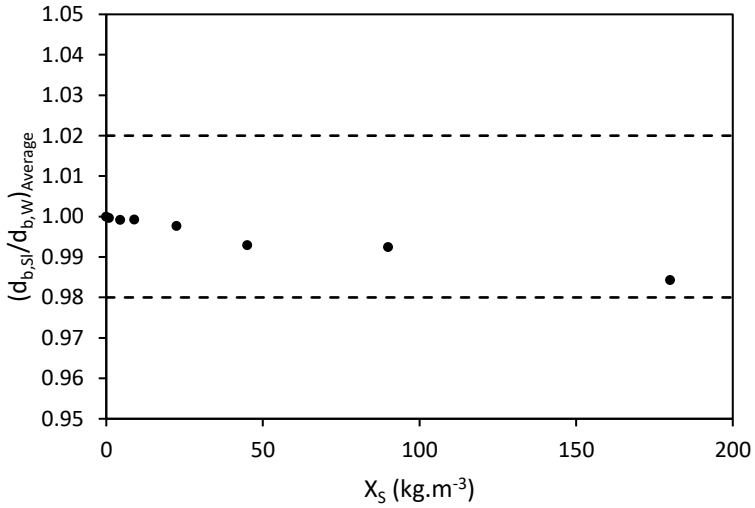

Figure 2.8 Variation of the average estimated bubble size. The dashed lines represent a variation of ±2%

Furthermore, a ratio of the Archimedes number in the slurry to the Archimedes number in tap water ($\frac{Ar_{Sl}}{Ar_w}$) has been defined (Eq.19), considering a constant bubble size, to highlight the impact of the clay content on this dimensionless number.

$$\frac{Ar_{Sl}}{Ar_w} = \left(\frac{\rho_{Sl}}{\rho_w}\frac{\mu_w}{\mu_{Sl}}\right)^2 \tag{19}$$

Figure 2.9 shows a comparison between the ratio of Archimedes numbers and the alpha factor as function of the solid volume fraction. Both the ratio of Archimedes numbers and the alpha factor decrease with the solid fraction volume and, hence, the clay concentration in the slurry, increase. Furthermore, a similar (but not completely identical) behavior of both curves can be noticed, and three phases can be identified.

The presence of solids in the slurry can influence the gas-liquid transfer via different mechanisms, i.e. i) by changing in apparent viscosity and density, leading to changes in the rheological properties and the buoyancy forces of the fluids; ii) by creating steric effects, producing bubble trajectory changes, increasing bubble residence time and producing bubble coalescence; iii) by adsorbing onto the gas-liquid surface (bubble contamination), causing a reduction in the effective transfer area and; iv) by adsorbing oxygen molecules on their surface, enhancing the transfer rate. One can then use these mechanisms to hypothesize the variations in the volumetric oxygen transfer coefficient in each phase observed.

In the first phase (I) ($\varepsilon_S < 0.025$; clay content < 1 % w/v), it is possible to observe a clear decrease in average α values which is not reflected by the $\frac{Ar_{Sl}}{Ar_w}$ ratio. During this phase, variations of apparent viscosity and apparent density are negligible $\left(\frac{Ar_{Sl}}{Ar_w} \approx 1\right)$. Thus, little influence of these physicochemical properties can be assumed and no impact on gas hold-up has been observed. Moreover, the volume occupied by the solids in the suspensions is not significant, meaning that the main mechanism influencing the $k_L a$ behavior can be assumed to be bubble contamination (mechanism iii previously described). This phenomenon has been addressed in the context of gas-liquid mass transfer in the literature. For instance, Ferreira et al. [46] reported that solid particles (expandable polystyrene and polyvinyl chloride beads) have generally a negative effect on the gas liquid transfer and this impact depends mainly on the size and density of the solid particles and its affinity for the gas phase. Mena et al. [48] found that very fine expandable polystyrene beads (d_p = 0.1µm) can act as impurities on the surface of the bubbles and block the mass transfer area. However, hollow glass beads with a bigger size particle (d_p = 9.6 µm) can avoid coalescence, stabilizing bubbles and increasing the transfer rate at low concentrations (< 3 vol.%). Even if the material and density of the solid particles studied by these researchers differ from those of clay particles, similar effects may be theorized for both systems. Accordingly, fine clay particles might obstruct the transfer area by attaching to the bubble surface and this can cause a decrease in the oxygen transfer rate (even at very low concentrations).

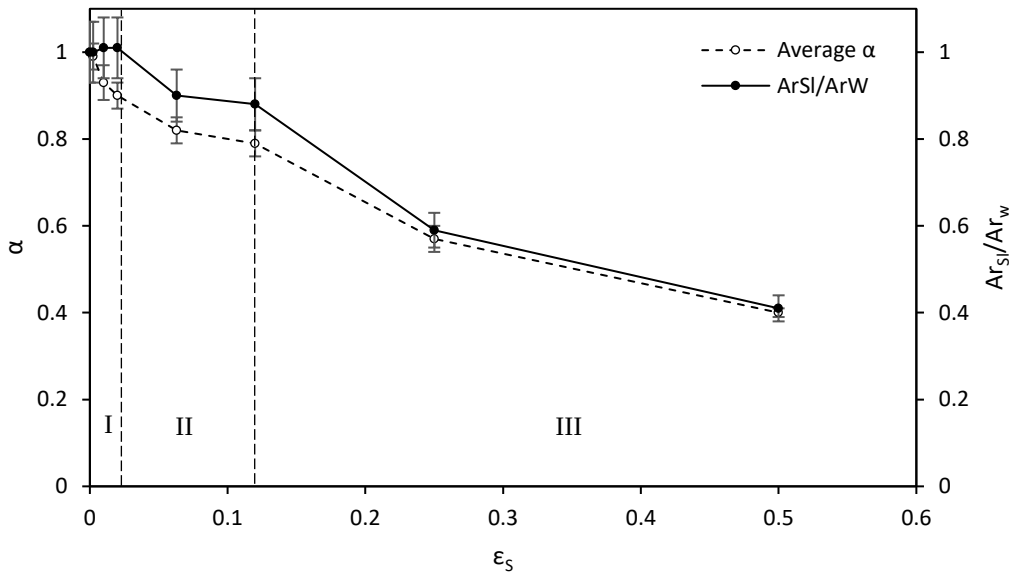

Figure 2.9 Average alpha factor and ratio of Archimedes number for different solid volume fractions

In the second phase (II) (ε_S between 0.025 and 0.063; equivalent to 1% and 5% w/v respectively), a slighter decrease in the values of α can be observed. On one hand, the density effect can still be neglected in this phase in comparison with viscous effects. In fact, for a clay content of 5% w/v, the slurry density increases only by 3% compared to water density. On the other hand, the viscosity increment can be highlighted by the decrease in the ratio of Archimedes number. These changes in viscosity (up to 10% from water viscosity) can lead to an increase in the drag force of ascending bubbles and retain them in the slurry. Additionally, the number of particles and the volume occupied by them have increased importantly. This means that probably steric effects (mechanism ii) start to play a role in the transfer [11].

Finally, in the third phase (III), the ratio of Archimedes number highly decreases with an increase in solid volume fraction, and both viscosity (as main factor) and density (as minor factor) start to have a significant influence on the surface renewal and the buoyancy forces of the bubbles, respectively (mechanism i). These changes trigger a more noticeable decrease in the oxygen mass transfer process.

Oxygen adsorption on clay (mechanism iv) has not been addressed in the literature as an important transfer mechanism. This is probably because of the much higher affinity of clay surface to water compared to non-polar gasses [50].

The fact that the decrease on $k_L a$ values, caused by the presence of solids, can be explained only by changes in the apparent viscosity and density of the slurry in phases II and III seems to confirm the hypothesis regarding the small effect of solids on the bubble size, the relative gas holdup and, hence, the bubble residence time. This suggests that clay presence significantly affects the specific transfer area (a) due to bubble contamination and steric effects. Similarly, solids may affect the oxygen transfer coefficient (k_L) during the phases II and III due to physicochemical changes and buoyancy effects.

Figure 2.10 shows the average alpha factor as a function of the average ratio of Archimedes numbers for each clay concentration, excluding the points corresponding the first phase, where neither viscosity nor density are involved in the decrease of oxygen transfer. A linear correlation with a slope of m = 0.91 and with R^2 = 0.99 (Eq. 20) has been calculated (valid for the ranges of experimental parameters shown in Table 2.1).

$$\frac{k_L a_{Sl}}{k_L a_W} = m \frac{Ar_{Sl}}{Ar_W} \tag{20}$$

By using Eq. 20, one can predict the oxygen transfer coefficient in slurry systems by only knowing the Bingham plastic viscosity, the density of the clay slurry and the oxygen transfer coefficient in tap water for the conditions tested in this study (at clay content >1% w/v) with an error of less than 15%. Figure 2.11 shows the correlation of experimental and predicted $k_L a$ values using the proposed correlation ($R^2 = 0.97$).

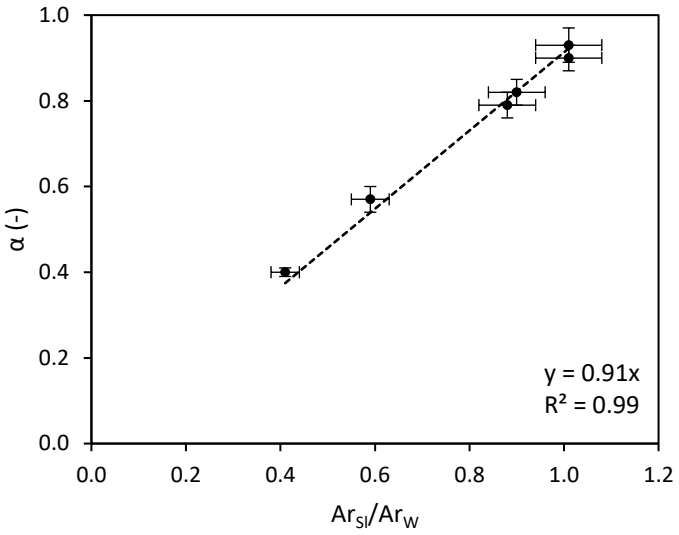

Figure 2.10 Alpha factor as a function of the ratio of Archimedes numbers

Figure 2.12 presents the model proposed for the calculation of the volumetric oxygen mass transfer coefficient. This model is valid for the gas mixing regime of this study and operational parameter ranges presented in Table 2.1.

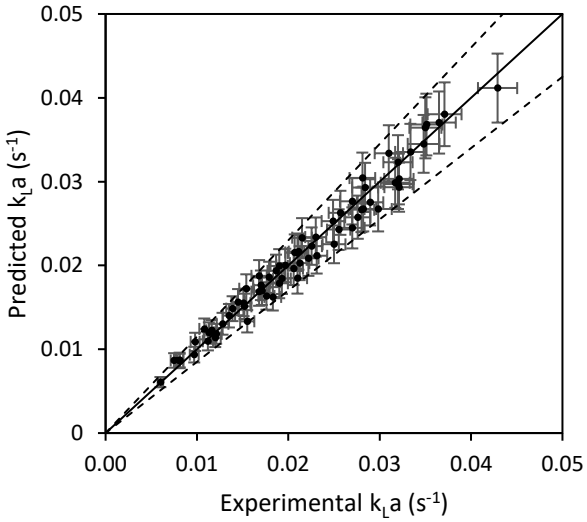

Figure 2.11 Dispersion of the oxygen transfer coefficient using the alpha model (Dashed lines represent 15% of deviation)

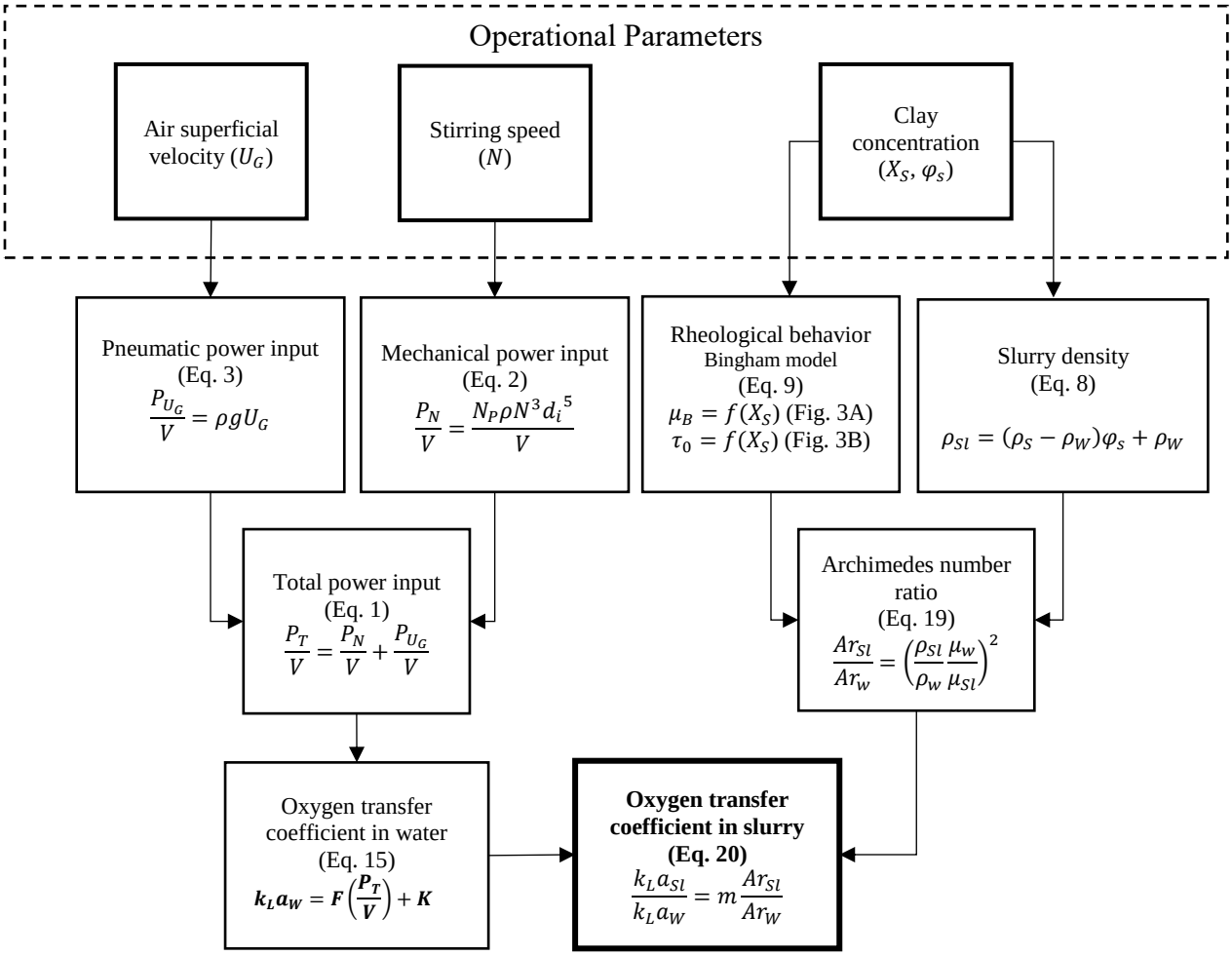

Figure 2.12 Model schematization for the estimation of the oxygen transfer coefficient in slurry phase at the conditions tested in this study

4. Conclusions

The present research focused on the study of the gas-liquid mass transfer in clay slurry phase at a wide range of solid volume fraction and atypical power input conditions (power input generated by aeration not negligible) and using an axial impeller (marine propeller) for mechanical agitation. In these conditions, the rheological behavior of the clay-water slurry can be modelled using the Bingham rheological model. Besides, the air bubbles are not homogeneously dispersed in the reactor and, as a consequence, the relative gas holdup of the system does not depend on the air superficial velocity or the clay content, except at low U_G, where clay content has a noticeable influence.

The volumetric oxygen mass transfer coefficient varies linearly with the total power input applied to the system and the alpha factor is independent of both the gas holdup and the total

power input, which means that it only depends on the clay concentration. This effect might be attributed to density and viscosity changes in the slurry, as well as bubble contamination. Furthermore, the latter might be responsible for the decrease of the volumetric oxygen mass transfer coefficient also at low solid volume fractions. A linear correlation between the alpha factor and the ratio of Archimedes number of the slurry to the one of water has been proposed. It is important to highlight that this model is applicable for the operational conditions tested in this research work. Further research is needed to assess the applicability in other gas mixing regimes. This can be achieved by extending the operational parameter ranges or by using different types of impellers.

Finally, as demonstrated in this study, clay presence in soils can strongly affect oxygen transfer in slurry systems. Therefore, during the design and operation of a slurry bioreactor, it is important to consider the clay content and the soil concentration as parameters that can affect the entire biodegradation process. Besides, it is known that the biomass can alter the physicochemical properties of the liquid phase [12]. It is important then to consider the effect of both solid particles interacting in the slurry phase and the effect of other operational parameters (such as stirring speed, air superficial velocity, pH and temperature) on this interaction and in the overall bioremediation process.

References

[1] A.M. Thayer, Bioremediation: Innovative Technology for Cleaning Up Hazardous Waste, Chem. Eng. News. 69 (1991) 23–44. doi:10.1021/cen-v069n034.p023.

[2] S. Colombano, A. Saada, V. Guerin, P. Bataillard, G. Bellenfant, S. Beranger, D. Hube, C. Blanc, C. Zornig, I. Girardeau, Quelles techniques pour quels traitements–Analyse coûts-bénéfices, Rapp. Final BRGM-RP-58609-FR. (2010).

[3] R. Boopathy, Factors limiting bioremediation technologies, Bioresour. Technol. 74 (2000) 63–67.

[4] I.V. Robles-González, F. Fava, H.M. Poggi-Varaldo, A review on slurry bioreactors for bioremediation of soils and sediments, Microb. Cell Factories. 7 (2008) 5. doi:10.1186/1475-2859-7-5.

[5] C. Trellu, A. Miltner, R. Gallo, D. Huguenot, E.D. van Hullebusch, G. Esposito, M.A. Oturan, M. Kästner, Characteristics of PAH tar oil contaminated soils—Black particles, resins and implications for treatment strategies, J. Hazard. Mater. 327 (2017) 206–215. doi:10.1016/j.jhazmat.2016.12.062.

[6] R.L. Crawford, D.L. Crawford, Bioremediation: Principles and Applications, Cambridge University Press, 2005.

[7] D.O. Pino-Herrera, Y. Pechaud, D. Huguenot, G. Esposito, E.D. van Hullebusch, M.A. Oturan, Removal mechanisms in aerobic slurry bioreactors for remediation of soils and sediments polluted with hydrophobic organic compounds: An overview, J. Hazard. Mater. 339 (2017) 427–449. doi:10.1016/j.jhazmat.2017.06.013.

[8] C. Fu, S. Pfanstiel, C. Gao, X. Yan, R. Govind, H.H. Tabak, Studies on contaminant biodegradation in slurry, wafer, and compacted soil tube reactors, Environ. Sci. Technol. 30 (1996) 743–750.

[9] F. Garcia-Ochoa, E. Gomez, Bioreactor scale-up and oxygen transfer rate in microbial processes: An overview, Biotechnol. Adv. 27 (2009) 153–176. doi:10.1016/j.biotechadv.2008.10.006.

[10] C. Duran, Y. Fayolle, Y. Pechaud, A. Cockx, S. Gillot, Impact of the activated sludge suspended solids on its non-Newtonian behavior and oxygen transfer in a bubble column, Chem. Eng. Sci. (2016). https://hal-upec-upem.archives-ouvertes.fr/hal-01394418.

[11] C. Freitas, J.A. Teixeira, Oxygen mass transfer in a high solids loading three-phase internal-loop airlift reactor, Chem. Eng. J. 84 (2001) 57–61. doi:10.1016/S1385-8947(00)00274-6.

[12] S.S. Alves, S.P. Orvalho, J.M.T. Vasconcelos, Effect of bubble contamination on rise velocity and mass transfer, Chem. Eng. Sci. 60 (2005) 1–9. doi:10.1016/j.ces.2004.07.053.

[13] J. Huang, T. Saito, Influences of gas–liquid interface contamination on bubble motions, bubble wakes, and instantaneous mass transfer, Chem. Eng. Sci. 157 (2017) 182–199. doi:10.1016/j.ces.2016.05.013.

[14] J.V. Littlejohns, A.J. Daugulis, Oxygen transfer in a gas–liquid system containing solids of varying oxygen affinity, Chem. Eng. J. 129 (2007) 67–74. doi:10.1016/j.cej.2006.11.002.

[15] S. Woo, J. Park, Estimation of oxygen transfer in soil slurry bioreactor, Biotechnol. Tech. 11 (1997) 713–716.

[16] G.R. Kasat, A.B. Pandit, Review on Mixing Characteristics in Solid-Liquid and Solid-Liquid-Gas Reactor Vessels, Can. J. Chem. Eng. 83 (2008) 618–643. doi:10.1002/cjce.5450830403.

[17] J.A. Sánchez Pérez, E.M. Rodríguez Porcel, J.L. Casas López, J.M. Fernández Sevilla, Y. Chisti, Shear rate in stirred tank and bubble column bioreactors, Chem. Eng. J. 124 (2006) 1–5. doi:10.1016/j.cej.2006.07.002.

[18] S. Hall, Rules of Thumb for Chemical Engineers, Elsevier Science, 2017. https://books.google.fr/books?id=S6jRDgAAQBAJ.

[19] J.O. Robertson, H.H. Rieke, G.V. Chilingar, Viscosity Measurements of Aqueos Clay Suspensions as a Tool for Determining Mineralogic Type of Clays, Sedimentology. 4 (1965) 181–187.

[20] M.K. Stenstrom, R.G. Gilbert, Effects of alpha, beta and theta factor upon the design, specification and operation of aeration systems, Water Res. 15 (1981) 643–654. doi:10.1016/0043-1354(81)90156-1.

[21] S. Gillot, A. Héduit, Prediction of alpha factor values for fine pore aeration systems, Water Sci. Technol. 57 (2008) 1265. doi:10.2166/wst.2008.222.

[22] M. Jamnongwong, K. Loubiere, N. Dietrich, G. Hébrard, Experimental study of oxygen diffusion coefficients in clean water containing salt, glucose or surfactant: Consequences on the liquid-side mass transfer coefficients, Chem. Eng. J. 165 (2010) 758–768. doi:10.1016/j.cej.2010.09.040.

[23] K. Norrish, The swelling of montmorillonite, Discuss. Faraday Soc. 18 (1954) 120–134.

[24] P.F. Luckham, S. Rossi, The colloidal and rheological properties of bentonite suspensions, Adv. Colloid Interface Sci. 82 (1999) 43–92. doi:10.1016/S0001-8686(99)00005-6.

[25] M.D. Foster, The relation between composition and swelling in clays, Clays Clay Miner. 3 (1954) 205–220.

[26] F. Gridi-Bennadji, G.L. Lecomte-Nana, J.-P. Bonnet, S. Rossignol, Rheological properties of montmorillonitic clay suspensions: Effect of firing and interlayer cations, J. Eur. Ceram. Soc. 32 (2012) 2809–2817. doi:10.1016/j.jeurceramsoc.2011.11.018.

[27] R. Keren, Rheology of mixed kaolinite-montmorillonite suspensions, Soil Sci. Soc. Am. J. 53 (1989) 725–730.

[28] J. Mewis, N.J. Wagner, Colloidal Suspension Rheology, Cambridge University Press, 2012. https://books.google.fr/books?id=Et6kZGtdiFsC.

[29] M.M. Ramos-Tejada, F.J. Arroyo, R. Perea, J.D.G. Durán, Scaling Behavior of the Rheological Properties of Montmorillonite Suspensions: Correlation between Interparticle Interaction and Degree of Flocculation, J. Colloid Interface Sci. 235 (2001) 251–259. doi:10.1006/jcis.2000.7370.

[30] E.-J. Teh, Y.K. Leong, Y. Liu, A.B. Fourie, M. Fahey, Differences in the rheology and surface chemistry of kaolin clay slurries: The source of the variations, Chem. Eng. Sci. 64 (2009) 3817–3825. doi:10.1016/j.ces.2009.05.015.

[31] M. Benna, N. Kbir-Ariguib, A. Magnin, F. Bergaya, Effect of pH on rheological properties of purified sodium bentonite suspensions, J. Colloid Interface Sci. 218 (1999) 442–455.

[32] A. Kapic, T.J. Heindel, Correlating Gas-Liquid Mass Transfer in a Stirred-Tank Reactor, Chem. Eng. Res. Des. 84 (2006) 239–245. doi:10.1205/cherd.05117.

[33] V.B. Rewatkar, A.J. Deshpande, A.B. Pandit, J.B. Joshi, Gas hold-up behavior of mechanically agitated gas-liquid reactors using pitched blade downflow turbines, Can. J. Chem. Eng. 71 (1993) 226–237.

[34] T.N. Zwietering, Suspending of solid particles in liquid by agitators, Chem. Eng. Sci. 8 (1958) 244–253. doi:10.1016/0009-2509(58)85031-9.

[35] A.A. Yawalkar, V.G. Pangarkar, A.A. Beenackers, Gas hold-up in stirred tank reactors, Can. J. Chem. Eng. 80 (2002) 158–166.

[36] M. Bouaifi, G. Hebrard, D. Bastoul, M. Roustan, A comparative study of gas hold-up, bubble size, interfacial area and mass transfer coefficients in stirred gas–liquid reactors and bubble columns, Chem. Eng. Process. Process Intensif. 40 (2001) 97–111.

[37] M. Martín, F.J. Montes, M.A. Galán, Mass transfer rates from bubbles in stirred tanks operating with viscous fluids, Chem. Eng. Sci. 65 (2010) 3814–3824.

[38] T. Moucha, V. Linek, K. Erokhin, J.F. Rejl, M. Fujasová, Improved power and mass transfer correlations for design and scale-up of multi-impeller gas–liquid contactors, Chem. Eng. Sci. 64 (2009) 598–604. doi:10.1016/j.ces.2008.10.043.

[39] B. Özbek, S. Gayik, The studies on the oxygen mass transfer coefficient in a bioreactor, Process Biochem. 36 (2001) 729–741. doi:https://dx-doi-org.fennec.u-pem.fr/10.1016/S0032-9592(00)00272-7.

[40] D.B. Mills, R. Bar, D.J. Kirwan, Effect of solids on oxygen transfer in agitated three-phase systems, AIChe J. 33 (1987) 1542–1549.

[41] O. Ozkan, A. Calimli, R. Berber, H. Oguz, Effect of inert solid particles at low concentrations on gas–liquid mass transfer in mechanically agitated reactors, Chem. Eng. Sci. 55 (2000) 2737–2740. doi:10.1016/S0009-2509(99)00532-1.

[42] J. Gimbun, C.D. Rielly, Z.K. Nagy, Modelling of mass transfer in gas–liquid stirred tanks agitated by Rushton turbine and CD-6 impeller: A scale-up study, Chem. Eng. Res. Des. 87 (2009) 437–451. doi:10.1016/j.cherd.2008.12.017.

[43] M. Martín, F.J. Montes, M.A. Galán, Bubbling process in stirred tank reactors II: Agitator effect on the mass transfer rates, Chem. Eng. Sci. 63 (2008) 3223–3234. doi:10.1016/j.ces.2008.03.035.

[44] A. Karimi, F. Golbabaei, M.R. Mehrnia, M. Neghab, K. Mohammad, A. Nikpey, M.R. Pourmand, Oxygen mass transfer in a stirred tank bioreactor using different impeller configurations for environmental purposes, Iran. J. Environ. Health Sci. Eng. 10 (2013) 1.

[45] F. Garcia-Ochoa, E. Gómez, Mass transfer coefficient in stirred tank reactors for xanthan gum solutions, Biochem. Eng. J. 1 (1998) 1–10.

[46] A. Ferreira, C. Ferreira, J.A. Teixeira, F. Rocha, Temperature and solid properties effects on gas–liquid mass transfer, Chem. Eng. J. 162 (2010) 743–752. doi:10.1016/j.cej.2010.05.064.

[47] A.A.C.M. Beenackers, W.P.M. Van Swaaij, Mass transfer in gas—liquid slurry reactors, Chem. Eng. Sci. 48 (1993) 3109–3139. doi:10.1016/0009-2509(93)80199-Z.

[48] P. Mena, A. Ferreira, J.A. Teixeira, F. Rocha, Effect of some solid properties on gas–liquid mass transfer in a bubble column, Chem. Eng. Process. Process Intensif. 50 (2011) 181–188. doi:10.1016/j.cep.2010.12.013.

[49] F. Garcia-Ochoa, E. Gomez, Theoretical prediction of gas–liquid mass transfer coefficient, specific area and hold-up in sparged stirred tanks, Chem. Eng. Sci. 59 (2004) 2489–2501. doi:10.1016/j.ces.2004.02.009.

[50] C. Volzone, J.G. Thompson, A. Melnitchenko, J. Ortiga, S.R. Palethorpe, Selective gas adsorption by amorphous clay-mineral derivatives, Clays Clay Miner. 47 (1999) 647–657.

CHAPTER 3

Study of the volatilization of light aromatic compounds

CHAPTER 3 – Study of the volatilization of light aromatic compounds

Gas-liquid mass transfer, part II: Volatilization of three aromatic compounds is studied in this chapter. Bubbel volatilization and surface volatilization are tested. Moreover, two models using the transfer of oxygen and water as reference compound are verified and compared.

Abstract

Volatilization of hydrophobic organic compound have been observed in many water, wastewater and soil treatment processes. This phenomenon may become particularly important when mechanical agitation and/or bubble aeration are supplied to the system. Several models able to predict and quantify the pollutant transfer to the gas phase have been developed, being the proportionality coefficient (PC) the most common model used. This model is based on the use of oxygen as the only reference compound, making necessary to estimate the resistance to transfer in the gas phase. This resistance might be of importance for some volatile organic compounds (VOCs) and all semi-volatile compounds. Therefore, in this study the use of the two-reference compound model (2RC) (i.e. oxygen and water) able to calculate both the liquid-side and the gas-side resistance was proposed. Additionally, the Henry's law constants for the hydrophobic organic compounds (HOCs), which plays a key role in the model estimations, were obtained in the same device that was used for the experimental calculation of the mass transfer coefficients. The influence of the power input on the gas-liquid mass transfer was also evaluated. The results of the estimations for both the PC model and the 2RC model showed similar results. However, the latter constitute a more robust method to estimate the gas-liquid mass transfer coefficient of any compound and can be extrapolated to all substances (including semi-volatile compounds). Finally, the relevance and limitations of both models were established.

Nomenclature

A	Interfacial area (m^2)
a	Interfacial area per unit of liquid volume ($m^2.m^{-3}$)
A_B	Total interfacial area between the bubbles and the liquid phase (m^2)
A_S	Interfacial area on the top surface of the liquid phase (m^2)
a_S	Interfacial area on the top surface of the liquid phase per unit of liquid volume ($m^2.m^{-3}$)
B	Constant in Eq. 53
C_G	Concentration in the gas phase ($kg.m^{-3}$)
$C_G^{ln}.$	Logarithmic mean of the inlet and outlet concentrations in gas phase ($kg.m^{-3}$)
C_G^*	Equilibrium concentration in the gas phase ($kg.m^{-3}$)
C_L	Concentration in the liquid phase ($kg.m^{-3}$)
C_L^*	Equilibrium concentration in the liquid phase ($kg.m^{-3}$)
D_G	Gas diffusivity ($m^2.s^{-1}$)
d_i	Impeller diameter (m)
D_L	Liquid diffusivity ($m^2.s^{-1}$)
DO	Dissolved oxygen ($mg.L^{-1}$)
H_C	Dimensionless Henry's constant (-)
K_G	Overall mass transfer coefficient defined from the gas phase ($m.s^{-1}$)
k_G	Individual mass transfer coefficient in the gas film ($m.s^{-1}$)
K_L	Overall mass transfer coefficient defined from the liquid phase ($m.s^{-1}$)
k_L	Individual mass transfer coefficient in the liquid film ($m.s^{-1}$)
m	Gas diffusivity exponent (-)
N	Stirring speed (s^{-1})
$\dot{N}$	Mass transfer rate ($kg.s^{-1}$)
N_P	Power number (-)
n	Liquid diffusivity exponent (-)
$\frac{P_N}{V}$	Mechanical power input ($W.m^{-3}$)
Q_G	Air flow rate ($m^3.s^{-1}$)
r_c	Surface renewal rate (s^{-1})
R_G	Gas-side resistance to transfer ($s.m^{-1}$)
R_L	Liquid-side resistance to transfer ($s.m^{-1}$)
R_T	Total resistance to transfer ($s.m^{-1}$)
S_d	Saturation degree (-)
S_p	Slope (s^{-1})
t	time (s)
t_c	Contact time (s)
t_r	Bubble residence time (s)
U_G	Air superficial velocity ($m.s^{-1}$)
V_G	Gas volume (m^3)
V_L	Liquid volume (m^3)

Greek letters

γ	Exponent in Eq. 53 (-)
δ_G	Shear rate (s^{-1})
δ_L	Gas holdup (-)
ρ	Density ($kg.m^{-3}$)

Sub-indexes

HOC	Relative to Hydrophobic Organic Compound
i	Relative to the interface
O_2	Relative to Oxygen
ref	Relative to a reference compound
W	Relative to Water

Super-indexes

B	Relative to bubble volatilization
in	Relative to the inlet
S	Relative to surface volatilization
out	Relative to the outlet
e	Estimated

Acronyms

2RC	Two-reference compound model
HOC	Hydrophobic organic compound
NAP	Naphthalene
PAH	Polycyclic aromatic hydrocarbons
PC	Proportionality coefficient model
PHE	Phenanthrene
TOL	Toluene
VOC	Volatile organic compound

1. Introduction

Over the last decades, the occurrence of hydrophobic organic compounds (HOCs) as pollutants in the aquatic environments and soils has become a major environmental concern. Among the pollutants concerned, many are volatile and semi-volatile and can thus be transferred to the atmosphere due to mass transfer processes. Physicochemical and biological processes are often used to remove these pollutants during wastewater treatment, water purification treatments and soil remediation. In general, these processes need mixing to improve the homogeneity and the reactor performance and/or the introduction of a gas phase by a diffuser (aerobic biological treatment, ozonation, electro-Fenton, etc.). In systems open to the atmosphere, the mechanical power input promotes the surface aeration of the reactor, but it favors simultaneously the transfer of the most volatile molecules to the gas phase. In the same way, bubble dispersion through the liquid phase favors the transfer of the desired gas and at the same time the stripping of some volatile and semi-volatile compounds. However, despite the environmental and public health issues, the volatilization process has been, in general, severely underestimated in wastewater treatment process [1] and even not considered in many research papers [2].

The most susceptible compounds to transfer are usually called volatile organic compounds (VOCs) and other compounds exhibiting the same behavior but in lesser extent (e.g. polycyclic aromatic compounds or PAHs) are frequently referred as “semi-volatile compounds”. In general, the Henry’s law constant determines the degree of volatilization of any compound [3]. However, the limit between the “volatile” and the “semi-volatile” categories is not clearly defined and there is no consensus in the literature regarding this topic. Furthermore, it is difficult to generalize because the extent of the volatilization does not only depend on the molecules properties but also on the local hydrodynamic conditions [4].

To predict the gas-liquid mass transfer rate of volatile and semi-volatile compounds, many authors have used oxygen as a reference molecule [5–7]. They relate its mass transfer coefficient to the mass transfer coefficient of oxygen using a proportionality factor that only depends on the ratio of the diffusion coefficients of the two molecules. This approach assumes that the mass transfer is controlled by the liquid-phase resistance. Nevertheless, this is only valid for very volatile compounds and, conversely, for less volatile compounds for which the gas phase resistance cannot be neglected more complex models should be used [8].

In this sense, two models have been proposed for semi-volatile molecules. The most complex is the sum of two reference compound resistances (or two-reference compound model, 2RC), in which, to estimate the mass transfer rate of the molecule considered, the mass transfer rate of two reference molecules need to be known; one whose transfer is controlled by the gas phase and one whose transfer is controlled by the liquid phase [9]. The second model uses the sum of resistances of the same reference molecule, requiring only one reference compound (in general oxygen). It is called the proportionality coefficient (PC) model. Unlike the 2RC model, the PC model is based only on the measurement of the liquid-phase resistance and the gas phase resistance is estimated and not experimentally measured [6]. Only very few studies have been performed to validate these models and no comparisons between them have been done. Therefore, there is a need to further investigate and to assess methodologies and models allowing to predict mass transfer of volatile and semi-volatile molecules. In addition, most models require values of Henry's law constant (H_C) of the targeted compound. Sander [10] has created an extensive compilation of this parameters and it is noticeable that for many compounds, and particularly for HOCs, the range of values can be very wide, comprising several orders of magnitudes in some cases. The H_C has a critical influence on the mass transfer coefficient estimation and inaccurate values can lead to important errors in the estimation of the volatilization rates [11].

For all these reasons, the main purpose of this research work was to study and to model the gas-liquid surface mass transfer process of HOCs using both the PC model and the 2RC model. Three HOCs: one VOC (toluene) and two PAHs (naphthalene and phenanthrene) were selected as model molecules for the volatile and semi-volatile groups for this research work. Additionally, oxygen and water mass transfer coefficients were obtained as they were employed as reference compounds in the modeling. Also, the Henry's law constants for the HOCs were experimentally calculated. Experimental and modeling results were used to elaborate a comparative analysis of both the PC and the 2RC model.

2. Mass transfer modeling

2.1. The two-film theory

According to the two-film theory of mass transfer, when a compound is transferred between two phases, it passes through two thin films that are formed on each side of the interface between these phases (Figure 3.1). The gradient of concentration in each layer decreases in the direction of the mass transfer and the relation of the concentrations at the interface is

given by the Henry's law (Eq. 21). Moreover, Henry's law defines also the equilibrium concentration of each phase through Eq. 22 and Eq. 23.

$$C_{G,i} = H_c C_{L,i} \tag{21}$$

$$C_G^* = H_c C_L \tag{22}$$

$$C_L^* = \frac{C_G}{H_c} \tag{23}$$

Three possible cases of mass transfer are depicted in Figure 3.1: (i) the transfer of a substance dissolved in the liquid phase, in this case an HOCs, into the gas phase, usually called volatilization; (ii) the transfer of a substance present in the gas phase, such as oxygen in air, into the liquid phase, called absorption; and (iii) the transfer of a liquid substance, such as water, to the gas phase at a temperature below its boiling point, known as evaporation.

If no accumulation in any of the thin layers is assumed, the mass transfer rate for any compound moving from the liquid phase to the gas phase is given by Eq. 24 (in the liquid film) and Eq. 25 (in the gas film). If the compound is moving in the other direction (from the gas phase to the liquid phase), an inversion of terms in the gradient will be enough to adjust these equations.

$$\dot{N} = k_L A\left(C_L - C_{L,i}\right) \tag{24}$$

$$\dot{N} = k_G A\left(C_{G,i} - C_G\right) \tag{25}$$

k_L and k_G represent the individual mass transfer coefficient corresponding to the liquid-phase layer and the gas-phase layer correspondingly, and A is the interfacial area through which the transfer occurs.

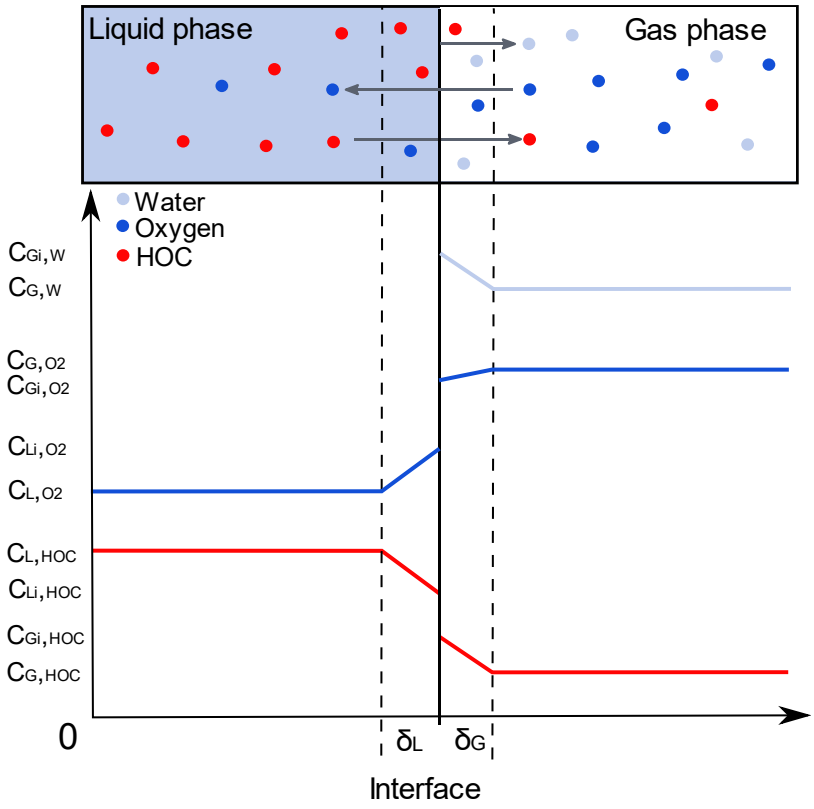

Figure 3.1 Two-film theory schema

Since no accumulation in the layers is assumed, Eq. 24 and. Eq. 25 can be equalized. Then, invoking Henry's law (Eq. 21-23), the transfer rate by unit of volume of a compound from the liquid phase to the gas phase can be calculated using either Eq. 26 or Eq. 27, depending on the phase in which the relation is applied, and defining the volumetric transfer area as $a = \frac{A}{V_L}$.

$$\frac{dC_L}{dt} = K_L a(C_L^* - C_L) \tag{26}$$

$$\frac{dC_L}{dt} = K_G a(C_G - C_G^*) \tag{27}$$

The overall volumetric mass transfer coefficient ($K_L a$) defined for the liquid phase in Eq. 26 is equal as the inverse of the sum of the reciprocals of the mass transfer coefficient of both the liquid layer and the gas layer (corresponding to a sum of resistances), as shown in Eq. 28. This coefficient is related to the one defined for the gas phase (in Eq. 27) by the Henry's law constant of the compound (Eq. 29).

$$K_L = \frac{1}{\frac{1}{k_L} + \frac{1}{H_C k_G}} \;\; ; \;\; \frac{1}{R_T} = \frac{1}{R_L} + \frac{1}{R_G} \tag{28}$$

$$K_G a = H_C K_L a \tag{29}$$

For certain compounds, the resistances to the mass transfer in one of the phases can be negligible compared to the other phase. This is often the case for gases, such as oxygen, that at standard conditions encounter very low resistance in the gas phase. Thus, the overall mass transfer coefficient (K_L) may be assimilated to the individual transfer coefficient of the liquid phase (k_L) (Eq. 30) and it is common to call these processes as "liquid-phase controlled mass transfer".

$$K_L a \cong k_L a \tag{30}$$

On the other hand, for the substances with a much higher affinity for the liquid phase, the mass transfer can be considered "gas-phase controlled", meaning that the resistance in the liquid film can be considered unimportant. In this case, the overall mass transfer coefficient may be approximated to the individual transfer coefficient of the gas phase (k_G) (Eq. 31).

$$K_G a \cong k_G a \tag{31}$$

The contribution of the resistance of each phase depends mainly on the Henry's law constant of the compound being transfer which, in turn, depends on the temperature of the system. Nevertheless, the hydrodynamic conditions can also have an important role in the resistance to mass transfer in each film [8].

2.2. Mass transfer coefficient and diffusivity

Most models indicate that the mass transfer coefficient in each layer is proportional to the diffusivity raised to some power, as mentioned by Munz and Robert [8] (Eq. 32 and Eq. 33) .

$$k_L \propto (D_L)^n \tag{32}$$

$$k_G \propto (D_G)^m \tag{33}$$

This means that, knowing the individual mass transfer coefficient in each layer of a reference compound and the exponent of the diffusivity term, it may be possible to estimate this parameter for any desired compound using Eq. 34 and Eq. 35.

$$\frac{k_L}{k_{L,ref}} = \left(\frac{D_L}{D_{L,ref}}\right)^n \tag{34}$$

$$\frac{k_G}{k_{G,ref}} = \left(\frac{D_G}{D_{G,ref}}\right)^m \tag{35}$$

Depending of the mass transfer theory used to relate the diffusivity coefficient and the mass transfer coefficient and its underlying assumptions, *m* and *n* can take several values. Table 3.1 shows the expression of the relation in Eq. 34 for the main mass transfer theories existing in the literature. Analogously, the same relations can be applied for the gas film (Eq. 35).

Table 3.1 Relation between the mass transfer coefficient and the diffusivity

Theory	Expression	Exponent n value	Reference
Two-film theory	$k_L = \frac{D_L}{\delta_L}$	1	[12]
Penetration theory	$k_L = 2\sqrt{\frac{D_L}{t_c}}$	0.5	[13]
Surface renewal theory	$k_L = \sqrt{D_L r_c}$	0.5	[14]

In general, one of the theories and its corresponding value for m and/or n are chosen. However, some authors have estimated these values from experimental data. In fact, by combining Eq. 28 and the ratio of diffusivities, it is possible to estimate the overall mass transfer coefficient or the exponents for the diffusivity terms using Eq. (36. However, no consensus exists among the authors on the ranges, and even much less, on the specific values that these exponents might take. For example, Arogo et al. [15] mention that the possible values are ranging between 0.15 and 1, Mihelcic et al. [5] describe typically values between 0.5 and 0.6, Soltanali and Shams Hagani [16] define a range from 0.1 to 0.8, and Munz and Roberts [8] have found in the literature values between 0.1 and 0.8 with an average of 0.6 for n and recommend values for both m and n within 0.5 and 0.67. Moreover, the factors that might influence these parameters are not completely understood.

$$\frac{1}{K_L a} = \frac{1}{k_{L,ref} a \left(\frac{D_L}{D_{L,ref}}\right)^n} + \frac{1}{H_C k_{G,ref} a \left(\frac{D_G}{D_{G,ref}}\right)^m} \tag{36}$$

2.3. Volatilization

Any compound is susceptible of being volatilized from the surface of the solution where it is dissolved. This is a phenomenon occurring in any natural or artificial water body. In wastewater treatment plants, as well as in soil or sediment slurry treatments, this can be a non-negligible transfer mechanism for a given contaminant during the process [4,17]. This is particularly true for volatile and semi-volatile compound with low degradation kinetics and in reactors using surface aeration [11]. For the specific case of surface volatilization, the mass transfer rate can be described using the Eq. 37 and Eq. 38.

$$V_L \frac{dC_L}{dt} = K_L^S A_S \left(C_L - C_L^{*,S}\right) \tag{37}$$

$$\text{where } K_L^S a_S = \frac{1}{\frac{1}{k_L^S a_S} + \frac{1}{H_C k_G^S a_S}} \tag{38}$$

It is common to consider the concentration of the volatile or semi-volatile compound negligible in the gas phase. This can be true or not depending on the system studied. For example, in open treatment facilities using only surface aeration, the volatilized compound can readily disperse into the atmosphere. However, in agitated covered reactors or poorly surface-aerated tanks, where the gas phase remains contained and in contact with the liquid phase for a certain period of time, the compound can easily accumulate in the gas phase, decreasing the potential gradient for volatilization. If the gas phase concentration is not correctly considered, an important error in the estimation of the mass transfer coefficient can be introduced.

In the case of bubbly flow systems, compounds can transfer from the liquid phase to the bubbles as they rise. This phenomenon (often called stripping) can become the main removal mechanism of volatile and semi-volatile recalcitrant compounds in aerated reactors [18]. Therefore, it is important to quantify the transfer by stripping in order to account for it in the general mass balance of the system.

By analogy with the surface aeration, the mass transfer rate by bubble volatilization is given by Eq. 39. However, in this case, the transfer area is the interface between the dispersed bubbles in the liquid phase and the liquid phase itself (A_B).

$$V_G \frac{dC_G}{dt} = K_L^B A_B \left(C_L - C_L^{*,B}\right) \quad (39)$$

Replacing Eq. 23 in Eq. 39 and integrating in time from the moment in which a bubble enters into the reactor and when it exits (i.e. the gas residence time) and for all the bubbles dispersed in the gas phase, Eq. 40 is obtained.

$$ln\left|1 - \frac{C_L^{*,B}}{C_L}\right| = -\frac{K_L^B a V_L}{H_C V_G} t_r \quad (40)$$

The residence time of the gas in the reactor is defined as $t_r = \frac{V_G}{Q_G}$. If Eq. 40 is rearranged by using the relations established in Eq. 41 derived from Henry's law, which defines the saturation degree, it is possible to obtain the concentration of the desired compound in the bubble when it reaches the surface of the liquid as a function of the mass transfer coefficient, the Henry's law constant and the operational parameters of the reactor: V_L and Q_G (Eq. (42).

$$\frac{C_L^{*,B}}{C_L} = \frac{C_G}{C_G^{*,B}} = S_d \quad (41)$$

$$S_d = 1 - e^{\frac{K_L^B a V_L}{H_C Q_G}} \quad (42)$$

3. Materials and methods

This study was divided in two parts. Firstly, an experimental part in which the surface mass transfer coefficients for oxygen, water and the targeted HOCs (i.e. toluene, phenanthrene and naphthalene) as a function of the mechanical power input were obtained, as well as the HOC Henry's law constants. Secondly, using the values obtained in the experimental part, two models to calculate the HOC volumetric mass transfer coefficient were tested: the proportionality coefficient model (PC) and the two-reference compound (2RC) model. With this purpose, necessary estimations of parameters belonging to each model were performed, minimizing the errors between the experimental HOC transfer coefficients and the estimated ones. Finally, both models were compared based on their robustness and their accuracy.

3.1. Experimental part

3.1.1. Reactor and operating conditions

The experiments were carried out in a standard 4.2-L glass reactor (working volume) with a thermal jacket controlled at 20 °C and four baffles. The dimensions of the reactor are specified by Pino-Herrera et al. [2].

Mechanical agitation was supplied by a motor with digital controlled stirring speed coupled to a single marine propeller ($d_i = D/3$). The reactor was operated varying the corresponding operational parameters per test in the ranges given in Table 3.2. The power input was calculated using the power number (Eq. 43). The power number N_P is constant and equal to 0.35 for a marine propeller at turbulent conditions ($Re > 10^4$), which is the case for all conditions tested in this study [19].

$$\frac{P_N}{V} = \frac{N_P \rho N^3 {d_i}^5}{V_L} \tag{43}$$

Table 3.2 Operational parameters used in this study

Reactor configuration		Operational parameter	Units	Range
A	B			
×		Air superficial velocity, U_G (×10^3)	m.s^{-1}	0
	×	Air superficial velocity, U_G (×10^3)	m.s^{-1}	1.53 – 8.87
×	×	Mechanical power input, $\frac{P_N}{V}$	W.m^{-3}	17.65 – 94.52

Two reactor set-up configurations were used: A) for water, oxygen and HOCs surface mass transfer, the gas phase was introduced to the reactor using a plastic tube passing through holes in the lid, directing the airflow to the wall of the reactor. In this way, when the gas phase enters the reactors, preferential pathways for a direct exit and perturbations on the liquid surface were avoided; and B) for Henry's law constant determination of HOCs, the gas phase was injected from the bottom of the reactor through a porous glass sparger connected to a three-port L-shaped valve, providing the choice between an airflow and a nitrogen flow as needed.

3.1.1. HOC Henry's law constant determination

According to Matter-Müller et al. [20], assuming that in a batch reactor only HOC volatilization occurs, a mass balance in the liquid phase of a reactor in which only bubble

volatilization occurs would lead to Eq. 44. Invoking Henry's law (Eq. 23) and using Eq. 41, it is possible to obtain Eq. 45.

$$V_L \frac{dC_L}{dt} = -Q_G C_G^{out} \tag{44}$$

$$C_G^{out} = S_d H_C C_L \tag{45}$$

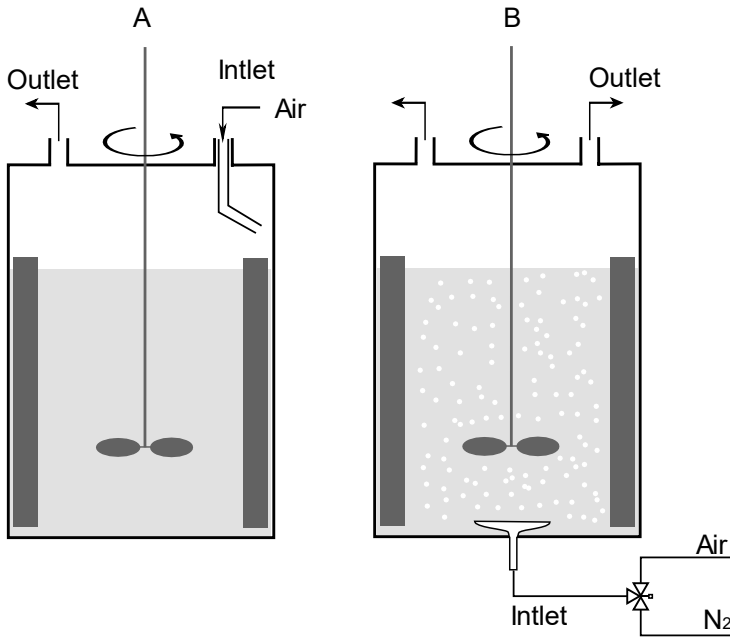

Figure 3.2 Experimental set-up: (A) Surface mass transfer and (B) Bubble mass transfer

Combining and rearranging Eq. 44 and Eq. 45, it is possible to obtain Eq. 46. If the concentration of the volatile compound in the liquid phase is recorded in time, a first order curve may be plotted and using Eq. 46, it would be possible to calculate the saturation degree and, hence, the diffused mass transfer coefficient. A linear correlation will be found between the natural logarithm of the normalized concentration of the volatilized product and time, and the slope of this correlation, Sp^B, will be defined by Eq. 47.

$$\frac{dC_L}{dt} = -\left(\frac{Q_G H_C}{V_L} S_d\right) C_L \tag{46}$$

$$Sp^B = -\frac{Q_G H_C}{V_L} S_d \tag{47}$$

Hsieh et al. [21] consider three cases regarding the saturation degree in the bubble: i) when $S_d \leq 0.1$, the slope, Sp^B is approximately equal to the diffused mass transfer coefficient; ii)

when $S_d \geq 0.99$, the bubbles will exit the liquid phase near saturation and the slope will approximate to $-\frac{Q_G H_C}{V_L}$ and iii) when $0.1 \geq S_d \geq 0.99$, the mass transfer coefficient must be calculated using the expressions in Eqs. 42 and 47. When bubble saturation (case ii) is reached in a range of air flows, a linear correlation between Sp^B and Q_G can be obtained and, using the slope of this correlation, it is possible to calculate accurately the Henry's law constant of a particular compound using Eq. 47 and assuming S_d = 1 [11].

Hydrophobic organic compounds used in this research work (toluene, naphthalene and phenanthrene) were obtained from Sigma-Aldrich chemicals (≥ 98% purity). Solvents (methanol and acetonitrile, HPLC grade) and phosphoric acid were obtained from VWR chemicals. Diffusivity of the compounds used in this study in air and water are shown in Table 3.3.

Table 3.3 Diffusivity of the compounds studied at 20¨C

Compound	Diffusivity in air (D_G) ($cm^2.s^{-1}$)	Diffusivity in water (D_L) ($cm^2.s^{-1}$)
Toluene (TOL)*	7.92×10^{-2}	8.4×10^{-6}
Naphthalene (NAP)*	5.9×10^{-2}	7.5×10^{-6}
Phenanthrene (PHE)*	5.4×10^{-2}	7.2×10^{-6}
Oxygen**	0.176	1.97×10^{-5}
Water**	0.26	-

* From Bedient et al. [22]
** From Cussler [23]

A solution of the three HOCs in water was prepared. For phenanthrene and naphthalene, a concentrated solution in methanol was previously made and 2 ml of this solution were added to 5 l of tap water, containing 3 ml of toluene. The amount of methanol in solution (< 0.04%) was low enough not to modify the HOC mass transfer in the system [24]. The solution was magnetically stirred until no droplets of toluene were observed and then filtered to remove any possible PAH crystals remaining suspended. The HOC solution (4.2 l) was added to the reactor.

For the Henry's law constant determination of selected HOCs, the reactor set-up configuration shown in Figure 3.2B was used. Samples of the liquid phase were taken before starting the introduction of the air flow and after, at appropriate times, and analyzed for HOC concentration. Experiments within the ranges of the operational parameters in Table 3.2 were performed. Samples were measured using an HPLC (Hitachi *LaChrom Elite® L-*

2400) coupled with UV/VIS detector (set to 254 nm) and a fluorescence detector (Excitation wavelength set to 250 nm and Emission wavelength set to 350 nm). The separation was performed using a RP C-18 end capped column (Purospher®, Merck) (5 mm, 25 cm × 4.6 mm) placed in an oven at 40 °C. The mobile phase was a mixture of water (with a pH adjusted to 2.5 using phosphoric acid) and acetonitrile (25:75 v/v) with a flow rate of 0.8 $ml.min^{-1}$ in isocratic mode. The injection volume was 20 µl.

3.1.2. Oxygen mass transfer coefficient determination

The oxygen transfer coefficients were obtained using the configuration shown in Figure 3.2B and were measured by the dynamic method (gassing out), described by García-Ochoa and Gomez [25]. Shortly, a nitrogen stream was injected to the system to remove the dissolved oxygen (DO). When the DO was less than 1 $mg.l^{-1}$, the nitrogen flow was interrupted, and the reactor was left open to the atmosphere. The curve of oxygen absorption was recorded using an inoLab® Oxi 7310 DO sensor connected to a Cellox 325 probe (WTW). From the oxygen absorption curves, the oxygen volumetric mass transfer coefficients ($k_{L,O_2}^{S}a_S$) in Eq. 48 were obtained, considering the response time of the electrode. The influence of power input on this parameter was measured within the range shown in Table 3.2.

$$\frac{dC_{L,O_2}}{dt} = k_{L,O_2}^{S}a_S\left(C_{L,O_2}^{\infty} - C_{L,O_2}\right) \tag{48}$$

3.1.3. Water mass transfer coefficient determination

The water transfer coefficients were obtained using the configuration shown in Figure 3.2A. An airflow was continuously introduced to the upper part of the experimental system and steady state conditions in the gas phase was reached. Then, the gas phase relative humidity and temperature was measured using a KIMO® AMI 310 multifunction meter at the inlet and the outlet of the reactor. The air flow was introduced in the gas phase from the top of the reactor, avoiding disturbances in the liquid surface and the saturation of the gas phase. The surface water transfer coefficient was subsequently obtained by performing a mass balance for the humidity in the gas phase (Eq. 49), knowing the psychrometric conditions of the air at the inlet and the outlet of the system. Several air flows were tested for the same agitation condition in order to check that this parameter did not affect the transfer coefficient. As in the case of oxygen mass transfer, the influence of power input on this parameter was measured within the range shown in Table 3.2.

$$C_{G,W}^{in} Q_G + k_{G,W} a\left(C_{G,W}^{\infty} - C_{G,W}^{ln}\right) = C_{G,W}^{out} Q_G \quad (49)$$

3.1.4. HOCs mass transfer coefficient determination

The overall HOC surface mass transfer coefficients were obtained using the reactor set-up configuration in Figure 3.2A. An HOC solution was prepared as explained in section 3.1.1 and introduced in the reactor (4.2 l). In the same way as for surface water transfer, an air flow was introduced from the top of the reactor through the lid avoiding disturbances in the liquid surface, in order to remove any accumulation of HOCs in the gas phase. In this case, HOC gas phase concentration was considered negligible, since the gas phase was continuously renewed ($C_L^{*,S}$ = 0). Therefore, Eq. 37 could be simplified to Eq. 50. A batch volatilization experiment where the HOC concentration was measured as a function of time led to a first order equation from which the HOC surface mass transfer coefficient was easily calculated. The influence of power input on this parameter was measured within the range shown in Table 3.2.

$$\frac{dC_L}{dt} = K_L^S a_S C_L \quad (50)$$

3.2. HOC mass transfer modeling

In this study, two models to predict the individual and the overall gas-liquid mass transfer coefficients of the HOCs were tested and compared. Both models are based on the sum of resistances (in Eq. 18) and the use of reference compounds. However, they differ in the use of one (PC model) or two (2RC model) substances as reference compounds. Figure 3.3 shows a schema of the parameter estimation followed in this study. Firstly, from the experimental data of this study and assumed parameters corresponding to each model, the HOC overall mass transfer coefficients for each condition of $\frac{P}{V}$ were calculated. Then, the error between these calculated coefficients and the experimental ones was minimized by modifying the initial assumed parameters. Once the minimal error was obtained, the estimated parameters for each model were analyzed and compared.

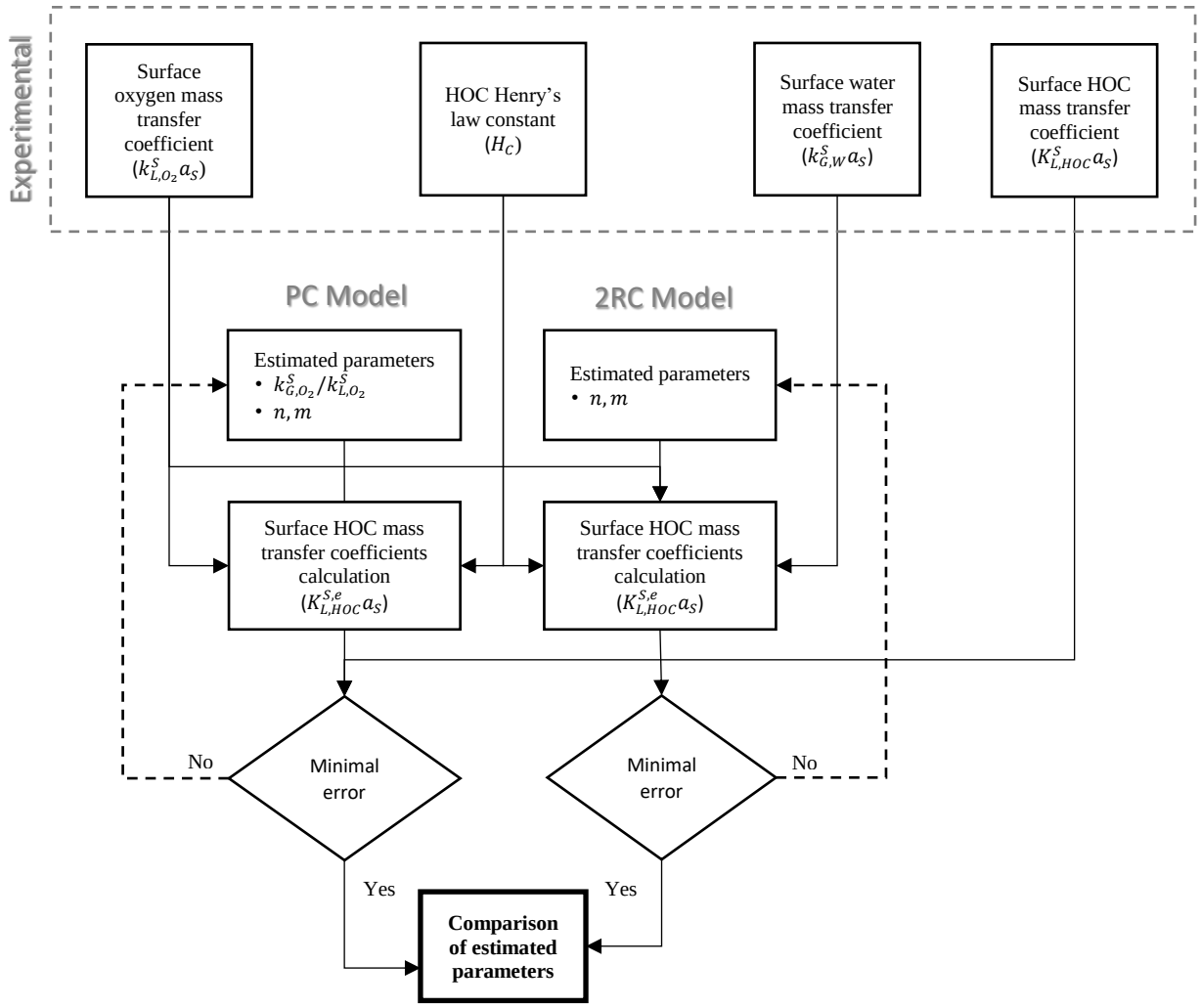

Figure 3.3 Modeling approach used in this study

3.2.1. 2RC model

In liquid-phase mass transfer processes, oxygen is often used as reference compound. The reason for this is that, during its transfer and due to its high H_C, the gas-phase resistance can be considered negligible and Eq. 30 can be applied. Conversely, in aqueous solutions, water presents a virtually non-existent transfer resistance in the liquid phase, which allows the use of Eq. 31 for this compound. Then, by means of both oxygen and water as reference compounds in Eq. 38, the HOC mass transfer coefficient could be estimated using Eq. 51, the sum of resistances of two reference compounds (2RC model). However, since in the literature there is not a consensus in either which value use for the diffusivity's exponents, n and m, or how they can be best estimated, they were fitted minimizing the error between the experimental values for the HOC mass transfer coefficients obtained in this research work and the calculated ones using Eq. 51.

$$\frac{1}{K_{L,HOC}^{S} a_S} = \frac{1}{k_{L,O_2}^{S} a_S \left(\frac{D_{L,HOC}}{D_{L,O_2}}\right)^n} + \frac{1}{H_C k_{G,W}^{S} a_S \left(\frac{D_{G,HOC}}{D_{G,W}}\right)^m} \quad (51)$$

3.2.2. PC model

Hsieh et al. [6] transformed Eq. 36 by using only oxygen as the reference compound and defining the proportionality coefficient (PC), Ψ, as shown in Eq. 52. This relation was also tested by fitting both exponents n and m, as well as the ratio of individual oxygen mass transfer coefficients ($k_{G,O_2}^{S} a_S / k_{L,O_2}^{S} a_S$).

$$(\Psi)^{-1} = \frac{K_{L,O_2}^{S} a_S}{K_{L,HOC}^{S} a_S} = \frac{1}{\left(\frac{D_{L,HOC}}{D_{L,O_2}}\right)^n} + \frac{1}{H_C\left(k_{G,O_2}^{S} a_S / k_{L,O_2}^{S} a_S\right)\left(\frac{D_{G,HOC}}{D_{G,O_2}}\right)^m} \quad (52)$$

Using the experimental data obtained in this research work, both models were tested and compared based on their accuracy and their robustness to predict HOC overall mass transfer coefficients.

4. Results and discussion

4.1. HOC Henry's law constant

To calculate the Henry's law constant by the method described in section 3.1.1, it is necessary to reach the compound saturation concentration when the bubbles leave the liquid phase in the reactor. Given that it was not possible to measure the gas phase concentration for the experiments performed in this study, indirect methods to assure the bubble saturation were used. Figure 3.4 shows the relation between the slope for bubble volatilization experiments tested and the air superficial velocity at different mechanical power inputs. In this figure it is possible to observe that the relation between the parameter Sp^B is linearly dependent to the air flow. Likewise, there is no significant effect of the mechanical power input on this parameter. These corroborations allow to draw the conclusion that, for the three molecules tested in this research work, the saturation case for Eq. 47 was reached [11].

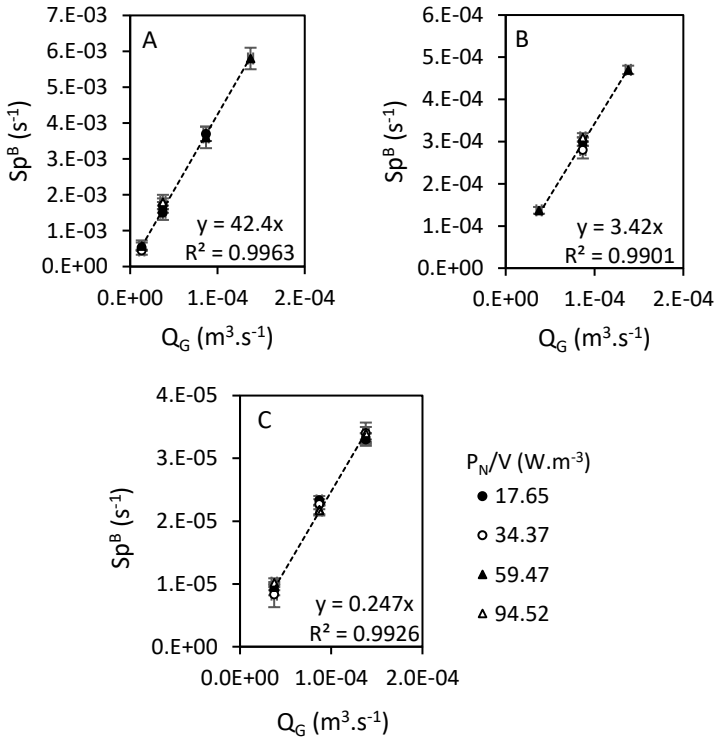

Figure 3.4 Slope for bubble volatilization of (A) toluene; (B) naphthalene and (C) phenanthrene as a function of the air flow rate and the mechanical power input

The results for the H_C calculation are shown in Table 3.4. The calculated values for the Henry's law constant are within the range of those found in the literature, which confirms the hypothesis of the bubble saturation.

Table 3.4 Henry's law constants calculated from Eq. 18 and considering bubble saturation (Sd>0.99)

Compound	Slope in Figure 3.4 (s^{-1})	Calculated Henry's law Constant (-)	Range of experimental H_C values*
Toluene	42.4	1.78×10^{-1}	$1.46\times10^{-1} – 5.26\times10^{-1}$
Naphthalene	3.42	1.44×10^{-2}	$6.84\times10^{-3} – 3.16\times10^{-2}$
Phenanthrene	0.247	1.04×10^{-3}	$9.77\times10^{-4} – 2.56\times10^{-3}$

*According to the H_C compilation made by Sander [10]

Additionally, it is interesting to observe that the Henry's law constants for HOCs presented in Table 3.4 show a wide range of values. This might be due to the different experimental set-ups and conditions in which they have been measured. Therefore, whenever possible, this parameter should be obtained experimentally.

4.2. Surface mass transfer

4.2.1. Oxygen and water

Figure 3.5 Influence of the power input on the surface mass transfer coefficient for (A) Oxygen and (B) Watershows the results of the test aiming to measure the influence of the mechanical power input on the surface mass transfer coefficient of oxygen and water. These coefficients for both oxygen and water are proportional to the power input and the trend for both cases follows a power type curve fit, which correspond to the findings reported in the literature for many compounds [6,8,25]. However, for the oxygen transfer, this increase seems to be relatively more important than for the water transfer. In fact, the value of the power in the function for the oxygen is almost five times higher than the one for the water.

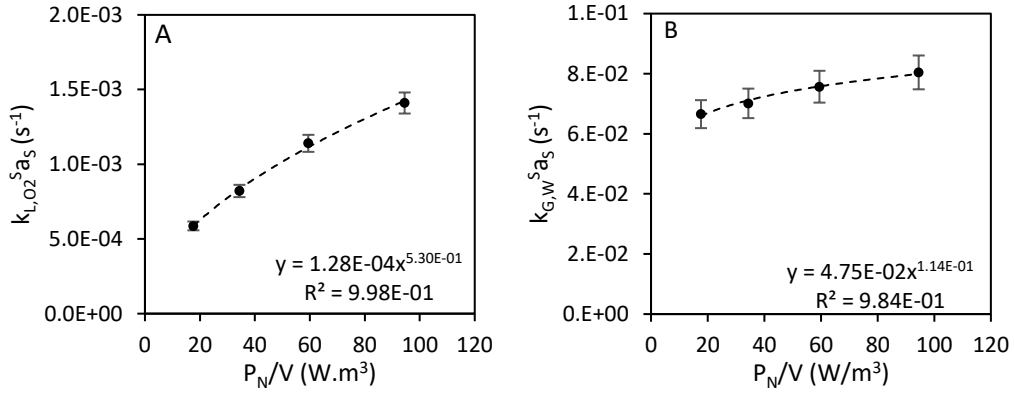

Figure 3.5 Influence of the power input on the surface mass transfer coefficient for (A) Oxygen and (B) Water

As the power input increases, two effects at the surface can be created. Firstly, since the agitation is being directly applied to the liquid phase, it induces a faster surface renewal (or a decreased film thickness) at the liquid side of the surface. Secondly, higher agitation produces an augmentation of the gas-liquid interfacial area due to surface deformation. This effect was visible to the naked eye in the reactor. Since oxygen is being transferred from the gas phase to the liquid phase, both phenomena affect its transfer. However, the continuous liquid phase is mainly constituted by water, which means that the water transfer occurs only in the gas phase. Hence, the first effect does not have any consequence and only the gas-liquid interfacial area modification is influencing this mechanism. These phenomena can explain the significant difference in the influence of the power input in the transfer of these two substances. Additionally, the exponent of the power relation for the oxygen transfer is in agreement with the results found by Hsieh et al. [6] for similar operating systems.

4.2.2. HOC

The influence of the power input on the surface transfer coefficient of the HOCs tested can be observed in Figure 3.6. As in the case of water and oxygen transfer, the surface volatilization coefficient of HOCs depends on the power input and the relation between the latter and the mass transfer coefficient can be assimilated to a power model in the form of Eq. 53 in the range of $\frac{P_N}{V}$ tested in this study. It is important to mention that the $K_L^S a_S$ for toluene at the highest power input was excluded from the graph, because it did not fit well in the figure. In fact, at the highest $\frac{P_N}{V}$, a surface breakage was observed, allowing some coarse bubbles to enter and remain for a short period of time in the liquid phase. Toluene is the most volatile of the three compounds tested and, due to its high Henry's law constant, a small increase in the transfer area may have had an important impact on its overall volumetric transfer coefficient. Conversely, the PAHs present a much lower volatilization kinetics (of one and two order of magnitude lower than toluene for naphthalene and phenanthrene respectively) and it seems unlikely that few coarse bubbles affected significantly the surface mass transfer process.

$$K_L^S a_S = B\left(\frac{P_N}{V}\right)^{\gamma} \tag{53}$$

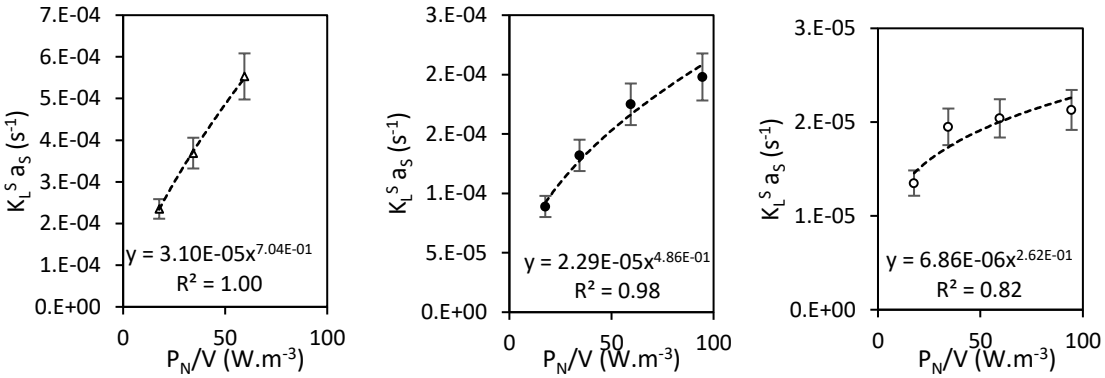

Figure 3.6 Influence of Power input on the surface mass transfer coefficient for (Δ) Toluene, (●) Naphthalene and (○) Phenanthrene

Figure 3.7 Linear correlations between the parameters in Eq. 33 and ln(H_C)displays the correlations found between the parameters in Eq. 53 and the Henry constant of the compounds tested. The natural logarithm of B depends linearly on the natural logarithm of the H_C for the compounds and in the range of power input tested in this study. Similarly, a linear dependence of γ and the natural logarithm of H_C can be also established for the HOCs, but not for the oxygen. This may be related to the fact that the gas resistance is negligible for the latter

compound and suggests that the linearity might be restrained to a specific range of H_C. In other words, γ might be related not only to the liquid-phase resistance, but also to the gas-phase resistance in the range of H_C tested in the present study.

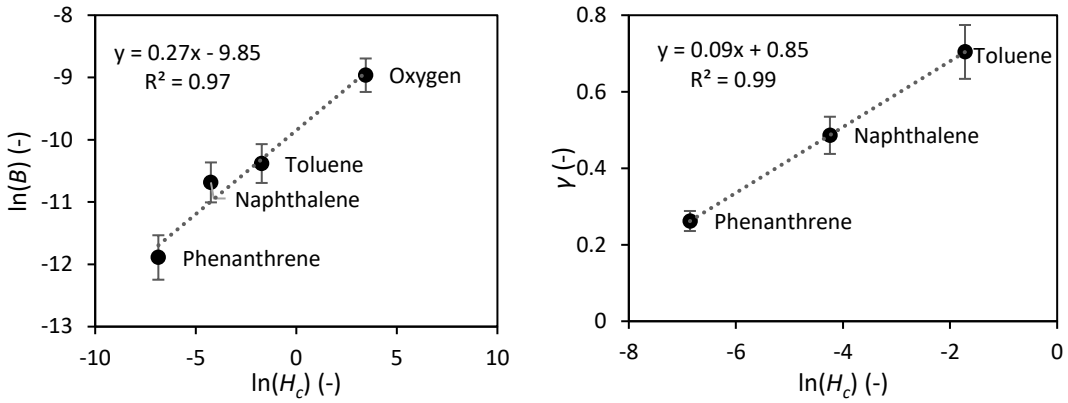

Figure 3.7 Linear correlations between the parameters in Eq. 33 and ln(H_C)

4.3. Modeling of Surface HOC mass transfer coefficient

As discussed in the section **Erreur ! Source du renvoi introuvable.**, HOC mass transfer coefficients can be predicted using Eq. 51. However, it is necessary to estimate the values for the exponents *m* and *n*. Several approaches for this estimation have been used in the literature, but, in general, they imply some assumptions, which are difficult to test experimentally. For example, Hsieh et al. [6] and Soltanali et Shams Hagani [16], as well as Munz and Roberts [8], assumed that both exponents are equal, due to the incertitude in their calculation and the lack of information regarding the parameters influencing them. Additionally, Munz and Roberts have found that the diffusivity exponents are virtually independent of the mixing intensity. Moreover, some authors, such as Chrysikopoulos et al. [26], Smith et al. [9] and Libra [27], have considered that the diffusivity exponents are dependent on the type of compound. With the purpose of estimating these exponents and studying the use of reference compounds for the volatilization of HOCs in this research work, two models were tested employing the experimental data obtained for the surface transfer of HOCs, water and oxygen: the proportionality coefficient model (PC) and the two-reference compound model (2RC).

The first model tested was the PC model, expressed by Eq. 52. The proportionality coefficient (Ψ) is defined to be used with oxygen as the only reference compound. This fact makes possible to neglect the resistance in the gas phase for the reference compound (due to the high H_C value for the oxygen). Therefore, the proportionality constant is widely applied for the

modeling of the transfer of volatile organic compounds (VOCs) in wastewater treatment facilities [5]. Many authors consider that the "volatile" characteristic of a compound is mainly given by its Henry's law constant. Though no definitive consensus on the matter, in general, compounds with $H_C \geq 0.19$ are considered volatile [28]. Besides, some authors consider that the liquid-phase resistance is only completely negligible for compounds with $H_C \geq 0.55$ [16].

In this study, toluene is placed around the limit of the "volatile" category. The PAHs (i.e. naphthalene and phenanthrene) are generally considered "semi-volatile" compounds [9,29], presenting a much more important gas-phase resistance [30]. Nevertheless, some authors also consider naphthalene as a volatile compound [6,31]. This proves that the limit in this regard is not completely well-defined, mainly because the rate of volatilization of a compound does not only depends on H_C, but also on the hydrodynamic properties of the phases where the transfer occur [21].

The parameters to be estimated for the PC model are the exponents of the diffusivity ratios (n and m) and the ratio of individual mass transfer coefficients for the oxygen ($k^S_{G,O_2}/k^S_{L,O_2}$). However, as Hsieh et al. [6] and Munz and Roberts [8] explain, the uncertainty regarding the exponents n and m probably exceeds the difference between them. Therefore, it was decided to assume that they are equal, and hence, decrease the degrees of freedom for the estimation. Additionally, since each individual mass transfer coefficient is influenced differently by the stirring in the reactor, their ratio changes with a variation of the power input. Instead, according to Munz and Robert [8], n and m seem not to be affected by this operational parameter. Therefore, the estimation was made assuming one $k^S_{G,O_2}/k^S_{L,O_2}$ per power input condition and only one $n = m$ for all of them.

The second model tested was the two-reference compound model (2RC), which is a more general approach than the PC model for the volatilization modeling of semi-volatile substances [16]. Yet, most authors use the latter due to the convenience of the utilization of only oxygen as a reference compound. Thus, very few research works have used other substances as reference compounds, much less for estimating the gas-side mass transfer coefficient. Monteith et al. [32] proposed the utilization of ammonia for this purpose due to its low Henry's law constant, but the ionization of this compound in water and the influence of pH on the mass transfer may complicate the experiments and the analytical processing of the data. In fact, high ion concentrations and changes in surface tension can modify the mass transfer coefficient of any compound [20]. Smith et al. [9] used water as a reference

compound for the surface mass transfer of semi-volatile compounds, which has several advantages when studying the mass transfer in aqueous system: firstly, its transfer has virtually no resistance in liquid-phase film; secondly, the measurement of water concentration in the gas phase is relatively easy to perform (by direct or indirect methods); and thirdly, it is an economic and quick method to obtain information for the gas-side mass transfer.

Therefore, to test the 2RC model, oxygen and water were used as a reference compounds for the liquid-side and gas-side mass transfer resistance, respectively. The parameters to be estimated in this model are both exponents of the diffusivity ratios n and m, and the same assumption regarding the equality of these parameters explained above was used in this case. Table 3.5 *Results of the PC model and the 2RC model fitting* shows the results for the fitting for both models, and Figure 3.8 and Figure 3.9 show the correlation between the experimental and the calculated values for the overall mass transfer coefficient of the three HOCs tested in this study for the PC model and the 2RC model respectively.

Observing the results of the fitting for the PC model, it is noticeable that most relative errors for all HOC at all power input conditions are lower or equal to 20%. Moreover, the plot between the calculated and the experimental overall mass transfer coefficients generates a good correlation (R^2 = 0.96). For the 2RC model, even if the relative errors of the mass transfer coefficients are rather higher than those of the PC model, the goodness of fit is slightly better (R^2 = 0.97), and most values are also within the 20% error.

The value for the exponent n, although within the ranges found in the literature, are higher than the typical values estimated for both models. Values of n close to 1 are usually related to systems with a continuous transfer, where the contact time between the phases is relatively long. Even if this is not typical for agitated reactors in turbulent mixing regimes, this result can be a consequence of the type of impeller used and the range of power input tested. This combination could generate a type of flow near the surface closer with higher lower surface renewal and higher interface contact time than those usually found for this type of systems.

Table 3.5 Results of the PC model and the 2RC model fitting

$\frac{P_N}{V}$ (W.m^{-3})	Diffusivity Exponents	$k^S_{G,O_2}/k^S_{L,O_2}$ (-)	Relative error (%)		
PC model			Phenanthrene	Naphthalene	Toluene
	$m = n$ (-)	Estimated			
17.65	1.00	76.8	0.25	25.8	0.18
34.37		76.5	0.21	18.4	11.1
59.47		56.7	0.16	5.57	19.4
94.52		47.4	0.33	3.72	-
2RC model					
	$m = n$ (-)	Calculated using estimated $m = n$			
17.65	0.92	76.8	10.7	36.3	7.75
34.37		57.8	14.8	11.9	5.97
59.47		44.9	11.1	0.85	14.9
94.52		38.6	9.0	0.01	-

*Not plotted in Figure 3.8
** Not plotted in Figure 3.9

Regarding the ratio of individual oxygen mass transfer coefficients ($k^S_{G,O_2}/k^S_{L,O_2}$), whilst this parameter is fitted for the PC model, it is possible to calculate it for the 2RC model by using the value obtained for $m(=n)$. For both models, these parameters are in general agreement with those found by Munz and Roberts [8], but much lower than those found by Hsieh [6]. This ratio is strongly dependent on the geometry and the hydrodynamic properties of the reactor. Therefore, a direct comparison is not always possible. Nonetheless, it is interesting to notice the ratio decreases as the mixing intensity augments. Considering that the power input was directly applied to the liquid phase and that the gas phase was fed with the same air flow input throughout all the experiments, this relation becomes logical. In fact, as the power input increases, the renewal rate at the liquid interface augments, increasing the k^S_{L,O_2}, while the gas interface remains almost unchanged (k^S_{G,O_2}virtually invariable). As a result, the global ratio of individual mass transfer coefficient decreases as the liquid stirring increases.

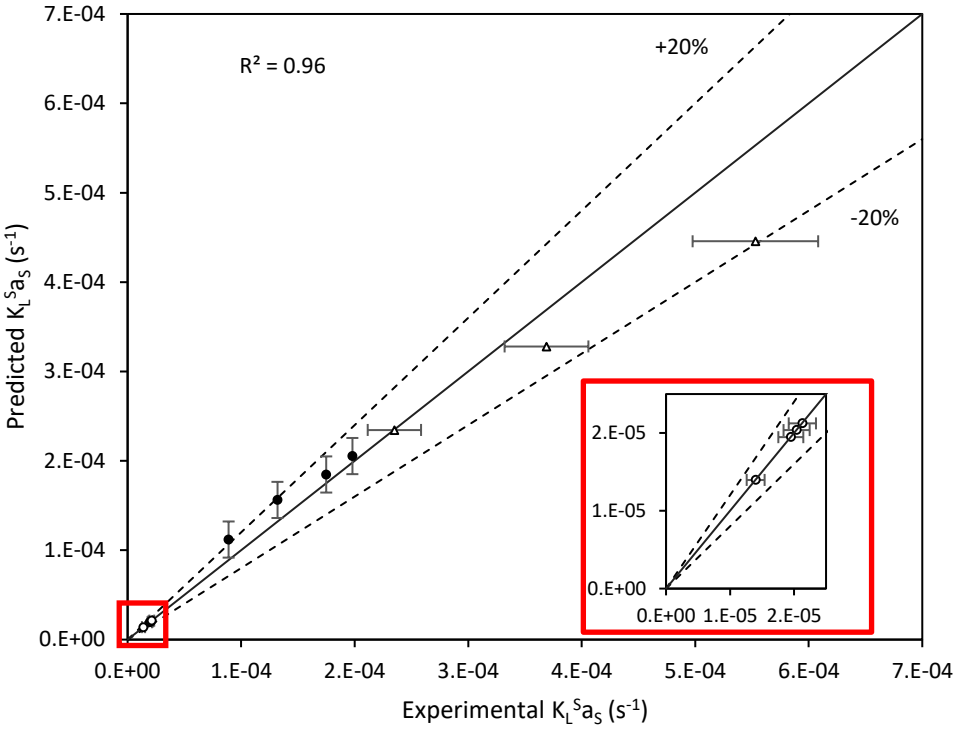

Figure 3.8 HOC mass transfer coefficients correlation for the PC model coefficient for (Δ) Toluene, (●) Naphthalene and (○) Phenanthrene

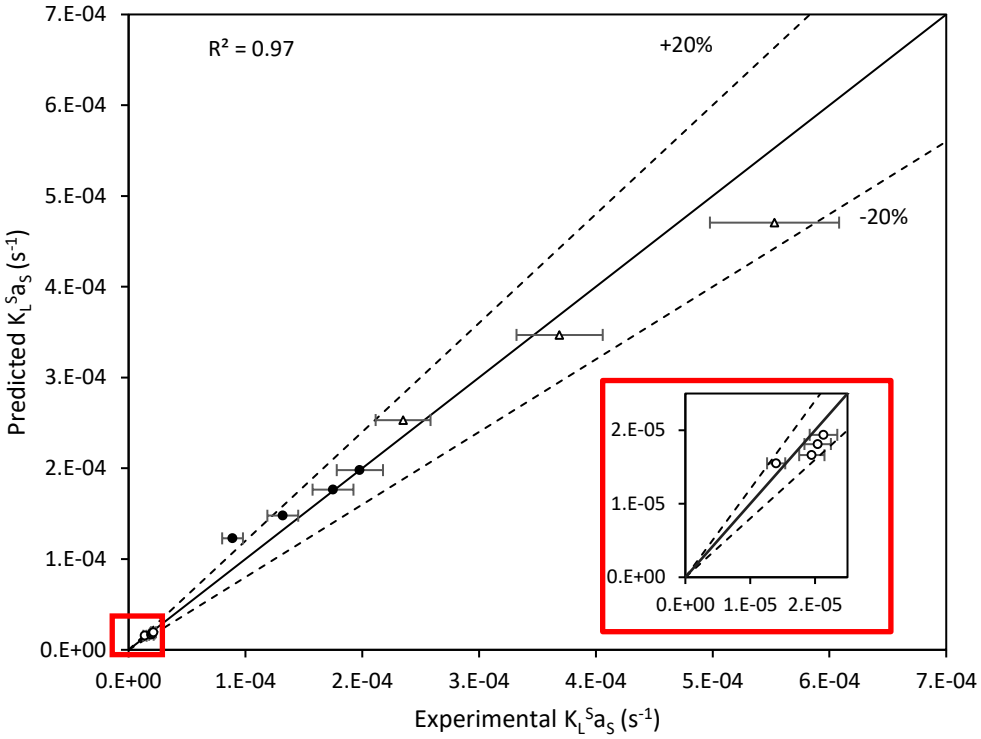

Figure 3.9 HOC mass transfer coefficients correlation for the 2RC model coefficient for (Δ) Toluene, (●) Naphthalene and (○) Phenanthrene

Besides, it can be noticed that for the $k^S_{G,O_2}/k^S_{L,O_2}$ values for PC model are slightly superior than those of the 2RC model. Moreover, in the case of the latter, the ratio presents a continuous decreasing as the power input increases for all the points, conversely to the first two power input conditions for the PC model. Plotting the results for this parameter for both models (and excluding the first point for the PC model) as functions of the power input (Figure 3.10), the similarity of their behavior becomes evident. Moreover, the functions follow a power type curve with exponents -0.42 and -0.48 for the 2RC model and PC model, respectively. These values are in agreement with the value found by Munz and Robert [8] for the same parameter (-0.422). Considering, that the degrees of freedom for this estimation were higher, the 2RC model shows to be preferable. Indeed, less assumptions must be made in order to obtain similar estimations, resulting in a more robust model.

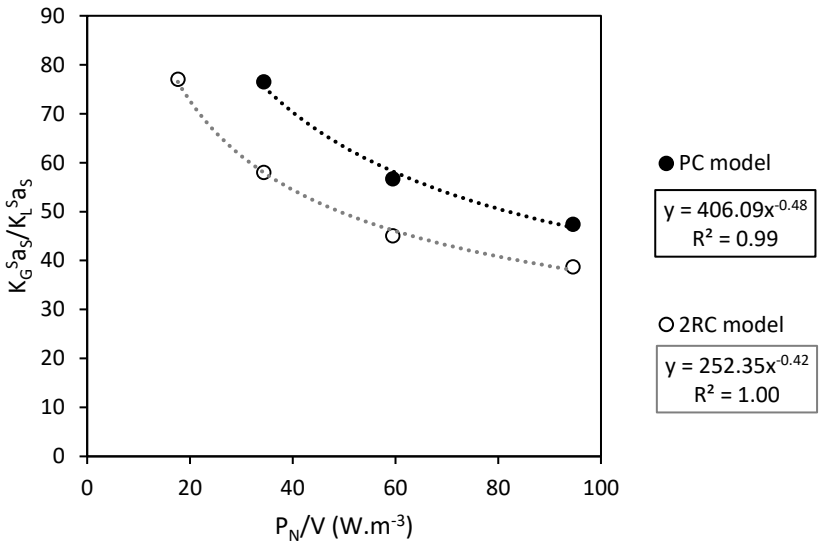

Figure 3.10 Ratio of individual oxygen mass transfer coefficients as a function of the power input for each model

Using the results of the 2RC model, the relative liquid resistance for each molecule as a function of the power input could be calculated (Figure 3.11). It is noticeable that the more than 90% of the resistance correspond to the liquid side for the toluene, which allow its classification as a "volatile" compound, as expected. On the other hand, phenanthrene (presenting less than 10% of resistance on the liquid side) and naphthalene (presenting between 30% and 50% for the power input conditions tested) can be categorized as "semi-volatile" substances. This means that, since three substances tested are comprised within a wide R_L/R_T range, the conclusions of this research work may be applicable to most volatile and semi-volatile substances.

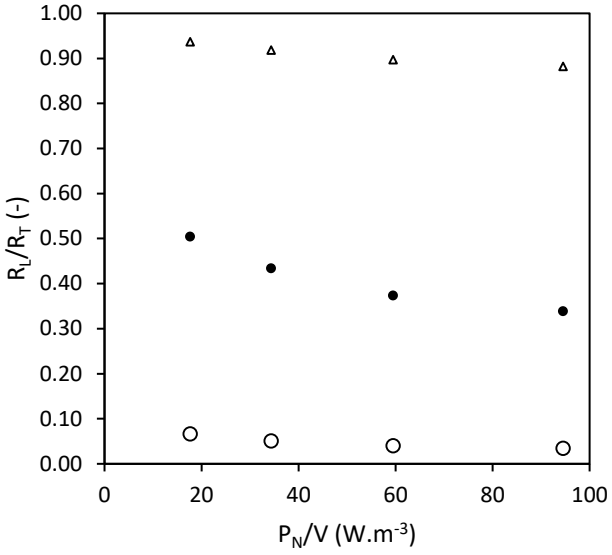

Figure 3.11 Relative liquid resistance for (Δ) Toluene, (●) Naphthalene and (○) Phenanthrene

5. Relevance and limitations of the models and the use water as reference compound

Traditionally, VOCs surface volatilization and stripping modeling considers that the gas-phase resistance is negligible. However, this assumption is not always correct because of the variability of the "volatile" condition of the compounds according to the system characteristics. Therefore, models that consider the gas phase resistance are a better option. Oxygen is a useful reference compound for many processes, particularly the aerobic ones in which its concentration in water constitute a key parameter. Therefore, the proportionality coefficient model (PC), which is based on this molecule is one of the most frequently used in the literature. Although the use of only one reference compound is an easy and practical way to calculate the mass transfer coefficient of other compounds, the prediction of overall mass transfer coefficient is limited to the ability to predict the oxygen transfer process, which, in turn, is limited to the parameters affecting only the liquid phase (since the gas resistance is negligible for this compound). In addition to this, two parameters should be either supposed or estimated for the specific system, i.e. the ratio of individual mass transfer coefficient and the exponent of the liquid diffusivity ratio. Hsieh et al. [6] explain that this ratio is generally assumed to be between 50 and 300 (with an average of 150), which is a wide range. Besides, this parameter varies according to the hydrodynamic conditions. As for the diffusivity ratio exponent, as mentioned in section 2.2, the values also are within wide ranges proposed in the literature. All this may lead to wrong estimations of the mass transfer coefficient.

One way to avoid the incertitude and/or the estimations errors is to find a manner to calculate the gas-phase resistance and to use the 2RC model. By directly estimating the individual mass transfer coefficients with the help of two reference compounds, this model allows a more robust way to obtain the gas-liquid mass transfer coefficient of any compound, volatile or not. This research work has proved that, for surface volatilization, the use of water as a reference compound produces similar results than the traditional PC model. The use of the 2RC model would avoid the introduction of errors associated to assumptions made for the ratio of individual mass transfer coefficients and knowing oxygen transfer behavior and water transfer behavior in the system will suffice to account for liquid-film and gas-film changes, respectively. Moreover, by the means of simple equipment, basic experiments on water transfer can be performed in almost any system to obtain the necessary information regarding the gas-phase resistance. This means that, if the reference compounds' gas-liquid transfer is characterized, the transfer of any volatile or semi-volatile compound can be extrapolated.

In this sense, the approach proposed in this paper can be used in wastewater treatment plants, slurry reactors or soil washing processes to quantify the gas-liquid mass transfer of compounds susceptible to volatilize. Nonetheless, the major limitation of this practice is that air saturation can easily and rapidly be reached, especially in systems with low or no gas phase circulation. The same limitation applies for aerated systems using bubble diffusers within the liquid phase in which, depending on the bubble size, few centimeters may be sufficient to reach the mass transfer equilibrium. For these cases, a similar approach, but using other substances allowing higher equilibrium concentrations in the gas phase can be used.

6. Conclusions

- Using the bubble aeration mode in the reactor, HOCs bubble concentrations reached mass transfer equilibrium, which allowed the calculation of the Henry's law constant for these compounds.
- The surface overall mass transfer coefficient of all compound tested in this study presented a power-type correlation with the mechanical power input.
- Correlations between the Henry's law constant and the parameters of the mentioned power-type correlation for the HOCs were found. These correlations can be used to estimate the value of the overall HOC mass transfer coefficient within the conditions used in this research work.
- Two model for estimating the diffusivity exponents were tested and compared: the proportionality coefficient (PC) model and the two-reference compound (2RC) model.

Both models presented similar results, showing that either only oxygen or both, oxygen and water, can be used as reference compounds to calculate the mass transfer coefficient.

- However, the 2RC is preferable for the cases where a reference compound with gas-film controlled mass transfer can be used, due to its higher robustness and its extrapolatable characteristics regarding hydrodynamic changes in both gas-side and liquid-side interfaces.

References

[1] J. Yang, K. Wang, Q. Zhao, L. Huang, C.-S. Yuan, W.-H. Chen, W.-B. Yang, Underestimated public health risks caused by overestimated VOC removal in wastewater treatment processes, Env. Sci Process. Impacts. 16 (2014) 271–279. doi:10.1039/C3EM00487B.

[2] D.O. Pino-Herrera, Y. Pechaud, D. Huguenot, G. Esposito, E.D. van Hullebusch, M.A. Oturan, Removal mechanisms in aerobic slurry bioreactors for remediation of soils and sediments polluted with hydrophobic organic compounds: An overview, J. Hazard. Mater. 339 (2017) 427–449. doi:10.1016/j.jhazmat.2017.06.013.

[3] Y. Luo, W. Guo, H.H. Ngo, L.D. Nghiem, F.I. Hai, J. Zhang, S. Liang, X.C. Wang, A review on the occurrence of micropollutants in the aquatic environment and their fate and removal during wastewater treatment, Sci. Total Environ. 473–474 (2014) 619–641. doi:10.1016/j.scitotenv.2013.12.065.

[4] M. Pomiès, J.-M. Choubert, C. Wisniewski, M. Coquery, Modelling of micropollutant removal in biological wastewater treatments: A review, Sci. Total Environ. 443 (2013) 733–748. doi:10.1016/j.scitotenv.2012.11.037.

[5] J.R. Mihelcic, C.R. Baillod, J.C. Crittenden, T.N. Rogers, Estimation of VOC Emissions from Wastewater Facilities by Volatilization and Stripping, Air Waste. 43 (1993) 97–105. doi:10.1080/1073161X.1993.10467120.

[6] C.-C. Hsieh, K.S. Ro, M.K. Stenstrom, Estimating emissions of 20 VOCs. I: Surface aeration, J. Environ. Eng. 119 (1993) 1077–1098.

[7] A.V. Padalkar, R. Kumar, Removal mechanisms of volatile organic compounds (VOCs) from effluent of common effluent treatment plant (CETP), Chemosphere. 199 (2018) 569–584. doi:10.1016/j.chemosphere.2018.01.059.

[8] C. Munz, P.V. Roberts, Gas- and liquid-phase mass transfer resistances of organic compounds during mechanical surface aeration, Water Res. 23 (1989) 589–601. doi:10.1016/0043-1354(89)90026-2.

[9] J.H. Smith, D.C. Bomberger, D.L. Haynes, Volatilization rates of intermediate and low volatility chemicals from water, Chemosphere. 10 (1981) 281–289.

[10] R. Sander, Compilation of Henry's law constants (version 4.0) for water as solvent, Atmospheric Chem. Phys. 15 (2015) 4399–4981. doi:10.5194/acp-15-4399-2015.

[11] D. Mackay, W.Y. Shiu, R.P. Sutherland, Determination of air-water Henry's law constants for hydrophobic pollutants, Environ. Sci. Technol. 13 (1979) 333–337. doi:10.1021/es60151a012.

[12] W.K. Lewis, W.G. Whitman, Principles of Gas Absorption., Ind. Eng. Chem. 16 (1924) 1215–1220. doi:10.1021/ie50180a002.

[13] R. Higbie, Penetration theory leads to use of the contact time in the calculation of the mass transfer coefficients in the two film theory, Trans Am Inst Chem Engrs 31. 365 (1935).

[14] P.V. Danckwerts, Significance of Liquid-Film Coefficients in Gas Absorption, Ind. Eng. Chem. 43 (1951) 1460–1467. doi:10.1021/ie50498a055.

[15] J. Arogo, R.H. Zhang, G.L. Riskowski, L.L. Christianson, D.L. Day, Mass Transfer Coefficient of Ammonia in Liquid Swine Manure and Aqueous Solutions, J. Agric. Eng. Res. 73 (1999) 77–86. doi:10.1006/jaer.1998.0390.

[16] S. Soltanali, Z. Shams Hagani, Modeling of air stripping from volatile organic compounds in biological treatment processes, Int. J. Environ. Sci. Technol. 5 (2008) 353–360. doi:10.1007/BF03326030.

[17] R.F. Lewis, SITE Demonstration of Slurry-Phase Biodegradation of PAH Contaminated Soil, Air Waste. 43 (1993) 503–508. doi:10.1080/1073161X.1993.10467149.

[18] K.-C. Lee, B.E. Rittmann, J. Shi, D. McAvoy, Advanced steady-state model for the fate of hydrophobic and volatile compounds in activated sludge, Water Environ. Res. 70 (1998) 1118–1131. doi:10.2175/106143098X123480.

[19] S. Hall, Rules of Thumb for Chemical Engineers, Elsevier Science, 2017. https://books.google.fr/books?id=S6jRDgAAQBAJ.

[20] C. Matter-Müller, W. Gujer, W. Giger, Transfer of volatile substances from water to the atmosphere, Water Res. 15 (1981) 1271–1279.

[21] C. Hsieh, R.W. Babcock, M.K. Stenstrom, Estimating Emissions of 20 VOCs. II: Diffused Aeration, J. Environ. Eng. 119 (1993) 1099–1118. doi:10.1061/(ASCE)0733-9372(1993)119:6(1099).

[22] P.B. Bedient, H.S. Rifai, C.J. Newell, others, Ground water contamination: transport and remediation., Prentice-Hall International, Inc., 1994.

[23] E.L. Cussler, Diffusion: mass transfer in fluid systems, Cambridge university press, 2009.

[24] Christoph Munz, Paul V. Roberts, Air-Water Phase Equilibria of Volatile Organic Solutes, J. Am. Water Works Assoc. 79 (n.d.). http://www.jstor.org/stable/41290598.

[25] F. Garcia-Ochoa, E. Gomez, Bioreactor scale-up and oxygen transfer rate in microbial processes: An overview, Biotechnol. Adv. 27 (2009) 153–176. doi:10.1016/j.biotechadv.2008.10.006.

[26] C.V. Chrysikopoulos, L.M. Hildemann, P.V. Roberts, Modeling the emission and dispersion of volatile organics from surface aeration wastewater treatment facilities, Water Res. 26 (1992) 1045–1052.

[27] J.A. Libra, Volatilization of organic compounds in an aerated stirred tank reactor, University of California Los Angeles, 1991. http://www.seas.ucla.edu/stenstro/d/d11.pdf (accessed December 11, 2016).

[28] Paul V. Roberts, Christoph Munz, Paul Dändliker, Modeling Volatile Organic Solute Removal by Surface and Bubble Aeration, J. Water Pollut. Control Fed. 56 (1984) 157-.

[29] L. Lucattini, G. Poma, A. Covaci, J. de Boer, M.H. Lamoree, P.E.G. Leonards, A review of semi-volatile organic compounds (SVOCs) in the indoor environment: occurrence in consumer products, indoor air and dust, Chemosphere. 201 (2018) 466–482. doi:10.1016/j.chemosphere.2018.02.161.

[30] K.T. Valsaraj, R. Ravikrishna, J.J. Orlins, J.S. Smith, J.S. Gulliver, D.D. Reible, L.J. Thibodeaux, Sediment-to-air mass transfer of semi-volatile contaminants due to sediment resusmension in water, Adv. Environ. Res. (1997) 13.

[31] V. Martí, J. De Pablo, I. Jubany, M. Rovira, E. Orejudo, Water-Air Volatilization Factors to Determine Volatile Organic Compound (VOC) Reference Levels in Water, Toxics. 2 (2014) 276–290. doi:10.3390/toxics2020276.

[32] H. D. Monteith, J. P. Bell, W. J. Parker, H. Melcer, R. T. Harvey, Effect of Bubble-Induced Surface Turbulence on Gas-Liquid Mass Transfer in Diffused Aeration Systems, Water Environ. Res. 77 (2005) 128–137.

CHAPTER 4

PAH sorption and desorption in soil

CHAPTER 4 – PAH sorption and desorption in soil

Liquid-solid mass transfer. In this chapter, the influence of soil content and composition on PAH sorption and desorption equilibria, as well as on PAH desorption kinetics is studied. A two-compartement; three-parameter model is used to fit the data obtained.

Abstract

Sorption and desorption processes are the main mechanisms controlling the behavior and fate of polycyclic aromatic hydrocarbons (PAHs) in soil. However, soil heterogeneity hampers the understanding of the transport and availability of such compounds in the environment. In this research, the sorption and desorption mechanisms of PAHs on different model soil components and their mixtures was to investigate through the study of equilibrium and kinetics using a mechanistic approach. The results show that the presence of clay affects the PAH sorption equilibrium controlled by the soil organic matter (SOM), probably due to a decrease of the available sorption sites by forming SOM-clay aggregates. The PAH kinetic desorption was modeled using a three-parameter, two-compartment model, in which each compartment represented each soil component (i.e. clay and SOM). A first order equation was used for each compartment. The PAH molecules with higher molecular weight and hydrophobicity tend to be sorbed in a higher proportion onto nonpolar sections of SOM than onto mineral surfaces. Soil concentration did not affect the desorption kinetic rate, meaning that the desorption may only depend on the surface equilibrium and not on the hydrodynamic conditions within the range of soil concentrations tested (2.5% - 10% w/v). The extrapolation of the results for real polluted soils was also discussed.

Nomenclature

C	Concentration in solid phase (mg.kg^{-1})
C_{eq}	Equilibrium concentration in the liquid phase (mg.l^{-1})
C_r	Reduced concentration (-)
C_T	Total concentration in soil (mg.kg^{-1})
f	PAH fraction in soil (-)
HI	Hysteresis index (-)
k_{clay}	First order kinetic constant for clay (h^{-1})
K_F	Freundlich isotherm coefficient (mg.kg^{-1}/(mg.l^{-1})$^{-1/n}$)
$K'_F.$	Modified Freundlich isotherm coefficient (mg.kg^{-1})
K_{OC}	Soil-water partition coefficient normalized to the carbon content (l.kg^{-1})
k_{SOM}	First order kinetic constant for soil organic matter (h^{-1})
n	Freundlich isotherm exponent (-)
q_{eq}	Equilibrium concentration in the sorbent (mg.kg^{-1})
S_{scl}	Supercooled liquid-state solubility (mg.l^{-1})
t	time (h)
T	Temperature (°C)
x	Mass fraction (-)

Greek letters

Φ	Relative concentration (-)

Sub-indexes

$clay$	Relative to clay
i	Relative to the soil component *i*
$sand$	Relative to sand
SOM	Relative to soil organic matter
0	Relative to the initial state

Super-indexes

d	Relative to desorption
s	Relative to sorption

Acronyms

B(a)P	Benzo(a)pyrene
FLA	Fluoranthene
HOC	Hydrophobic organic compound
NAP	Naphthalene
PAH	Polycyclic aromatic hydrocarbon
PHE	Phenanthrene
PYR	Pyrene
SOM	Soil organic matter

1. Introduction

Polycyclic aromatic hydrocarbons (PAHs) are known to be recalcitrant pollutants, present in many contaminated sites and with a tendency to accumulate on geomaterials and organic matter by different mechanisms [1]. Due to their high toxicity and mutagenicity, great concern has been given to their fate in the environment and many removal techniques have been proposed [2]. There is a common consensus on the fact that PAH sorption and desorption processes are the main mechanisms controlling the behavior and fate of these pollutants in soil and sediments [3]. However, the complexity regarding the composition and interactions between soil particles and materials complicate the comprehension of these systems. Interactions between PAHs and geosorbents can be ruled by molecule physicochemical properties, surface properties, active sites availability and hydrodynamic conditions [4].

Additionally, heterogeneity of sorbents in the environment hinders the understanding and prediction of the transport and the availability of these compounds. The type of sorbent can play a major role on the release of PAHs into the environment. For instance, several studies have proved that the presence of organic matter is a key factor in this process [5,6]. On the other hand, regarding the mineral soil constituents, clay materials tend to accumulate a much higher readily available concentration of these pollutants than sand materials, due to their higher specific surface area [7]. Although numerous studies on these topics have been carried out, a better understanding of the releasing mechanisms in individual soil fractions and their interactions with the different soil surfaces is still needed. Studies on real contaminated soils give some insights regarding the sorption and desorption processes, but many site-specific factors, such as pollution aging and weathering, limit the applicability of the results to other soils. In addition, the best fitting models for desorption kinetics found in the literature only differentiate between a “rapid” and a “slow” desorbing fraction [8,9], giving little information about the physical meaning of these fractions in terms of soil constituents. Thus, the study of simplified systems could help to isolate individual interactions and better comprehend them.

The main objective of this study is to investigate and understand the sorption and desorption mechanisms of PAHs on different soil components and their mixtures, through the study of equilibrium and kinetic experiments by using a mechanistic approach. Model soil components were used in order to isolate individual interactions: montmorillonite clay was chosen as a model for mineral surfaces, while sphagnum peat was used as soil organic matter (SOM). The impact of the type of soil sorbent and its composition was studied in equilibrium conditions.

Likewise, the influences of sorbent concentration and composition, molecule properties and hydrodynamic conditions on the desorption process was tested on kinetic experiments.

2. Materials and methods

2.1. Sorbents

The clay used was provided by Argiles du Bassin Méditerranéen (France), and was composed of at least 65% of Sardinian montmorillonite (from Italy), with a particle size lower than 40 µm under ambient conditions. The chemical analysis of the clay was provided by the supplier. Sphagnum peat (95% organic matter) was used as a source of SOM. It was wet sieved at 200 µm and dried at 60 °C, prior to utilization. Artificial soil was prepared by thoroughly mixing montmorillonite and sphagnum peat at the desired proportion.

2.2. Phenanthrene sorption and desorption equilibria

A concentrated phenanthrene solution was prepared by dissolving phenanthrene crystals (98% purity, Sigma-Aldrich) in methanol (HPLC grade, VWR). This solution was used to prepare an aqueous stock solution of phenanthrene in tap water. The concentration of methanol in water never exceeded 0.1% (v/v), which can be considered negligible [10]. Sodium azide (Sigma-Aldrich) was added up to a concentration of 100 $mg.l^{-1}$ with the purpose of avoiding microbial growth. Six concentration levels of the aqueous phenanthrene solution were obtained by serial dilutions, adding a 100-$mg.l^{-1}$ solution of sodium azide. Phenanthrene sorption isotherms were determined by mixing the aqueous solution at each concentration level with the sorbent in glass centrifuge tubes in duplicates. Three soil compositions were tested: pure clay, pure SOM and an artificial soil composed by 90% clay and 10% SOM (in mass/mass percent). The desorption isotherm for the latter soil composition was determined using the phenanthrene-loaded soil in each glass centrifuge tube from the sorption experiment and adding a 100-$mg.l^{-1}$ solution of sodium azide.

The soil-aqueous solution mixtures were left for equilibration at 20°C in an orbital shaker and then analyzed for aqueous phenanthrene concentration at the 7^{th} and 8^{th} day of incubation. After verifying that the concentration of the solutions did not change between these two consecutive days, they were centrifuged and analyzed for phenanthrene soil concentration. The supernatant was discarded and extraction of phenanthrene was performed by ultrasonication with methanol as solvent. Each extraction was repeated three times, with the methanol supernatant collected and mixed for phenanthrene analysis.

The phenanthrene analysis was performed using an *LaChrom Elite® L-2400* HPLC (Hitachi) coupled with UV/VIS detector (set to 254 nm) and a fluorescence detector (Excitation wavelength set to 250 nm and Emission wavelength set to 350 nm). The separation was performed using a RP C-18 end capped column (Purospher®, Merck) (5 mm, 25 cm × 4.6 mm) placed in an oven at 40 °C. The mobile phase was a mixture of water and methanol (20:80 v/v) with a flow rate of 1.0 $ml.min^{-1}$ in isocratic mode. The injection volume was 20 µl.

2.3. Desorption kinetics

The influence of soil concentration and soil composition on the PAH desorption kinetics was studied. The conditions tested are shown in Table 4.1. The experiments were performed in reactors with 1-l working volume, magnetically agitated using PTFE magnetic bars and covered with a PTFE cap. For each experiment, the reactors were fed with water and the desired amount of PAH spiked soil, as well as Amberlite® XAD®-2 (Supelco) to create an infinite sink for desorption [11,12]. For each condition, the mass of Amberlite added represented only 10% of the soil mass in order to avoid significant changes in the rheology and hydrodynamic conditions of the system. Samples were collected at the beginning of the experiments and at appropriate time intervals for the analysis of aqueous and soil PAH concentration. PAHs were extracted from soil using the extraction method described in section 2.2.

Table 4.1 Experimental conditions tested for PAH desorption kinetic tests

Clay mass fraction (-)	Soil concentration (%m/v)				
	10.0	7.5	5.0	2.5	1.0
1	×				
0.9	×	×	×	×	
0.8	×				
0	×				×

Soil was spiked using a solution of PAHs in acetone based on the procedure proposed by Northcott and Jones [13]. In short, after addition of the acetone solution containing the desired mass of PAHs to the dry soil, the mixture was thoroughly mixed. Once the slurry was homogenized, it was left under a hood at ambient temperature to let the solvent evaporate. The mixture was often stirred during the drying phase to allow a homogeneous evaporation of the solvent and an even distribution of the PAHs in the soil. Once dried, the soil was crushed and homogenized one more time.

Desorption kinetics was tested for five PAHs (Sigma-Aldrich): naphthalene (NAP), phenanthrene (PHE), fluoranthene (FLA), pyrene (PYR) and benzo(a)pyrene (B(a)P). PAHs were analyzed using an HPLC (Shimadzu). The separation was performed using a Phenomenex Luna C18 column (250 × 4.6 mm, 5 µm) in an oven at 40°C connected to a UV detector set at 254 nm. Eluent was a mixture of acetonitrile and water (3:1), 1.8 ml.min^{-1} in isocratic mode and the injection volume was 20 µl. PAHs (with at least 98% purity) and acetonitrile were provided by Sigma-Aldrich.

3. Model

3.1. Sorption Equilibrium

Sorption equilibrium is often modelled using the Freundlich equation, given by Eq. (54.

$$q_{eq} = K_F {C_{eq}}^{1/n} \tag{54}$$

One of the main limitations of the Freundlich isotherm model is that the Freundlich constant (K_F), which can be translated as a measure of the affinity of the compound for the adsorbent, depends on the exponent n. This makes the comparisons between several K_F difficult when n is different (even for the same adsorbent). Nonetheless, Carmo et al. [14] proposed a method to homogenize this parameter, making it independent of n. They proposed that, instead of directly using the equilibrium concentration in Eq. (54, a ratio between C_{eq} and the supercooled liquid-state solubility (S_{scl}) should be used (Eq. (55).

$$q_{eq} = {K'}_F {C_r}^{1/n} \tag{55}$$

where $C_r = \frac{C_{eq}}{S_{scl}}$, which can be approximated to the activity of the solute in water. S_{scl} for a given compound depends on the melting point, the aqueous solubility and the temperature and, therefore, can be considered constant at isotherm conditions. This leads to a modified Freundlich parameter (${K'}_F$) which is independent of n and can be calculated from the Freundlich constant, K_F, as shown in Eq (56. This value represents more clearly the sorbent characteristics. The equilibrium data was modeled using Eq. (55).

$${K'}_F = K_F {S_{scl}}^{1/n} \tag{56}$$

3.2. Desorption kinetics

Typically, in heterogeneous systems, sorbed compounds are distributed in different materials and fractions of these materials, each one with different desorption kinetic rates. For instance, soil is composed of silicate particles (sand and silt), agglomerates of clay platelets and organic matter. According to Geerdink et al. [15], the overall desorption rate of PAHs in soil can be modelled as a sum of individual rates corresponding to each soil fraction (Eq. (57).

$$\frac{dC_T}{dt} = f_{SOM}\frac{dC_T}{dt} + f_{clay}\frac{dC_T}{dt} + f_{sand}\frac{dC_T}{dt} \tag{57}$$

Eq. (57 can be rewritten, using the mass fractions of each soil fraction, as shown in Eq. (58.

$$\frac{dC_T}{dt} = x_{SOM}\frac{dC_{SOM}}{dt} + x_{Clay}\frac{dC_{clay}}{dt} + x_{sand}\frac{dC_{sand}}{dt} \tag{58}$$

Thus, the desorption rate of each fraction can be calculated individually. To do this, in many cases a simple first model suffice (Eq. (59).

$$\frac{dC_i}{dt} = -k_i C_i \tag{59}$$

In this study, only clay and SOM were used as soil fractions, thus the sand fraction term in Eq. (57 was considered equal to 0. Also, to integrate this equation using a first order model for each fraction (Eq. (59), it is necessary to consider the relative initial concentration of PAHs sorbed on each fraction (Eq. (60) and normalize by the total PAH initial concentration (Eq. (61). The solution of the integration with all these considerations, given in Eq. (62, corresponds to a three-parameter, two-compartment model.

$$\phi_{SOM,0} = \frac{C_{SOM,0}}{C_{T,0}}\ ;\ \phi_{clay,0} = \frac{C_{clay,0}}{C_{T,0}}\ ;\ \phi_T = \frac{C_T}{C_{T,0}} \tag{60}$$

$$x_{SOM}\phi_{SOM,0} + x_{clay}\phi_{clay,0} = 1 \tag{61}$$

$$\phi_T = x_{clay}\phi_{clay,0}e^{-k_{clay}t} + (1 - x_{clay}\phi_{clay,0})e^{-k_{SOM}t} \tag{62}$$

Experimental results for desorption were modeled using Eq. (62. Fitting parameters were the ratio of the initial concentration of PAHs in the clay to the total initial concentration ($\phi_{clay,0}$),

and the first order PAH desorption kinetic constants from clay (k_{clay}) and SOM (k_{SOM}). Error between the estimated normalized concentration and the experimental one (ϕ_T) were minimized in order to obtain the best fit.

4. Results and discussion

4.1. Sorption equilibrium

4.1.1. Individual soil components

Figure 4.1 shows the results of phenanthrene sorption isotherms, determined individually for each soil component (i.e. clay and SOM). It is noticeable that the K'_F for SOM is three orders of magnitude higher than that for the clay sorption. These results are in agreement with those found in the literature for both clay (i.e. 77.9 mg.kg^{-1}) and SOM (i.e. 66575 mg.kg^{-1}). For example, Hundal et al. [16] found values of K'_F in orders of magnitude between 10^1 and 10^2 mg.kg^{-1} for several types of montmorillonites, and Wang et al. [17] obtained a values between 10^3 and 10^4 for several types of SOM.

The higher phenanthrene sorption ability of SOM compared to that of clay can be explained by the higher affinity of phenanthrene for SOM. In general, the partition of any compound between water and a solid surface is controlled by several physicochemical factors, i.e. temperature, surface area, affinity between the sorbent and the compound, and sorption active sites availability [18]. Clays are materials known for their high specific surface areas (with an order of magnitude of 10^3-10^4 m^2.g^{-1} for some smectites, such as hectorite and montmorillonite) due to their sheet configuration, usually having neutral or negative charged surfaces. These characteristics make clay an excellent adsorbent for many compounds. On the other hand, SOM includes a large number of substances from all sizes and with possibly very different physicochemical properties (e.g. organic polymers, lipids, polysaccharides, and proteins). Wershaw [19] developed a model for humic materials, in which a general structure of SOM is explained. According to him, humic substances present in SOM can contain ionizable negative carboxylate groups with their counter ions, non-ionizable polar groups and nonpolar hydrophobic sections. These characteristics give amphiphile characteristics to the substance, creating active sorption sites for many compounds. Besides, many of the natural SOM found in nature possess specific surface areas within an order of magnitude of 10^0 [17] (much lower than clay), although this can significantly vary due to the heterogeneity of the material. As hydrophobic compounds, PAH interactions with the different materials of the soil are mainly driven by hydrophobic forces [20]. Comparing the type of surfaces that both

materials present, it becomes obvious that the latter offers more attractive sorption active sites for hydrophobic substances.

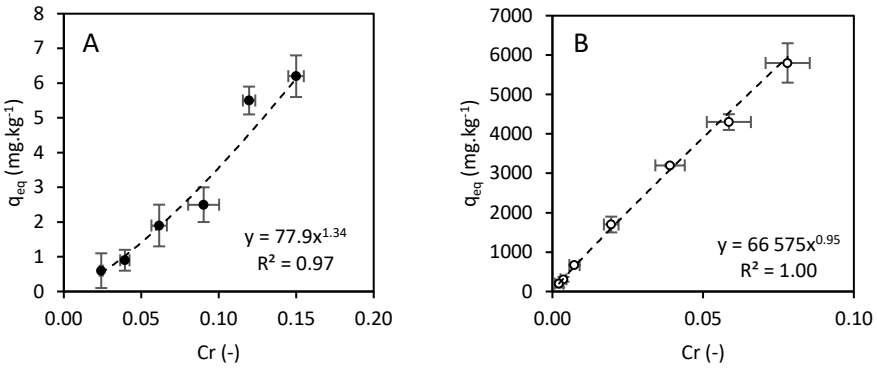

Figure 4.1 Phenanthrene sorption isotherms on (A) Clay and (B) Soil organic matter

Additionally, the exponent value of the Freundlich equation $(1/n)$ for the clay isotherm denotes a cooperative sorption process, corresponding to the findings of Müller et al. [7]. According to the authors, phenanthrene sorption mechanisms correspond to capillary condensation in the meso- and micro-pores of the clay particles (sheet structure). On the other hand, the exponent coefficient of the Freundlich equation for the SOM approximates to 1. Linear and quasi-linear isotherms for this material were also found by Wang et al. [17]. This type of isotherm is typical of equilibrium at low concentrations, meaning that sorption saturation was far from being attained in the range of conditions tested in this study.

4.1.2. Artificial soil

Figure 4.2A shows the comparison between the experimental and theoretical isotherms, with the latter calculated using the parameters for the individual materials' isotherms (as displayed in Figure 4.1). The modified Freundlich equation parameters for the experimental isotherm were similar to those found by Carmo et al. [14] ($K'_F = 683$ mg.kg^{-1} and $1/n = 0.61$), using the clay fraction (predominantly smectite) of a real soil and having about 5% of organic carbon content. The theoretical isotherm was calculated using the mass balance given in Eq. (63) and the individual Freundlich equation corresponding to each soil component.

$$q_{eq} = x_{clay} q_{eq,clay} + x_{SOM} q_{eq,SOM} \tag{63}$$

Theoretically, given the higher affinity between hydrophobic organic compounds (HOCs) and the organic matter, SOM should control the sorption equilibrium of phenanthrene [18]. However, the experimental isotherm presents a lower modified Freundlich coefficient (K'_F), as well as a lower Freundlich exponent (n^{-1}). This can be explained by the interactions between the materials in the soil. Humic acids and humic-like substances are able to bind with clay particles and form aggregates and complexes that interact differently with HOCs in the system [19]. Clay-SOM bonds include polyvalent cation bridges, ligand exchange and weak interactions, such as van der Waals forces and hydrogen bonds [21]. This phenomenon can significantly reduce the number of active sites available for the sorption of phenanthrene in both materials. Additionally, SOM can release soluble substances to the aqueous phase (usually called dissolved organic matter, or DOM) which can compete with other substances for sorption places on the solid materials and retain other compounds in solution, acting as surfactants and forming micelles [22]. The combination of all these effects may result in a diminution of the K'_F value, which, in the case of this study, was of approximately one order of magnitude.

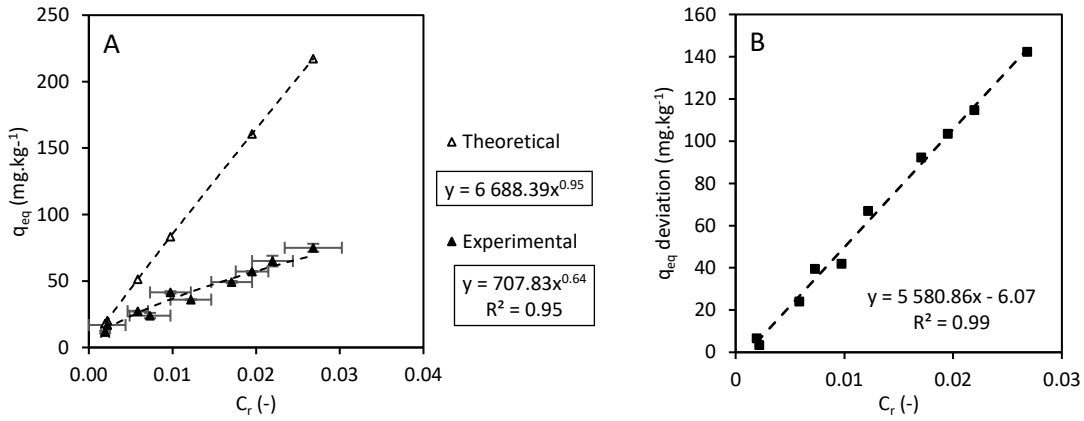

Figure 4.2 Comparison of theoretical and experimental phenanthrene sorption isotherms in artificial soil: (A) curves (B) experimental deviation of the equilibrium soil concentration from the theoretical values

Moreover, it is possible to observe that, at low reduced concentrations (C_r), both isotherms seem to have similar values, which implies that, close to this region and probably for lower concentration values, the experimental points correspond to the theoretical ones (and hence they are far from saturation). However, as C_r increases, the experimental soil values decrease in relation with the theoretical ones. To better illustrate this relation, the deviation of the experimental q_{eq} values from the theoretical ones was plotted in Figure 4.2B. The deviation depends linearly on the reduced equilibrium concentration and when it is equal to 0, the reduced concentration is approximately of 1×10^{-3}. Below this concentration, the correlation

has no longer a physical meaning and the experimental values approach the theoretical curve. From the linearity of this correlation, the modification of the active sites in the SOM-clay system for sorption probably remains unchanged in relation with the phenanthrene concentration, implying that the number of active sites is constant for any specific Clay/SOM concentration. Then, the experimental isotherm takes a convex form ($1/n < 1$), which means that the sorbent saturation is being approached due to the occupation of the active sorption sites by the SOM-clay interactions.

4.1.3. Hysteresis

Figure 4.3 shows the sorption and desorption isotherms for the artificial soil composed of 90% clay and 10% SOM used in this study. The results showed that differences between the sorption and desorption isotherms were negligible. In some cases, interactions between the sorbed compound and the soil components can cause some irreversible effects on the sorption and desorption processes. This phenomenon is called hysteresis and, according to Wu and Sun [3], can be due to three effects, i.e. chemical or physical entrapment in SOM-clay colloids or in DOM, diffusion and irreversible sorption on SOM and non-equilibrium conditions at the end of the isotherms experiments. The first two effects can be observed in aged and/or weathered contaminated soil. For recently polluted soil, slow diffusion in SOM and micropores (such as clay interlayer space) may be less important. The hysteresis index (HI), calculated as shown in Eq. (64), is typically used to measure the extent of this phenomenon.

$$HI = \left. \frac{{q_e}^d - {q_e}^s}{{q_e}^s} \right|_{T,C_{eq}} \tag{64}$$

Since the isotherm experiments were made in a relative short equilibration time (1 week), the interactions caused by aging and weathering described by Wu and Sun [3] did not occur and no significant irreversible effects could be noticed. Indeed, the hysteresis index calculated using both isotherms was always lower than 5%. Moreover, the sorption experiments were assumed to have reached the equilibrium when the concentration in the liquid phase did not change within 24 h. This time is significantly lower than the characteristic time for the apparent diffusivity of PHE in different types of soil found in the literature (between 10^2 and 10^5 h) [9]. Thus, diffusion into the micropores during 24 h may have been negligible.

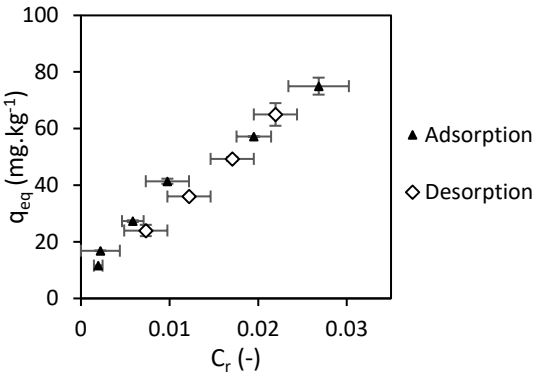

Figure 4.3 Phenanthrene sorption and desorption isotherms in artificial soil

4.2. Desorption kinetics

4.2.1. Experimental results

Figure 4.4 shows the results for the desorption kinetic experiments, at a constant soil concentration (10% m/v), varying the clay and SOM fractions, as well as the curve at 1% of pure SOM. For all the PAHs tested, the fastest desorption rate was obtained for the soil containing pure clay, and the slowest was observed for the pure SOM. The curve for the soil containing a mixture between these two conditions (10% m/v with $x_{clay} = 0.9$ and $x_{SOM} = 0.1$) exhibited a behavior between that of the two pure compounds. Increasing the SOM content at the same soil concentration ($x_{clay} = 0.8$ and $x_{SOM} = 0.2$) induced a slower desorption rate. These results show that, at constant soil concentration conditions, higher SOM contents lead to slower desorption kinetic rates. In contrast, Figure 4.5 shows the desorption curves for four different concentrations, at the same soil composition ($f_{clay} = 0.9$). In this case, it is possible to observe that the curves have a similar shape and no clear trend between the soil concentration and the rate can be established.

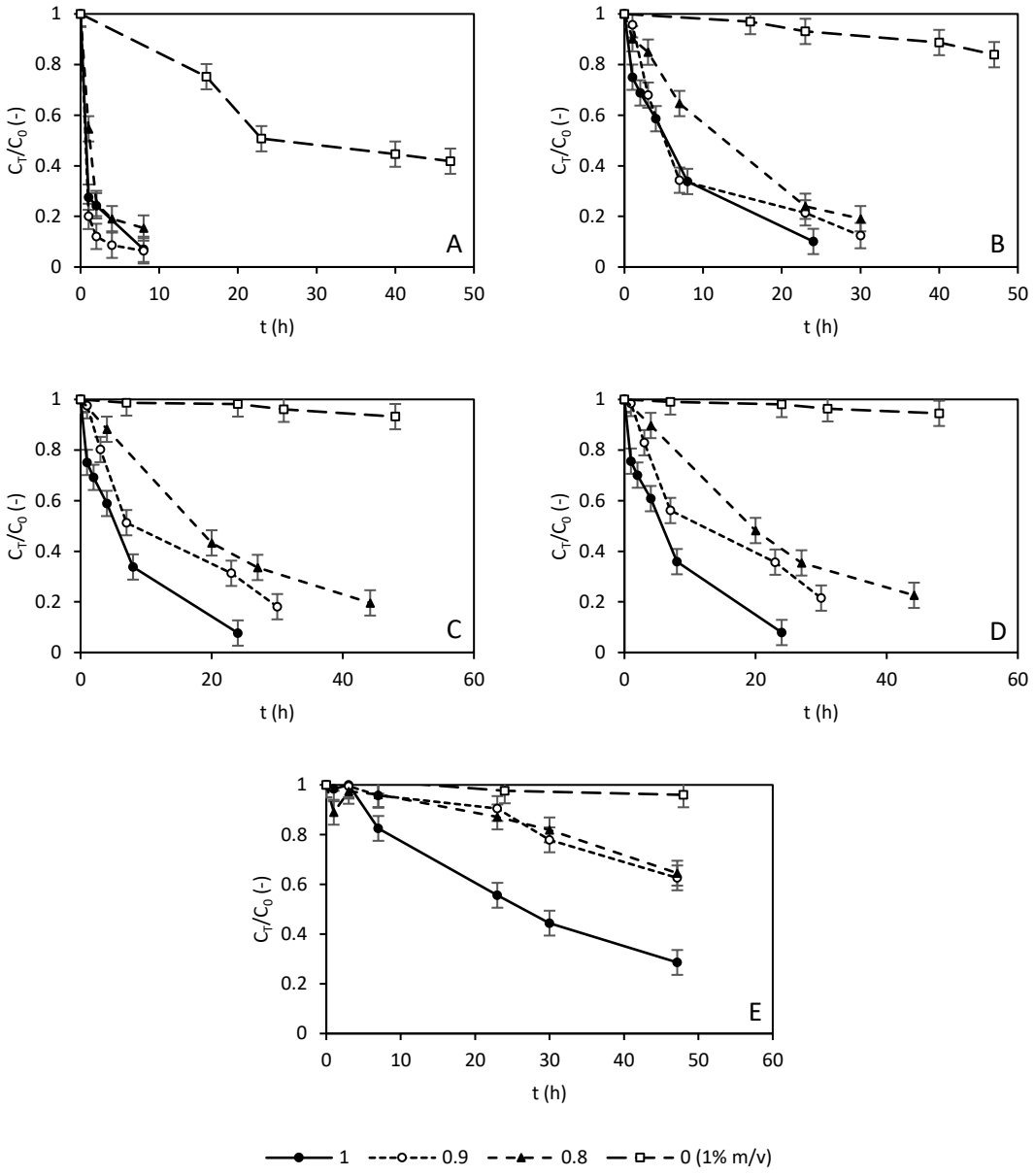

Figure 4.4 Desorption curves at different clay mass fractions for (A) naphthalene; (B) phenanthrene; (C) fluoranthene; (D) pyrene; and (E) benzo(a)pyrene

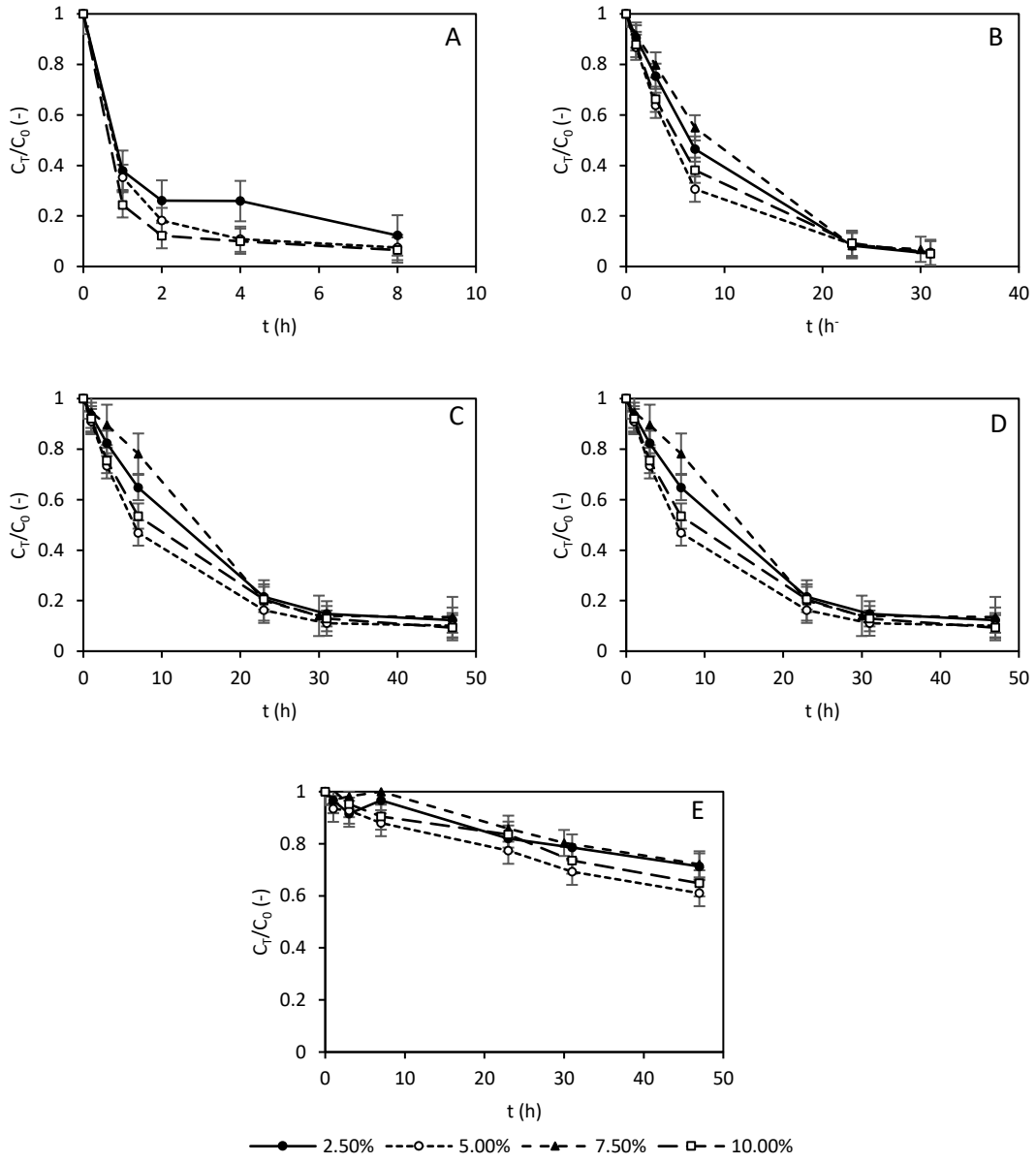

Figure 4.5 PAH desorption kinetics at different soil concentration (%m/v) for (A) naphthalene; (B) phenanthrene; (C) fluoranthene; (D) pyrene; and (E) benzo(a)pyrene

4.2.2. Modeling

Given the results shown in section 4.2.1, the fitting of the desorption curves was pursued using Eq. 9 under three conditions: i) the desorption kinetic constant for clay (k_{clay}) is the same for all experiments done at the same soil concentration; ii) the desorption kinetic constant for SOM (k_{SOM}) is the same for all experiments done at the same soil concentration; and iii) the initial PAH concentration in clay ($\phi_{clay,0}$) and, hence, in SOM are the same for the experiments done at the same soil composition. Assuming hypothesis (i) and (ii) means

that the desorption rate of each soil fraction does not depend on the soil composition, while hypothesis (iii) supposes an ideal homogeneity of PAHs in the spiked soil. In fact, soil containing the same ratio clay/SOM was spiked and homogenized in a unique batch, validating hypothesis (iii).

Results of the modeling are shown in Table 4.2. A good correlation was found between the experimental normalized concentrations and the estimated ones (Figure 4.6), with $R^2 = 0.97$ and most individual errors lower than 20%.

Table 4.2 Results of the fit for the kinetic model

Compound	Soil concentration (% m/v)	x_{clay} (-)	f_{clay} (-)	f_{SOM} (-)	k_{clay} (h^{-1})	k_{SOM} (h^{-1})
NAP	2.5	0.9	0.90	0.10	8.23×10^{-1}	1.40×10^{-2}
	5	0.9	0.90	0.10	1.11	1.50×10^{-2}
	10	1	1.00	0.00	1.55	-
		0.9	0.90	0.10	1.55	1.88×10^{-2}
		0.8	0.79	0.21	1.55	1.88×10^{-2}
	1	0	0.00	1.00	-	1.88×10^{-2}
PHE	2.5	0.9	0.94	0.06	1.34×10^{-1}	3.92×10^{-3}
	5	0.9	0.94	0.06	1.60×10^{-1}	3.07×10^{-3}
	7.5	0.9	0.94	0.06	1.33×10^{-1}	3.23×10^{-3}
	10	1	1	0	1.36×10^{-1}	-
		0.9	0.94	0.06	1.36×10^{-1}	4.56×10^{-3}
		0.8	0.78	0.22	1.36×10^{-1}	4.56×10^{-3}
	1	0	0.00	1.00	-	4.56×10^{-3}
FLA	2.5	0.9	0.88	0.12	9.48×10^{-2}	1.00×10^{-3}
	5	0.9	0.88	0.12	1.21×10^{-1}	4.00×10^{-3}
	7.5	0.9	0.88	0.12	1.00×10^{-1}	2.00×10^{-3}
	10	1	1.00	0.00	1.07×10^{-1}	-
		0.9	0.88	0.12	1.07×10^{-1}	2.00×10^{-3}
		0.8	0.69	0.31	1.07×10^{-1}	1.46×10^{-3}
	1	0	0.00	1.00	-	1.46×10^{-3}
PYR	2.5	0.9	0.85	0.15	8.55×10^{-2}	2.00×10^{-3}
	5	0.9	0.85	0.15	1.18×10^{-1}	5.00×10^{-3}
	7.5	0.9	0.85	0.15	9.31×10^{-2}	3.00×10^{-3}
	10	1	1.00	0.00	1.06×10^{-1}	-
		0.9	0.85	0.15	1.06×10^{-1}	1.00×10^{-3}
		0.8	0.67	0.33	1.06×10^{-1}	1.22×10^{-3}
	1	0	0.00	1.00	-	1.22×10^{-3}
B(a)P	2.5	0.9	0.48	0.52	1.85×10^{-2}	2.65×10^{-4}
	5	0.9	0.48	0.52	3.21×10^{-2}	2.58×10^{-4}
	7.5	0.9	0.48	0.52	1.69×10^{-2}	2.64×10^{-4}
	10	1	1.00	0.00	2.65×10^{-2}	-
		0.9	0.48	0.52	2.65×10^{-2}	2.73×10^{-4}
		0.8	0.32	0.68	2.65×10^{-2}	2.73×10^{-4}
	1	0	0.00	1.00	-	2.73×10^{-4}

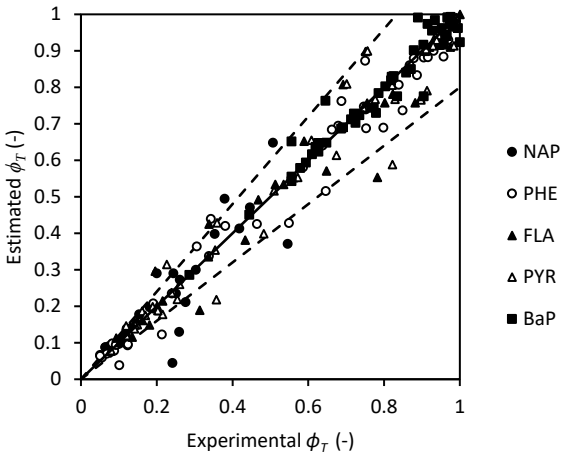

Figure 4.6 Experimental vs estimated relative concentration for the desorption kinetic modelling

A two-compartment three-parameter model, similar to Eq. (62, has already been reported [8,9]. However, in most cases, the terms represent a "rapid" and a "slow" desorption fraction. It is interesting to notice that for Barnier et al. [8], Weber and Kim [4] and Johnson et al. [9] the values of the "rapid" kinetic constant are in the same order of magnitude of those found for clay in this study, regardless if they used spiked or real aged polluted soil. On the other hand, in their studies, values for the "slow" kinetic desorption constant are more variable, including several orders of magnitudes (10^{-4} to 10^{1} h^{-1}), depending on the type of soil.

Müller et al. [7] demonstrated that sand materials have a lower PAH adsorption capacity than clay due to its lower surface area. Nevertheless, if these parameters are normalized by the surface area, partition coefficients result to be equivalent. This could mean that the mechanisms by which the PAHs are adsorbed onto both sand and clay materials are similar and, hence, desorption mechanisms could be affected by similar parameters. The implications of this idea, in addition to the results of the present study, could indicate that the "rapid" desorption rate correspond to the desorption from mineral surfaces in the soil. In contrast, the high variability of the types of SOM in soil, as well as factors such as aging and weathering, may alter and change the characteristics of the bonds between PAHs and carbonaceous materials [5]. Chemical reactions with the sorbent (chemisorption), diffusion into glassy organic matter (black carbon particles) and other processes can affect the final desorption rate from these materials, meaning that the "slow" desorption could correspond to SOM.

In addition, from the model fitting, the initial PAH distribution among the soil components was calculated (Figure 4.7). In general, low molecular weight PAHs, such as naphthalene and phenanthrene, were distributed homogenously according to the mass fraction of clay and

SOM for both soil composition tested. These results contrast with the equilibrium isotherm ones (in section 4.1), from which it was demonstrated that SOM possesses a higher PAH sorption capacity. When SOM is present during soil spiking, most PAHs are expected to be strongly attracted to SOM, having a much higher concentration on it. Nevertheless, since the soil spiking was not performed with water but acetone (a less polar solvent of rapid evaporation) in this study, hydrophobic effects were less influencing, particularly for light molecular weight PAHs. Therefore, NAP and PHE were almost equally distributed among the soil mass fractions of clay and SOM.

On the other hand, PAHs with 4 rings (FLA and PYR) were slightly more concentrated on SOM. For B(a)P, concentration on SOM was always superior to 50%, even if the maximum mass fraction of this material was 20%. This means that for high molecular weight PAHs, the spiking solvent was polar enough to observe the hydrophobic effects on the pollutant distribution in the different soil fractions and favor the sorption onto SOM. This means that the soil contamination method controls the distribution of the PAHs in the soil.

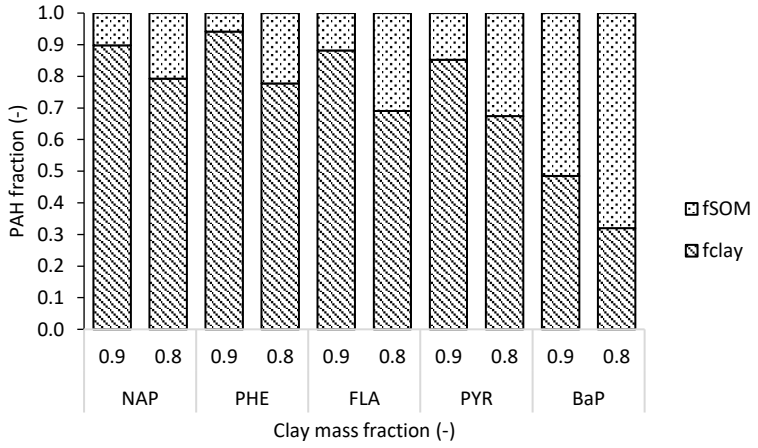

Figure 4.7 Fitted PAH initial distribution on the soil components according to the soil mass fraction

Regarding the effect of the soil concentration on the desorption rate, Figure 4.8 shows that no clear effect in either the k_{clay} or k_{SOM} for pure materials can be established. In a previous work [23], it was demonstrated that clay concentration changes the viscosity of the slurry and, hence, the hydrodynamic conditions of the systems. The fact that soil concentration, within the range tested, had not noticeable influence on the desorption kinetic constant could mean that the PAH desorption process is mainly controlled by the attachment and detachment of the molecules from the active site (i.e. the equilibrium process).

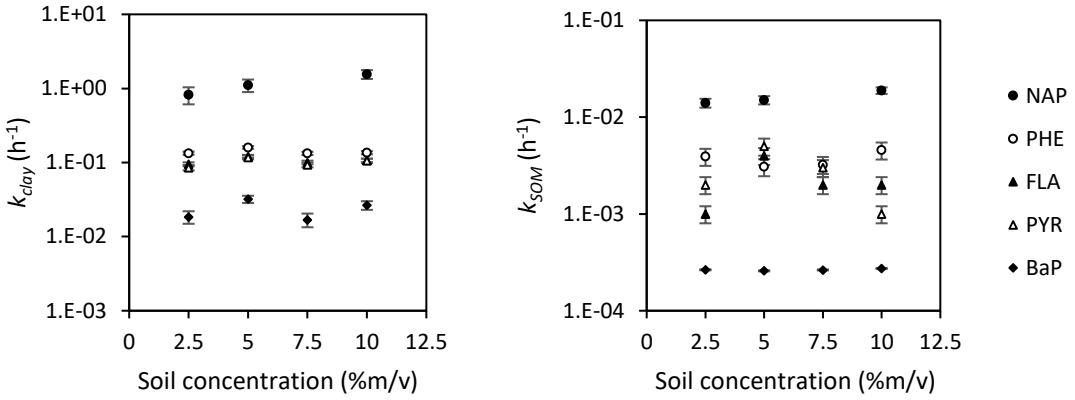

Figure 4.8 Influence of the soil concentration in the slurry on the desorption kinetic constants for (A) clay and (B) SOM

In fact, power-type correlations, shown in Figure 4.9, were found of the first order kinetic constants for both clay and SOM, and the normalized organic carbon to water partition coefficient (K_{OC}). Moreover, it is interesting to observe that the exponents of the power-type correlation for both materials is similar, which might indicate that the relation between the equilibrium and kinetic parameters involve similar types of interactions. These correlations corroborate the hypothesis that the PAH desorption kinetics for these materials are mainly controlled by the physicochemical properties of both, sorbent and PAH molecule, and the affinity between these materials (hydrophobicity). Additionally, the constant of proportionality of the power function for desorption from clay is higher than that for SOM. This can be due to the stronger hydrophobic interactions on SOM than on clay, as discussed in section 4.1.

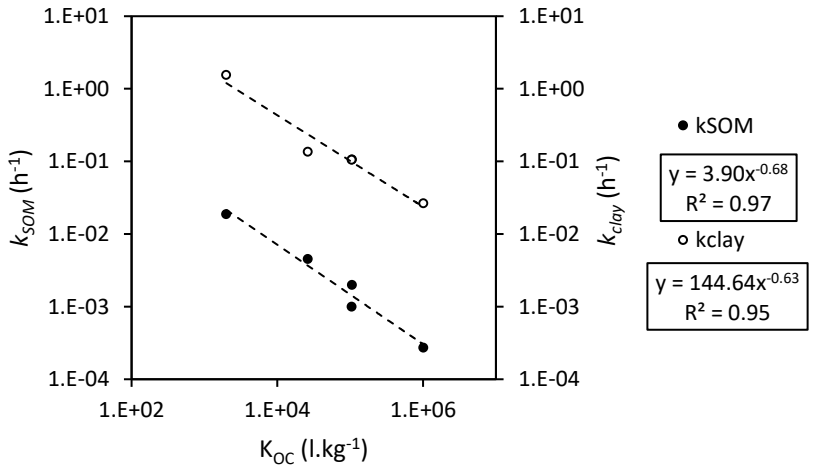

Figure 4.9 Estimated desorption kinetic constants for the pure fractions as a function of KOC (from NJDEP, 2008 [24])

5. Extrapolation of the results for real contaminated soil

The results of this study show that the main interactions of PAHs with soil components are of hydrophobic nature. However, the strength of the associations as well as soil components interactions determine the fate of PAHs in the environment [19]. Therefore, SOM type and content in soil are important factors to consider when potential treatments are being evaluated [19]. Likewise, an important feature often neglected in many studies seeking the remediation of specific real contaminated soils is the history of the soil pollution and its influence on the PAH distribution and remediation. In this regard, origin, aging and weathering are of highly importance.

For instance, regarding the pollution origin, if the contaminants were brought to the geosorbents via an aqueous phase (in the same way as the sorption equilibrium process carried out in this research work), it is probable that they will mostly adsorb onto the hydrophobic parts of the SOM. However, if a process similar to the soil spiking used in this study occurs, in which less polar organic solvents are the carriers of these contaminants, the distribution might be more uniform according to the mass fractions of the soil components.

Additionally, aging could have a great influence on the pollutant desorption kinetics, predominantly from SOM [25]. It was demonstrated by this study that desorption kinetics of recent polluted soil depends mainly on surface equilibrium processes. Nonetheless, this behavior can change due to contaminant pore diffusion and chemisorption processes [5,20]. On the other hand, the compartment model developed in this research study could explain the behavior and fate of pollutants in the soil. For example, sorbents exposed to continuous contact with aqueous phases (such as sediments) could easily release the contaminants from the mineral surfaces (or “rapid” desorption fractions) and even redistribute them toward the most hydrophobic parts of the soil [26]. Consequently, it is important to consider the historic factors of the polluted site in order to best decide on the remediation treatment to apply.

6. Conclusions

The objective of the present study was to determine the influence of clay and SOM in the PAH sorption-desorption equilibrium process, as well as the effect of soil concentration and composition on the PAH desorption kinetics. From the results, the next conclusion were drawn:

- Even if SOM controls the PAH sorption equilibrium, clay presence can interfere, probably by reducing the available sorption sites by forming SOM-clay aggregates. Hysteresis was negligible for short time PAH sorption equilibration.
- Desorption kinetics was modelled as the sum of individual desorption rates for each soil component using a three-parameter, two-compartment model. First order equations were defined for each compartment.
- Distribution of PAH concentration in each fraction depends on the way the soil was contaminated. In any case, PAH molecules with a higher molecular weight (and a higher hydrophobicity) tend to be sorbed in higher proportion onto nonpolar sections of SOM than onto mineral surfaces.
- Soil concentration did not affect the desorption kinetic rate. This means that desorption may only depend on the surface equilibrium (and, hence, on the physicochemical properties of the molecule and the sorbent) and not on the hydrodynamic conditions in the soil concentration range tested in this study.
- A power-type correlation was found for the first order kinetic constants for both materials, clay and SOM, and the normalized organic carbon to water partition coefficient (K_{OC}), meaning that the PAH desorption from these fractions of soil is mainly controlled by the affinity between the compound and the sorbent (hydrophobicity).
- Pollution origin, aging and weathering determine the fate of PAHs in soil and environment.

References

[1] S. Hussain, M. Arshad, D. Springael, S.R. SøRensen, G.D. Bending, M. Devers-Lamrani, Z. Maqbool, F. Martin-Laurent, Abiotic and Biotic Processes Governing the Fate of Phenylurea Herbicides in Soils: A Review, Crit. Rev. Environ. Sci. Technol. 45 (2015) 1947–1998. doi:10.1080/10643389.2014.1001141.

[2] S. Gan, E.V. Lau, H.K. Ng, Remediation of soils contaminated with polycyclic aromatic hydrocarbons (PAHs), J. Hazard. Mater. 172 (2009) 532–549. doi:10.1016/j.jhazmat.2009.07.118.

[3] W. Wu, H. Sun, Sorption–desorption hysteresis of phenanthrene – Effect of nanopores, solute concentration, and salinity, Chemosphere. 81 (2010) 961–967. doi:10.1016/j.chemosphere.2010.07.051.

[4] W.J. Weber, H.S. Kim, Optimizing Contaminant Desorption and Bioavailability in Dense Slurry Systems. 1. Rheology, Mechanical Mixing, and PAH Desorption, Environ. Sci. Technol. 39 (2005) 2267–2273. doi:10.1021/es049565b.

[5] C. Trellu, A. Miltner, R. Gallo, D. Huguenot, E.D. van Hullebusch, G. Esposito, M.A. Oturan, M. Kästner, Characteristics of PAH tar oil contaminated soils—Black particles, resins and implications for treatment strategies, J. Hazard. Mater. 327 (2017) 206–215. doi:10.1016/j.jhazmat.2016.12.062.

[6] G. Cornelissen, Ö. Gustafsson, T.D. Bucheli, M.T.O. Jonker, A.A. Koelmans, P.C.M. van Noort, Extensive Sorption of Organic Compounds to Black Carbon, Coal, and Kerogen in Sediments and Soils: Mechanisms and Consequences for Distribution, Bioaccumulation, and Biodegradation, Environ. Sci. Technol. 39 (2005) 6881–6895. doi:10.1021/es050191b.

[7] S. Müller, K.U. Totsche, I. Kögel-Knabner, Sorption of polycyclic aromatic hydrocarbons to mineral surfaces, Eur. J. Soil Sci. 58 (2007) 918–931. doi:10.1111/j.1365-2389.2007.00930.x.

[8] C. Barnier, S. Ouvrard, C. Robin, J.L. Morel, Desorption kinetics of PAHs from aged industrial soils for availability assessment, Sci. Total Environ. 470–471 (2014) 639–645. doi:10.1016/j.scitotenv.2013.10.032.

[9] M.D. Johnson, T.M. Keinath, W.J. Weber, A Distributed Reactivity Model for Sorption by Soils and Sediments. 14. Characterization and Modeling of Phenanthrene Desorption Rates, Environ. Sci. Technol. 35 (2001) 1688–1695. doi:10.1021/es001391k.

[10] W.J. Weber, W. Huang, A distributed reactivity model for sorption by soils and sediments. 4. Intraparticle heterogeneity and phase-distribution relationships under nonequilibrium conditions, Environ. Sci. Technol. 30 (1996) 881–888.

[11] M.H. Huesemann, T.S. Hausmann, T.J. Fortman, Does bioavailability limit biodegradation? A comparison of hydrocarbon biodegradation and desorption rates in aged soils, Biodegradation. 15 (2004) 261–274.

[12] L. Lei, M.T. Suidan, A.P. Khodadoust, H.H. Tabak, Assessing the Bioavailability of PAHs in Field-Contaminated Sediment Using XAD-2 Assisted Desorption, Environ. Sci. Technol. 38 (2004) 1786–1793. doi:10.1021/es030643p.

[13] G.L. Northcott, K.C. Jones, Developing a standard spiking procedure for the introduction of hydrophobic organic compounds into field-wet soil, Environ. Toxicol. Chem. 19 (2000) 2409–2417.

[14] A.M. Carmo, L.S. Hundal, M.L. Thompson, Sorption of Hydrophobic Organic Compounds by Soil Materials: Application of Unit Equivalent Freundlich Coefficients, Environ. Sci. Technol. 34 (2000) 4363–4369. doi:10.1021/es000968v.

[15] M.J. Geerdink, M.C. van Loosdrecht, K.C.A. Luyben, Model for microbial degradation of nonpolar organic contaminants in a soil slurry reactor, Environ. Sci. Technol. 30 (1996) 779–786.

[16] L.S. Hundal, M.L. Thompson, D.A. Laird, A.M. Carmo, Sorption of Phenanthrene by Reference Smectites, Environ. Sci. Technol. 35 (2001) 3456–3461. doi:10.1021/es001982a.

[17] G. Wang, S. Kleineidam, P. Grathwohl, Sorption/desorption reversibility of phenanthrene in soils and carbonaceous materials, Environ. Sci. Technol. 41 (2007) 1186–1193.

[18] X. Cui, W. Hunter, Y. Yang, Y. Chen, J. Gan, Biodegradation of pyrene in sand, silt and clay fractions of sediment, Biodegradation. 22 (2011) 297–307. doi:10.1007/s10532-010-9399-z.

[19] R.L. Wershaw, A new model for humic materials and their interactions with hydrophobic organic chemicals in soil-water or sediment-water systems, J. Contam. Hydrol. 1 (1986) 29–45.

[20] W. Chen, H. Wang, Q. Gao, Y. Chen, S. Li, Y. Yang, D. Werner, S. Tao, X. Wang, Association of 16 priority polycyclic aromatic hydrocarbons with humic acid and humin fractions in a peat soil and implications for their long-term retention, Environ. Pollut. 230 (2017) 882–890. doi:10.1016/j.envpol.2017.07.038.

[21] M.V. Lützow, I. Kögel-Knabner, K. Ekschmitt, E. Matzner, G. Guggenberger, B. Marschner, H. Flessa, Stabilization of organic matter in temperate soils: mechanisms and their relevance under different soil conditions - a review, Eur. J. Soil Sci. 57 (2006) 426–445. doi:10.1111/j.1365-2389.2006.00809.x.

[22] H. Yu, G. Huang, C. An, J. Wei, Combined effects of DOM extracted from site soil/compost and biosurfactant on the sorption and desorption of PAHs in a soil–water system, J. Hazard. Mater. 190 (2011) 883–890. doi:10.1016/j.jhazmat.2011.04.026.

[23] D.O. Pino-Herrera, Y. Fayolle, S. Pageot, D. Huguenot, G. Esposito, E.D. van Hullebusch, Y. Pechaud, Gas-liquid oxygen transfer in aerated and agitated slurry systems with high solid volume fractions, Chem. Eng. J. 350 (2018) 1073–1083. doi:10.1016/j.cej.2018.05.193.

[24] NJDEP, Chemical Properties for Calculation of Impact to Ground Water Soil Remediation Standards, (2008). doi:10.7282/T3Z0385G.

[25] B.J. Reid, K.C. Jones, K.T. Semple, Bioavailability of persistent organic pollutants in soils and sediments—a perspective on mechanisms, consequences and assessment, Environ. Pollut. 108 (2000) 103–112.

[26] J.W. Talley, U. Ghosh, S.G. Tucker, J.S. Furey, R.G. Luthy, Particle-scale understanding of the bioavailability of PAHs in sediment, Environ. Sci. Technol. 36 (2002) 477–483.

CHAPTER 5

Culture enrichment and biodegradation kinetics

CHAPTER 5 – Culture enrichment and biodegradation kinetics

Biodegradation. In this chapter, a mixed culture from a real PAH-contaminated soil was acclimated to phenanthrene consumption and enriched with co-substrates to test their effect in PAH biodegradation kinetics. The effect of the presence of a surfactant in the broth was also tested.

Abstract

A key issue regarding the polycyclic aromatic hydrocarbon (PAH) biodegradation by mixed cultures is their ability to adapt to environmental changes. Depending of the characteristics of these changes, synergetic or antagonistic effects, which affect the extent and the rate of the PAH utilization, could arise. The goal of this work was to study the effect of the acclimation, co-substrate enrichment and surfactant presence on the PAH-degradation ability of a mixed culture obtained from a PAH-contaminated soil. Phenanthrene was used as the sole carbon source for the culture acclimation. Two co-substrates (i.e. naphthalene, glucose) and a zwitterionic surfactant (lauryl betaine) and some of their combinations were used for culture enrichment. The PAH degradation ability of the cultures was measured by their consumption kinetics, biomass production and overall efficiency. Results showed that PAHs containing non-aromatic rings are less degraded by cultures enriched with only-aromatic PAHs. As a co-substrate of phenanthrene-degrading cultures, glucose incremented the biomass amount produced. However, microorganisms developed were less efficient to degrade phenanthrene certainly due to a less PAH degrading specified biomass development. Lauryl betaine strongly inhibited the phenanthrene-degrading capacity and the bacterial growth, even when glucose was present as co-substrate. The substrate used in the acclimation and enrichment of the culture plays an important role in its PAH biodegradation capacity and change adaptability.

1. Introduction

Polycyclic aromatic hydrocarbons (PAHs) are a group of toxic and recalcitrant compounds present in many contaminated sites. They represent a major environmental concern and, thus, numerous removal techniques for these family of compounds have been developed. Among the existing technologies, biological treatments are considered as one of the less expensive and most environmentally friendly techniques in almost any polluted matrix (water, soil, sediments, etc.) [1,2]. For this reason, the scientific community has dedicated significant time and effort to the understanding of the diverse mechanisms by which microorganisms degrade these pollutants. Identification of PAH-degrading strains, biodegradation pathways hypothesis and microbial consortia behavior towards the utilization of these compounds have been widely studied [3–6].

A key topic regarding the PAH biodegradation by mixed cultures is their ability to adapt to environmental changes [7]. Depending on the characteristics of these changes, synergetic or antagonistic effects, affecting the extent and the rate of the PAH utilization, could arise [8]. The understanding of these effects may allow the development of more resistant and efficient PAH-degrading cultures for specific applications. However, despite the growing knowledge on these topics during the last three decades, specific interactions between microorganisms, co-substrates and other substances that could be present during the degradation process need to be further studied. For instance, PAH degradation in presence of naphthalene as a co-substrate could result in either a positive or a negative effect [9,10]. Another example is the use of surfactants; in many soil and sediment remediation treatments, surfactants are used to increase the aqueous solubility and the mobility of hydrophobic organic compounds in order to enhance the bioavailability of these pollutants [11,12]. Nonetheless, they can also inhibit and even be toxic for many microorganisms [13].

Therefore, the general objective of this work is to study the effect of the acclimation, co-substrate enrichment and surfactant presence on the PAH-degradation ability of a mixed culture obtained from a PAH-contaminated soil. Phenanthrene was used for the culture acclimation. Two co-substrates (i.e. naphthalene, glucose) and a zwitterionic surfactant (lauryl betaine) and some of their combinations were used for culture enrichment. The PAH degradation ability of the cultures was measured by their consumption kinetics, biomass production and overall efficiency.

2. Materials and methods

Experiments were divided in five phases depicted in Figure 5.1. The first phase consisted in the isolation of a mixed culture from a PAH polluted soil and its acclimation to phenanthrene degradation as sole carbon source (section 2.2). The second phase consisted in the evaluation of the PAH degradation ability of the acclimated culture (section 2.3). In the third phase, cultures were enriched using specific co-substrate and in the presence of a surfactant in order to evaluate the effect of these substances in the biomass production (section 2.4). The fourth phase consisted in the assessment of the effect of the co-substrates and surfactant on the ability of the enriched culture to degrade phenanthrene (also section 2.4). Finally, the fifth phase consisted in the re-acclimation of the enriched cultures to phenanthrene consumption and the evaluation of its ability to degrade this molecule (section 2.5).

2.1. Chemicals and culture medium

All the PAHs used were provided by Sigma-Aldrich with a purity of (at least) 98%. Reagent grade salts and glucose were provided either by Merck or by VWR chemicals. Culture medium for all the experiments performed in this study was a modified Bushnell-Hass (BH) culture medium. It was constituted by $MgSO_4$ (0.2 $g.l^{-1}$), $CaCl_2$ (0.02 $g.l^{-1}$), KH_2PO_4 (1 $g.l^{-1}$), K_2HPO_4 (1 $g.l^{-1}$), $FeCl_3$ (0.025 $g.l^{-1}$) and NaCl (0.2 $g.l^{-1}$). Nitrogen source was provided by adding a proper amount of a NH_4Cl solution (10 $g.l^{-1}$) in order to obtain a substrate COD/N ratio of 10 in the broth in each experiment.

2.2. Culture development and acclimation

A PAH-degrading culture was developed using a real PAH-contaminated clayey soil from the north of France as inoculum. 5 g of soil were added to a 250-ml Erlenmeyer flask containing 200 ml of modified BH medium and few phenanthrene crystals as only source of carbon. The mixture was magnetically stirred in an incubator at 20°C for one week. After this incubation period, 10 ml of the culture were added to a second 250-ml Erlenmeyer flask and 90 ml of minimal BH medium and few phenanthrene crystal were added. This operation was repeated weekly for a period of 2 month, and every 3 weeks on average for a period of 6 months, according to the solution turbidity and the PHE consumption (crystals disappearance). Dissolved oxygen was measured at selected times using an inoLab® Oxi 7310 DO sensor connected to a Cellox 325 probe (WTW) to verify aerobic conditions in the flask.

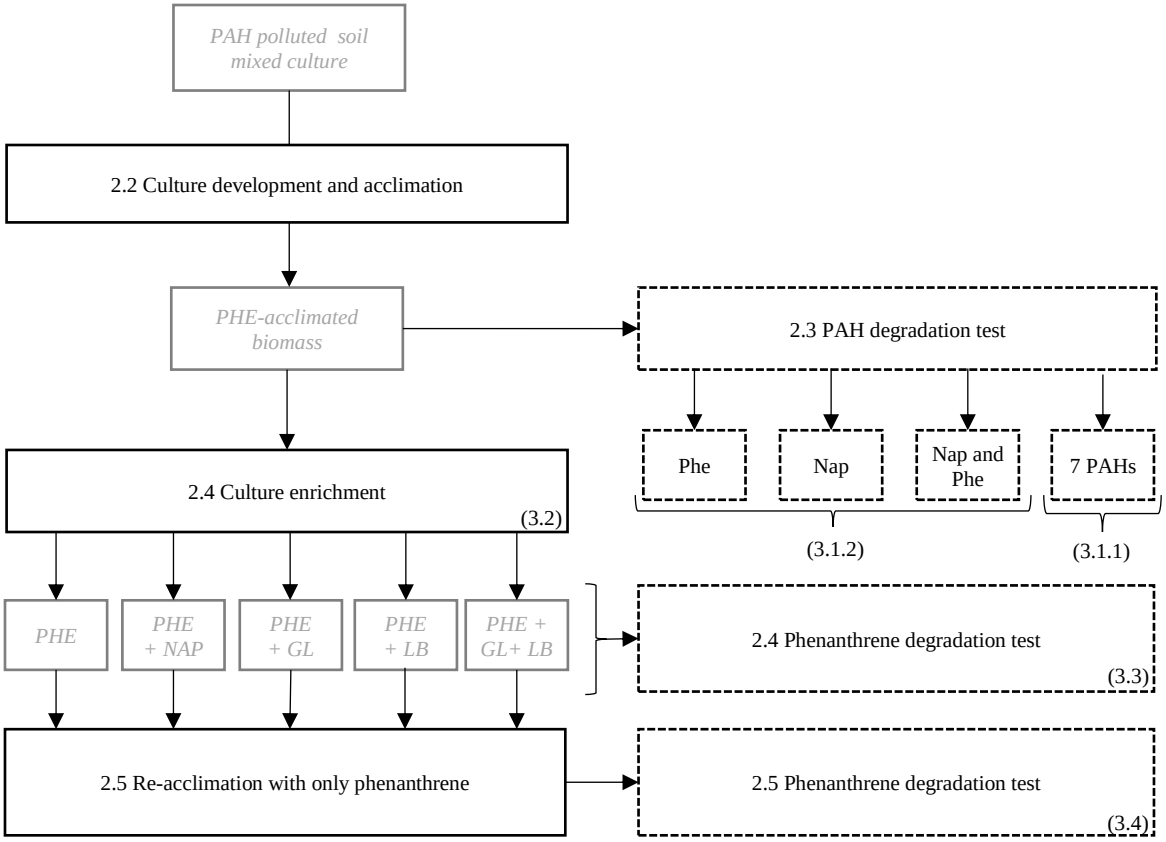

Figure 5.1 Experimental approach, (——) cultures, (——) selective pressure, and (-----) kinetic experiments. Number in parenthesis indicate the section in which the corresponding topic is discussed.

2.3. PAH biodegradation by acclimated cultures

The PHE-acclimated cultures were tested for PAH biodegradation. To do this, four different PAH aqueous solutions (below the limit of solubility) were prepared with respect to the different PAH used. Their name and PAH constituents are reported on Table 5.1. The ability of the microbial consortium to degrade the different PAH combination was assessed by measuring the decreasing in the PAH concentration in time.

With this purpose, samples were taken from the acclimated culture, centrifugate and washed three times with a sodium chloride solution (9 $g.l^{-1}$) to concentrate the biomass and avoid carrying phenanthrene from the culture development in the tests. These samples were used as inocula for the biodegradation experiments. PAH mixture solutions were prepared in a modified BH medium by adding solid PAH crystal. The solutions were magnetically stirred for 24 h and then filtered to remove remaining solids. Biodegradation experiments were performed in 100-ml septum capped culture bottles. PAH solutions were added to the bottles. Nitrogen, in the form of ammonium, was also added to the bottles in order to respect a COD to N ratio of 10. The bottles were inoculated with the washed acclimated cultures. Liquid

samples (0.5 ml) were taken at regular intervals using glass syringes in order to follow the PAH biodegradation kinetics.

Table 5.1 PAH solutions tested for degradation by the PHE-acclimated culture

PAH solution name	PAHs content in solution
NAP	Naphthalene
PHE	Phenanthrene
NAP + PHE	Naphthalene and phenanthrene
7 PAHs	Naphthalene, acenaphthene, phenanthrene, anthracene, fluoranthene, pyrene and benzo(a)pyrene

2.4. Culture enrichment with co-substrates or surfactant

Since the growing of the microorganism biomass in aqueous phase was limited by the solubility of phenanthrene, the PHE-acclimated cultures were used to create enriched cultures with different co-substrates. Samples of the PHE-acclimated culture were washed and centrifugated, then resuspended in 3 ml of a NaCl solution (9 $g.l^{-1}$) and kept at -20°C until their use. Five enriched cultures were prepared, according to Table 5.2, to test the effect of two co-substrates (i.e. naphthalene, glucose) and a zwitterionic surfactant (lauryl betaine) and some of their combinations in the culture development.

Table 5.2 Co-substrate and surfactant used for culture enrichment

Culture name	Co-substrate and/or surfactant used (amount)
PHE	Phenanthrene (20 mg; solid)
NP	Phenanthrene (20 mg; solid) and naphthalene (100 mg; solid)
PG	Phenanthrene (20 mg; solid) and glucose (2 $g.l^{-1}$)
PLB	Phenanthrene (20 mg; solid) and lauryl betaine (0.1% m/v)
PGLB	Phenanthrene (20 mg; solid), glucose (2 $g.l^{-1}$) and lauryl betaine (0.1% m/v)

250-ml Erlenmeyer flasks were filled with 20 mg of phenanthrene crystals, the corresponding co-substrate, minimal BH medium and an ammonium chloride solution (C/N ratio was kept at 10:1) to reach a volume of 197 ml. Initial glucose concentration was 2 g.l-^{1} and LB concentration was 0.5% (v/v) in the respective bottles containing these compounds. The acclimation period lasted 1 month, and the resulting biomass was measured as particulate COD. After the enrichment phase, cultures were washed, centrifugated, resuspended in 3 ml of a NaCl solution (9 $g.l^{-1}$) and frozen for future use.

2.5. Phenanthrene re-acclimation and degradation ability

With the purpose of observing the effect of the culture enrichment on the kinetic behavior of the phenanthrene-degrading microorganisms, enriched cultures were re-acclimated for 1 week using phenanthrene as the only carbon source, and then their phenanthrene-degradation ability re-assessed by kinetic experiments. The protocol for kinetic biodegradation, detailed in section 2.3, was repeated using only phenanthrene as substrate.

2.6. Analytical methods

PAH concentrations were measured using an HPLC (Hitachi *LaChrom Elite® L-2400)* coupled with UV/VIS detector (set to 254 nm) and a fluorescence detector (Excitation wavelength set to 250 nm and Emission wavelength set to 350 nm). The separation was performed using a RP C-18 end capped column (Purospher®, Merck) (5 mm, 25 cm × 4.6 mm) placed in an oven at 40.0 °C. The mobile phase was a mixture of water (with a pH adjusted to 2.5 using phosphoric acid) and acetonitrile (25:75 v/v) with a flow rate of 0.8 $ml.min^{-1}$ in isocratic mode. The injection volume was 20 µl. Culture COD values were measured using a Merck Millipore COD cell test Spectroquant® 114541.

3. Results and discussion

3.1. PAHs biodegradation by phenanthrene acclimated culture

3.1.1. Biodegradation of 7 PAHs

The two main issues regarding culture development and acclimation with PAHs are generally the toxicity and the low bioavailability in aqueous phase of these pollutants. Phenanthrene is however characterized by a low toxicity and a relatively higher solubility compared to other PAHs. For these reasons, this PAH was chosen for the acclimation phase and the kinetic tests in this work. Biodegradation kinetics and efficiency curves after 50h are displayed on Figure 5.2 and Figure 5.3.

In Figure 5.2 one can observe that the fastest PAH degraded is phenanthrene (without a lag phase). For all the other PAHs, a lag phase from 0 to 17 h was observed. The absence of lag phase for phenanthrene may be explained by the fact that the culture acclimation was done using this compound as sole source of carbon, meaning that microorganisms were prepared to immediately degrade this compound. It seems that around 17 h, the concentration of phenanthrene had been reduced to less than 50% of the initial concentration, and probably the stress linked to the competition for this substrate might have pushed the microorganism to adapt and consume the other molecules present in the broth .

On the other hand, it is common to find in the literature that low-molecular-weight PAH biodegradation exhibits faster kinetics than the biodegradation of PAHs with a higher number of rings, even when cultures are enriched with several PAHs [9]. Thus, the following order in term of kinetics of degradation was expected: naphtalene>acenaphtene>anthracene-phenanthrene>fluoranthene>Pyrene>Benzo(a)-pyrene. In the present study, anthracene, was the second fastest PAH degraded, followed by naphthalene. Even if the latter should be degraded easier than most PAHs [1,2], it was consumed after phenanthrene and anthracene (Figure 5.2). This can be explained by the phenanthrene acclimation process. Anthracene, as phenanthrene, is a three-ring PAH and is the closest to phenanthrene in terms of molecular structure.

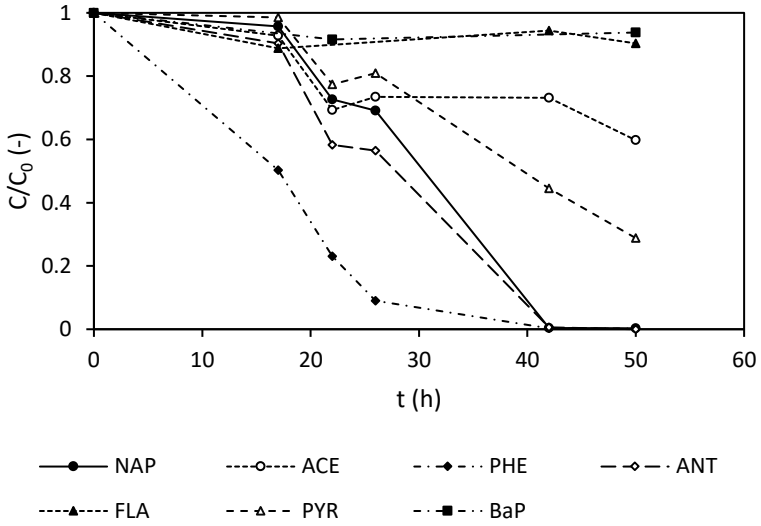

Figure 5.2 PAH biodegradation kinetic curves using acclimated culture (error bars not included for clarity)

Fluoranthene, pyrene and benzo(a)pyrene are considered as high molecular weight PAHs (HMW PAHs). This type of compounds are known to be recalcitrant pollutants, hard to biodegrade by non-specialized microorganisms. Nevertheless, pyrene, a four-ring PAH, was faster (and at higher extent) biodegraded than acenaphthene (three-ring PAH). The reason for this is that phenanthrene and pyrene degrading microorganisms display a similarity in the metabolic utilization of these compounds [8,14]. Fluoranthene and benzo(a)pyrene were only slightly degraded, even after 50h (≤10%) (Figure 5.3). This result agrees with the work of Hilyard et al. [15], in which cultures developed with only naphthalene or phenanthrene as sole carbon source were not able to degrade neither of these two molecules.

Regarding acenaphthene degradation, it is surprising that this molecule, being a low molecular weight PAH, was only 40% degraded (Figure 5.3). Anthracene and fluoranthene

have in their structure non-aromatic five-carbon rings, while all the other PAHs present in the mixture have only aromatic rings. This suggests a connection between the PAH rings' aromaticity and the ability of the phenanthrene-acclimated culture to degrade the molecules. However, no information about this relation was found in the literature and further investigation is needed to explain this apparent association. On the other hand, Beckles et al. [9] showed that for their mixed culture, the presence of acenaphthene caused a total inhibition on fluoranthene degradation, which may also have been the case for this study.

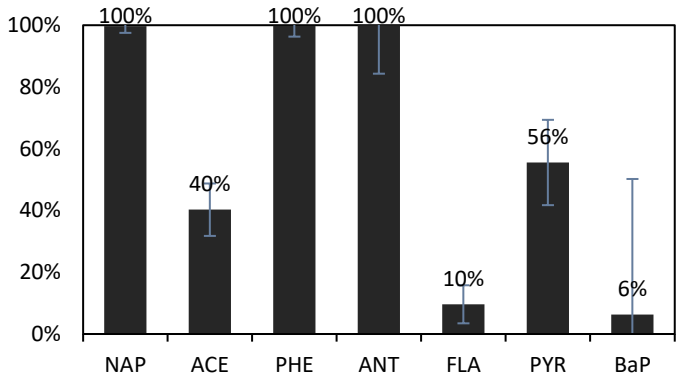

Figure 5.3 PAH biodegradation efficiency after 50 h

3.1.2. Co-substrate influence on the degradation of naphthalene and phenanthrene

Figure 5.4 shows the results of phenanthrene and naphthalene degradation kinetics as sole carbon source or in combination with other co-substrates after the acclimation with only phenanthrene. One can observe that both naphthalene and phenanthrene were the fastest degraded when they individually were the only carbon source than in the presence of other PAHs. By contrast, the combination of naphthalene and phenanthrene as co-substrates resulted in the slowest biodegradation rates for both compounds. Some authors have shown that naphthalene-degrading bacteria and degraders of other PAHs are not necessarily the same. Naphthalene can act as an inhibitor for other PAH-degraders [10,16,17]. This can explain the decreasing in the phenanthrene biodegradation kinetics when both molecules were present in the broth.

In contrast, this negative co-metabolic effect was not observed for the biodegradation test using 7 PAHs, since the degradation curve of naphthalene, when introduced alone, is similar to the one with the 6 other PAHs (Figure 5.4) . It is possible that synergetic interactions caused by the presence of other PAHs, such as anthracene or acenaphthene are behind this apparently contradictory observation [8]. As an example, Beckles et al. [9], observed that, in

their microbial consortia, fluoranthene was degraded only when naphthalene was present in the medium. This co-metabolic dependence is often explained by the enzymatic induction of one or several substrates [17]. However, the synergetic or antagonistic interactions are specific of the combination of strains present in the mixed culture, and further test are needed to prove the hypothesis here proposed.

The effect of phenanthrene acclimation was also evident in these tests. In fact, the active phenanthrene-acclimated culture were characterized by a lag phase for naphthalene degradation. Nevertheless, it is noticeable that this lag phase was less significant when no phenanthrene was present in the solution. In this case, the microbial community, facing the lack of other carbon sources in the broth, might have to faster adapt to the presence of naphthalene and its alternative consumption.

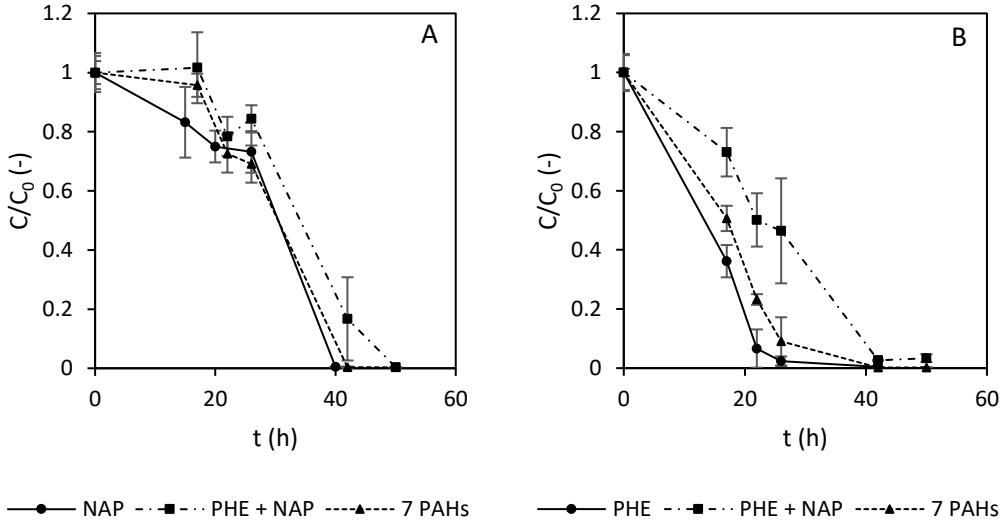

Figure 5.4 Effect of PAH co-substrates on (A) naphthalene and (B) phenanthrene biodegradation

3.2. Influence of co-substrate enrichment on culture development

Two different effects were tested. Firstly, since the biomass produced using phenanthrene as the only carbon source is limited by the aqueous solubility of this molecule, a more soluble PAH (i.e. naphthalene) and glucose were used as co-substrates in order to try to increment the bacterial density in the culture. Secondly, the effect of the presence of a zwitterionic surfactant (lauryl betaine) was investigated.

Figure 5.5 shows pictures of the cultures after 1 month of incubation and Table 5.3 displays the initial theoretical substrate COD, as well as the optical density at 600 nm for the enriched cultures at the end of the experiment. Biodegradation products of PAHs are known to be green-orange colored [18]. By comparing the pictures for the different enriched cultures, it is

possible to observe that more concentrated products were obtained for the cultures using only PAHs as substrates. The cultures using naphthalene or glucose as co-substrates, respectively, developed higher turbidity (and hence biomass) than the original one. This was expected, since the initial theoretical substrate COD for these cultures was also higher. Nevertheless, even if the OD values are not representative of the living biomass content, these results seem to infer that the PHE culture was the most efficient one regarding the production of biomass from lower content of the initial substrate COD.

Table 5.3 Optical density of enriched culture after 1 month

Culture	Initial theoretical substrate COD (mg O_2)	Optical Density 600 nm (AU)
PHE	59.2	0.359
PHE + NAP	359.2	0.865
PHE + GL	487.2	0.835
PHE + LB	541.8	0.073
PHE + GL + LB	1017.2	0.151

Culture with glucose as co-substrate had a high biomass content, but a lighter green color, which suggests a lower concentration on PAH biodegradation products in solution and, hence a lower PAH consumption. In the presence of the easily degradable glucose, a more important bacterial growth was observed. However, the use of this co-substrate probably also led to a less PAH-specific degradation. On the other hand, cultures containing LB produced less biomass than those having the same co-substrates but without the surfactant, suggesting that LB acted as an inhibitor of bacterial growth at the concentration tested.

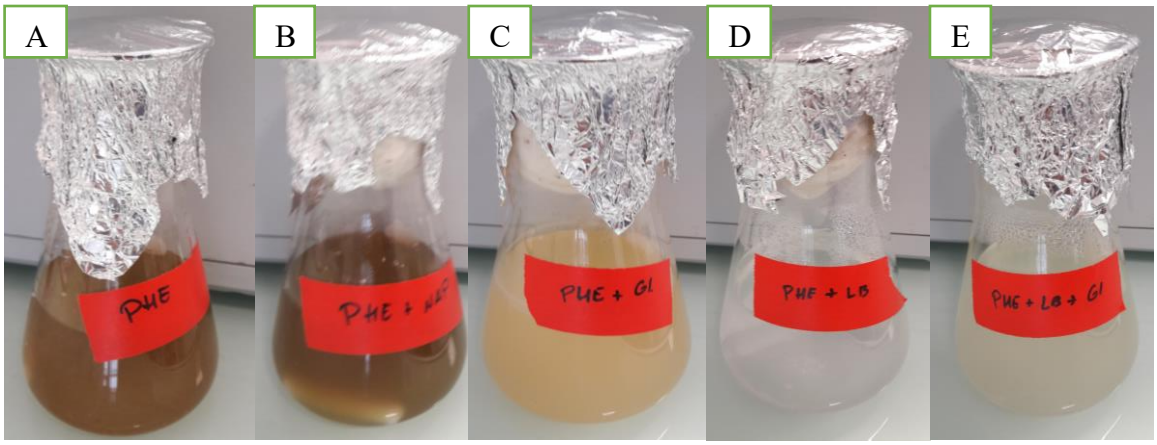

Figure 5.5 Culture enrichment in the presence of (A) phenanthrene; (B) phenanthrene and naphthalene; (C) phenanthrene and glucose; (D) phenanthrene and LB;(E) phenanthrene, glucose and LB.

Ability of enriched culture to degrade phenanthrene

The degradation kinetics curves (normalized concentration of phenanthrene versus time) are represented on Figure 5.6 for all the enriched cultures, except the PHE + LB culture. The reason for this is that the amount of biomass developed in the enrichment process was not enough to implement all the degradation tests for this culture. It was decided that it would be used for the last kinetic experiment (section 3.3). Alternatively, PHE + GL + LB culture was re-enriched using two substrate combination: i) phenanthrene and glucose, named as PHE + GL + (LB); and ii) phenanthrene and LB, named as PHE + (GL) + LB. For this test, initial inocula biomass COD for each culture was the same (20 mg $O_2.l^{-1}$), allowing a direct comparison of the kinetic curves (Figure 5.6).

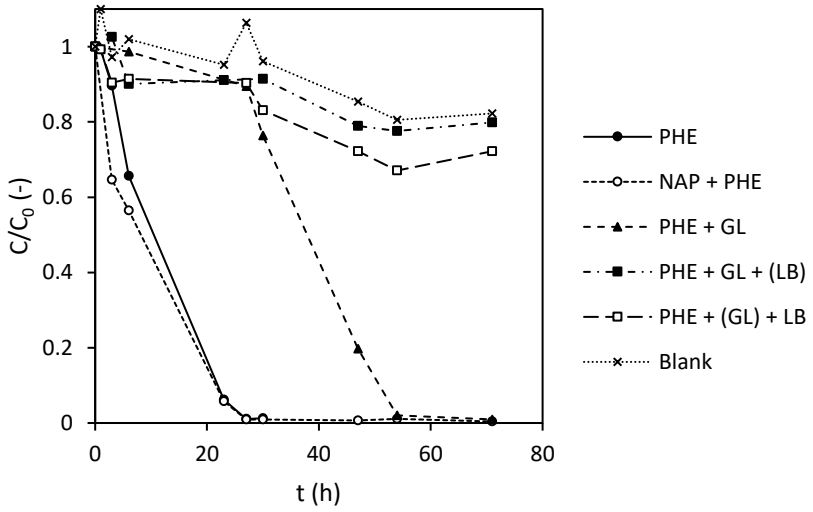

Figure 5.6 Phenanthrene biodegradation kinetics curves for the enriched cultures. Error bars are not included for clarity. The curves traced are the result of the average of duplicates.

The results show that only the PAH activated inocula (PHE and NAP + PHE) were able to completely degrade phenanthrene (>99%) within the first 24 h. In this case, the antagonistic co-substrate effect of naphthalene was not observed, presumably because, at this point, the mixed culture was specialized in the degradation of both PAHs due to the selective pressure that it endured. Mueller et al. [19] demonstrate that the strength of this mixtures resides in their ability to adapt to different conditions and substrate combinations. In consequence, they recommend the use of mixed cultures over single strains for degradation of several PAHs.

Phenanthrene degradation was also observed in PHE + GL culture. However, the cultures are characterized by a lag phase of more than 24 h. This seems to indicate that this bacterial consortium needed a new acclimation period, probably due to the fact that it was a less specific phenanthrene-degrading microbial community and it was already adapted to glucose

consumption. Additionally, even if in the section 3.2 the existence of LB-resistant strains was observed, phenanthrene degradation was practically inexistent during this test. This confirms the strong inhibition effect of the zwitterionic surfactant on the isolated microbial community at the concentration used in this study.

3.3. Ability of enriched culture to degrade phenanthrene after phenanthrene re-acclimation

Figure 5.7 displays the kinetic curves for the aqueous phenanthrene biodegradation performed by the enriched cultures re-acclimated with phenanthrene. According to the results, all cultures were able to degrade more than 95% of the substrate within 24 h. The biodegradation curves follow a first order kinetic model, given by the equation:

$$\frac{dS}{dt} = -k_B S$$

where S is the substrate concentration, k_B is the first-order biodegradation kinetic constant and t is time. Table 5.4 shows the kinetics constants normalized by the initial biomass COD for each culture. The fastest phenanthrene-degrading culture by biomass unit was the one selected only on phenanthrene, which seems to indicate that all co-substrates tested in this study produced slower mixed cultures. This may seem logical because of the successful acclimation of this culture, which increased its phenanthrene-consuming specificity. Moreover, it is possible to observe that slowest phenanthrene-degrading consortium was PHE + GL. This confirms the hypothesis about the diminution of PAH-degradation specificity in this culture. These results are in agreement with those of Trzesicka-Miynarz and Ward [20], who also observed that the use of glucose as co-substrate of a fluoranthene-degrading mixed culture reduced its fluoranthene-specific degradation ability compared to the use of this PAH as the only substrate.

Table 5.4 First-order biodegradation kinetic constants for enriched cultures reactivated with PHE

Culture	k_B (h^{-1})	Biomass initial COD (mg)	$k_{b,X}$ ($mg_{COD}^{-1}.h^{-1}$)	R^2
PHE	0.232	0.189	1.23	1.00
PHE + NAP	0.154	0.231	0.67	0.99
PHE + GL	0.057	0.179	0.32	0.92
PHE + LB	0.188	0.207	0.91	0.99
PHE + GL + LB	0.417	0.427	0.98	0.98

The use of naphthalene as co-substrate reduced the biodegradation kinetic rate for phenanthrene degradation. As explained in section 3.1, antagonistic interactions between naphthalene and phenanthrene as co-substrate have been observed by several researchers. Bouchez et al. [17], who isolated six PAH-degrading strains, found out that stains isolated on naphthalene as the sole substrate were not able to metabolize other PAHs. Moreover, they observed that this PAH was toxic for other strains. Shuttleworth and Cerniglia [10] also showed that naphthalene inhibited several individual PAH-degrading strains. In all these studies, these observations are related to the higher naphthalene solubility compared to other PAHs. A significant amount of naphthalene dissolved in the water increases the exposure of microorganisms to this compound. As a consequence, toxic soluble by-products are accumulated faster, and negatively impact some microbial strains. It is possible that the mixed culture isolated in this study contained some strains able to degrade both PAHs, and other able to degrade only phenanthrene and to which naphthalene could have been toxic. The population of the latter could have been diminished during the enrichment, explaining the low biomass/substrate efficiency and the slower biodegradation kinetics.

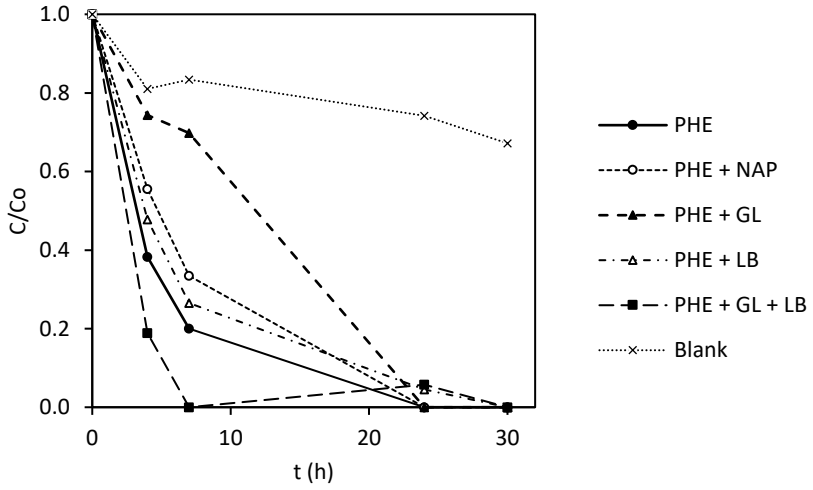

Figure 5.7 Phenanthrene biodegradation kinetic curves for enriched cultures after the phenanthrene re-acclimation. Error bars are not included for clarity. The concentration are the result of the average of duplicates.

In addition, the biodegradation kinetic rate of the cultures enriched in the presence of LB was less affected and values for the biomass normalized kinetic constant are similar for both set of co-substrates, PHE and PHE + GL. Since the cultures showed a growing inhibition effect in the presence of LB during the enrichment phase, one can hypothesize that there were LB-resistant phenanthrene-degrading strains present in the original culture that exhibited a similar behavior to the original culture regarding phenanthrene degradation. However, they were not

active during the previous test (section 0), meaning that they probably needed a higher re-acclimation time. The addition of glucose increased the biomass of the total LB resistant bacteria and slightly increased the biomass specific kinetic rate.

4. Conclusions

The main objective of this study was to investigate the selective pressure induced by different co-substrates on the PAH degradation ability of a microbial community coming from a PAH-contaminated soil acclimated to phenanthrene. Figure 5.8 shows the main conclusions obtained.

- PAHs containing non-aromatic rings are less degraded by cultures enriched with only aromatic PAHs.
- Heavy PAHs were less degraded, probably because the culture was acclimated using a light PAH.
- An antagonist effect was observed in the co-metabolism of phenanthrene and naphthalene by the phenanthrene-acclimated culture.
- As a co-substrate of phenanthrene-degrading cultures, glucose incremented the biomass amount produced. However, microorganisms developed were less efficient to degrade phenanthrene certainly due to a less PAH degrading specified biomass development.
- The surfactant lauryl betaine had a strong inhibitory effect on the bacterial growth of the cultures enriched with glucose and phenanthrene. However, the phenanthrene-degradation capacity remained almost unaffected.
- The substrates used in the acclimation and enrichment of the culture plays an important role in its PAH biodegradation capacity and change adaptability.

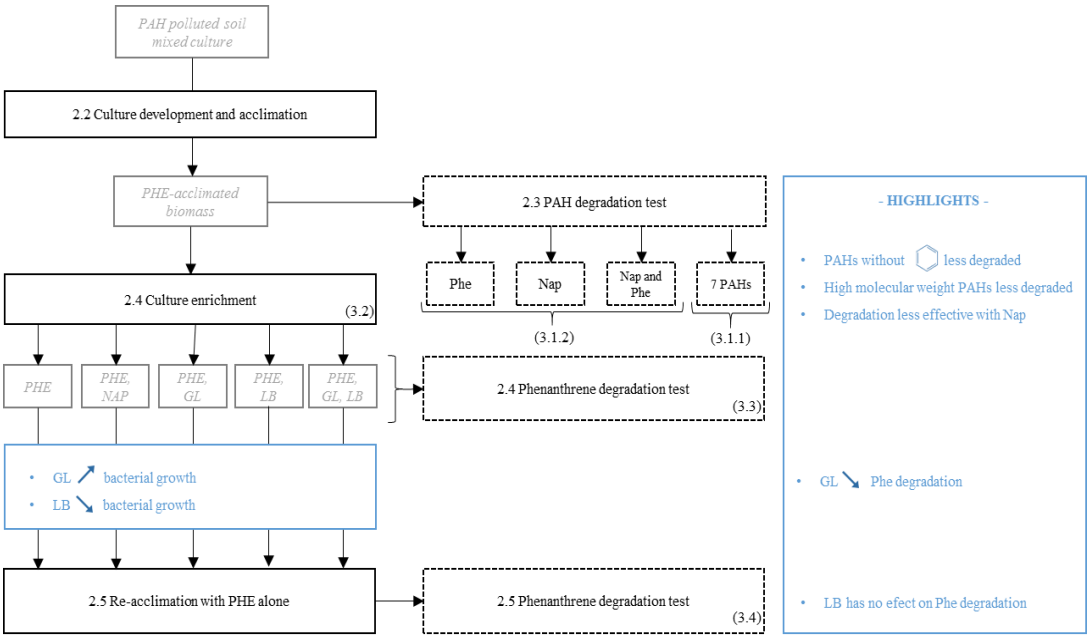

Figure 5.8 Main conclusions obtained in this study

References

[1] A.M. Thayer, Bioremediation: Innovative Technology for Cleaning Up Hazardous Waste, Chem. Eng. News. 69 (1991) 23–44. doi:10.1021/cen-v069n034.p023.

[2] M.C. Tomei, A.J. Daugulis, Ex Situ Bioremediation of Contaminated Soils: An Overview of Conventional and Innovative Technologies, Crit. Rev. Environ. Sci. Technol. 43 (2013) 2107–2139. doi:10.1080/10643389.2012.672056.

[3] C.E. Cerniglia, Biodegradation of polycyclic aromatic hydrocarbons, Biodegradation. 3 (1992) 351–368.

[4] A.K. Haritash, C.P. Kaushik, Biodegradation aspects of Polycyclic Aromatic Hydrocarbons (PAHs): A review, J. Hazard. Mater. 169 (2009) 1–15. doi:10.1016/j.jhazmat.2009.03.137.

[5] X.-Y. Lu, T. Zhang, H.H.-P. Fang, Bacteria-mediated PAH degradation in soil and sediment, Appl. Microbiol. Biotechnol. 89 (2011) 1357–1371. doi:10.1007/s00253-010-3072-7.

[6] R.A. Kanaly, S. Harayama, Biodegradation of high-molecular-weight polycyclic aromatic hydrocarbons by bacteria, J. Bacteriol. 182 (2000) 2059–2067.

[7] M. Wu, L. Chen, Y. Tian, Y. Ding, W.A. Dick, Degradation of polycyclic aromatic hydrocarbons by microbial consortia enriched from three soils using two different culture media, Environ. Pollut. 178 (2013) 152–158. doi:10.1016/j.envpol.2013.03.004.

[8] M. Molina, R. Araujo, R.E. Hodson, Cross-induction of pyrene and phenanthrene in a Mycobacterium sp. isolated from polycyclic aromatic hydrocarbon contaminated river sediments, 45 (1999) 10.

[9] D.M. Beckles, C.H. Ward, J.B. Hughes, Effect of mixtures of polycyclic aromatic hydrocarbons and sediments on fluoranthene biodegradation patterns, Environ. Toxicol. Chem. 17 (1998) 1246–1251. doi:10.1002/etc.5620170708.

[10] K.L. Shuttleworth, C.E. Cerniglia, Bacterial degradation of low concentrations of phenanthrene and inhibition by naphthalene, Microb. Ecol. 31 (1996). doi:10.1007/BF00171574.

[11] J.-L. Li, B.-H. Chen, Surfactant-mediated Biodegradation of Polycyclic Aromatic Hydrocarbons, Materials. 2 (2009) 76–94. doi:10.3390/ma2010076.

[12] F.A. Bezza, E.M. Nkhalambayausi Chirwa, Biosurfactant-enhanced bioremediation of aged polycyclic aromatic hydrocarbons (PAHs) in creosote contaminated soil, Chemosphere. 144 (2016) 635–644. doi:10.1016/j.chemosphere.2015.08.027.

[13] A. Tiehm, Degradation of Polycyclic Aromatic Hydrocarbons in the Presence of Synthetic Surfactants, APPL Env. MICROBIOL. 60 (1994) 6.

[14] S. Gaskin, R. Bentham, Comparison of enrichment methods for the isolation of pyrene-degrading bacteria, Int. Biodeterior. Biodegrad. 56 (2005) 80–85. doi:10.1016/j.ibiod.2005.04.004.

[15] E.J. Hilyard, J.M. Jones-Meehan, B.J. Spargo, R.T. Hill, Enrichment, Isolation, and Phylogenetic Identification of Polycyclic Aromatic Hydrocarbon-Degrading Bacteria from Elizabeth River Sediments, Appl. Environ. Microbiol. 74 (2008) 1176–1182. doi:10.1128/AEM.01518-07.

[16] W.T. Stringfellow, M.D. Aitken, Competitive Metabolism of Naphthalene, Methylnaphthalenes, and Fluorene by Phenanthrene-Degrading Pseudomonads, APPL Env. MICROBIOL. 61 (1995) 6.

[17] M. Bouchez, D. Blanchet, J. Vandecasteele, Degradation of polycyclic aromatic hydrocarbons by pure strains and by defined strain associations: inhibition phenomena and cometabolism, Appl. Microbiol. Biotechnol. 43 (1995) 156–164.

[18] Y. Ho, M. Jackson, Y. Yang, J.G. Mueller, P.H. Pritchard, Characterization of fluoranthene- and pyrene-degrading bacteria isolated from PAH-contaminated soils and sediments, J. Ind. Microbiol. Biotechnol. 24 (2000) 100–112. doi:10.1038/sj.jim.2900774.

[19] J.G. Mueller, P.J. Chapman, P.H. Pritchard, Action of a Fluoranthene-Utilizing Bacterial Community on Polycyclic Aromatic Hydrocarbon Components of Creosote, APPL Env. MICROBIOL. 55 (1989) 6.

[20] D. Trzesicka-Mlynarz, O.P. Ward, Degradation of polycyclic aromatic hydrocarbons (PAHs) by a mixed culture and its component pure cultures, obtained from PAH-contaminated soil, Can. J. Microbiol. 41 (1995) 470–476. doi:10.1139/m95-063.

CHAPTER 6

Slurry bioreactor and general discussion

CHAPTER 6 – Slurry bioreactor and general discussion

Slurry bioreactor treatment. This chapter presents the performance of a slurry bioreactor treating artifically polluted soil. The effect of the presence of soil organic matter is analyzed. A general discussion is developed using the leassons learned in the previous chapters in order to explain the observation made in the remediation process.

Abstract

Soil slurry bioreactor is an advantageous technology to treat polluted soil. It allows the control of several operational parameters influencing the biodegradation process. However, the process operation can be very complex and the internal functioning of the pollutant removal mechanisms is not completely understood. Therefore, this chapter aims to use the individual processes exposed in the previous chapters of this thesis, to better understand this technology. The chapter is divided in two parts: the first part consists in the experimental analysis of a slurry bioreactor treating artificial polluted soil, whereas the second part involves the lessons learned during this research to explain some of the observations made in the first part. The mechanistic approach developped in this investigation can be used as a generic method to study the slurry bioreactor treatment for any type of soil, different pollutants and microbial communities, as well as additional operating conditions.

1. Introduction

Soil slurry bioreactor is a bioremediation technology used to treat the fine fraction of the polluted soils. There are several known advantages in the use of this kind of system. For instance, the use of a reactor can enhance the gas-liquid and solid-liquid mass transfer, causing an increase of the bioavailability of contaminants [1]. More importantly, it permits to control several operational parameters such as pH, temperature, soil concentration, aeration and agitation rate, etc., which significantly influence the final biodegradation rate of the pollutants [2]. This gives to the slurry reactors an advantage over other biodegradation processes on the degradation of recalcitrant compounds [3].

However, the processes involved can be very complex and, even after several decades of research on this topic, there is still a lack of knowledge about the mechanisms that impact the removal of the pollutants. Most studies on bioslurry focus on the biological aspects of the remediation process. Thus, the interactions between the gas-liquid mass transfer, the solid-liquid mass transfer and the pollutant biodegradation need to be further investigated.

Therefore, the main goal of this chapter is to study the interactions between processes in a soil slurry bioreactor. The chapter is divided in two parts. The first part corresponds to the experimental analysis of a soil slurry bioreactor treating an artificial polluted soil. For a better understanding of the process, a simplified system was used. Clay and sphagnum peat were used as starting materials to create an artificial soil of known proportions. Phenanthrene was selected as model molecule due to its physicochemical properties, which allow the simultaneous observation of gas-liquid transfer, solid-liquid transfer and biodegradation process in a similar time scale. A batch slurry reactor was run in which phenanthrene concentration in soil and in aqueous phase was followed. Other parameters such as the concentration of selected degradation products, chemical oxygen demand (COD) in solid and soluble phase, nitrogen in different forms and the microorganisms' oxygen uptake were also measured with the purpose of describing the process occurring in the reactor.

The second part of the chapter aims to relate the previous chapters of this thesis, in which individual gas-liquid transfer, solid-liquid transfer and biodegradation processes were studied, with the slurry bioreactor remediation experiment performed in the first part of the present chapter. This part shows how the conclusions found in the previous stages of the investigation can be used to better understand the interactions between the removal mechanisms and consists in the general discussion of this thesis. Likewise, it shows the implications of the

various mechanisms highlighted on the optimization, the choice of the operating conditions and the practical implementation of the process.

2. Experimental part

2.1. Materials and methods

2.1.1. Reactor

The experiments were carried out in a standard 4.2-L glass reactor (working volume) with a thermal jacket controlled at 20 °C and four baffles. The dimensions of the reactor are specified in chapter 2. Mechanical agitation in the reactor was supplied by a motor with digital controlled stirring speed coupled to a single marine propeller. Aeration was provided from the bottom of the reactor using a porous glass. The reactor was connected to an air-tight respirometry cell with temperature control and magnetic agitation.

2.1.2. Soil and chemicals

For this study, an artificial soil was created, using two materials: clay and soil organic matter (SOM). Clay was provided by Argiles du Bassin Méditerranéen (France). It was composed of at least 65% of Sardinian montmorillonite, with a particle size lower than 40 µm in ambient conditions. The chemical analysis of the clay was provided by the supplier. Sphagnum peat (95% organic matter) was used as source of SOM. It was wet sieved at 200 µm and dried at 60°C, prior utilization. An artificial soil was created by mixing clay and sieved sphagnum peat, at a 90:10 clay/SOM mass proportion. The mixture was thoroughly homogenized for several minutes. Phenanthrene and two of its biodegradation products (i.e. 1-hydroxy-2-napthoic acid and 2-napthol) (98% purity) were provided by Sigma-Aldrich.

Soil spiking was achieved using a solution of phenanthrene in acetone based on the procedure proposed by Northcott and Jones [4]. In brief, after addition of the acetone solution containing the desired mass of phenanthrene to the dry soil, the mixture was thoroughly mixed. Once the slurry was homogenized, it was left under a hood at ambient temperature to let the solvent evaporate. The mixture was often stirred during the drying phase to allow a homogeneous evaporation of the solvent and an even distribution of the phenanthrene in the soil. Once dried, the soil was crushed and homogenized one more time. It was left at ambient conditions covered with a loose aluminum foil piece for several months until use.

2.1.3. Slurry bioreactor treatment

A slurry bioreactor treatment in batch mode was performed to study the remediation of an artificial phenanthrene-polluted soil at two different compositions: 100% clay and the prepared artificial soil (90:10 clay/SOM). The reactor was loaded with the polluted soil and a phosphate-buffer solution (pH 7.5) prepared in tap water to obtain a 10% w/v soil concentration. A concentrated ammonium chloride solution was added in order to provide for a bioavailable nitrogen source at a concentration of 30 mg $N\text{-}NH_4^+.1^{-1}$ (equivalent to a theoretical phenanthrene COD:N ratio ≈ 10). The reactor was inoculated with a phenanthrene-acclimated culture, enriched with naphthalene and phenanthrene as co-substrate (see chapter 4). Initial inoculum biomass COD was approximately 8 mg COD l^{-1}. Reactor was covered, and the gas exhaust was connected to a column containing 40 g of Amberlite® XAD®- 2 (Sigma-Aldrich) to recover the volatilized compounds from the solution. Agitation (500 rpm) and aeration through the porous glass diffusor (8.69 $m^3.s^{-1}$) were started. 15-ml samples of the slurry were collected, processed and analyzed periodically.

2.1.4. Analytical methods

The slurry was sampled to measure total slurry COD and nitrogen content. To determine phenanthrene concentration in soil, slurry samples were centrifuged at 10,000 rpm to separate the solid phase and the aqueous phase. The extraction of phenanthrene from the solid phase was performed by ultrasonication with methanol as solvent and then centrifugated. Each extraction was repeated three times, the solvent supernatants were collected each time, mixed and set aside for phenanthrene analysis. The aqueous phase was used to determine soluble PHE, 1H2NA and 2NAP concentrations, soluble COD and soluble nitrogen content, selected cation concentrations (Na^+, NH_4^+, K^+, Mg^{+2} and Ca^{+2}), as well as nitrate (NO_3^-) and nitrite (NO_2^-) concentrations.

Phenanthrene, 1H2NA and 2NAP analyses were performed using a *LaChrom Elite® L-2400* HPLC (Hitachi, Japan) coupled with UV/VIS detector (set to 254 nm) and a fluorescence detector (excitation wavelength set to 250 nm and emission wavelength set to 350 nm). The separation was performed using a RP C-18 end capped column (Purospher®, Merck) (5 mm, 25 cm × 4.6 mm) placed in an oven at 40°C. The mobile phase was a mixture of water and methanol (20:80 v/v) with a flow rate of 1.0 $ml.min^{-1}$ in isocratic mode. The injection volume was 20 µl. Anion and cation concentrations were determined using ion chromatography (ThermoFisher: ICS1100 Ion Pac AS15, at 30°C with eluent generator cartridge EGC III KOH for anions; ICS1100 Ion Pac CS16, at 30 °C using a 0.4 mM solution of sulfuric acid as

eluent for cations). Dissolved oxygen (DO) was measured using an inoLab® Oxi 7310 DO sensor connected to a Cellox 325 probe (WTW). The oxygen uptake rate (OUR) was determined by measuring at different times the decrease in the DO concentration in the respirometry cell in order to characterize microbial activity. Total slurry COD and soluble COD was performed using the standard, closed reflux, titrimetric APHA 5520 method [5].

2.2. Results and discussion

2.2.1. Polluted clay remediation

In this section, the results of the remediation of the phenanthrene-contaminated soil with a composition of 100% clay using the soil slurry bioreactor treatment are presented and discussed.

2.2.1.1. Phenanthrene removal

The phenanthrene removal as well as the pH evolution are displayed in Figure 6.1A. Phenanthrene sorbed in soil, initially at a concentration of 890 $mg.kg^{-1}$, decreased over time at a constant removal rate during the first 40 h. After this period, the removal rate increased and the phenanthrene was completely removed within the first 70 h of treatment. One can observe that, as phenanthrene is being consumed, a pH diminution of the slurry occurs (Figure 6.1A). The minimum in the pH value corresponds to the complete removal of phenanthrene in the solid phase. The acidification of the system may be explained by the CO_2 production, suggesting a successful biodegradation of phenanthrene. This can be confirmed by an observed augmentation of the carbonate ion concentration in solution (data not shown). After the total depletion of PHE in the soil, pH returns to the initial value and remains quasi stable after 90 h. This value corresponds to the pH obtained in a previous test for clay-buffer mixtures (pH 7.9-8.0).

Figure 6.1B displays the evolution of the oxygen consumption rate. An increase of the OUR was observed in parallel with the total phenanthrene concentration decrease. The maximum OUR value measured corresponds to 70 h (when there is no longer phenanthrene sorbed in soil). The need of a higher amount of oxygen at this point could mean the presence of phenanthrene and/or biodegradable products in the aqueous phase, which were still being degraded after 60 h. A diminution in the OUR can be observed after 140 h, indicating a decrease in the microbial activity, certainly associated to the lack of biodegradable substances.

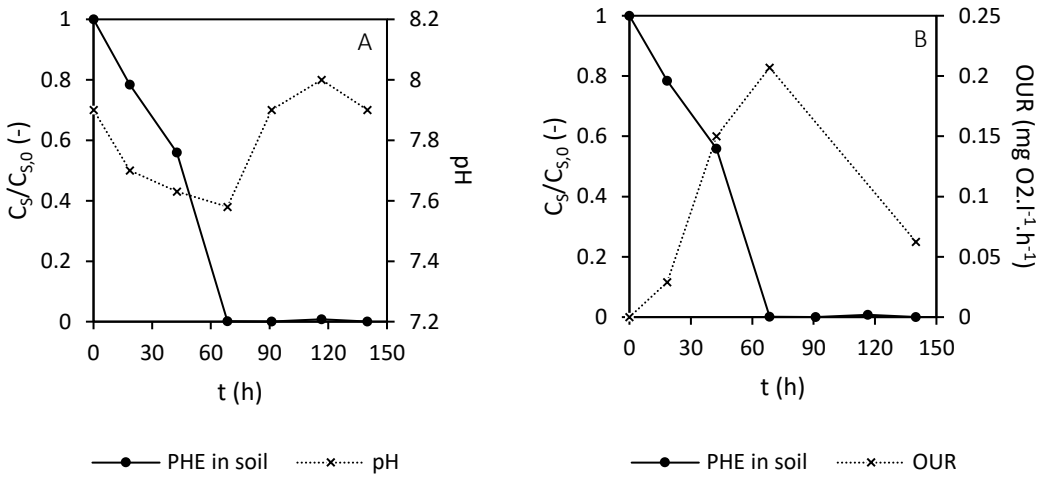

Figure 6.1 Comparison of phenanthrene disappearance with (A) pH evolution and (B) oxygen uptake rate

It is also important to consider that the phenanthrene loss in the reactor was not entirely due to the biodegradation process. In fact, around 5% of the initial amount of phenanthrene was recovered from the Amberlite® XAD®-2 column, which corresponds to losses by volatilization.

2.2.1.2. Biodegradation products

Two specific biodegradation products of phenanthrene were followed in the aqueous phase: 1-hydroxy-2-naphtoic acid (1H2NA) and 2-napthol (2NAP). The choice of these two compounds was based on their presence on many mineralization pathways proposed for the microbial degradation of phenanthrene in the literature [6–9]. Soluble phenanthrene concentration was also followed over time. Figure 6.2A, B, C and D display the evolution of the concentrations of soluble phenanthrene, 1H2AC and 2NAP, as well as the sorbed concentration of PHE, respectively. By comparing Figure 6.2A and D, one can observe that the evolution of dissolved phenanthrene follows the same trend as phenanthrene concentration in the solid phase. After 60 h, more than 95% of phenanthrene was removed from both solid and liquid phase. However, it seems that a small amount of this compound (< 0.01 $mg.l^{-1}$) remained in solution during the second half of the experiment.

On the other hand, after less than 24 h, 1H2NA was already detected in solution, whereas 2NAP mainly appeared after 68 h. This is in accordance with several biodegradation pathways proposed in the literature for phenanthrene biodegradation with pure strains where 1H2NA was produced before the detection 2NAP [6]. Additionally, some authors claim that

2NAP can also be a by-product produced by the decarboxylation of the 2-hydroxy-1-naphtoic acid, another phenanthrene metabolite and isomer of 1H2NA [10].

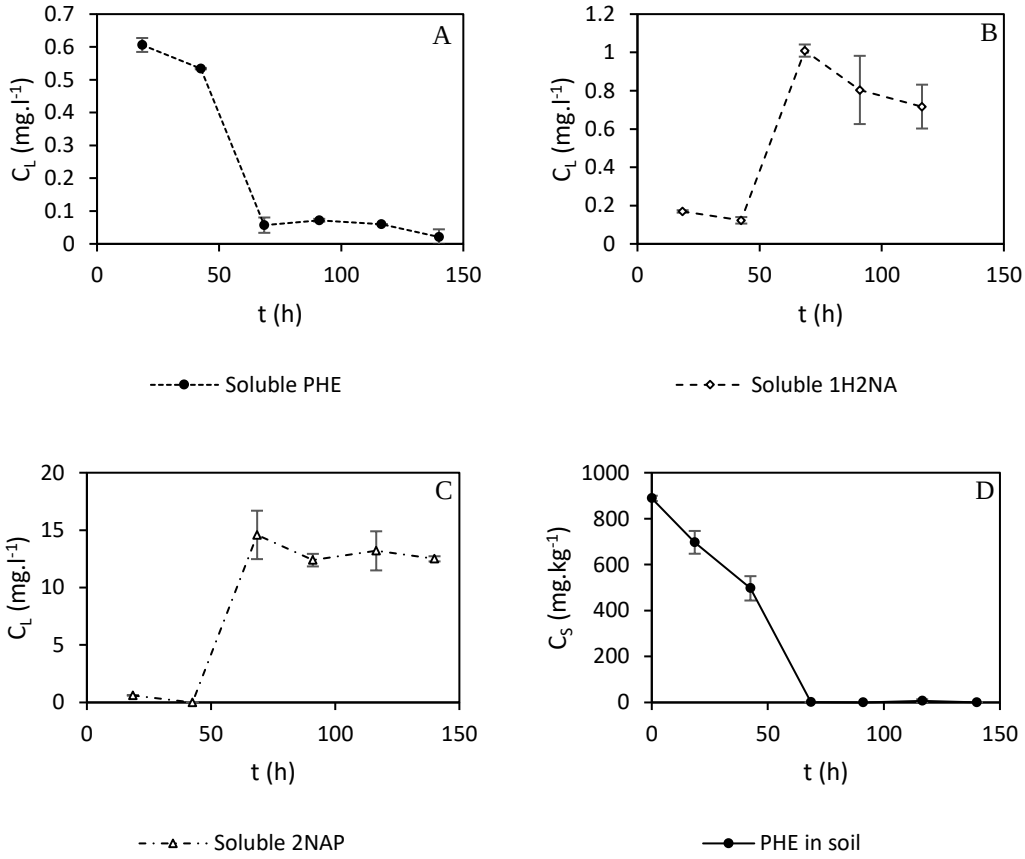

Figure 6.2 Evolution of (A) soluble phenanthrene, (B) soluble 1H2AC, (C) soluble 2NAP concentrations and (D) phenanthrene concentration in soil in time

Concentrations of 1H2NA peaked at 68 h and slowly decreased in concentration afterwards, confirming the transitory accumulation of biodegradation metabolites. However, 2NAP reached a concentration plateau after 90 h, which indicates that this product was probably no longer utilized. Two reasons for this could be hypothesized: i) the mixed culture used in this experiment was not capable to use this compound as substrate; and/or ii) the microbial community was inhibited by this substance. This could also explain the small concentration of phenanthrene remaining in solution. Several research works have proved either the inability of some pure strains to degrade 2NAP or the toxic effect of this compound on specific bacterium [6,11]. For instance, Tao et al. [12] found that 2NAP was only degraded in the presence of phenanthrene, 1H2NA and other phenanthrene metabolites by a *Sphingomonas* strain, indicating that enzyme induction was needed. Additionally, Mallick et al. [6] showed that 2NAP and other similar substances were dead-end products of the biodegradation process for

a *Staphylococcus* strain. However, at this point, no definitive conclusions can be given for the mixed culture used and further investigation on this topic is needed.

2.2.1.3. Total and aqueous COD dynamics

COD evolution for slurry, aqueous phase and phenanthrene in soil (theoretical values calculated from soil concentration) are shown in Figure 6.3. It is important to mention that clay COD was measured, resulting in a value of 125 mg $O_2.l^{-1}$. In the figure, the total slurry COD decrease during the first 72 h of treatment can be observed, corresponding to the removal of phenanthrene from the solid phase. Once passed this time, it seems to stabilize around 210 mg $O_2.l^{-1}$. On the other hand, soluble COD increases during the first 48 h, reaching a maximum of approximately 150 mg $O_2.l^{-1}$. Even if no exact value was measured at 70 h (technical problems with the method due to an out-of-range value), the soluble COD concentration at this point was even higher than at 48h. This confirms the accumulation of biodegradation products in the aqueous phase observed in the previous section (2.2.1.2). After 90 h, soluble COD stabilizes around 35 mg $O_2.l^{-1}$, indicating that some soluble degradation products remained in the aqueous phase and that the microbial community was probably not able to completely mineralize them. Furthermore, the theoretical 2NAP COD values represent at least 90% of the soluble COD remaining in solution.

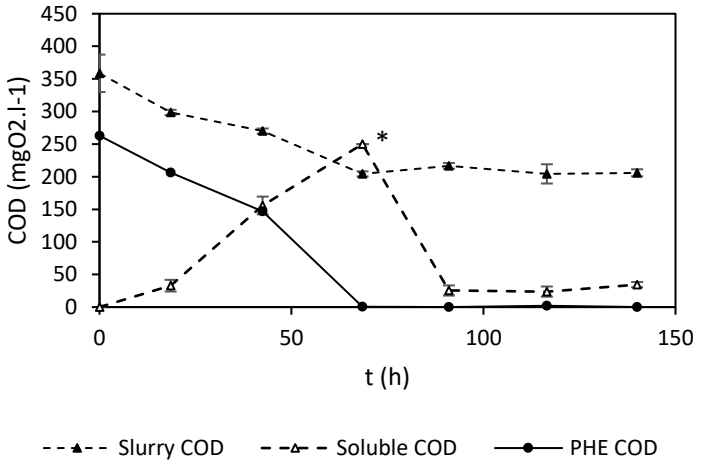

*Figure 6.3 Evolution of slurry COD, soluble and theoretical phenanthrene COD over time in the reactor (*reference value, the real value was not measured due to technical problems with the method)*

2.2.1.4. Nitrogen utilization

The evolution of different nitrogen species and fractions of the slurry in the reactor is illustrated in Figure 6.4. Total slurry nitrogen decreases with a quasi-constant slope over time during all the experiment. A similar behavior can be observed for soluble total nitrogen. This

can be explained by a loss of nitrogen due to ammonia volatilization. Observing the individual species, it appears that nitrate (coming from the tap water) remains fairly constant during the treatment. However, the dynamics of ammonium is similar to the one of sorbed phenanthrene. It decreases steadily during the first 70 h of experiments and reaches a plateau at a very low concentration when phenanthrene concentration has almost disappeared. Thus, a biological utilization of this nitrogen source, combined with the ammonia volatilization, can be assumed.

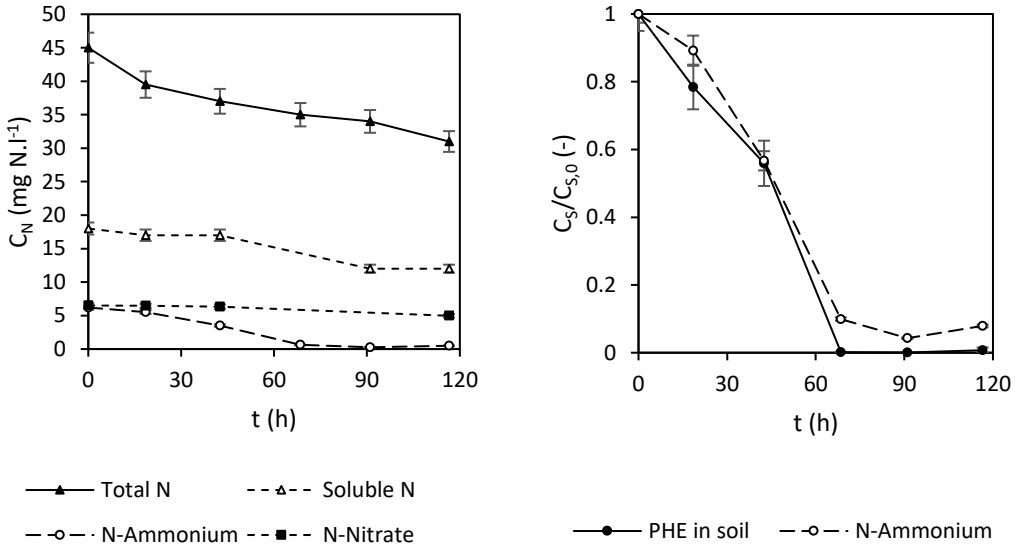

Figure 6.4 Nitrogen evolution in time. (A) Total, aqueous, ammonium and nitrate (B) comparison between ammonium and sorbed phenanthrene removal

Nonetheless, in sections 2.2.1.1 and 2.2.1.3, it was demonstrated that microbial degradation activity continued after 70 h, which means that nitrogen consumption should have also continued. One can suppose two reasons to justify the late nitrogen consumption (after 70 h) was not reflected in the ammonium consumption. Firstly, it is possible that microorganisms had already transformed the nitrogen from ammonium into extracellular polymeric substances (EPS) or biosurfactants. These substances can contain nitrogen compounds [13], which could have been later reutilized as nitrogen sources. Secondly, clay could have served as an ammonium reservoir. According to the supplier, clay used in this study have a cation exchange capacity higher than 1.2 meq.g^{-1}, which allows this material to exchange the cations in its structure (mainly Na^+ and Ca^{+2}) by other cations in solution [14]. Table 6.1 shows the initial concentration of selected cations in the buffer solution before and after adding the clay to the water to form the slurry. One can observe that highly concentrated ions in the buffer solution (such as K^+ and NH_4^+) declined in concentration after the slurry creation. Conversely, Na^+ concentration augmented significantly in the slurry compared to the buffer solution. It

becomes clear that ammonium was sorbed by the clay and probably released as it was consumed in the solution.

Table 6.1 Selected cation concentrations in the buffer solution and in aqueous phase throughout the experiment

Sample	Cation concentration ($mg.l^{-1}$)				
	Sodium (Na^{+})	Potassium (K^{+})	Magnesium (Mg^{+2})	Calcium (Ca^{+2})	Ammonium (NH_4^{+})
Buffer solution in tap water	10.5	51.8	4.3	15.0	30.0
Slurry (Buffer solution + clay)	40.1	18.6	4.5	13.5	8.0

2.2.2. Artificial soil: SOM effect

In this section, a comparison between results of the treatment of the polluted clay and the polluted artificial soil with the slurry bioreactor is presented and discussed.

2.2.2.1. Phenanthrene removal and biodegradation products

Table 6.2 shows a comparison between selected parameters at the initial conditions and after 72 h of treatment for clay and artificial soil. For phenanthrene removal, one can observe that the disappearance rate was significantly slower. This indicates that SOM presence in the reactor caused a reduction in the biodegradation rate of phenanthrene in around 25%, probably due to bioavailability decrease. Three factors could affect the phenanthrene bioavailability: i) a reduction in the desorption rate (see chapter 3); ii) a substrate competition with carbon sources provided by SOM; and iii) a reduction in the homogeneity of the slurry. Indeed, due to a lower density, SOM had the tendency to separate from the slurry mixture and float on the liquid surface. Despite the presence of phenanthrene after 72 h of treatment, the lower degradation rate can also be observed in the lower OUR at this time for artificial soil, considering that the value measured at this time in both experiments was the maximum for both experiments. After 90 h the concentration of phenanthrene in soil for the artificial soil decreased to zero, which demonstrated that the remediation process, although slower, was also successful in the presence of SOM.

Regarding the biodegradation products for artificial soil, both 1H2NA and 2NAP were already present at the beginning of the experiment. Possibly, phenanthrene-degrading microorganisms were already present in this soil before the experiment. Since the soil was prepared several months in advance, some bacteria and/or fungus from air could have developed taking advantage of the water retention capacity of SOM. This could also explain

the lower initial phenanthrene concentration observed (in fact, both soils were spiked in the same conditions). Conversely to clay slurry treatment, in which by-products accumulate in the aqueous phase, these substances seem to only slightly change their concentration after 72 h. Additionally, for both substances, the concentration is one order of magnitude lower than that in clay slurry. SOM, being a versatile adsorbent, could have partially sequestered these substances [15].

Table 6.2 Comparison of parameters for clay and artificial soil at initial conditions and after 72 h of bioslurry treatment

Parameter	Clay		Artificial soil	
	Initial	After 72h	Initial	After 72h
Sorbed PHE concentration (mg kg^{-1})	890	1.3	730	55
Soluble 1H2NA concentration (mg l^{-1})	0	1.0	0.14	0.08
Soluble 2NAP concentration (mg l^{-1})	0	14.6	2.4	3.6
OUR (mg O_2 l^{-1} h^{-1})	0	0.21	0	0.15
Soluble NH_4^+ concentration (mg l^{-1})	8.0	0.8	2.5	1.8

2.2.2.2. Nitrogen utilization

Initial ammonium concentration in the slurry is also lower in the presence of SOM, which can be explained by the capacity of SOM to exchange and complex cations [14]. In fact, humic acids and other humic-like substances can entrap ammonium within their structure, reducing the concentration of this cation in the liquid phase. On the other hand, after 72 h, the concentration of ammonium was only slightly modified. It is possible that other nitrogen sources were available in the SOM. Indeed, peat can contain both organic nitrogen and ammonium ions in its structure [16]. Thus, other nitrogen sources, different from the ammonium provided in the buffer solution, could have been used by the bacteria.

3. General discussion

3.1. Interactions between mass transfer and biodegradation mechanisms in the soil slurry bioreactor

To remove hydrophobic contaminants from soil using a slurry bioreactor, a series of processes should occur. First, pollutants have to be released (or desorbed) from soil. Microorganisms must have access to these pollutants and to several nutrients. In addition, for aerobic microorganisms, oxygen must be readily available. Only when these conditions are fulfilled, biodegradation process can start. However, other processes, which are not necessarily related

to the biotransformation of the pollutants, could happen at the same time. For instance, targeted contaminants could volatilize or resorb in other fractions of soil. In order to simplify and better understand these mechanisms, one can classify them into three groups: i) gas-liquid transfer processes; ii) solid-liquid transfer processes; and iii) biodegradation processes. These mechanisms take place simultaneously in the reactor and can influence one another. Chapter 1 shows an overview of the study of these phenomena in slurry bioreactors during the last decades and highlights some of their interactions, which are driven by the physicochemical properties of the soil and pollutants, as well as the reactor's operational parameters.

Table 6.3 Summary of the effects of the operational parameters tested in this study on the mechanisms occurring in a slurry bioreactor

Mechanism	Chapter	Operational parameter	Effect on kinetics*	Observations
Surface oxygen transfer	3	Stirring speed	+	
Bubble oxygen transfer	2	Stirring speed	+	
		Air superficial velocity	+	
		Soil content	–	No effect on the other parameters' influence on OT
Surface volatilization	3	Stirring speed	+	
Bubble volatilization	3	Stirring speed	+	
		Air superficial velocity	+	
Desorption	4	Soil concentration	No apparent effect	
		SOM content	–	
Phenanthrene biodegradation	5	Co-substrates enrichment (naphthalene and glucose)	–	Biomass production increase
		Surfactant presence	No apparent effect	Biomass production decrease

* (+) positive correlation ; (–) negative correlation

During this research work, the influence of some of these parameters on the mentioned mechanisms has been investigated using selected aromatic compounds. A qualitative summary of the effects of operational parameters is provided in Table 6.3. Characteristic times for individual mechanisms have been calculated from the results obtained in each chapter of this thesis manuscript (Figure 6.5). They give information about the relative speed of the process in the conditions tested in this study. Moreover, they can explain some of the observations regarding phenanthrene removal in the slurry bioreactor experiments developed

during this chapter. In this section, connections between the individual mechanisms exposed in the previous chapters (summarized in Table 6.3) and the soil remediation treatment performed using a soil slurry bioreactor are brought to light.

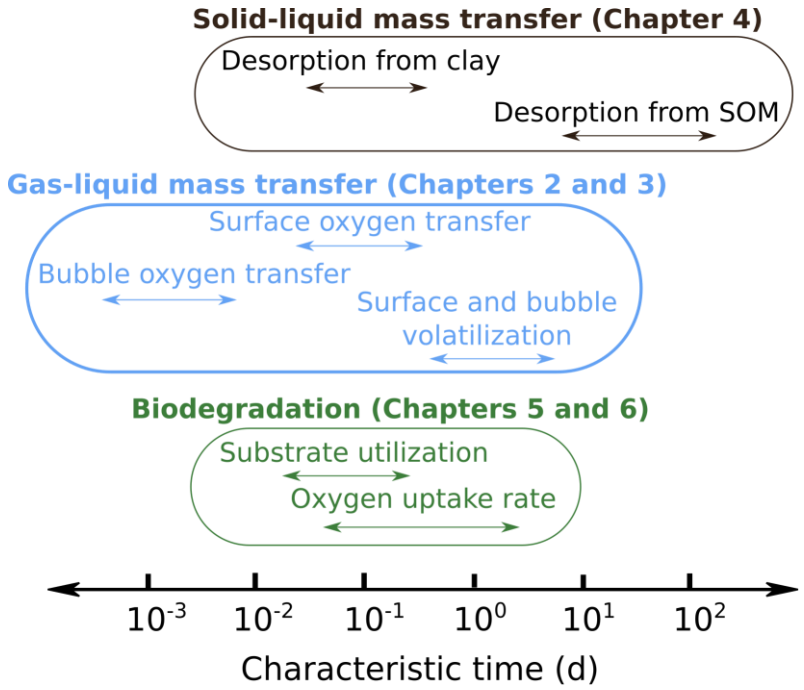

Figure 6.5 Characteristic time ranges for phenanthrene obtained in this research study

3.1.1. Pollutant bioavailability

A substrate is considered bioavailable when microorganisms have access to it in order to metabolize it. One of the reasons why PAHs are considered recalcitrant pollutants resides in their tendency to remain sorbed in soil and other solid surfaces, which can be explained by their hydrophobicity [17]. Substrate are generally more bioavailable when they are solubilized in the aqueous phase [18]. Thus, PAH desorption could constitute a key mechanism in the degradation rate of these pollutants. Comparing the characteristic time of phenanthrene desorption from clay, obtained in chapter 4, and that of its utilization by the microbial community (from chapter 5), one can observe that both mechanisms share a similar range. This means that desorption may be a limiting step in the phenanthrene removal in the reactor. This hypothesis becomes almost a certainty when SOM is present in the soil, given the much higher desorption characteristic time from this material (by two orders of magnitude). In fact, this effect was observed in the slurry treatment of the soils with and without SOM, in which

the overall phenanthrene biodegradation efficiency after 72 h was reduced by approximately 25% in the presence of 10% of SOM in soil (Table 6.2). Besides, no effect of the agitation rate was observed on the desorption process, which means that low stirring speed can be used to optimize the energy consumption of the treatment, without affecting the pollutant bioavailability.

Nonetheless, some microorganisms are able to accelerate the desorption rate by producing extracellular polymeric substances (EPS) and/or biosurfactants, which can increase the apparent solubility of hydrophobic compounds in aqueous solutions. Even if no tests regarding the production of such substances were performed for the slurry treatment, an evident increase of slurry viscosity (to the naked eye) during the clay remediation occurred. It might indicate the production of some of these biomolecules [19]. However, a (noticeable) viscosity augmentation was not observed for the artificial soil. The reason of this difference might reside in the utilization of SOM as substrate. In other words, given that phenanthrene was the only source of carbon in the polluted clay treatment, stress due to lack of bioavailable and easily biodegradable substrate could have impulsed the microorganisms to produce extracellular substances to increase the desorption rate [20]. As a consequence, a thickening of the slurry occurred. Conversely, in the case of artificial soil, the presence of SOM could have avoided such stress and, thus limited the excretion of extracellular substances.

Another mechanism that could influence the availability of pollutants in aqueous solutions is their volatilization. Even if, in Figure 6.5, it is possible to observe that phenanthrene biodegradation kinetics is in general faster than volatilization kinetics, these two processes could compete in the phenanthrene removal from the reactor, particularly at early stages of the treatment. As a matter of fact, after inoculation, most cultures need an adaptation period before they start the biodegradation process. During this period, the main pollutant removal mechanism is gas-liquid transfer [21]. In consequence, longer lag phases imply higher losses by volatilization, which may require an additional treatment of the exhaust gas stream and increase the complexity and cost of the treatment. For polluted clay remediation, a lag phase was not observed, probably due to the fact that its duration was shorter than the time lapse between the beginning of the experiment and the first sample (18.5 h), and the losses by volatilization reached only 5% of the total initial phenanthrene amount in soil.

The relatively low volatilization removal could also be explained by the findings exposed in chapter 3. In summary, gas-phase saturation by the aromatic compounds tested occurred during the bubble rise through the reactor. The fast saturation in the relatively small volume

of the reactor used in this investigation might be linked to the bubble size. The gas sparger used for all experiences was indeed a porous glass, producing a fine air dispersion that could easily be saturated at the conditions of the reactor. According to the results of chapter 3, if only surface aeration would have been used to provide oxygen, losses for volatilization could have been similar to those find in this experiment (same order of magnitude for the characteristic times for both types of volatilization). Furthermore, it was demonstrated in chapter 3 that lighter aromatic compounds (with henry constant's values > 0.01) exhibit much faster volatilization rates than phenanthrene. For these substances, a factual competition between the pollutant volatilization and biodegradation during all the treatment could occur.

3.1.2. Oxygen availability

Oxygen availability is important for the aerobic biodegradation process [22]. Characteristic times measured in this study show that bubble oxygen transfer is at least one order of magnitude higher than oxygen uptake rate. This means that the supply of oxygen was excessive for the most part of the biodegradation process, mainly because the amount of pollutants, of biomass and organic matter in the reactor was relatively low, compared to other treatments using similar aeration conditions [22,23]. On the other hand, surface oxygen transfer share the same range of characteristic times than OUR, which means that oxygen could become a limiting reagent for the respiration process at high biomass concentrations with only surface aeration. Additionally, to reach higher oxygen transfer rates, higher stirring speeds or air flow would be needed (see chapter 2), causing an increase in the energy requirements of the reactor. Chapter 3 showed that both aeration and agitation accelerate the volatilization rates for the low-molecular-weight aromatic hydrocarbons. Therefore, a compromise between enough oxygen supply and low pollutant volatilization should be reached, which could be translated in a low aeration rate. According to Figure 6.5, this would allow sufficient oxygen supply for microorganisms and at the same time would minimize the volatilization losses due to their fast saturation.

3.2. Considerations for the extrapolation for real contaminated soils

The conclusion drawn from this research work can be extended for the treatment of real contaminated soil. However, it is necessary to consider additional aspects such as history, aging and weathering of the pollution, in order to further understand the interaction between the removal mechanisms [24]. As shown in chapter 4, the origin and weathering of the pollution can determine the distribution of the pollutants in the soil, modifying their behavior

in the reactor. Moreover, aging can cause pollutant sequestration and chemisorption, reducing the pollutant biodegradable fraction in soil [25].

Similarly, soil composition must be considered in the selection of the operational conditions. Clay can modify the gas-liquid transfer and the slurry rheological properties (see chapter 2), whereas SOM can significantly affect the pollutant desorption rate (see chapter 4). These effects can be regulated by controlling the soil concentration in the slurry. Likewise, effect of sand on the treatment should be considered when studying the real soil cases [26,27].

Therefore, the type of soil is an important aspect to consider. For instance, since sand is a denser material than clay, sandy soils would require a higher stirring speed to maintain a homogeneous suspension, which implies a higher energy consumption. On the other hand, clayey soils seem to be the ideal type of soils for this treatment [1]. However, different types of clays can cause different effect on the viscosity and the hydrodynamic properties of the slurry, affecting differently the oxygen transfer processes [28]. Additionally, soil organic matter in real soil can come from numerous types of substances and may produce different effects than those shown in chapters 4 and 6 [29–31]. Furthermore, with the soil weathering, clay-SOM aggregates are likely to form in the soil matrix, creating a new element that could play an important role in the bioavailability of the pollutants [15].

In real polluted soils, indigenous microorganisms are present and probably already acclimated to the specific type of soil pollution. They can serve as starting point for the culture enrichment, which likely would increase the pollutant-specificity biodegradation [32]. Also, the presence and type of SOM can influence the structure of the microbial communities. Certain strains or combinations of them could be able to degrade this soil component and modify the population dynamics regarding the consumption of the targeted contaminants. Furthermore, slurry rheological properties, and hence the transfer processes, could change in function of the different cultures and the extracellular substances that they could produce.

4. Conclusions

This chapter was divided in two parts. The experimental part allowed the demonstration of the complete bioremediation process of an artificial phenanthrene-polluted soil for two different compositions, from which the next conclusions were drawn:

- Artificial phenanthrene-polluted soil was successfully remediated using a soil slurry bioreactor.

- OUR and pH proved to be practical parameters to follow the microbial activity in the reactor.
- Degradation products were not completely removed from the aqueous phase, probably due to the lack of adaptation of microorganisms to consume these substances and/or their toxic effect on the microbial community.
- Ammonium was consumed by bacteria at a similar rate than phenanthrene for clay remediation and thus seems to be the preferential nitrogen source for microorganisms. However, for the artificial soil containing SOM, nitrogen could have been consumed in other forms provided by this material.
- SOM caused a decrease in the biodegradation rate, which can be explained by the lower bioavailability of phenanthrene when this material was present, combined with a possible accessibility of other carbon sources given by SOM in detriment of the phenanthrene consumption.

Furthermore, the experimental part provided the necessary information for the development of a general discussion about the interactions between the mechanisms occurring in a soil slurry bioreactor, which were individually studied in the previous chapters of this thesis, with phenanthrene as a model molecule. From the general discussion the next points can be highlighted:

- The pollutant bioavailability was limited by the desorption process, particularly when SOM was present in the soil.
- Phenanthrene volatilization might have been the major removal process during the lag phase of the biodegradation process.
- Low agitation rates and stirring speeds can be used to optimize the compromise between oxygen transfer and phenanthrene volatilization, as well as the energy consumption of the reactor, without affecting the phenanthrene bioavailability.

The results of this research work can be extrapolated to the study of the soil slurry bioreactor for real contaminated soil remediation, but several considerations should be made, i.e. type of soil, type of SOM, aging and weathering, and the presence of indigenous microorganisms, among others. In any case, the mechanistic approach used in this investigation can be seen as a generic method and can be used to study and better understand the slurry bioreactor treatment for any type of soil, different pollutants and microbial communities, as well as additional operating conditions. Moreover, the development of a mathematical model including the individual mechanisms models developped in this study, as well as the

interactions between them could constitute a powerful tool for the optimization of this treatment. The study of the slurry bioreactor treatment on a real contaminated soil could serve for adjusting the modeling parameters for specific-soil remediation.

References

[1] I.V. Robles-González, F. Fava, H.M. Poggi-Varaldo, A review on slurry bioreactors for bioremediation of soils and sediments, Microb. Cell Factories. 7 (2008) 5. doi:10.1186/1475-2859-7-5.

[2] D.O. Pino-Herrera, Y. Pechaud, D. Huguenot, G. Esposito, E.D. van Hullebusch, M.A. Oturan, Removal mechanisms in aerobic slurry bioreactors for remediation of soils and sediments polluted with hydrophobic organic compounds: An overview, J. Hazard. Mater. 339 (2017) 427–449. doi:10.1016/j.jhazmat.2017.06.013.

[3] S.C. Wilson, K.C. Jones, Bioremediation of soil contaminated with polynuclear aromatic hydrocarbons (PAHs): a review, Environ. Pollut. 81 (1993) 229–249.

[4] G.L. Northcott, K.C. Jones, Developing a standard spiking procedure for the introduction of hydrophobic organic compounds into field-wet soil, Environ. Toxicol. Chem. 19 (2000) 2409–2417.

[5] 5220 CHEMICAL OXYGEN DEMAND (COD), Standard Methods for the Examination of Water and Wastewater, (2017). doi:10.2105/SMWW.2882.103.

[6] S. Mallick, S. Chatterjee, T.K. Dutta, A novel degradation pathway in the assimilation of phenanthrene by Staphylococcus sp. strain PN/Y via meta-cleavage of 2-hydroxy-1-naphthoic acid: formation of trans-2,3-dioxo-5-(2'-hydroxyphenyl)-pent-4-enoic acid, Microbiology. 153 (2007) 2104–2115. doi:10.1099/mic.0.2006/004218-0.

[7] L. Rehmann, G.P. Prpich, A.J. Daugulis, Remediation of PAH contaminated soils: Application of a solid–liquid two-phase partitioning bioreactor, Chemosphere. 73 (2008) 798–804. doi:10.1016/j.chemosphere.2008.06.006.

[8] S. Gao, J.-S. Seo, J. Wang, Y.-S. Keum, J. Li, Q.X. Li, Multiple degradation pathways of phenanthrene by Stenotrophomonas maltophilia C6, Int. Biodeterior. Biodegrad. 79 (2013) 98–104. doi:10.1016/j.ibiod.2013.01.012.

[9] R.-H. Peng, A.-S. Xiong, Y. Xue, X.-Y. Fu, F. Gao, W. Zhao, Y.-S. Tian, Q.-H. Yao, Microbial biodegradation of polyaromatic hydrocarbons, FEMS Microbiol. Rev. 32 (2008) 927–955. doi:10.1111/j.1574-6976.2008.00127.x.

[10] D. Ghosal, J. Chakraborty, P. Khara, T.K. Dutta, Degradation of phenanthrene via meta-cleavage of 2-hydroxy-1-naphthoic acid by Ochrobactrum sp. strain PWTJD: Biodegradation of phenanthrene by Ochrobactrum sp., FEMS Microbiol. Lett. 313 (2010) 103–110. doi:10.1111/j.1574-6968.2010.02129.x.

[11] N.V. Balashova, I.A. Kosheleva, N.P. Golovchenko, A.M. Boronin, Phenanthrene metabolism by Pseudomonas and Burkholderia strains, Process Biochem. 35 (1999) 291–296. doi:10.1016/S0032-9592(99)00069-2.

[12] X.-Q. Tao, G.-N. Lu, Z. Dang, C. Yang, X.-Y. Yi, A phenanthrene-degrading strain Sphingomonas sp. GY2B isolated from contaminated soils, Process Biochem. 42 (2007) 401–408. doi:10.1016/j.procbio.2006.09.018.

[13] H.-C. Flemming, J. Wingender, The biofilm matrix, Nat. Rev. Microbiol. 8 (2010) 623–633. doi:10.1038/nrmicro2415.

[14] C.S. Helling, G. Chesters, R.B. Corey, Contribution of Organic Matter and Clay to Soil Cation-Exchange Capacity as Affected by the pH of the Saturating Solution1, Soil Sci. Soc. Am. J. 28 (1964) 517. doi:10.2136/sssaj1964.03615995002800040020x.

[15] R.L. Wershaw, A new model for humic materials and their interactions with hydrophobic organic chemicals in soil-water or sediment-water systems, J. Contam. Hydrol. 1 (1986) 29–45.

[16] F.J. Sowden, H. Morita, M. Levesque, Organic nitrogen distribution in selected peats and peat fractions, Can. J. Soil Sci. 58 (1978) 237–249. doi:10.4141/cjss78-028.

[17] X.-X. Zhang, S.-P. Cheng, Z. Cheng-Jun, S. Shi-Lei, Microbial PAH-degradation in soil: degradation pathways and contributing factors, Pedosphere. 16 (2006) 555–565.

[18] X.-Y. Lu, T. Zhang, H.H.-P. Fang, Bacteria-mediated PAH degradation in soil and sediment, Appl. Microbiol. Biotechnol. 89 (2011) 1357–1371. doi:10.1007/s00253-010-3072-7.

[19] C. Duran, Y. Fayolle, Y. Pechaud, A. Cockx, S. Gillot, Impact of the activated sludge suspended solids on its non-Newtonian behavior and oxygen transfer in a bubble column, Chem. Eng. Sci. (2016). https://hal-upec-upem.archives-ouvertes.fr/hal-01394418.

[20] J.D. Desai, I.M. Banat, Microbial production of surfactants and their commercial potential., Microbiol. Mol. Biol. Rev. 61 (1997) 47.

[21] R.F. Lewis, SITE Demonstration of Slurry-Phase Biodegradation of PAH Contaminated Soil, Air Waste. 43 (1993) 503–508. doi:10.1080/1073161X.1993.10467149.

[22] F. Garcia-Ochoa, E. Gomez, V.E. Santos, J.C. Merchuk, Oxygen uptake rate in microbial processes: An overview, Biochem. Eng. J. 49 (2010) 289–307. doi:10.1016/j.bej.2010.01.011.

[23] F. Garcia-Ochoa, E. Gomez, Bioreactor scale-up and oxygen transfer rate in microbial processes: An overview, Biotechnol. Adv. 27 (2009) 153–176. doi:10.1016/j.biotechadv.2008.10.006.

[24] B.J. Reid, K.C. Jones, K.T. Semple, Bioavailability of persistent organic pollutants in soils and sediments—a perspective on mechanisms, consequences and assessment, Environ. Pollut. 108 (2000) 103–112.

[25] W. Chen, H. Wang, Q. Gao, Y. Chen, S. Li, Y. Yang, D. Werner, S. Tao, X. Wang, Association of 16 priority polycyclic aromatic hydrocarbons with humic acid and humin fractions in a peat soil and implications for their long-term retention, Environ. Pollut. 230 (2017) 882–890. doi:10.1016/j.envpol.2017.07.038.

[26] S. Müller, K.U. Totsche, I. Kögel-Knabner, Sorption of polycyclic aromatic hydrocarbons to mineral surfaces, Eur. J. Soil Sci. 58 (2007) 918–931. doi:10.1111/j.1365-2389.2007.00930.x.

[27] F. Beolchini, L. Rocchetti, F. Regoli, A. Dell'Anno, Bioremediation of marine sediments contaminated by hydrocarbons: Experimental analysis and kinetic modeling, J. Hazard. Mater. 182 (2010) 403–407. doi:10.1016/j.jhazmat.2010.06.047.

[28] R. Keren, Rheology of mixed kaolinite-montmorillonite suspensions, Soil Sci. Soc. Am. J. 53 (1989) 725–730.

[29] R.G. Luthy, G.R. Aiken, M.L. Brusseau, S.D. Cunningham, P.M. Gschwend, J.J. Pignatello, M. Reinhard, S.J. Traina, W.J. Weber, J.C. Westall, Sequestration of hydrophobic organic contaminants by geosorbents, Environ. Sci. Technol. 31 (1997) 3341–3347.

[30] J.W. Talley, U. Ghosh, S.G. Tucker, J.S. Furey, R.G. Luthy, Particle-scale understanding of the bioavailability of PAHs in sediment, Environ. Sci. Technol. 36 (2002) 477–483.

[31] C. Trellu, A. Miltner, R. Gallo, D. Huguenot, E.D. van Hullebusch, G. Esposito, M.A. Oturan, M. Kästner, Characteristics of PAH tar oil contaminated soils—Black particles, resins and implications for treatment strategies, J. Hazard. Mater. 327 (2017) 206–215. doi:10.1016/j.jhazmat.2016.12.062.

[32] M. Wu, L. Chen, Y. Tian, Y. Ding, W.A. Dick, Degradation of polycyclic aromatic hydrocarbons by microbial consortia enriched from three soils using two different culture media, Environ. Pollut. 178 (2013) 152–158. doi:10.1016/j.envpol.2013.03.004.

[33] M.C. van Loosdrecht, J. Lyklema, W. Norde, A.J. Zehnder, Influence of interfaces on microbial activity., Microbiol. Rev. 54 (1990) 75–87.

[34] R. Sardeing, P. Painmanakul, G. Hébrard, Effect of surfactants on liquid-side mass transfer coefficients in gas–liquid systems: A first step to modeling, Chem. Eng. Sci. 61 (2006) 6249–6260. doi:10.1016/j.ces.2006.05.051.

General conclusions and perspectives

GENERAL CONCLUSIONS AND PERSPECTIVES

1. General conclusions

The investigation of the PAH removal mechanisms in a soil slurry bioreactor through a mechanistic approach helped to elucidate the influence of the physicochemical characteristics of the PAHs and the soil components, as well as certain operational parameters on the mass transfer and biodegradation processes. From each chapter, the next conclusions can be drawn.

1.1. Chapter 2: Gas-liquid oxygen transfer

The objective of this chapter was to study the influence of the stirring speed, the air superficial velocity and the clay concentration on the gas-liquid mass transfer. The results showed that the volumetric oxygen mass transfer coefficient varies linearly with the total power input (mechanical and pneumatic) applied to the system at the conditions tested. Also, the oxygen transfer is significantly affected by the soil content. This effect might be attributed to density and viscosity changes in the slurry, as well as bubble contamination. A linear correlation between the alpha factor (which is the relative diminution of the oxygen transfer coefficient in the presence of soil) and the ratio of the Archimedes number of the slurry to the one of water was proposed. Further research is needed to assess the applicability of the correlation in other gas mixing regimes. This can be achieved by extending the operational parameter ranges or by using different types of impellers.

It was demonstrated that clay presence in soils can strongly affect oxygen transfer in slurry systems. Therefore, during the design and operation of a slurry bioreactor, it is important to consider the clay content and the soil concentration as parameters that can affect the entire biodegradation process. Besides, biomass can modify the physicochemical properties of the liquid phase. Thus, it is important to consider the effect of both solid particles interacting in the slurry phase and the effect of other operational parameters on this interaction and in the overall bioremediation process.

1.2. Chapter 3: PAH volatilization

The main purpose of chapter 3 was to study the influence of the stirring speed and of physicochemical properties of molecules on the volatilization of selected light aromatic compounds. The experiments demonstrated that bubble aeration in the reactor led to the PAH saturation of the bubbles. This allowed the calculation of the Henry's law constant of these compounds. On the other hand, the PAH surface mass transfer coefficient showed a power-type correlation with the mechanical power input. Moreover, correlations between the Henry's law constant and the parameters of this power-type correlation were proposed. These

correlations can be used to estimate the value of the overall HOC mass transfer coefficient within the conditions tested.

To appropriately model the gas-liquid mass transfer coefficient., two models were compared. The proportionality coefficient (PC) model and the two-reference compound (2RC) require knowing the mass transfer coefficient of one and two reference compounds respectively. Both models presented similar results, showing that either only oxygen or both, oxygen and water, can be used as reference compounds to calculate the mass transfer coefficient. However, the 2RC model is preferable, due to its higher robustness and its extrapolatable characteristics regarding hydrodynamic changes in both gas-side and liquid-side interfaces.

1.3. Chapter 4: PAH sorption-desorption

In this chapter, the influence of soil concentration in the slurry and soil composition (SOM content) on the sorption-desorption equilibrium and the desorption kinetics was assessed. The results indicate that PAH sorption equilibrium is mainly controlled by soil organic matter. However, clay presence can modify this phenomenon, probably by reducing the available sorption sites forming SOM-clay aggregates. Additionally, sorption hysteresis was negligible for the short time PAH sorption equilibration.

On the other hand, desorption kinetics was modelled as the sum of individual desorption rates for each soil component using a three-parameter, two-compartment model, in which first order equations were defined for each compartment. Soil concentration did not affect the desorption kinetic rate. This means that desorption may only depend on the surface equilibrium (and, hence, on the physicochemical properties of the molecule and the sorbent) and not on the hydrodynamic conditions at the range of soil concentration tested.

A power-type correlation was found for the first order kinetic constants for both materials, clay and SOM, and the organic-carbon normalized soil to water partition coefficient (K_{OC}), meaning that the PAH desorption from these fractions of soil is mainly controlled by the compound hydrophobicity. Additionally, PAH molecules with a higher molecular weight (and a higher hydrophobicity) tend to be sorbed in higher proportion onto nonpolar SOM than onto mineral surfaces. Pollution origin, aging and weathering determine the fate of PAHs in soil and environment.

1.4. Chapter 5: Biodegradation and culture enrichment

The goals of chapter 5 were to test the effect of co-substrate and the presence of a surfactant on the PAH biodegradation kinetics and on the ability of the microbial community to adapt to environmental changes. From the results, it was concluded that PAHs containing non-

aromatic rings are less degraded by cultures enriched with only-aromatic PAHs. Also, HMW PAHs are less degraded, when culture acclimation is done using LMW PAHs.

Moreover, when glucose is used as co-substrate of phenanthrene-degrading cultures, biomass production is incremented. However, the microbial community becomes less efficient at phenanthrene degradation. In addition, the surfactant lauryl betaine had a strong inhibitory effect on the bacterial growth, even when the phenanthrene-degradation capacity of the cultures was not affected. The substrates used in the acclimation and enrichment of the culture plays an important role in its PAH biodegradation capacity and change adaptability.

1.5. Chapter 6: Slurry bioreactor

This chapter allowed the demonstration of the complete bioremediation process of artificial phenanthrene-polluted soils. The experiment demonstrated that the polluted soils were successfully remediated using a soil slurry bioreactor. Both OUR and pH proved to be practical parameters to follow the microbial activity in the reactor. Nonetheless, the targeted degradation products were not completely removed from the aqueous phase, probably due to the lack of adaptation of microorganisms or to their toxic effect on the culture.

Besides, SOM caused a decrease in the biodegradation efficiency of 25%, which can be explained by the lower bioavailability of phenanthrene when this material was present, combined with a possible bioaccessibility of other carbon sources provided by SOM in detriment of the phenanthrene consumption.

1.6. Chapter 6: Interactions between the PAH removal mechanisms

In the general discussion, some interactions between the mechanisms were identified using the soil slurry bioreactor experiment. For instance, the pollutant bioavailability was limited by the desorption process, particularly when SOM was present in the soil. Also, volatilization can be the major removal process during the lag phase of the biodegradation process. As a conclusion, for the slurry bioreactor tested, low agitation rates and stirring speeds can be used to optimize the compromise between oxygen transfer and phenanthrene volatilization, as well as the energy consumption of the reactor, without affecting the phenanthrene bioavailability.

The results of this research work can be extrapolated to the study of the soil slurry bioreactor for real contaminated soil remediation. However, it is necessary to consider the characteristics and composition of the soil and the presence of indigenous microorganisms. The mechanistic approach used in this investigation can be seen as a generic method and can be used to study and better understand the slurry bioreactor treatment for any type of soil, different pollutants and microbial communities, as well as additional operating conditions

2. Limitations of this study

The characterization of the sorbents (clay and SOM) could not be performed for this study. Given that desorption is one of the most important aspects of the slurry bioreactor treatment, sorbent characterization could elucidate specific features of the sorbents surface, such as the specific surface area or the type of active sites, that can help to better understand the sorption-desorption process. Likewise, biomass measurement methods were difficult to implement. Techniques, such as the most probable number (MPN) and counting plates were tested, with no success. Problems regarding the repeatability, precision and robustness of these methods were encountered. Information about the biomass growth and yield are necessary to model the biodegradation process. The dynamic population analysis and the microorganisms' identification could enhance the comprehension of the culture and allow a better comparison with the studies in the literature. Additionally, in chapter 2, bubble size was considered to be constant during the process at constant agitation and aeration conditions. This assumption was based on theoretical relations. The difficulty for the determination of this parameter resides in the presence of solids in suspension. Indeed, the most common methods for the measuring of bubble size are based on optical techniques, which can be heavily affected by soil presence. Nonetheless, the quantification of this parameter could improve the validity of the hypothesis and conclusions derived from chapter 2.

3. Perspectives and scientific challenges

In general, the studies found in the literature regarding the soil slurry bioreactor technology consider the process as a black box and the influence of operational parameters is measured only on the pollutant removal efficiencies, without understanding the mechanisms leading to those efficiencies. Therefore, the objective of this thesis project was to develop a mechanistic approach in order to elucidate the processes behind that black box.

Although many of the main removal mechanisms and their interactions were brought to light by this study, several questions remain to be answered. In this section, some of these questions, necessary to advance towards a better comprehension of the soil slurry bioreactor functioning, are proposed.

- It seems that, when acclimated enriched cultures are used as inocula, the desorption process could be the limiting step for soil bioremediation, if one considers that microorganisms consume the pollutants only in their soluble form. However, bacterial attachment to solid surfaces can be an important mechanism. Are the microorganisms

able to attach to the soil particles (by forming biofilms)? Can they metabolize the pollutants when they are still sorbed? What is the influence of the type of surface on this attachment (SOM, clay)? Can bacteria/clay/SOM aggregates be formed? What could the structure of these aggregates be? How could they influence the hydrodynamic properties of the slurry? Is this the reason why there was an increase in the slurry viscosity in our experiments?

- In the slurry bioreactor process, the production of biopolymers and/or biosurfactants during the degradation due to a carbon source stress was hypothesized. Then, what are the factors that affect the production of these substances by microorganisms? Does variating other nutritional limitations enhance EPS or biosurfactant production? Does the hydrodynamic stress due to a high shear rates (high stirring speed) induce an important EPS production and, in turn, the attachment of microorganisms on soil particles and the formation of strong and large aggregates?
- In general, surfactants have an important influence on the gas-liquid transfer [34]. If biosurfactants are produced in the reactor, what is the influence of these substances on the gas-liquid mass transfer and the pollutant removal?
- Biodegradation products were not completely degraded in the reactor. Were these degradation products toxic or was the microbial community simply not able to degrade them? What would their influence as co-substrate be on the culture acclimation and enrichment?
- Regarding the resilience of the enriched cultures, what is the influence of pH and temperature in the culture enrichment process? How these parameters affect the PAH biodegradation kinetics and biomass growth? Would the antagonistic and synergetic effects of co-substrate change with these parameters?

Furthermore, given that the desorption mechanism was the limiting step for the soil remediation in our study, technologies improving this step should be further investigated. Two solutions are proposed: the integration of the reactor with a system of desorption assisted by ultrasound and the study of the secretion of biosurfactants and other extracellular polymers by the cultures in the reactor. Finally, since biodegradation products remain in the aqueous solution, it is necessary to characterize the wastewater produced in order to evaluate a cleanup strategy. The coupling with other processes, such as chemical or electro-chemical treatments can be interesting for this purpose. Likewise, clean soil fate and disposal strategies must be further addressed.

APPENDIX

APPENDIX

Appendix I – Valorization of the PhD research work

Papers in peer-reviewed journals:

D.O. Pino-Herrera, Y. Pechaud, D. Huguenot, G. Esposito, E.D. van Hullebusch, M.A. Oturan, Removal mechanisms in aerobic slurry bioreactors for remediation of soils and sediments polluted with hydrophobic organic compounds: An overview, J. Hazard. Mater. 339 (2017) 427–449. doi:10.1016/j.jhazmat.2017.06.013.

D.O. Pino-Herrera, Y. Fayolle, S. Pageot, D. Huguenot, G. Esposito, E.D. van Hullebusch, Y. Pechaud, Gas-liquid oxygen transfer in aerated and agitated slurry systems with high solid volume fractions, Chem. Eng. J. 350 (2018) 1073–1083. doi:10.1016/j.cej.2018.05.193.

Two more articles, based on Chapters 3 and 4, are being prepared and will be soon submitted for peer-review process.

Conferences

Oral presentations:

- **Pino-Herrera D.O.**, Pechaud Y., Fayolle Y., Pageot S., Huguenot D., Oturan N., Esposito G., van Hullebusch E.D., Oturan M.A. (2017) **Experimental Analysis and Modeling of Mechanisms involved in the PAH-contaminated Soil Treatment using a Slurry Bioreactor**, Oral presentation, 14th International Conference on Sustainable Use and Management of Soil, Sediment and Water Resources (AquaConSoil 2017), Lyon, France, June 26-30, 2017.
- **Pino-Herrera D.O.**, Pechaud Y., Fayolle Y., Pageot S., Papirio S., Huguenot D., Esposito G., van Hullebusch E.D., Oturan M.A. (2017) **Solid-Liquid and Gas-Liquid Mass Transfer of PAHs in Soil Slurry Bioreactor**s, Keynote oral presentation, 13th International Conference on Gas–Liquid and Gas–Liquid–Solid Reactor Engineering (GLS-13), Brussels, Belgium, August 20-23, 2017.
- **Pino-Herrera D.O.,** Pechaud Y., , Huguenot D., Oturan N., Esposito G., van Hullebusch E.D., Oturan M.A. (2017) **Experimental Analysis and Modeling of the Gas-Liquid Mass Transfer in a Slurry Bioreactor treating PAH-contaminated Soil.** Fourth International symposium on Bioremediation and Sustainable Environmental Technologies . Battelle conferences, Miami, USA, May 22-25, 2017.

- **Pino-Herrera D.O**., Fayolle Y., van Hullebusch E.D., Huguenot D., Esposito G., Oturan M.A., Pechaud, Y. (2018) **Experimental analysis and modelling of bioslurry reactor treating PAHs contaminated soil: an overview**, 2018 - Contaminated Site Management in Europe: Sustainable Remediation and Management of Soil, Sediment and Water (CSME-2018) and Oxidation and Reduction Technologies for Treatment of Soil and Groundwater (EORTs-2018) October 22-25, 2018

Poster presentation:

- **Pino-Herrera D.O.**, Pechaud Y., Papirio, S., Fayolle Y., Huguenot D., Esposito G., van Hullebusch E.D., Oturan M.A. (2018). **Treatment of PAH-contaminated soil using a soil slurry bioreactor: Experimental analysis and modeling**, Intersol 2018, 17th edition, Paris, France, March 27-29, 2018.

Summer school presentations:

- **Pino-Herrera D.O.**, Pechaud Y., Huguenot D., Esposito G., van Hullebusch E.D., Oturan M.A. **Remediation of PAH contaminated soils: Experimental analysis and modeling of a soil slurry bioreactor**, Summer school on Contaminated Soils. Université Paris-Est Marne-la-Vallée, June 29 – July 3 2015.
- **Pino-Herrera D.O.**, Pechaud Y., Huguenot D., Esposito G., van Hullebusch E.D., Oturan M.A. **Remediation of PAH contaminated soils: Experimental analysis and modeling of a soil slurry bioreactor,** Summer School on Contaminated Sediments: Characterization and Remediation. UNESCO-IHE, Delft, The Netherlands, May 25-27 2016.
- **Pino-Herrera D.O.**, Pechaud Y., Papirio S., Fayolle Y., Huguenot D., Pageot S., Esposito G., van Hullebusch E.D., Oturan M.A. **Mass transfer mechanisms in a soil slurry bioreactor**, Oral presentation, Biological Treatment of Solid Waste Summer School, Gaeta, Italy, June 26-30, 2017.

Appendix II – Chapter 2: Supplementary data

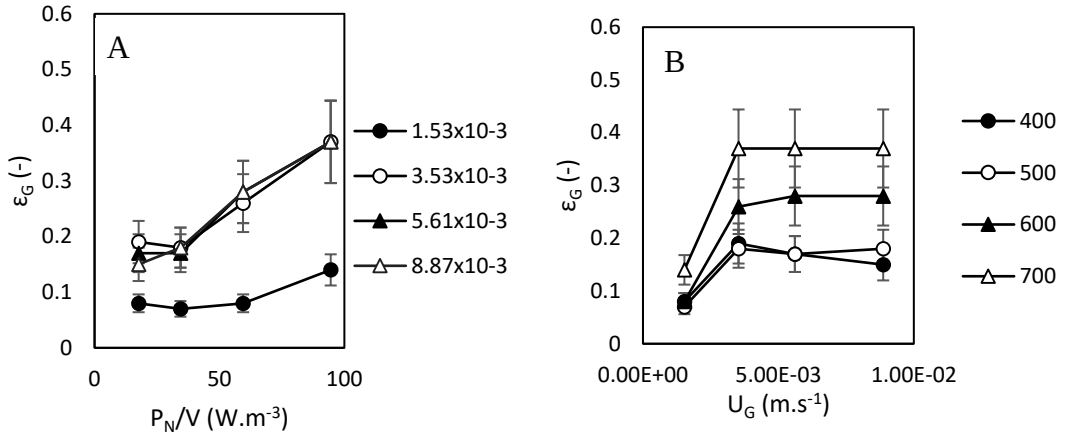

Figure S1 Gas holdup for tap water; A: Effect of power input for different air superficial velocities (in m.s^{-1}); B: Effect of air superficial velocity for different stirring speeds (in rpm)

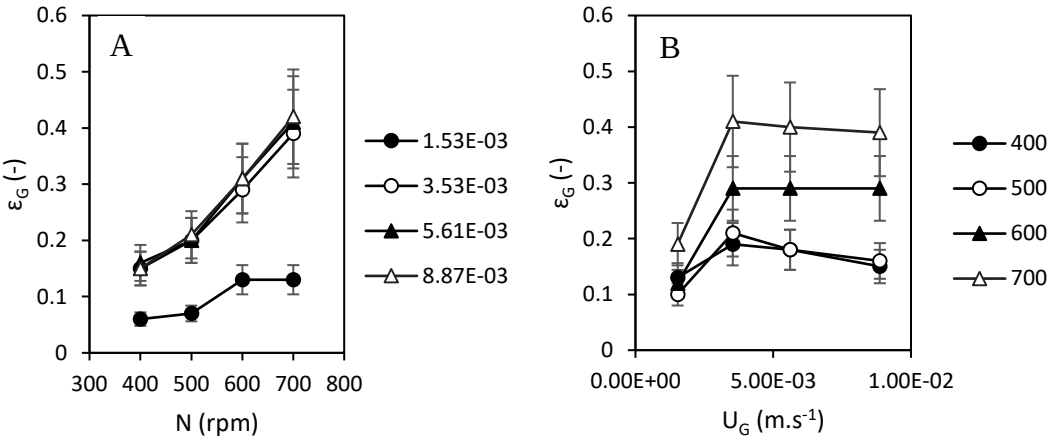

Figure S2 Gas holdup at 0.1% w/v clay concentration; A: Effect of stirring speed for different air superficial velocities (in m.s^{-1}); B: Effect of air superficial velocity for different stirring speeds (in rpm)

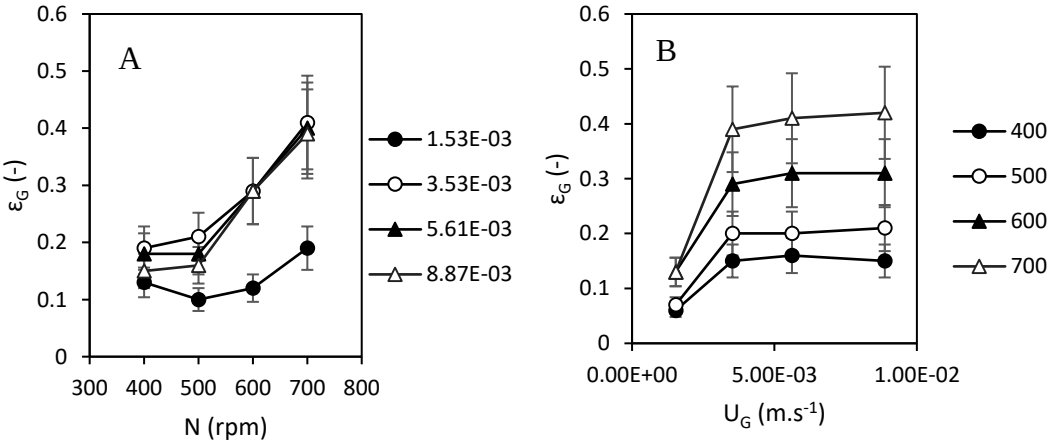

Figure S3 Gas holdup at 0.5% w/v clay concentration; A: Effect of stirring speed for different air superficial velocities (in m.s^{-1}); B: Effect of air superficial velocity for different stirring speeds (in rpm)

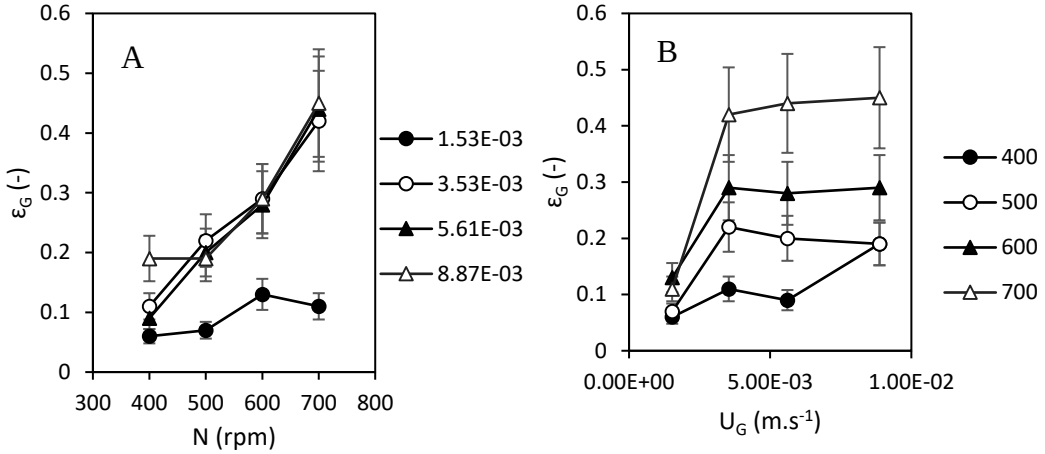

Figure S4 Gas holdup at 1% w/v clay concentration; A: Effect of stirring speed for different air superficial velocities (in m.s-1); B: Effect of air superficial velocity for different stirring speeds (in rpm)

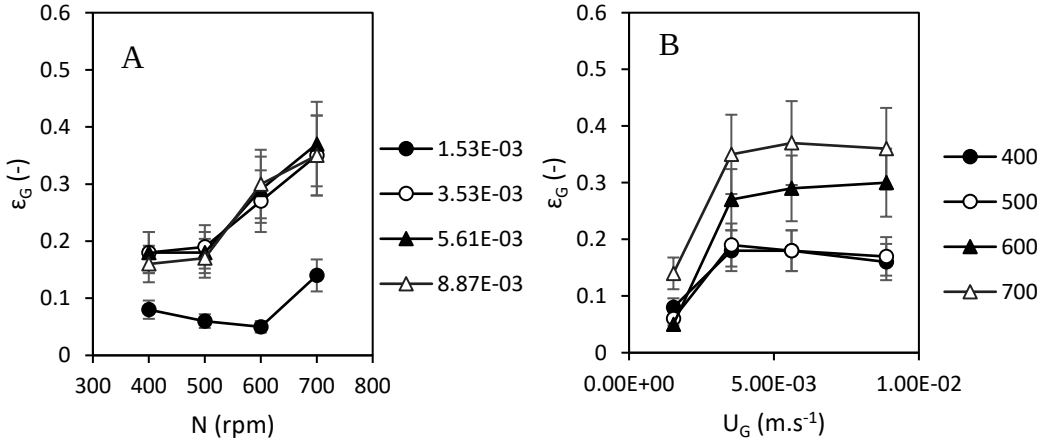

Figure S5 Gas holdup at 2.5% w/v clay concentration; A: Effect of stirring speed for different air superficial velocities (in m.s-1); B: Effect of air superficial velocity for different stirring speeds (in rpm)

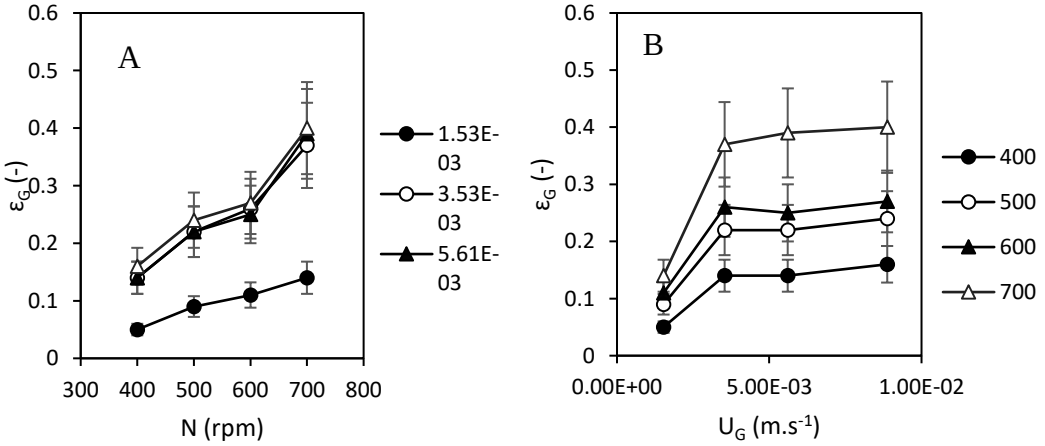

Figure S6 Gas holdup at 5% w/v clay concentration; A: Effect of stirring speed for different air superficial velocities (in m.s-1); B: Effect of air superficial velocity for different stirring speeds (in rpm)

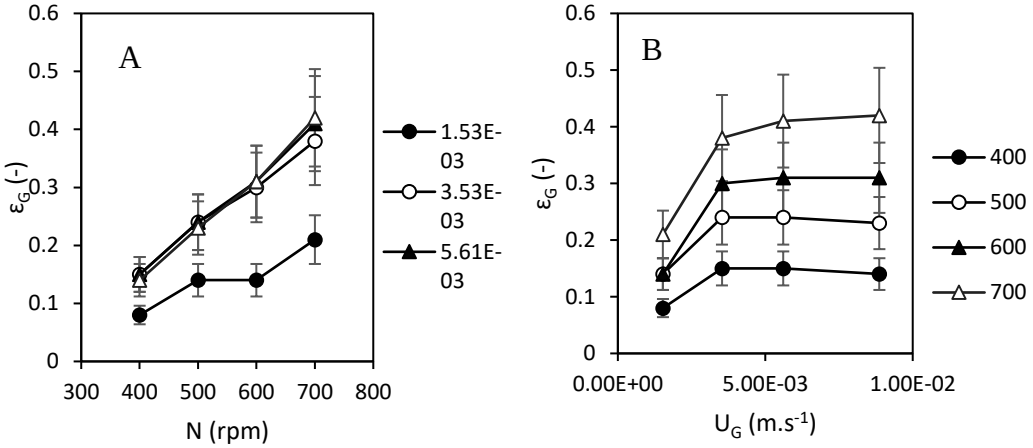

Figure S7 Gas holdup at 10% w/v clay concentration; A: Effect of stirring speed for different air superficial velocities (in m.s-1); B: Effect of air superficial velocity for different stirring speeds (in rpm)

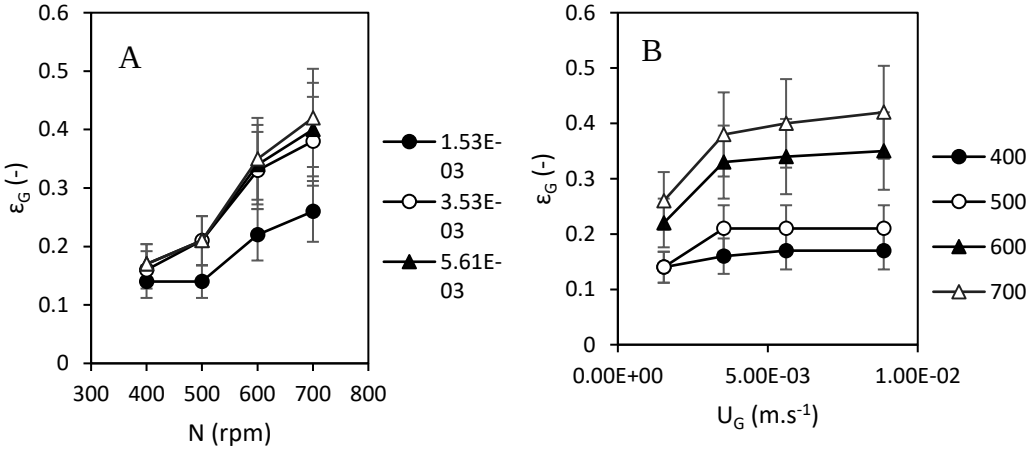

Figure S8 Gas holdup at 20% w/v clay concentration; A: Effect of stirring speed for different air superficial velocities (in m.s-1); B: Effect of air superficial velocity for different stirring speeds (in rpm)